AN ABSTRACT OF THE THESIS OF

Derik W. Kleibacker for the degree of Master of Science in Geology
Presented on November 28, 2001.
Title: Sequence Stratigraphy and Lithofacies of the middle Eocene upper McIntosh and Cowlitz Formations, Geology of the Grays River Volcanics, Castle Rock – Germany Creek Area, Southwest Washington.

Abstract approved: Redacted for privacy
Alan R. Niem

A composite 732-m thick section in Germany Creek of middle Eocene upper McIntosh and lower Cowlitz Formations, as well as the lower Grays River Volcanics, was studied using bio-, magneto- and lithostratigraphy to construct a sequence stratigraphic framework and assess hydrocarbon exploration potential. The upper McIntosh Formation forms a complete 3rd order depositional cycle that includes shallow marine, tide- and wave-dominated sandstones (upper McIntosh sandstone member) and overlying bathyal to outer-shelf siltstone (upper McIntosh siltsone member). The upper McIntosh Formation correlates to Chrons C19r (41.5 – 42.5 Ma) and lower Chron 19n (41.5 – 41.2 Ma). A 3rd order sequence boundary straddling Chron 19n (41.2 – 41.5 Ma) shows truncation of the highstand upper McIntosh siltstone by prograding lowstand shoreface parasequences of the lower Cowlitz Formation. The overlying (300 m thick) shoreface transgressive (TST) and highstand system tracts (HST) of the Cowlitz Formation range in age from 41.5 – 41.2 Ma to 39.35 ±0.36 Ma. The Cowlitz Formation HST of the study area chronostratigraphically correlates to the reservoir Clark and Wilson sandstone member of the Mist Gas Field Cowlitz Formation and to informal unit 1A and lower unit 1B of the type-Cowlitz Formation, southwest Washington.

The Grays River Volcanics of the study area are subdivided by an intra-formational unconformity defining the upper (~150-m thick; 38.6 – 36.8 Ma) and lower (1250-m thick; 40.1 – 39 Ma) Grays River Volcanics subunits. Two subalkaline olivine-

augite tholeiitic basalt flows of the lower Grays River Volcanics conformably overlying the Cowlitz Formation in Germany Creek were $^{40}Ar/^{39}Ar$ dated at 40.09 ±0.34 Ma and 39.35 ±0.36 Ma. The tholeiitic upper Grays River basalt unconformably overlies the lower Grays River Volcanics and the Cowlitz Formation. Numerous sub-parallel, northeast and minor northwest trending Grays River dikes ($^{40}Ar/^{39}Ar$ dated at 39.98 ±0.29 and 39.56 ±0.41 Ma) attest to extension of the study area during the eruption of the Grays River Volcanics.

The Oligocene Lincoln Creek Formation (~70 m) consists of bioturbated tuffaceous siltstone and interbedded silty sandstone with casts and molds of articulated mollusks. Geochemistry, normal polarity, and dikytaxitic texture of the 50-60 m thick Grande Ronde basalt are indicative of the Sentinel Bluffs unit (15.6 Ma) (Columbia River Basalt Group).

The Arkansas Anticline and three fault sets: (1) north-northwest- and (2) northwest-trending dextral oblique-slip faults, and (3) subordinate northeast-trending conjugate sinistral oblique-slip faults are related to two periods of deformation. They are: (1) dextral transtension resulting in horst and graben style faulting, beginning 40 – 39.5 Ma and terminating prior to the eruption of the upper Grays River volcanics (38.6 Ma); (2) post-middle Miocene period of dextral transpression, including dextral reactivation of normal faults and associated broad regional northwest-trending folding (e.g. Arkansas Anticline).

Small normal fault block similar to the Mist Gas Field provide structural traps throughout southwest Washington. Petrography of micaceous lithic arkoses of the upper McIntosh sandstone and Cowlitz Formation indicates reservoir-quality sandstones with an estimated porosity of 16-19%. The most likely hydrocarbon exploration play involves the subtidal to shoreface upper McIntosh Formation sandstone member.

Sequence Stratigraphy and Lithofacies of the middle Eocene upper McIntosh and Cowlitz Formations, Geology of the Grays River Volcanics, Castle Rock – Germany Creek Area, Southwest Washington

by
Derik W. Kleibacker

A THESIS

submitted to

Oregon State University

in partial fulfillment of
the requirements for the
degree of

Master of Science

Presented November 28, 2001
Commencement June 2002

Master of Science thesis of Derik W. Kleibacker presented on November 28, 2001.

APPROVED:

Redacted for privacy

Major Professor, representing Geology

Redacted for privacy

Head of the Department of Geosciences

Redacted for privacy

Dean of the Graduate School

I understand that my thesis will become part of the permanent collection of Oregon State University libraries. My signature below authorizes release of my thesis to any reader upon request.

Redacted for privacy

Derik W. Kleibacker, Author

ACKNOWLEDGEMENTS

I am extremely grateful of the generous financial support from Weyerhaeuser Corporation, under the supervision of Dave Pauli and George Sharp, which made this thesis possible. Additional support for aerial photos, thin section mounting and basalt geochemistry was provided by the Washington Department of Natural Resources, thanks to Dr. Tim Walsh and Karl Wegmann. My major professor, Dr. Alan Niem, beyond helping to secure funding for this project, provided me the tools and opportunity to grow as a geologist, for this I am thankful. Critical reviews of this manuscript by Dr. Alan Niem, Wendy Niem, and committee members Dr. Robert Lillie and Dr. Reed Glasmann clarified this thesis, for their expertise and time I am grateful.

Special thanks are also given to Russ Evarts of the U.S. Geological Survey for precious time in the field and sharing his knowledge of the geology of southwest Washington. Dr. Paul Hammond of Portland State University provided enthusiastic help and stimulating discussion. Dr. Elizabeth Nesbitt of the University of Washington Burke Museum kindly provided key paleoenvironmental information from molluscan fauna samples, for her expertise I am thankful. Emeritus geologist, Dr. Weldon Rau, analyzed foraminiferal assemblages from the area, also providing key paleoenvironmental and age data for the project. Jeff Grieff, volunteer at the Burke Museum, provided further foraminiferal assemblage identification and interpretation. Dr. Donald Prothero of Occidental College, Los Angeles, California was gracious enough to include the Germany Creek sections in his paleomagnetic study of the Cowlitz and Hamlet

formations of northwest Oregon and southwest Washington. The magnetic data proved to be an integral part of this thesis. Teachers such as Mrs. Sullivan, V.J. Ansfield, and Gary Johnson stoked my interest in geology. Former OSU student and friend of the Cowlitz, Chuck Payne, paved the way for my thesis by his thorough work. Fellow students Drew Erickson and Sebastian Geiger, as well as Telly Mikel, always had room for me in their homes and time for good conversation over a cold beer. Mike Parker, BP, was a mentor and friend throughout the thesis project.

I am also thankful to my parents, Wilson and Carol, who encouraged curiosity and rewarded independent thinking. Of all those who gave to help this project, my wife Annie gave the most. This thesis is due to her support and hard work.

TABLE OF CONTENTS

Page

INTRODUCTION..... 1

Research Objectives..... 3

Location of the Map Area..... 4

Geologic Setting..... 5

Methods of Investigation..... 10

STRATIGRAPHY AND LITHOFACIES OF THE UPPER MCINTOSH AND LOWER COWLITZ FORMATIONS..... 14

Previous Work..... 14

Age Determination of Strata..... 17

Upper McIntosh Formation..... 17
Lower Cowlitz Formation..... 18
Grays River Volcanics..... 21
Lincoln Creek Formation..... 21

Upper McIntosh Formation..... 23

Distribution..... 23
Upper McIntosh Formation Sandstone Unit Lithofacies..... 24
Upper McIntosh Formation Siltstone Unit Lithofacies..... 30
Depositional Environments..... 35
Upper McIntosh Sandstone unit..... 35
Upper McIntosh Siltstone unit..... 38

Lower Cowlitz Formation..... 40

Background..... 40
Contact with the McIntosh Formation..... 42
Lithofacies of the lower Cowlitz Formation..... 43
Germany Creek..... 43

TABLE OF CONTENTS (Continued)

Page

Monahan Creek....52
Arkansas Creek Area.... 55
Depositional Environments of the lower Cowlitz Formation....58
Germany Creek.... 58
Monahan Creek.... 64
Arkansas Creek 65
Summary.... 66

Magnetic Stratigraphy of the upper McIntosh and lower Cowlitz formations.... 68

Sequence Stratigraphy of the upper McIntosh and lower Cowlitz formations.... 72

SEDIMENTARY PETROLOGY OF THE UPPER MCINTOSH AND LOWER COWLITZ FORMATIONS....81

Background.... 81

Lithic-Arkosic Sandstones.... 82

Siltstones and Lithic Sandstones.... 90

Summary.... 94

STRATIGRAPHY, PETROLOGY, AND GEOCHEMISTRY OF THE GRAYS RIVER VOLCANICS AND ASSOCIATED SEDIMENTARY UNITS.... 96

Local Age Determination.... 99

Magnetic Stratigraphy....101

Grays River Volcanics Stratigraphy....105

Lower Grays River Volcanics.... 107
Upper Grays River Volcanics.... 113

Dikes of the Grays River Volcanics.... 117

TABLE OF CONTENTS (Continued)

Page

Petrology and Geochemistry 120
Grays River Sedimentary Units 121
Lower Grays River Lava Flows 123
Upper Grays River Lava Flows 126
Grays River Dikes 129

Conclusions and Interpretations 132

LINCOLN CREEK FORMATION 139

GRANDE RONDE BASALT 141

QUATERNARY UNITS 144

Modern Landslide Deposits 144

Lahar Deposits of A.D. 1980 145

Lahar Deposits (Qshu1) 145

Terrace Deposits 146

MIDDLE EOCENE TO LATE EOCENE REGIONAL CORRELATION AND STRATIGRAPHIC RELATIONSHIPS OF SOUTHWEST WASHINGTON AND NORTHWEST OREGON 147

Regional Magnetic Correlatons 148

Surface to Subsurface Regional Stratigraphic Correlations 151

STRUCTURAL GEOLOGY 156

Regional Tectonics and Structure 156

Local Structure 161

Summary 169

TABLE OF CONTENTS (Continued)

Page

HYDROCARBON POTENTIAL 171

Potential Reservoirs 172

Potential Seals 173

Structural Traps 173

Hydrocarbon Generation and Migration 174

Previous Exploration 176

Future Exploration 177

GEOLOGIC HISTORY 179

CONCLUSIONS 188

REFERENCES 197

APPENDICES 204

Appendix A (Microfauna) 205

Appendix B (Macrofauna) 207

Appendix C (Point Count Data) 209

Appendix D (Basalt Geochemistry) 210

Appendix E ($^{40}Ar/^{39}Ar$ Age Dates) 214

Appendix F (Paleomagnetic Results) 218

LIST OF FIGURES

Figure		Page
1.	Boundary and location of thesis area, Cowlitz County, southwest Washington (modified from Payne, 1998)	6
2.	Regional geologic map of southwest Washington and northwest Oregon highlighting Eocene and Oligocene sedimentary and volcanic units (modified from Payne, 1998; Walsh et al., 1987 and Robertson, 1997)	8
3.	Southwest Washington to northwest Oregon stratigraphic correlation chart	19
4.	Upper McIntosh Formation sandstone unit description	25
5.	Sedimentary structures of the upper McIntosh Formation sandstone unit, North Germany Creek section	29
6.	Upper McIntosh Formation siltstone unit measured section description and interpreted depositional environments	31
7.	Sedimentary structures of the upper McIntosh Formation siltstone unit (NGC)	34
8.	Prograding, wave-dominated shoreface successions of the basal Cowlitz Formation and unconformable contact with the upper McIntosh Formation siltstone	44
9.	Sedimentary structures of the basal Cowlitz Formation (NGC)	48
10.	Lithofacies of the lower Cowlitz Formation of Germany Creek, Cowlitz Co., Washington	51
11.	Monahan Creek measured section description and interpreted depositional environments of the Cowlitz Formation	54
12.	Lithofacies of the Cowlitz Formation exposed along a road cut near Arkansas Creek (N ½ of 36 – T10 R3; PlateI)	57

LIST OF FIGURES (Continued)

Figure Page

13. Profile of onshore-offshore depositional environments related to sedimentary structures and inchnofacies of the McIntosh Formation and shallow marine units of the Cowlitz Formation (slightly modified from Payne, 1998; Berkman,1990 and Robertson, 1997)..... 59

14. Magnetic stratigraphy of the Germany Creek sections..... 70

15. Surface to subsurface correlation and sequence stratigraphy of the Germany Creek measured sections and the Quigley No.1 (1925) exploratory well. Lithology and thicknesses of Quigley No.1 from driller's log..... 79

16. QFL ternary sandstone classification diagram (Folk, 1974) comparing mineralogic characteristics of reservoir and potential reservoir sandstones of the region..... 83

17. Photomicrograph of micaceous, carbonaceous lithic arkose from the upper McIntosh Formation sandstone (sample 916E, Plates I and II)..... 84

18. Photomicrograph of porous micaceous, lithic-arkosic sandstone of the Cowlitz Formation (sample G815B, Plates I and II)..... 86

19. A) SEM image of a partially dissolved K-spar grain rimmed by later-stage smectite overgrowths in Cowlitz Formation sandstone sample G81B.
B) XRD patterns from the clay-sized, <2 micron fraction of sample G815B, showing a sharp-peaked, organized Mg-smectite..... 87

20. Photomicrographs of Cowlitz and McIntosh Formation siltstones.
A) Sample 811B (Cowlitz Fm.) ripple- to parallel-laminated lower shoreface siltstone.
B) Sample 914H (upper McIntosh siltstone), bathyal turbidite siltstone..... 89

21. Lithic sandstones of the Cowlitz and upper McIntosh formations.
A) Sample GC916C, glauconitic, lithic sandstone from the base of a possible condensed section.
B) Poorly sorted, basaltic sandstone of the Cowlitz Formation, sample G901C.....92

LIST OF FIGURES (Continued)

Figure — Page

22. Grays River Volcanics outcrop and subcrop map showing locations of radiometric ages and magnetic polarity results..... 102

23. Magnetic polarity chart and radiometric age dates of the Grays River Volcanics, eastern Willapa Hills..... 106

24. Outcrop pictures of the Grays River sedimentary units.
   A) Basaltic conglomerate interbed below subaerial lava flow (Germany Creek, SE ¼, Sec. 14, T9N, R4W; Plate I)
   B) Lignite bed (30-cm thick) in tuffaceous terrestrial sandstone (Tgvst, Plate I, Sec. 12, T9N, R4W)
   C) Coarsening-upward, carbonaceous leaf-bearing tuff and siltstone, Tgvs2 (NW ¼ Sec. 1, T9N, R3W; Plate I road exposure)..... 109

25. Outcrop photographs of upper Grays River basalt flows.
   A) Quarry with radial-jointed upper Grays River basalt, ~14-m thick. (Sec. 24, T10N, R4W)
   B) Road exposure of blocky, 15-m thick subaerial lava flow with less resistant scoriaceous top (NW ¼, Sec. 32, T10N, R4W)
   C) Reddish oxidized scoriaceous flow-base breccia and overlying bent relict-flow colonnade (Sec. 3, T9N, R3W)..... 116

26. A) Radial glomeroporphyritic plagioclase phenocrysts of the 3-4 m thick interior of a 12-m thick Grays River dike, sample 914L (Germany Creek, Plate I)
   B) Typical jointed dark gray, aphyric Grays River dike intruding tan, fine-grained middle Eocene Cowlitz Formation sandstone along the South Germany Creek section, near interval 3 (Plate II)..... 119

27. A) Lowermost Grays River Volcanic strata – unit 1 (sample GR8A). Coarse-grained, shallow-marine basaltic sandstone.
   B) Lower Grays River Volcanic terrestrial strata (sample 628GB). Coarse-grained, scoriaceous basaltic sandstone..... 122

LIST OF FIGURES (Continued)

Figure Page

28. A) Basalts of the Grays River Volcanics from the thesis area plotted on a total alkali vs. SiO2 (TAS) diagram using normalized weight percentage based IUGS classification scheme of Le Bas et al., 1986.
B) Iron enrichment diagram of Miyashiro (1974). Most samples plot as subalkaline tholeiitic basalt; three samples plot as subalkaline basaltic andesite. (modified from Payne, 1998)..... 125

29. Photomicrographs of lower Grays River lava flows..... 127

30. Photomicrographs of Grays River dikes..... 131

31. Diagram illustrating the chonostratigraphic, magnetostratigraphic and geochemical relationships of the Grays River volcanics of the study area.... 133

32. MgO vs. TiO2 and TiO2 vs. P2O5 variation diagrams for informal Grande Ronde flow units from Reidel et al., (1989). Normal polarity sample 51706 is plotted as a red cross, most closely affiliated with 1a, Sentinel Bluffs unit..... 142

33. Regional magnetic polarity correlations of the middle to late Eocene McIntosh-Hamlet and Cowlitz formations of northwest Oregon and southwest Washington..... 149

34. Residual wavelength-filtered gravity anomaly map and volcanic geology map superimposed to show relationship of dense subsurface crustal blocks of the Siletzia terrane to mapped surface volcanic units (modified from Finn et al., 1991; Walsh et al., 1987; Robertson, 1997; and Payne, 1998)..... 157

35. Schematic geologic map of the Chehalis Basin and bounding uplifts. schematic north-south cross section A-A' and southwest-northeast cross section B-B' are based on data from outcrop and borehole studies, seismic reflection profiles, and magnetotelluric surveys (Stanely et al., 1994)..... 160

36. Aerial photo showing lineations in the Germany Creek drainage basin, western study area, northwest Cowlitz Co., Washington..... 164

37. Schematic paleogeographic reconstructions of the (A) lowstand tide-dominated upper McIntosh sandstone member, ~42 Ma; and the (B) highstand prograding shoreface deposits of the lower Cowlitz Formation, ~40 Ma..... 184

LIST OF PLATES

Plate

I: Geologic Map of the Germany Creek – Castle Rock Area, Cowlitz County, southwest Washington.

II: Stratigraphy and Lithofacies of the middle Eocene McIntosh and Cowlitz Formations, and Grays River Volcanics; Germany Creek, Cowlitz County, southwest Washington.

III: Surface and Subsurface Stratigraphic Cross-Section of middle to late Eocene rock units, northwest Oregon to southwest Washington.

Sequence Stratigraphy and Lithofacies of the middle Eocene upper McIntosh and Cowlitz Formations, Geology of the Castle Rock-Germany Creek Area, southwest Washington

INTRODUCTION

The stratigraphy of the middle to upper Eocene sedimentary sequences and forearc basaltic volcanic units of southwest Washington records a complex depositional history of seamount accretion, deltaic sedimentation and forearc deformation. Recent stratigraphic studies have focused on the Eocene hydrocarbon-bearing units within and surrounding the Chehalis basin of southwest Washington (Stanley et al., 1994; Flores and Johnson, 1995; Payne, 1998; Prothero et al., 2001). Motivated by the discovery of natural gas pools in the late Eocene Cowlitz Formation of nearby northwest Oregon, investigators have centered on increasing the stratigraphic resolution of the area to define exploration targets and determine step-out possibilities in the correlative units of southwest Washington.

A tool that has been employed by these recent studies is the use of sequence stratigraphy to define unconformably bounded sequences of relatively conformable strata and their depositional systems. Biostratigraphy and magnetostratigraphy of the middle to late Eocene section of the study area provide relative stratigraphic information useful in correlating sequences and sequence boundaries. Many associations of forearc basin deltaic/marine sequences of the McIntosh and Cowlitz formations inter-stratified with subaerial tholeiitic volcanism of the Grays River Volcanics provide opportunities for chronostratigraphic correlation. Also, the onset of nearby Cascadia calc-alkaline arc-

volcanism is recorded in tuff beds within the Cowlitz Formation. The interbedded lava flows and tuff beds provide excellent stratigraphic markers for radiometric dating.

The study area occupies a strategic location between the type section Cowlitz and McIntosh Formations in the Chehalis basin of southwest Washington and the producing Cowlitz Formation sands of the Mist Gas Field in the Nehalem basin of northwest Oregon. One objective of the study is to determine the stratigraphic relationships of the middle to late Eocene units of the study area with the type Cowlitz and McIntosh Formations of Washington and with the Cowlitz Formation of northwest Oregon. Studies by Payne (1998), Armentrout (1985), Robertson (1997), Kenitz (1997), Livingston (1966), Wells (1981), have aided greatly to the geologic understanding of the region and thesis area.

Identification of the lithofacies and interpretation of depositional environments of the mid- upper-Eocene sedimentary units is critical in determining the reservoir potential of the mixed intra-basinal basaltic volcanic and extra-basinal arkosic deltaic depositional system. Lithofacies are defined as a body of rock containing combinations of lithology, biological and physical structures that are different from the bodies of rock above, below, and adjacent (e.g. ripple-laminated siltstone facies or bioturbated massive arkosic sandstone facies) (Walker, 1992). Lithofacies successions (e.g. a coarsening- and thickening-upward shoreface succession) allow for paleo-environmental reconstruction when an individual facies could have formed in different depositional environments, such as heterolithic ripply siltstones of an intertidal estuarine or marine lower shoreface depositional environment (Walker, 1992). Understanding the spatial and temporal

proximity of the Eocene deltaic depositional systems with the intra-basinal growing volcanic highs can help determine the reservoir quality and production possibilities of the sandstone bodies (Armentrout and Suek, 1985).

In order to achieve these objectives, detailed stratigraphic measurement, sampling and dating of a 318 m section of lower Cowlitz and lower Grays River Volcanics and a 734 meter section of uppermost McIntosh, lower Cowlitz Formation and lower Grays River Volcanics along Germany Creek provided both lithofacies descriptions and stratigraphic control. Geologic mapping of the area at 1:24,000 scale allowed interpretations of the depositional and geologic histories of the volcanic centers, deltaic sedimentation, and the interaction between them.

RESEARCH OBJECTIVES

The primary goal of this study is to determine the stratigraphic relationships of the upper Eocene sedimentary and volcanic units exposed in the thesis area to the type-section Cowlitz and McIntosh Formations of southwest Washington and to the Cowlitz Formation of the Mist Gas Field in northwest Oregon (Figure 1, 2). Tying the measured section lithofacies to subsurface data provides a "key" to interpreting electric well log and cutting description data near the thesis area. Thanks to the work of Payne (1998), a close correlation of the lithofacies of the type-section Cowlitz Formation to the 1 Zion electric well-log was possible. Correlation between the 1 Zion well-log and the author's Germany Creek section was accomplished by Ar^{40}/Ar^{39} radiometric dates, magnetostratigraphy, biostratigraphy, and matching lithofacies descriptions. The

Germany Creek section was also lithologically correlated to cutting descriptions from the driller's log of Quigley No. 1, a well located near the center of the thesis area (Plate III). Detailed descriptions of the lithofacies, recognition of marine flooding surfaces and parasequence sets within the upper McIntosh and lower Cowlitz Formations helped resolve the depositional environments of the upper Eocene units.

Another objective of the study was to produce a geologic map (1:24,000 scale) and structural cross sections of the thesis area, allowing increased definition of the geologic history and structure of the area. The integration of the stratigraphy and geologic mapping with petrographic analysis of the Cowlitz and McIntosh formations was undertaken to determine the reservoir potential of sandstones, possible source rocks and prospective traps.

LOCATION OF MAP AREA

The thesis area is located in the eastern Willapa Hills, southwest of the Chehalis basin in northwest Cowlitz County, southwest Washington (Figure 1, 2). Bordered by Germany Creek on the west and the Cowlitz River on the east, the town of Castle Rock lies on the southeastern edge of the 154 square kilometer (63 square mile) area. The best exposures in the area generally occur along creekbeds in low summer flow, including Monahan Creek, Arkansas Creek, Delameter Creek, Germany Creek and its tributaries. Logging roads and numerous county highways provide access to roadcrop exposures throughout the area.

GEOLOGIC SETTING

The major structural feature of southwest Washington is the arcuate basement uplift forming the Willapa Hills (Wells and Coe, 1985). Middle Eocene submarine basalts and interbedded siltstone of the Crescent Formation are exposed in the core of the uplift. These rocks are believed to have formed in a continental-margin rift setting (Wells et al., 1984; Snavely, 1987; Babcock et al., 1992, Stanley et al., 1996), possibly associated with a leaky transform fault or hot spot system. An average K-Ar age of ~ 49 Ma is reported for this area of the Crescent Formation basalts (Duncan, 1982). These rocks at least partially correlate with the Siletzia accreted oceanic terrain, which comprises the basement for Tertiary forearc basins in the Oregon and Washington Coast Ranges. When this thick (15-30 km) oceanic crust of the Farallon Plate collided with the North American plate about 50 Ma, it was too buoyant to subduct and was accreted to the continent. A new subduction zone formed farther to the west, on the outer contintental shelf of present-day western Washington.

Gravity and magnetic data (Finn, 1991) indicate that Siletzia consists of many discrete blocks. Differential clockwise rotation of these small crustal blocks is attributed to Cascadia oblique subduction and consequent north-south transcurrent faulting developing northwest-trending conjugate faults in southwest Washington (Armentrout, 1987). Although paleomagnetic evidence suggests clockwise rotation of 30° or more for much of the Tertiary section (Wells and Coe, 1985), most previous basin analyses have been given in present geographic coordinates (Chan and Dott, 1986; Armentrout, 1987; Robinson, 1997, Payne, 1998). This study follows the same convention.

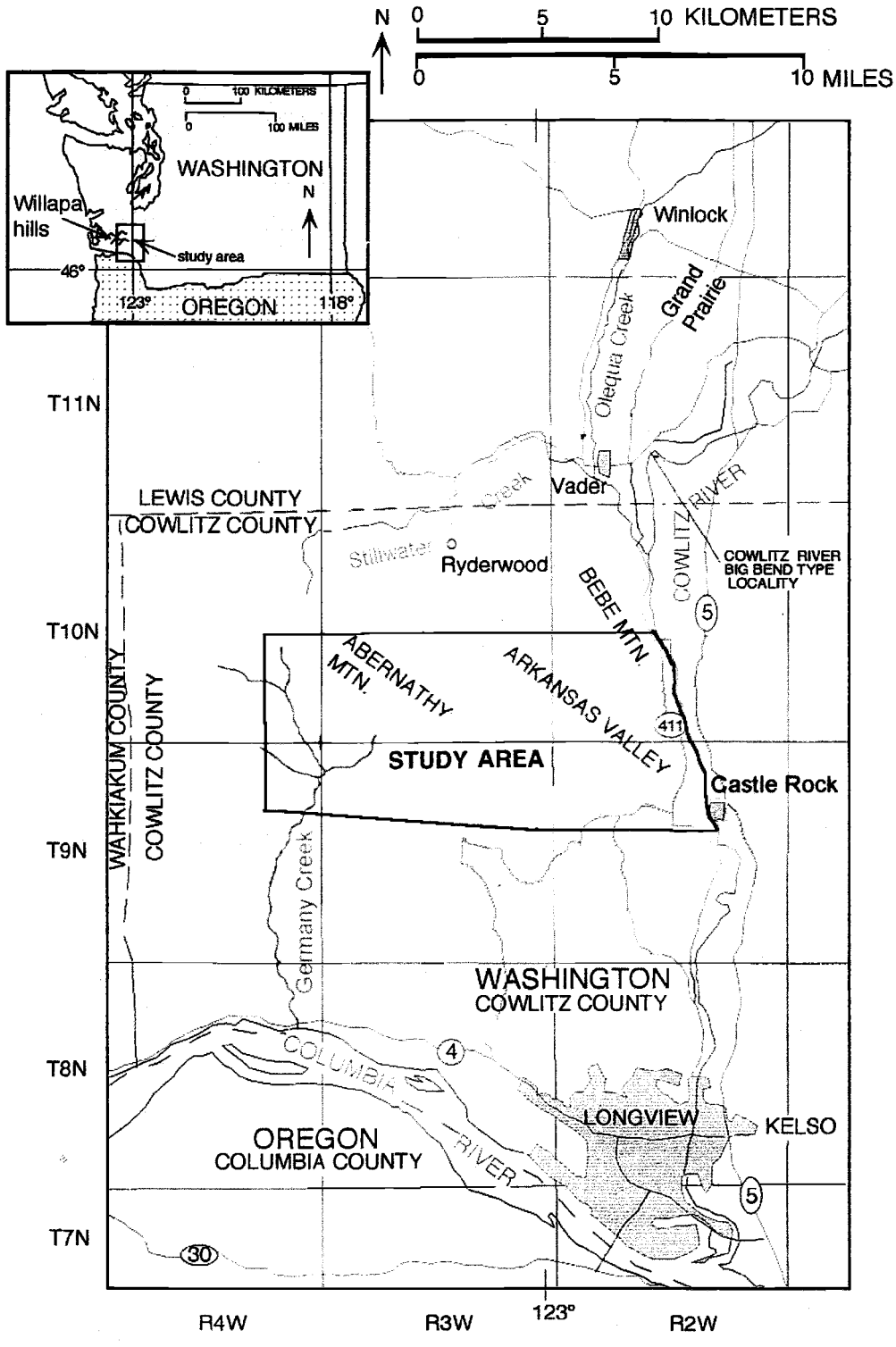

Figure 1. Boundary and location of the thesis area, Cowlitz County, southwest Washington (modified from Payne, 1998).

In southwest Washington, deformation of the Crescent basalts began during the middle Eocene (~48 Ma), initiating uplift of the Willapa Hills (Wells and Coe, 1985). The plate-boundary relocation and subsequent differential shear rotation of these crustal blocks is recognized in the geologic record as the earliest unconformity bounded sequence preserved in southwest Washington (Armentrout, 1987).

The thesis area is on the southwest edge of the Chehalis basin and the northeast flank of a Bougeur gravity high separating the Nehalem and Chehalis basins (Figure 2, 34). The gravity high has been related to the subsurface presence of a thick discrete crustal block of middle Eocene Crescent Formation (Siletzia), as well as a thick surface-subsurface pile (at least 1200 m) of overlying upper Eocene Grays River Volcanics (Kenitz, 1997).

Rapid subsidence of the Siletzia terrane in the middle to late Eocene due to crustal extension formed a forearc basin extending from present-day southern Oregon to Vancouver Island, Canada (Niem et al., 1992). At the southern edge of the Chehalis basin, bathyal mudstone and minor arkosic sandstone of the McIntosh Formation onlap the Crescent volcanic basement in the Willapa Hills, suggesting the area formed an Eocene basement high attributed to seamount topography at the top of the Crescent Formation (Stanley et al., 1994). Alternatively, Wells and Coe (1985) attribute the onlapping of the middle and upper Eocene sedimentary units as a result of the uplifted Crescent Formation basement, i.e. Willapa Hills uplift, forming a paleo-bathymetric high within the subsiding forearc basin.

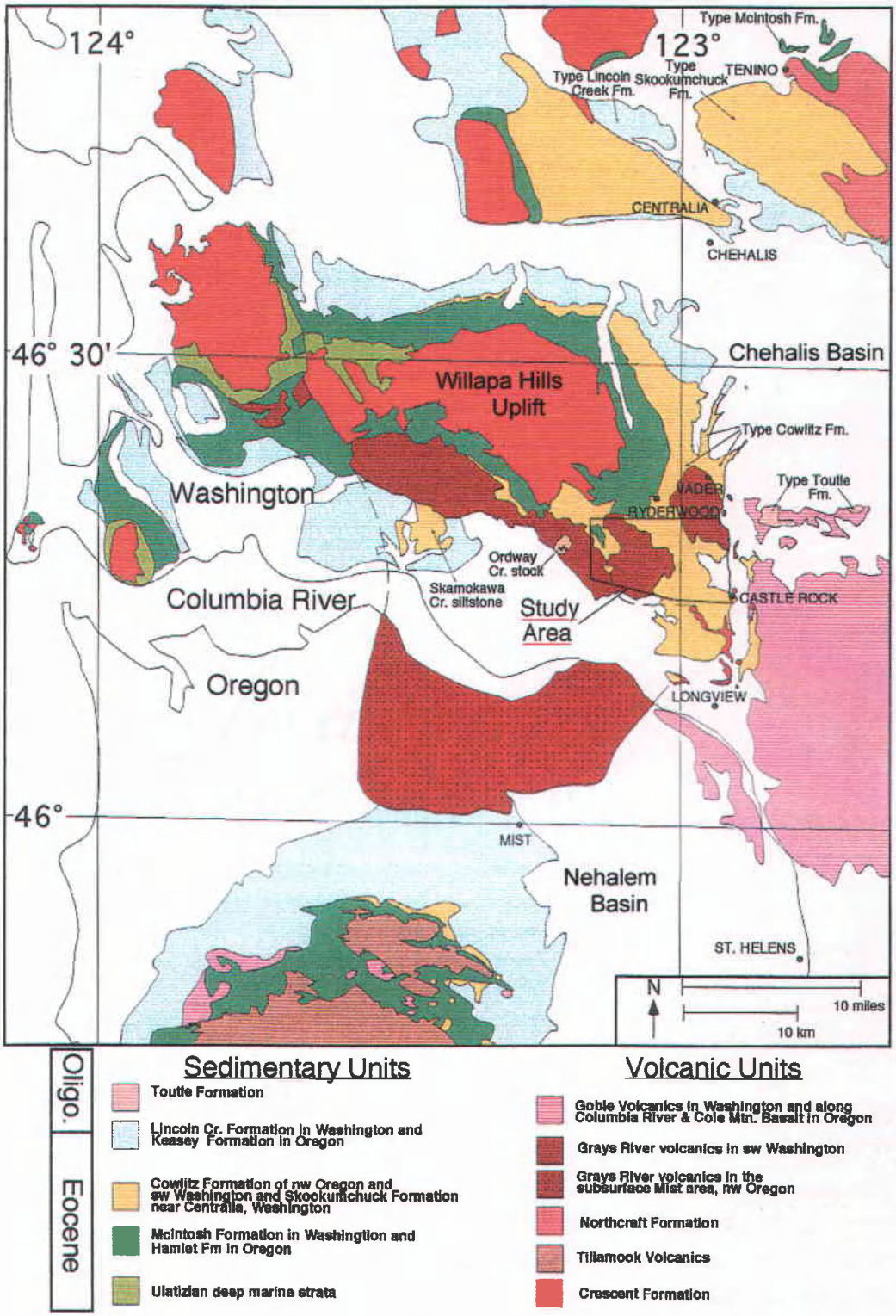

Figure 2. Regional geologic map of southwest Washington and northwest Oregon highlighting Eocene and Oligocene sedimentary and volcanic units (modified from Payne, 1998; Walsh et al., 1987 and Robertson, 1997).

Renewed basaltic volcanism during the middle to late Eocene produced forearc shield volcanoes of the Tillamook Volcanics (>42.4 Ma) in northwest Oregon and the petrologically equivalent Grays River Volcanics (41.4 – 36.8 Ma) of southwest Washington (Kenitz, 1997; Niem et al., 1992). These growing volcanic highs further subdivided the forearc basin into smaller marine depositional centers (Niem et al., 1992), encroaching on the southern edge of the Chehalis Basin by 40.1 Ma (this study). Slope mudstones and turbidites of the McIntosh Formation were deposited in deeper areas of the basins between subaerial volcanic highs.

Eventually, the middle and late Eocene (~48 to ~37 Ma) unconformity-bound sequence of marine sedimentary rocks prograded westward, transgressing the lower to middle Eocene (>~48 Ma) Crescent Formation forearc basement. Rocks of this paleogene sequence include the McIntosh Formation, Cowlitz Formation, and the Grays River Volcanics (Armentrout and Suek, 1985).

The middle to late Eocene Cowlitz Formation, composed of arkosic, micaceous deltaic/shelfal sandstones, prograded westward covering the deep-marine middle Eocene McIntosh mudstones and subsiding Tillamook Volcanics in northwest Oregon. The Cowlitz delta represents the marine equivalent of the largely non-marine coal-rich Skookumchuck Formation of the Chehalis basin, part of the extensive deltaic/coastal plain system of the Eocene Puget Group (Buckovic, 1979). The source areas of the micaceous arkosic sandstones of the Puget Group were granitic batholiths and metamorphic core complexes of the North American continent to the east, including the Idaho batholith. In the thesis area, the shallow marine Cowlitz Formation was overriden

by growing a Grays River basaltic high at 40.1 – 39.6 Ma. Continuing forearc tholeiitic basaltic volcanism (upper Grays River Volcanics) and Western Cascade calkaline arc volcanism (Goble Volcanics) occurred during and after deposition of the Cowlitz Formation (Phillips et al., 1989).

Unconformably overlying the late Eocene sequence in the forearc basin is a basal basaltic conglomerate, well developed along structural highs, grading upward into tuffaceous marine siltstone of the latest Eocene - Oligocene Lincoln Creek Formation (Keasy Formation of northwest Oregon) (Armentrout, 1987). This unconformity is the second major sequence boundary in southwest Washington (Armentrout, 1987).

Renewed tectonism in the early to middle Miocene is reflected in the angular unconformable relationship of many underlying Tertiary units to the overlying middle Miocene (~16 Ma) Columbia River Basalt flows (Grande Ronde basalt in thesis area). The Oregon and Washington Coast Ranges have been tilted and slightly folded from middle Miocene to the present as a result of active oblique subduction of the Juan de Fuca oceanic plate beneath the North American continental plate (Snavely, 1987).

METHODS OF INVESTIGATION

Two summers of field work (1999 and 2000) were spent measuring and describing the stratigraphic-section along Germany Creek (Plate II), collecting macro- and microfaunal assemblages and rock samples, paleomagnetic sampling of strata and volcanics, and mapping the geology of the thesis area. Detailed measurement and lithofacies description of the upper McIntosh, lower Cowlitz formations and the lower

Grays River Volcanics was conducted using a Jacob staff and Abney level along a 5.5 mile traverse of Germany Creek beginning at 46° 16.74' latitude and 123° 06.91' longitude; ending at 46° 19. 54' latitude and 123° 07.73' longitude. Additional subsurface stratigraphic data were gleaned from driller's log cutting descriptions of the Castle Rock Oil and Gas Company's Quigley No.1 well drilled in 1925. Detailed geologic mapping at 1:24,000 scale was aided by the use of Hampton Tree Farms logging road maps, 1:6000 scale ortho-corrected aerial photos and the Elochoman Lake, Abernathy Mountain, and Castle Rock U.S.G.S. 7.5-minute topographic maps.

A total of 138 samples were collected for analysis. Nine basaltic flows and dike localities and twenty-one sandstones and siltstones were collected for thin section petrography. Most sample locations were marked using a hand-held Garmin 12-channel GPS. Twenty-six molluscan fossil localities were collected for identification by Dr. Liz Nesbitt of the University of Washington Burke Museum, greatly enhancing the interpretation of depositional environments. Thirteen foraminifer samples were prepared and sent to Jeff Grieff of the Burke Museum and Dr. Weldon Rau, emeritus micropaleontologist, Washington Department of Natural Resources, for additional age and paleobaythymetry determination. Of these, seven were barren of foraminifer.

Thirty-nine sites along the Germany Creek section were sampled for magnetostratigraphic analysis. Three horizontally oriented samples were collected per site using simple hand tools. The samples were sent to Dr. Don Prothero of Occidental College, Los Angeles, California for analysis on a 2G cryogenic magnetometer at the paleomagnetics laboratory of the California Institute of Technology.

Nine lava samples were spatially oriented with a Brunton compass in outcrop and collected for magnetic polarity measurements using a portable fluxgate magnetometer in the lab. Fourteen basalts were analyzed for major and trace element geochemistry using a Rigaku x-ray fluorescence unit (XRF) and ICP by Dr. Peter Hooper at Washington State University, Pullman, through the assistance of Washington Department of Natural Resources. Two Grays River lava flows in depositional contact with shallow marine Cowlitz Formation, and two Grays River dikes along Germany Creek were prepared and submitted to Dr. Robert Duncan of the College of Oceanic and Atmospheric Science, Oregon State University, Corvallis for Ar^{40}/Ar^{39} incremental-heating age dating using a laser-fusion mass spectrometer.

Petrographic analyses of the McIntosh and Cowlitz Formations sandstones included description of twenty-one arkosic and mixed arkosic-volcanic thin sections. Four arkosic sandstones were K-feldspar stained for sandstone modal compositions. These four sandstones were also impregnated for visual porosity estimates. Four hundred points were counted and categorized into 19 variables for these samples. Identification of clay minerals forming the matrix of one sandstone sample was accomplished using a Phillips Automated X-ray diffractometer (XRD) under the supervision of Dr. Reed Glasmann of the Geosciences Department, Oregon State University. Scanning electron microscopy was also conducted on this sample under the direction of Al Soeldner at the Botany Department, OSU to determine the diagentic history of the sandstone.

Additionally, biostratigraphic information was used from earlier studies of the area, including five foraminifer localities collected by Livingston (1966). Dr. Paul

Hammond, emeritus professor of Portland State University, also supplied major and minor element XRF tuff geochemistry results from two sample sites within the thesis area. Major oxide and minor trace element XRF geochemistry from the basalt at Castle Rock (Tia) was provided from Phillips et al. (1989).

STRATIGRAPHY AND LITHOFACIES OF THE UPPER MCINTOSH AND LOWER COWLITZ FORMATIONS

PREVIOUS WORK

The type McIntosh Formation located near McIntosh Lake eight kilometers north of Tenino, Washington, consists of several hundred meters of dark-gray tuffaceous siltstone and mudstone (Snavely et al., 1951). Ray Wells (1981), modifying a two member convention for the middle Eocene McIntosh Formation introduced by Pease and Hoover (1957), remapped the McIntosh Formation in the northern and eastern Willapa Hills. The two informal members consist of (1) a lower member of arkosic to basaltic sandstone and siltstone, and (2) an upper member of siltstone and some thin-bedded sandstone (Wells, 1981). In the Ryderwood area, five km north of the thesis area, Wells (1981) mapped a massive to cross-bedded, micaceous arkosic sandstone in the basal part of the upper member of the McIntosh Formation.

Near the type area of the McIntosh Formation, ~300 m of pyroclastics, flow breccia and subaerial basaltic andesite and andesite flows of the Northcraft Formation overlie and interfinger with the McIntosh Formation (Snavely et al., 1958; Payne, 1998). Both the McIntosh and Northcraft formations are overlain in local angular unconformity by the middle to upper Eocene coal-rich Skookumchuck Formation (Snavely et al., 1951; Snavely et al., 1958). Cyclic shallow-marine and sandy, coal-bearing coastal-plain facies of the Skookumchuck Formation may be correlative with the dominantly shallow marine sandstone facies of the type Cowlitz Formation in southwest Washington (Flores and Johnson, 1995; Payne, 1998).

C. E. Weaver (1912, 1937) defined the type section Cowlitz Formation to include 4,300 feet (1292 m) of fossiliferous sandy siltstone and coal exposed in Olequa Creek and the Big Bend fossil locality of the Cowlitz River (Figure 1, 2). Henriksen (1956) expanded the definition of the Cowlitz Formation to include a deep-marine mudstone and minor arkosic sandstone, the "Stillwater Creek Member", along with the original "Olequa Creek Member" in his mapping of the area. Ray Wells (1981) remapped the "Stillwater Creek Member" as McIntosh Formation and restricted the Cowlitz Formation to Weaver's original definition of the formation, consisting of friable, micaceous arkosic sandstone interbedded with carbonaceous siltstone, volcanoclastics and sub-bituminous coal beds (Wells, 1981).

Payne (1998) proposed an informal lithostratigraphic division of five units in the 1,292 m (~4300 ft.) thick Cowlitz Formation at the type locality, north of the thesis area~ 15 km (Figure 1). The basal unit consists of several prograding, wave-dominated shoreface, lithic-arkosic sandstone parasequence sets and associated coal-bearing delta plain facies associations. Unit 2 is defined by thickening and coarsening-upward storm-dominated, hummocky-bedded shelf to delta-front arkosic sandstone parasequence sets, interbedded with minor middle and outer shelf siltstone and mudstone. Unit 3 is in unconformable contact with the shallow marine unit 2, and consists of an incised valley fill of fining upwards subtidal, intertidal, and supratidal facies associations. A conformably overlying fourth unit consists of wave-dominated shoreface arkosic sandstone and offshore bioturbated mudstone facies. Unit 5 unconformably overlies unit

4 and consists of deep marine laminated siltstone, turbidites, and submarine channel sandstones (Payne, 1998).

Livingston (1966), in reconnaissance geologic mapping of the Longview-Kelso area for ferruginous bauxite potential, mapped the Germany Creek – Abernathy Mountain part of the thesis area at 1:62,500 scale. He mapped the contact with the Cowlitz Formation and overlying Grays River Volcanics (mapped then as Goble Volcanics), and showed repetition of Cowlitz Formation along a northwest-trending fault in Sec. 1, T 9 N, R 4 W (Plate I). Information from Livingston's (1966) molluscan and foraminifer assemlages are incorporated into the thesis, and aided in defining the poorly exposed Lincoln Creek Formation in the thesis area.

Although Livingston (1966) did not map any Lincoln Creek Formation in the thesis area, he reported a Refugian age benthic foraminifer locality at the SE ¼ of Sec. 5, T 9 N, R 4 W. Livingston interpreted the tuffaceous siltstone to be interbeds within the Goble (Grays River) Volcanics. Wells (1981) mapped this tuffaceous siltstone as Lincoln Creek Formation. The Lincoln Creek Formation was originally defined from exposures of massive, concretionary, tuffaceous siltstone and minor fine-grained sandstone at Lincoln Creek, west of Centralia (Snavely et al., 1958) (Figure 1).

AGE DETERMINATION OF STRATA

Upper McIntosh Formation

Rau (1958) assigned strata of the upper McIntosh Formation exposed along Stillwater Creek (~5 km north of the study area) to the lower to middle Narizian stages (~43 to ~39 Ma) (Figure 3). The uppermost 180 meters, Rau restricted to the late Narizian stage based on the presence of the *Bulimina schenki-Plectofrondicularia cf. P. jenkinsi* bathyal foraminifer zone. The late Narizian corresponds to the middle to late Eocene, about 39 Ma to 35.3 Ma (Berggren et al., 1995) (Figure 3). In a foraminifer study of the upper McIntosh Formation (Stillwater Creek Member, Henriksen, 1958), Yett (1979) also determined the sections to be late Narizian in age. The *Bulimina schenki-Plectofrondicularia cf. P. jenkinsi* assemblage is also found in the deeper water facies of the Skookumchuck Formation in upper to middle bathyal water depths (Rau, written communication, 2000). A zircon fission-track date of 39.2 ±2.7 Ma was reported by Brandon and Vance (1992, in Flores and Johnson, 1995) from a tuff bed in coal deposits of the Skookumchuck Formation 30 km north of the thesis area.

Three picked foraminifer samples of the upper McIntosh Formation from Germany Creek were sent to Jeff Grieff of the University of Washington Burke Museum and Weldon Rau for foraminifer species identification, paleobathymetry estimation and age determination. Samples 914F, 914I, and 916D contain bathyal assemblages identified by W. Rau as characteristic of his *Bulimina schenki-Plectofrondicularia cf. P.*

jenkinsi zone of the upper part of the Narizian Stage (~39 to 35.3 Ma) (Rau, written communication, 2000). However, based on integrating dated lava flows overlying the Germany Creek sections with section magnetostratigraphy, the upper McIntosh Formation of the study area must be older than ~39 to 40 Ma. The upper McIntosh bathyal siltstone and subtidal bar sandstone of Germany Creek best correlates with Chron 19r (41.5 – 42.5 Ma). This finding places the *Bulimina schenki-Plectofrondicularia cf. P. jenkinsi* assemblage in the early Narizian, pushing the first appearance of the zone back from about 39 Ma to 41.5 – 42.5 Ma (see Magnetic Stratigraphy section). The unconformable contact between the upper McIntosh and Cowlitz formations correlates to Chron 19n (>41.2 – <41.5 Ma).

Lower Cowlitz Formation

Yett (1979) determined that foraminifer from the Olequa Creek Cowlitz Formation type-section locality to be late Narizian in age. Benthic foraminifer identified by Weldon Rau from the Cowlitz Formation of the South Germany Creek section were assigned a shallow, inner shelf water depth of late Narizian age (this study, sample GCBM). The lower Cowlitz Formation magnetostratigraphy best correlates to Chron 18r (40.1 – 41.2 Ma, slightly older than the late Narizian) and the lower part of Chron 18n (38.4 – 40.1 Ma) (see Figure 14).

Irving et al. (1996) obtained an Ar^{40}/Ar^{39} age of 38.9 ±0.1 Ma by fusion of potassic oligoclase grains from a 1.5 m thick tuff bed in Olequa Creek of the middle Cowlitz Formation, unit 3 of Payne (1998).

Figure 3. Southwest Washington to northwest Oregon stratigraphic correlation chart. Modified from Payne (1998) based on magnetic polarity results from this study. (1 Berggren et al., 1995; 2 McDougall, 1996 *in* Payne, 1998; 3 Prothero and Armentrout, 1985; 4 Bukry, 1975; 5 Robertson, 1997; 6 Phillips, 1987; 7 Evarts, 1998 *in* Payne, 1998; 6 Flores and Johnson, 1995; 9 Schasse, 1987.)

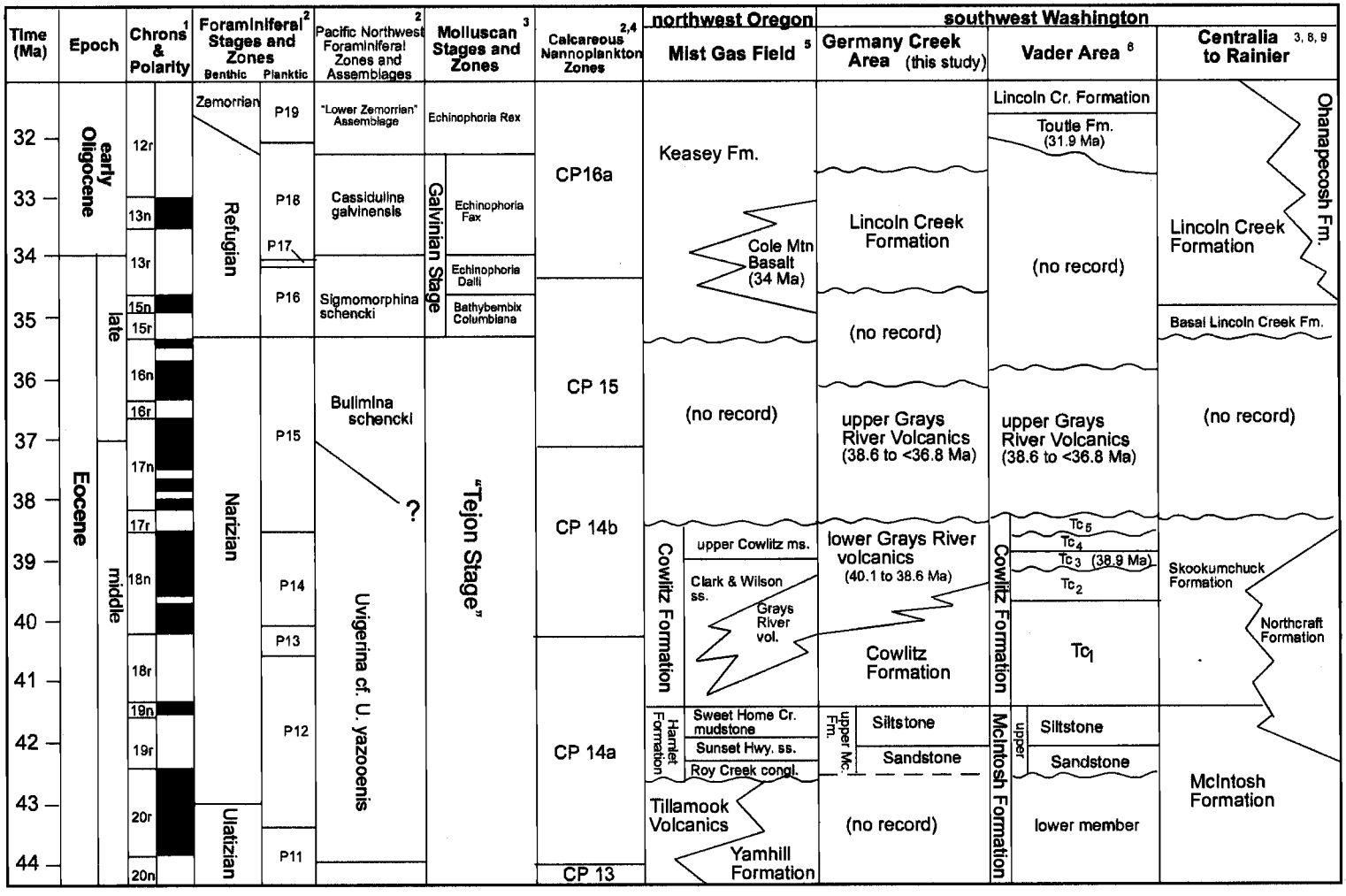
Time (Ma)
Epoch
Chrons & Polarity
Foraminiferal Stages and Zones
Benthic
Planktic
Pacific Northwest Foraminiferal Zones and Assemblages
Molluscan Stages and Zones
Calcareous Nannoplankton Zones
northwest Oregon
Mist Gas Field
southwest Washington
Germany Creek Area (this study)
Vader Area
Centralia to Rainier
32
33
34
35
36
37
38
39
40
41
42
43
44
Eocene
Oligocene
early
late
middle
12r
13n
13r
15n
15r
16n
16r
17n
17r
18n
18r
19n
19r
20r
20n
Zemorrian
Refugian
Narizian
Ulatizian
P19
P18
P17
P16
P15
P14
P13
P12
P11
"Lower Zemorrian" Assemblage
Cassidulina galvinensis
Sigmomorphina schencki
Bulimina schencki
Uvigerina cf. U. yazooenis
Echinophoria Rex
Galvinian Stage
Echinophoria Fax
Echinophoria Dalli
Bathybembix Columbiana
"Tejon Stage"
CP16a
CP 15
CP 14b
CP 14a
CP 13
Keasey Fm.
Cole Mtn Basalt (34 Ma)
(no record)
Cowlitz Formation
upper Cowlitz ms.
Clark & Wilson ss.
Grays River vol.
Hamlet Formation
Sweet Home Cr. mudstone
Sunset Hwy. ss.
Roy Creek congl.
Tillamook Volcanics
Yamhill Formation
Lincoln Creek Formation
(no record)
upper Grays River Volcanics (38.6 to <36.8 Ma)
lower Grays River volcanics (40.1 to 38.6 Ma)
Cowlitz Formation
upper Mc. Fm.
Siltstone
Sandstone
(no record)
Lincoln Cr. Formation
Toutle Fm. (31.9 Ma)
(no record)
upper Grays River Volcanics (38.6 to <36.8 Ma)
Cowlitz Formation
Tc5
Tc4
Tc3 (38.9 Ma)
Tc2
Tc1
McIntosh Formation
upper
Siltstone
Sandstone
lower member
Ohanapecosh Fm.
Lincoln Creek Formation
Basal Lincoln Creek Fm.
(no record)
Skookumchuck Formation
Northcraft Formation
McIntosh Formation

Figure 3.

~44 Ma to ~37 Ma (Rarey, 1985) (Figure 3). Molluscan fauna of the Cowlitz Formation correspond to the "Tejon" molluscan stage of California (Nesbitt, 1995) (Figure 3).

Grays River Volcanics

In the thesis area, two Grays River subaerial lava flows in depositional contact with the lower Cowlitz Formation have been Ar^{40}/Ar^{39} dated. Sample GC-1 from the base of the Grays River Volcanics and the top of the 318-m thick South Germany Creek section yielded an Ar^{40}/Ar^{39} whole rock plateau age of 40.09 ±0.34 Ma. Sample GC-2 from the base of the Grays River Volcanics and the top of the 733-m thick North Germany Creek section yielded an Ar^{40}/Ar^{39} whole rock plateau age of 39.35 ±0.36 Ma. These age dates allowed the magnetic polarity results of both the measured sections to be correlated to the magnetic time scale of Berggren et al. (1995) (Figure 3). The upper age of the lower Grays River Volcanics is constrained by unconformably overlying upper Grays River lava flows dated at ~38.6 to 36.8 Ma from southern Abernathy Mountain and Bebe Mountain (Payne, 1998) (Plate I, III). Eight kilometers to the south of the thesis area, an Ar^{40}/Ar^{39} whole rock plateau age of 40.3 ±0.3 Ma from a Grays River intrusion in the Cowlitz Formation of Coal Creek was determined by Irving et al. (1996).

Lincoln Creek Formation

Age determinations of the Lincoln Creek Formation rely on molluscan and foraminifer age diagnostic assemblages. The Lincoln Creek Formation in Olequa Creek, sixteen kilometers north of the thesis area, contains molluscan fossil assemblages referred

to the middle Galvinian (~33.5 Ma) stage of Armentrout (1975). Benthic foraminifer assemblages from the Olequa Creek section have been assigned to the Refugian (latest Eocene - early Oligocene) *Sigmomorphina schencki* zone of Rau (~35.3 to ~33.8 Ma) (Yett,1979). Livingston (1966) reports a benthic foraminifer sample (sample 612, Plate I, Appendix) identified by Rau as equivalent to the *Sigmomorphina schencki* assemblage of Refugian age from a tuffaceous siltstone in the thesis area. This unit has been mapped as Lincoln Creek Formation in this study and by Wells (1981). The Narizian/Refugian boundary has been placed at about 35.3 Ma by Berggren et al. (1995).

UPPER MCINTOSH FORMATION

Distribution

The upper McIntosh Formation crops out in the northwestern corner of the thesis area and is described in the base of the North Germany Creek section, section interval 39 – 32 (index map, Plate II). Outcrops beyond the creek bed are rare. Exposures were nearly continuous in the upper reaches of Germany Creek in the summer of 1999 when the section was measured, but a minor landslide covered interval 38 – 36 in the spring of 2000. About twenty-five meters of the section was projected in from the west fork of Germany Creek at interval 35 (index map, Plate II), due to poorer exposures along the main (east) fork of Germany Creek.

The upper McIntosh Formation has not previously been recognized in the study area (Livingston, 1966; Wells, 1981). This is likely explained by its poor outcrop exposure and the presence of 132 meters of shallow marine arkosic sandstone at the base of the 286 meter thick section of upper McIntosh Formation exposed in Germany Creek, leading previous authors to place the unit in the Cowlitz Formation. However, a relatively thin 162 meters of silty foraminifer-bearing mudstone and minor thin-bedded turbidites overlying the basal arkosic sandstone provides evidence for naming this unit the upper McIntosh Formation. This overlying silty mudstone contains late Narizian middle and upper bathyal foraminifers associated with distal turbidite facies consistent with a middle and upper bathyal depositional environment. On the basis of lithology and interpreted depositional environment, the unit is more consistent with the McIntosh

Formation siltstones and mudstones than with the Cowlitz Formation. Further, the basal sandstone consists of tidally-bedded lowstand deposits and shoreface strata in a retrogradational parasequence set. These characteristics are reported in the basal arkosic sandstone of the upper McIntosh Formation on regional strike, ~6 km to the north of the Germany Creek exposure by Payne (1998). For a more complete discussion of the regional stratigraphy and correlation of the Germany Creek sections, see pg 148.

Upper McIntosh Formation Sandstone Unit Lithofacies

The only continuous section of upper McIntosh sandstone found in the thesis area occurs in the NW ¼ of Sec. 25, T 10 N, R 4 W (Plate I, index map Plate II). The 132-m thick basal sandstone of the upper McIntosh Formation is 51% exposed with a sandstone to siltstone ratio of 1:2 (Plate II). The bottom 52 meters of the section is dominated by tidally-formed facies and sedimentary structures. This part of the section consists of two recognizable coarsening- and thickening-upward tidally-formed parasequences (Figure 4). The overlying 80 meters of the upper McIntosh sandstone unit are dominated by wave-formed shoreface facies sedimentary structures.

The lowest exposure of the measured section in Germany Creek is an 80-cm bed of micaceous carbonaceous mudstone with minor carbonaceous plant fragments and ripple-laminated heterolithic siltstone (~10%). This mudstone-dominated bed grades

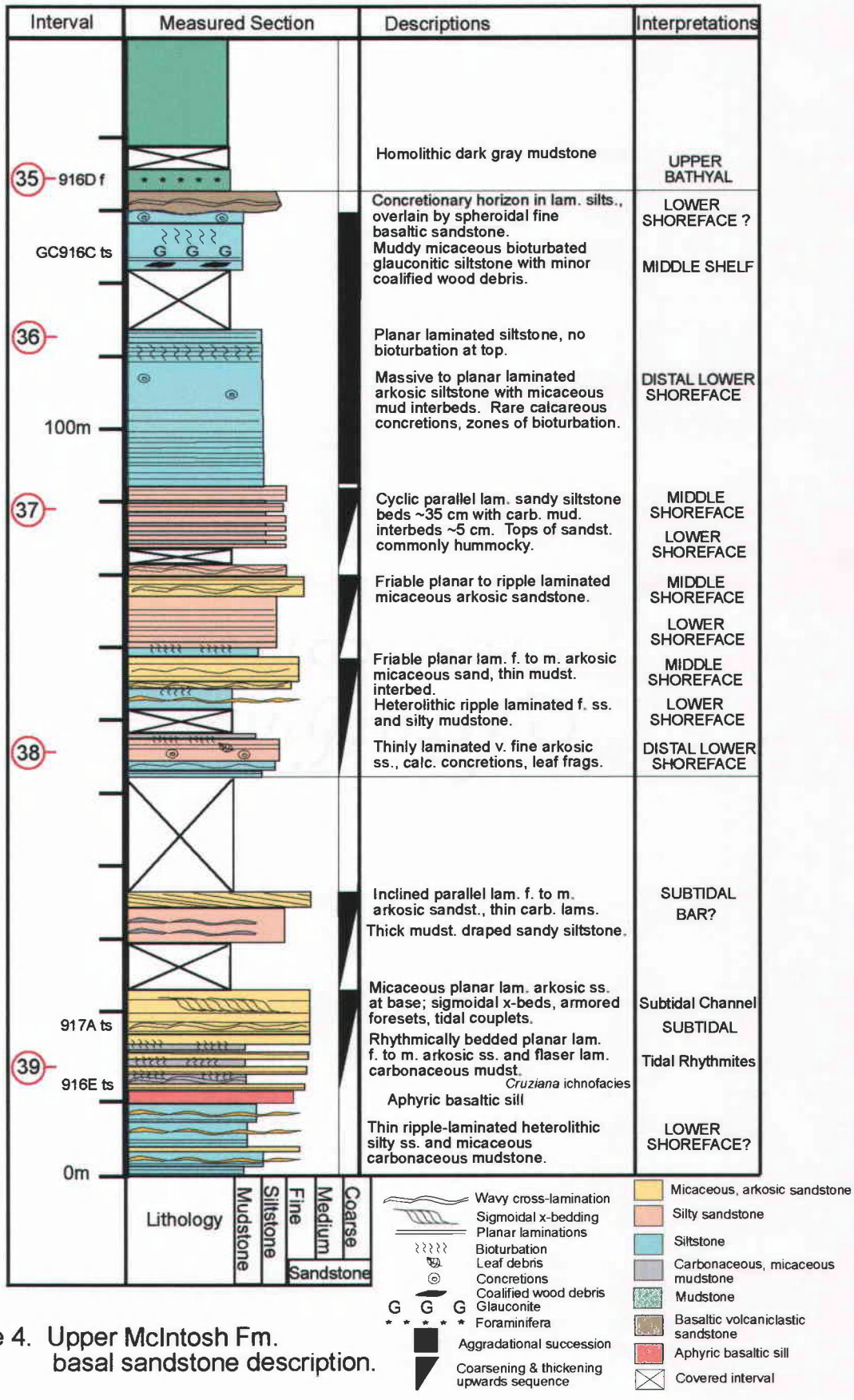

Figure 4. Upper McIntosh Fm. basal sandstone description.

evenly into a heterolithic laminated siltstone (~50%), with very thin ripple-laminated micaceous carbonaceous mudstone and a few fine- to medium-grained planar laminated friable arkosic sandstone beds (~30 cm). The interval is 9.9 meters thick. Above this interval is a 2.3-meter thick Grays River aphyric basaltic sill with baked upper and lower contacts and rare vesicles near the upper contact.

Above the sill is a 6.4-meter thick interval consisting of two repetitions of planar to ripple-laminated siltstone and highly carbonaceous laminated mudstone beds, and bioturbated fine- to medium-grained arkosic sandstone beds (Figure 5). The lowest beds of the cycle consist of baked finely laminated arkosic siltstone and carbonaceous mudstone, grading to planar laminated siltstone containing micaceous carbonaceous laminae (~1.8 m). A 10-cm thick overlying bed of progressively thicker and darker carbonaceous laminae is abruptly overlain by a planar-laminated fine- to medium-grained arkosic sandstone (7.5 cm thick)(thin section 916E). This sandstone has a bioturbated gradational upper contact (*Cruziana* ichnofacies) with ripple- to flaser-bedded carbonaceous mudstone and siltstone, marking the beginning of the next cycle (Figure 5).

Abruptly overlying the dark, carbonaceous mudstone of the second cycle is a vertically-stacked planar-laminated fine-grained arkosic sandstone bed (~35 cm), bounded at the top by a thin (2 cm) wavy carbonaceous mudstone lamina (Figure 5). Above this interval, a mud-draped ripple-laminated arkosic sandstone couplet (5 cm) overlies a planar laminated arkosic sandstone bed (25 cm) (thin section 917A). Overlying the carbonaceous mud couplets is a 2.3-meter thick sigmoidally cross-bedded, medium-grained arkosic sandstone with micaceous carbonaceous mudstone-draped

foresets (Figure 5). Other sedimentary structures include mudstone rip-up clasts, contorted cross-bedding, and tidal bundles (Figure 5).

Stratigraphically above this sequence is a 6.7-meter thick interval composed of a rippled silty arkosic sandstone bed with thick carbonaceous mudstone-drapes (flasers) overlain by an inclined parallel laminated fine- to medium-grained arkosic sandstone. This is the last interval in the upper McIntosh sandstone unit that consists of tide-dominated sedimentary structures.

Fifteen meters of cover separate the underlying tide-dominated parasequences from the overlying wave-dominated shoreface parasequences. Repetition due to faulting and drag-folding of the section occurs at this location (NW ¼ of Sec.25, T 10 N, R 4 W). Approximately 22 meters of section were repeated (Plate II, interval 38). The wave-dominated upper part of the upper McIntosh Formation sandstone unit is 80 meters thick. It consists of at least three coarsening- and thickening-upward parasequences and one aggradational sequence.

At section interval 38 (Plate II), a coarsening-upward parasequence consists of thinly laminated muddy siltstone grading upwards into bioturbated silty sandstone with carbonaceous leaf fragments (3.6 m), interbedded at the top with 3-4 cm thin carbonaceous mudstone beds. Above this interval is a 7.6-m coarsening- and thickening-upward succession, beginning with a heterolithic ripple-laminated siltstone and mudstone, that becomes more bioturbated at the top. This interval is overlain by a 4.2-m friable, planar-laminated fine- to medium-grained micaceous arkosic sandstone. The next 11-meter thick parasequence is defined by a sharp basal contact of thin carbonaceous

siltstone above an underlying friable, planar-laminated, arkosic sandstone, representing a marine flooding surface. The parasequence coarsens upward to planar-laminated silty sandstone and is capped by a 2.3-m thick friable, planar to ripple-laminated micaceous arkosic sandstone.

At section interval 37 (Plate II), a long, well-exposed logging road cut parallel to Germany Creek was measured and described in the summer of 1999. This section has since failed, causing a minor landslide that blocked the mainline road in the summer of 2000. The toe of the slide has redirected the flow of the east (main) fork of Germany Creek. The interval begins with a 1.1 meter thick heterolithic siltstone to very fine micaceous arkosic sandstone (80%) and thin discontinuous, bioturbated micaceous mudstone laminae (20%). Overyling the heterolithic facies is a 6.8-meter thick succession of at least eleven cyclic, planar-laminated, very fine-grained arkosic sandstone beds, 22-50 cm thick (section interval 37, Plate II, Figure 4). The sandstone beds are separated by 5-7 cm thick light gray, wavy-laminated micaceous mudstone. The tops of the buff-colored sandstone beds are commonly hummocky to planar laminated (Figure 5).

This "cyclic sandstone" interval is overlain by a 21-meter thick massive to planar-laminated siltstone. At its base, the interval contains minor mudstone-draped siltstone, lenticular bedding and very fine-grained rippled sandstone (3.6 m). A thinly laminated to massive siltstone (12.4 m) overlies the lower facies, followed by a calcareous concretionary zone overlain by a mottled, micaceous siltstone bed. The uppermost 1.9 meters of the interval contains planar laminations and no bioturbation (section interval 36, Plate II, Figure 4).

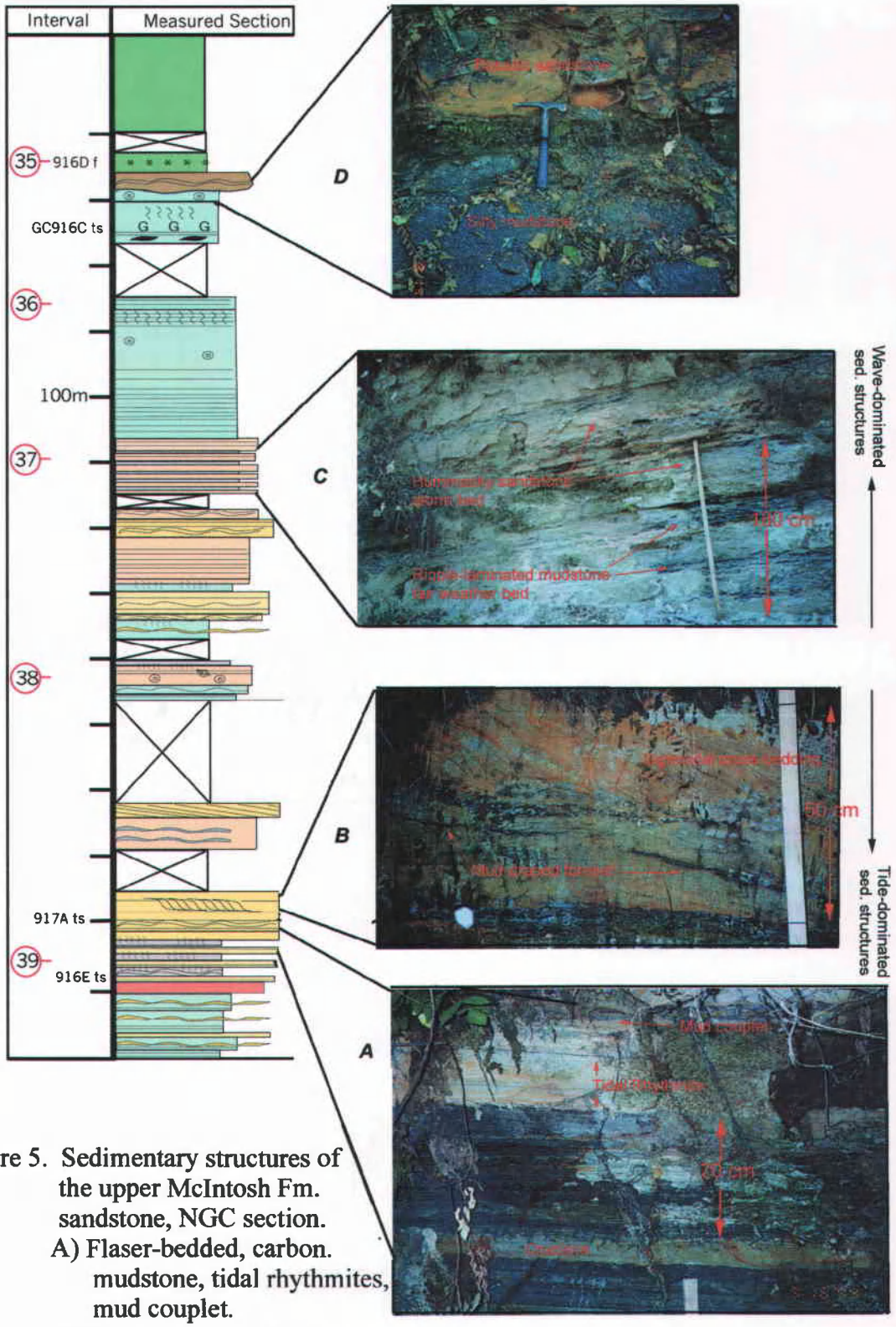

Figure 5. Sedimentary structures of the upper McIntosh Fm. sandstone, NGC section.
A) Flaser-bedded, carbon. mudstone, tidal rhythmites, mud couplet.
B) Sigmoidal cross-bedding, mud drapes.
D) Silty mudstone overlain by basaltic sandstone.

Due to poor exposures of the section in the east fork of upper part of Germany Creek, the section between intervals 36 and 35 is projected in the section from the west fork (see index map, Plate II). Exposures of interval 36 to 35 begin with a muddy micaceous, bioturbated, medium gray glauconitic siltstone (thin section GC916C), containing pieces of coalified woody debris (3-5 cm long). The 6.5-m thick siltstone displays chippy weathering and is thinly bedded (~30 cm). The section grades upward into an ellipsoidal calcareous concretionary horizon (Figure 5) and is abruptly overlain by a spheroidally weathered dark brown fine-grained basaltic sandstone (2.2 m thick) (Figures 4, 5).

Upper McIntosh Formation Siltstone Unit Lithofacies

The lower shoreface re-worked, fine-grained basaltic sandstone of the uppermost part of the upper McIntosh Formation basal sandstone unit is abruptly overlain by deep marine dark homolithic blocky mudstone. The contact and abrupt change in water depth between the two units represents the uppermost flooding surface of the upper McIntosh sandstone in Germany Creek. This contact also corresponds to the lowest part of the 163-m thick upper McIntosh siltstone. The upper McIntosh siltstone is described from the North Germany Creek section intervals 35 – 32, Plate II (123 meters to 286 meters). The section is 65 % exposed along the banks of Germany Creek from the NW ¼ of Sec. 25 to the S ½ of Sec. 36, T 10 N, R 4 W (Plate I, II). The section is dominated by gray- to

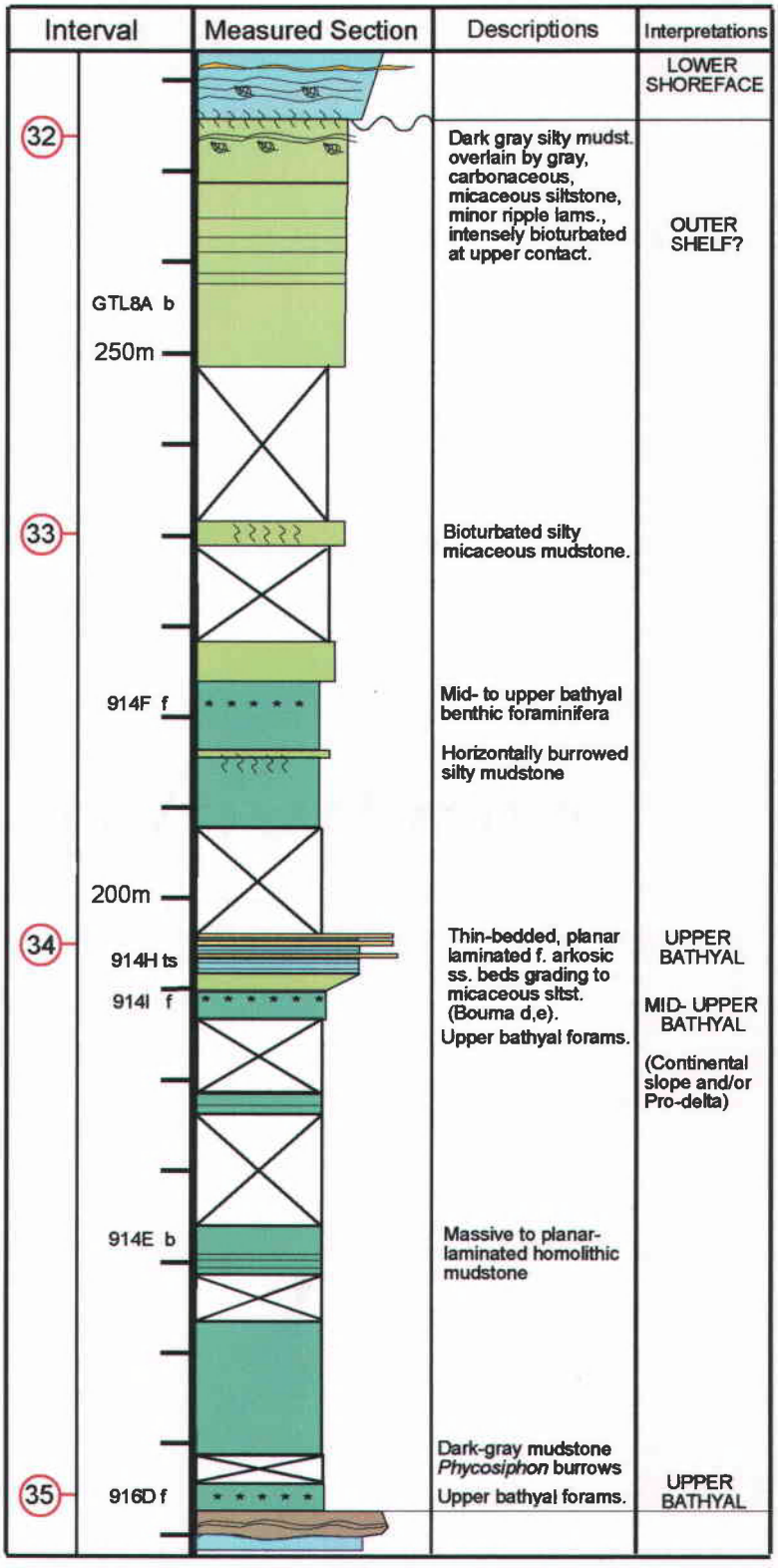

Figure 6. Upper McIntosh Formation siltstone measured section description and interpreted depositional environments (10 meter intervals, see Figure 4 for symbols and key).

Silty mudstone

dark-gray deep marine silty mudstone and siltstone, with a minor interval at least 6.6 meters thick (section interval 33) of thinly bedded fine-grained arkosic turbidite sandstone and silty mudstone.

Section interval 35 to 34 is composed of dark-gray, bathyal benthic foraminifer-bearing mudstone and minor silty mudstones (Plate II, Figure 6). Hook-shaped deep marine *Phycosiphon* burrows are present in locally bioturbated horizons. Bedding is massive to planar-laminated. Numerous recent shallow landslides have exposed this stretch of section along Germany Creek.

Even, thin-bedded, parallel laminated fine-grained arkosic sand beds (3-6 cm) (thin section 914H) with sharp bottom contacts that grade upward into micaceous siltstone intervals (turbidite d,e divisions) are exposed at interval 34 (Plate II, Figure 6, 7). The micaceous siltstone intervals are 10 to 20 cm thick, with *Phycosiphon* burrows (thin section 914H). At its base, this unit grades upward to a dark upper bathyal mudstone (foraminifer sample 914I). The upper part of the 6.6-meter section is not exposed.

Between section intervals 34 and 35, at meter 221(Plate II, Figure 6) a dark gray foraminifer-bearing massive mudstone is exposed. Further upsection (interval 33), zones of bioturbation dominated by horizontal burrows become more common in silty mudstones. Numerous thin (< 1-m thick), vertical basaltic dikes act as walls, holding-up the nearly-flat lying, incompetent silty mudstones along this interval of the Germany Creek streambed.

The uppermost part of the upper McIntosh siltstone unit (interval 32) contains at least 22 meters of dark, laminated, micro-micaceous silty mudstone gradationally overlain by a massive to ripple-laminated gray carbonaceous siltstone (~4 m thick, from meters 280 – 284, Plate II, Figure 6). The carbonaceous siltstone is in turn abruptly overlain by an intensely bioturbated, fine-grained heterolithic ripple-laminated arkosic sandstone (40%) and micaceous carbonaceous mudstone (60 %) of the lowest Cowlitz Formation.

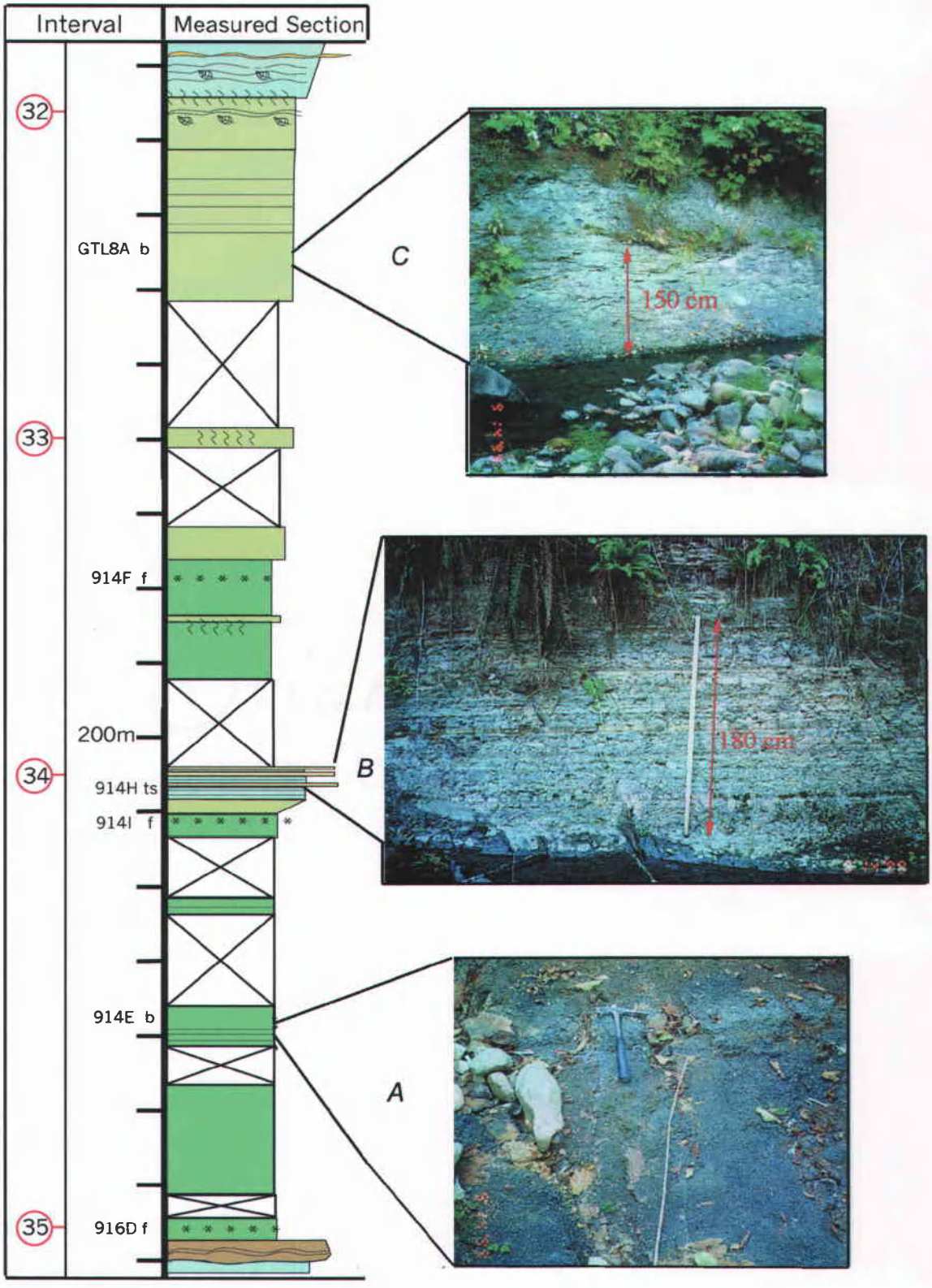

Figure 7. Sedimentary structures of the upper McIntosh Fm. siltstone (NGC).
A) Dark gray, foraminifer-bearing homogeneous mudstone.
B)Thin rhythmically-bedded turbidite siltstone and mudstone.
C) Massive to parallel laminated light gray shelfal muddy siltstone.

Depositional Environments

Upper McIntosh Formation sandstone unit

The 52-meter thick lowest interval of the upper McIntosh sandstone contains at least two coarsening-upwards, tide-dominated, subtidal bar or shoal facies associations (section interval 39, meters 9-37, Plate II, Figure 5). The two coarsening-upwards facies associations represent the following depositional environments and lithofacies: (1) distal subtidal bars (vertically-stacked tidal rhythmites and flaser-bedded sandstone, siltstone and carbonaceous mudstone, *Cruziana* ichnofacies), and (2) subtidal-channel megaripple cross-bedded (sigmoidal and tangential cross-beds), mud-couplet and mudstone-draped cross-bedded arkosic sandstone (Figures 4, 5). The *Cruziana* ichnofacies (Figure 5) can occur in subtidal or sublittoral environments, in moderate energy settings (Pemberton et al., 1992). A mud couplet indicates the presence of two slackwater stages during a flood-ebb cycle. This feature is characteristic of the subtidal zone (Nio and Yang, 1991). These facies are interpreted to have formed on prograding tidal sandbars, perhaps along the delta front of a tide-dominated delta prograding into an estuary, or a sandy estuary mouth.

However, the lowest 9 meters of the interval (North Germany Creek section, Plate II) consist of wave-rippled siltstones and interbedded micaceous mudstones that may represent the lower- to middle-shoreface depositional environment. The contact between the underlying wave-rippled facies and the overlying subtidal facies is obscured due to intrusion and baking by an aphyric Grays River basaltic sill at or next to the contact. Due

to the juxtaposition of lower- to middle-shoreface deposits directly underlying the subtidal deposits, a sequence boundary may exist between the units.

Van Wagoner and others, (1992), described a similar association in the Cretaceous (Campanian) Prince River Formation from the Book Cliffs of Utah. In the lower part of the Sego member of the Prince River Formation, wave-rippled siltstones and interbedded mudstones below a sequence boundary are overlain by thin, fine-grained, current-rippled sandstones with abundant interbedded clay drapes and thin layers of bioturbation. The sequence boundary generally is directly overlain by a lag of red clay clasts. The upper sandstone beds gradually thicken upward into fine- to medium-grained, sigmoidal cross-bedsets up to 1-m thick, with clay drapes on the foreset lamina (Van Wagoner et al., 1990). These Cretaceous estuarine sandstones represent a lowstand systems tract during the early stages of a relative sea level rise, filling an incised valley on the continental shelf.

Alternatively it is possible that the underlying rippled siltstones and micaceous mudstones are the prodelta basinward equivalents of prograding medium-grained estuarine sandstones and are conformable with the overlying estuarine sandstones (Van Wagoner et al., 1990). In this case, the sequence boundary would a distal correlative conformity of a proximal incised-valley unconformity (Van Wagoner et al., 1992). However, lower-shoreface, hummocky-bedded sandstones are not lateral-facies equivalents of estuarine strata (Van Wagoner et al., 1992). Due to lack of exposure of the units underlying the ripple-bedded siltstones, adequate facies associations of the interval are not available to further refine the identification of the depositional environment

(either normal marine lower shoreface or tide-dominated prodelta deposits). It is possible that the tide-dominated deltaic units, if conformably overlying the shoreface rippled siltstones, are part of a highstand system tract tide-dominated delta extending seaward onto a regressive shelf.

Overlying the tide-dominated facies associations at interval 38 (Plate II, Figure 4) are three wave-dominated coarsening- and thickening-upward shoreface parasequences and possibly one aggradational sequence. The contact between the lower 52-m thick tide-dominated interval and the upper 80-m thick wave-dominated interval is covered. Inferred depositional environments and lithofacies associations include: (1) distal lower shoreface (thinly laminated very fine-grained arkosic sandstone and interbedded micaceous mudstone), (2) lower shoreface (heterolithic ripple-laminated fine-grained arkosic sandstone and silty mudstone) and (3) middle shoreface storm and fair-weather beds (friable planar to ripple-laminated micaceous arkosic sandstone, hummocky cross-stratified fine-grained arkosic sand, ripply bioturbated silty carbonaceous mudstone).

Section interval 38, (meters 53 to 81, Plate II, Figure 4) consists of two progradational lower to middle shoreface parasequences capped by friable planar to ripple-laminated fine-grained arkosic sandstone. The sandstone capping the upper parasequence is slightly thinner and is in turn overlain by a finer and thinner bedded coarsening- and thickening-upwards sequence of lower to middle shoreface storm and fair-weather mudstone beds ("cyclic sands", Figure 5). Abruptly overlying the storm and fair-weather bed parasequence (section interval 37) is a uniform grain-size aggradational sequence of massive to planar laminated siltstone. This parasequence stacking pattern

defines a retrogrational parasequence set of a transgressive systems tract (Van Wagoner, 1992).

Together, the tide-dominated parasequences of the lower part of the upper McIntosh sandstone unit and the shoreface parasequences of the upper part of the upper McIntosh sandstone unit most likely define a lowstand to transgressive systems tract progression. A tide-dominated delta is interpreted to have been deposited along a partially flooded embayment or incised valley on the shelf during the early stages of a sea level rise. As sea level continued to rise most of the shelf flooded, ending tide-dominated deposition and depositing wave-dominated lower and middle shoreface succesions across the flooded shelf (Van Wagoner et al., 1992).

Upper McIntosh Formation siltstone unit

The 163-meter thick bathyal mudstone and siltstone of the upper McIntosh Formation directly underlies the micaceous arkosic shoreface sequences of the Cowlitz Formation and abruptly overlies the upper McIntosh Formation lower shoreface sandy siltstones. The lowest part of the upper McIntosh Formation siltstone (interval 35) contains upper bathyal benthic foraminifers (Rau, written communication, 2000, sample 916D, Appendix A). The presence of small (1-3 mm) hook-shaped *Phycosiphon* burrows indicates some oxygenated bottom-water conditions in these deep-marine basinal mudstones (Payne, 1998). Glauconitic silty mudstones, extensive bioturbation, and

concretionary zones lying directly beneath this bathyal mudstone may indicate a starved shelf and formation of a condensed section through hemipelagic sedimentation.

About 50 meters above sample 916D (interval 34), multiple normal graded to massive very thin arkosic sandstone beds with sharp basal contacts grading to planar laminated silty mudstone at the top are interpreted as distal turbidites. Directly underlying the distal turbidite facies is a foraminifer-bearing mudstone interval of the *Bulimina schenki-Plectofrondicularia cf. P. jenkinsi* zone, indicating an upper bathyal water depth of deposition (Rau, written communication, 2000). Also in this assemblage was *Globigerina bulloides*, the only planktonic species found in the upper McIntosh siltstone in Germany Creek. Its presence indicates a depositional environment that was exposed to the open ocean (Grieff, written communication, 2000).

Between section intervals 34 and 33, another middle to upper bathyal foraminiferal assemblage (sample 914F, Appendix A) and chippy mudstone indicates hemipelagic muds and silts accumulated slowly in this deep-marine basin. Beginning at interval 33, a slight decrease in water depth may be indicated by the increased amount of silt and bioturbation in the upper McIntosh siltstonetone member of Germany Creek. This may suggest a more oxygenated depositional environment, such as the outer shelf. About 40 meters above interval 33, at interval 32, the siltstone is abruptly overlain by thin-bedded heterolithic fine arkosic sandstone and micaceous, carbonaceous mudstone of the sand-rich Cowlitz Formation.

LOWER COWLITZ FORMATION

Background

Following the work of others (Weaver, 1912, 1937; Wells, 1981), the Cowlitz Formation of the study area is restricted to shallow marine/deltaic facies associations of fossiliferous micaceous arkosic sandstone, interbedded carbonaceous siltstone, volcaniclastics and sub-bituminous coal beds. In order to determine the lithofacies, thickness, and stratigraphy of the Cowlitz Formation in the thesis area, stratigraphic sections were measured and described along Germany Creek, Monahan Creek and Arkansas Creek (Plate I).

Among these, the North Germany Creek section (Plate II) contains the thickest measured section of Cowlitz Formation in the study area at 374 meters with 65% exposure. The South Germany Creek section contains a correlative 241-meter thick section of Cowlitz Formation (Plate II) with 66% exposure. Both sections are conformably overlain by subaerial basaltic Grays River Volcanics lava flows that have been Ar^{40}/Ar^{39} dated (this study). The South Germany Creek section is overlain by a lava flow dated at 40.09 ±0.34 Ma. The North Germany Creek Cowlitz Formation section overlies the upper McIntosh Formation siltstone unit, which is overlain by a Grays River lava flow dated at 39.35 ±0.36 Ma (Plate II).

A 110-meter thick section of Cowlitz Formation micaceous arkosic sandstone and carbonaceous siltstone along Monahan Creek (NE ¼ of Sec. 12, T 9 N, R 3 W) was measured and described (Figure 11). However, this section with 51 % exposure was less

continuous than the Germany Creek sections due to a ~37-meter covered interval making accurate measurement difficult. An estimated 69-meter thick section of landslide exposed cliffs along Arkansas Creek (SW ¼ of Sec. 24, T 10 N, R 3 W) provided a continuous but relatively thin stratigraphic section. Other field exposures are mainly restricted to roadcuts and minor landslide scarps throughout the study area (outcrop localities are shown on Plate I).

Multiple prograding lower shoreface to upper shoreface and foreshore facies associations are common to all measured sections described in the thesis area. No coal was encountered. Facies associations are dominated by wave and storm influenced sedimentary structures such as oscillatory ripple-laminated siltstone overlain by friable hummocky and swaley bedded arkosic sandstone with interbedded micaceous arkosic siltstone. Tide-influenced sedimentary structures such as mud-draped ripples and mud-draped foresets are infrequently encountered. All 19 Cowlitz Formation molluscan fossil assemblages gathered from the measured sections and outcrops of the thesis area were identified by Dr. Elizabeth Nesbitt of the University of Washington Burke Museum as indicative of normal shallow marine depositional environments.

Based on matching lithofacies, similarities in thickness and stratigraphic position, the Cowlitz Formation sections from Germany Creek have a close lithologic correlation to Payne's (1998) informal lithostratigraphic unit 1A of the basal Cowlitz Formation type-section in Stillwater and Olequa Creek, roughly 10 km to the north. Payne's (1998) unit 1 consists of numerous prograding, wave-dominated shoreface, lithic-arkosic sandstone successions (unit 1A) and coal-bearing delta plain facies associations (unit 1B).

Although the Monahan Creek and Arkansas Creek sections are thinner, the strat exposed in those sections are also consistent with unit 1A prograding shoreface successions. This study uses the phrase "lower Cowlitz Formation" to describe the lithostatigraphic position of the 374-meter thick basal Cowlitz Formation of the thesis area. For a more complete discussion of the regional lithologic, magnetic and chronostratigraphic correlation of the study area Cowlitz Formation, see pg 148.

Contact with McIntosh Formation

The contact of the basal Cowlitz Formation with the underlying McIntosh Formation is exposed in the North Germany Creek section (Plate II) along an upper cliff face on the east bank of Germany Creek (S ½ of Sec. 36, T 10 N, R 4 W, Plate I) (Figure 7, 8). At the contact, a 4-meter thick mottled gray carbonaceous siltstone in the upper McIntosh formation grades from micaceous silty mudstone at its base up to a sharp, scoured contact with fine-grained heterolithic ripple-laminated micaceous carbonaceous mudstone (60%) and fine arkosic sandstone of the Cowlitz Formation (Figure 8). Minor submarine truncation of the upper McIntosh Formation siltstone, along with a basinward shift in facies from middle shelf mudstone below the truncation to lower shoreface heterolithic mudstone and sandstone above, indicates a sequence boundary separating the shoreface sequences of the Cowlitz Formation from the deep marine upper McIntosh Formation.

Lithofacies of the lower Cowlitz Formation

Germany Creek

The most continuous exposures of the lithofacies of the Cowlitz Formation in the study area occur in the North Germany Creek (NGC) and correlative South Germany Creek (SGC) measured sections (Figure 9) (Plate II). Eight lithofacies (a through h) recognized in the Cowlitz Formation in Germany Creek are: (a) massive silty mudstone (middle shelf), (b) interbedded carbonaceous mudstone and thin-bedded ripple-laminated micaceous silty sandstone (shelf to shoreface), (c) bioturbated ripple-laminated carbonaceous, micaceous siltstone (lower shoreface), (d) heterolithic fine-grained sandstone and carbonaceous, micaceous siltstone (lower to middle shoreface), (e) massive to hummocky cross-stratified medium-grained sandstone (middle shoreface), (f) planar-laminated medium-grained sandstone (upper shoreface to foreshore), (g) pebbly basaltic sandstone (wave-reworked volcaniclastic debris flow deposits and channelized sandstone), and (h) tangentially cross-bedded arkosic sandstone (distributary bar or channel).

The lowest coarsening- and thickening-upward 54-meter thick shoreface sequence described from the North Germany Creek section contains lithofacies b through f (Figure 8, section interval 32 – 30, Plate II). The bottom 17 meters of the sequence consists of progressively more thickly bedded and sandier, bioturbated (*Cruziana*), carbonaceous mudstone and wave ripple-laminated siltstone. (lithofacies b and d). Above this heterolithic facies association are 4-meters of massive light gray fine- to medium-grained micaceous arkosic sandstone and ellipsoidal (10-35 cm diameter) calcareous concretions

Figure 8. Lithofacies descriptions of prograding, wave-dominated shoreface successions of the basalCowlitz Formation and unconformable contact (sequence boundary) with the shelf to upper bathyal upper McIntosh Formation siltstone member.

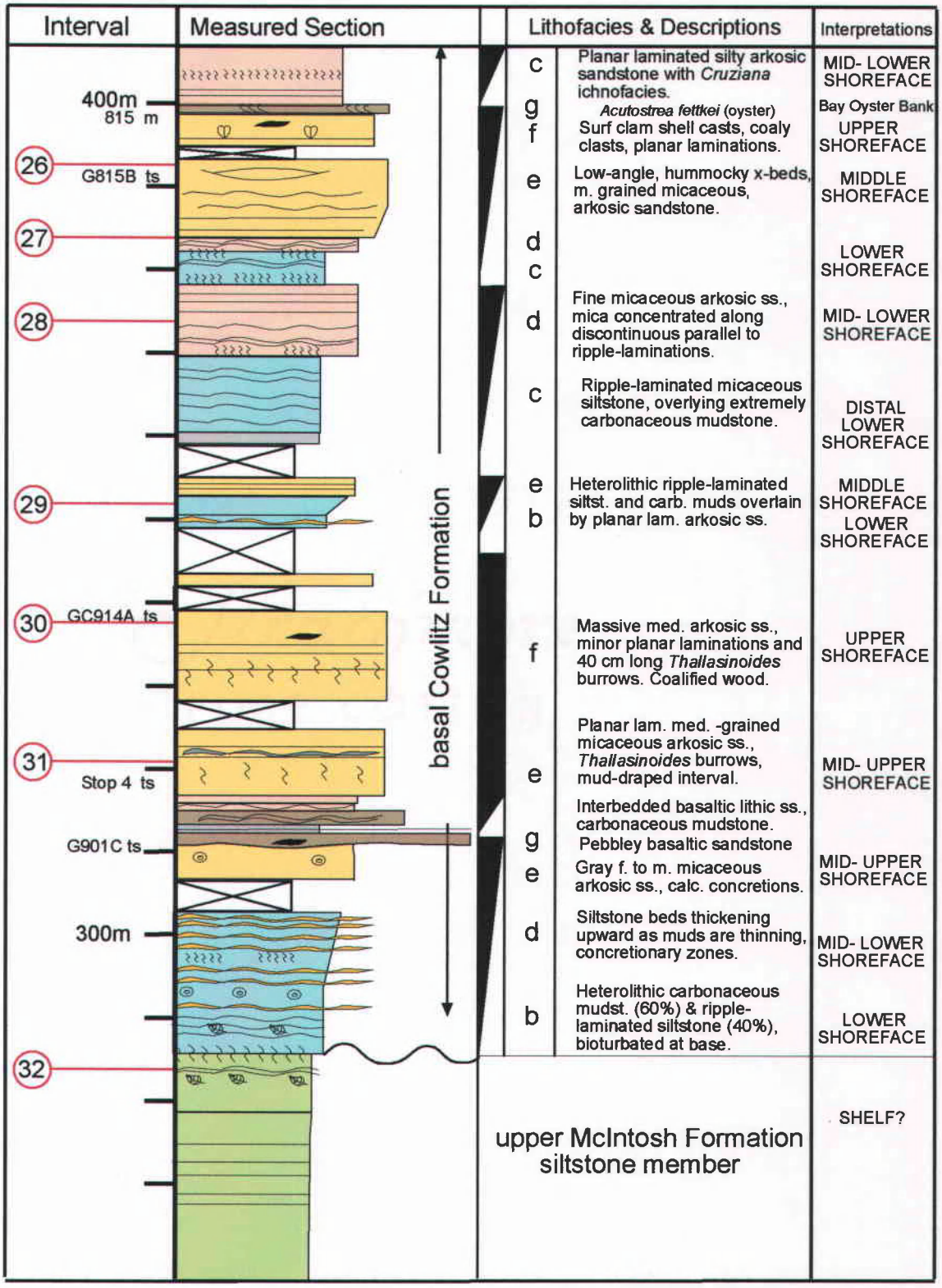
Interval
Measured Section
Lithofacies & Descriptions
Interpretations
400m
815 m
26
G815B ts
27
28
29
30
GC914A ts
31
Stop 4 ts
G901C ts
300m
32
basal Cowlitz Formation
c
Planar laminated silty arkosic sandstone with Cruziana ichnofacies.
MID- LOWER SHOREFACE
g
Acutostrea fettkei (oyster)
Bay Oyster Bank
f
Surf clam shell casts, coaly clasts, planar laminations.
UPPER SHOREFACE
e
Low-angle, hummocky x-beds, m. grained micaceous, arkosic sandstone.
MIDDLE SHOREFACE
d
c
LOWER SHOREFACE
d
Fine micaceous arkosic ss., mica concentrated along discontinuous parallel to ripple-laminations.
MID- LOWER SHOREFACE
c
Ripple-laminated micaceous siltstone, overlying extremely carbonaceous mudstone.
DISTAL LOWER SHOREFACE
e
b
Heterolithic ripple-laminated siltst. and carb. muds overlain by planar lam. arkosic ss.
MIDDLE SHOREFACE
LOWER SHOREFACE
f
Massive med. arkosic ss., minor planar laminations and 40 cm long Thallasinoides burrows. Coalified wood.
UPPER SHOREFACE
e
Planar lam. med. -grained micaceous arkosic ss., Thallasinoides burrows, mud-draped interval.
MID- UPPER SHOREFACE
Interbedded basaltic lithic ss., carbonaceous mudstone.
g
Pebbley basaltic sandstone
e
Gray f. to m. micaceous arkosic ss., calc. concretions.
MID- UPPER SHOREFACE
d
Siltstone beds thickening upward as muds are thinning, concretionary zones.
MID- LOWER SHOREFACE
b
Heterolithic carbonaceous mudst. (60%) & ripple-laminated siltstone (40%), bioturbated at base.
LOWER SHOREFACE
upper McIntosh Formation siltstone member
SHELF?

Figure 8.

(lithofacies e to f) (Figure 8). Scoured into the upper contact of the arkosic sandstone interval is a 1 meter thick pebbly basaltic sandstone bed, grading upward into fine basaltic sandstone and interbedded clay-altered tuffaceous mudstone. Overlying the basaltic sandstone is a nearly continuous 27-meter thick arkosic sandstone interval, capping the lowest coarsening-upward sequence of the lower Cowlitz Formation (Figure 8). At section interval 31 this sandstone succession contains a 10-cm thick carbonaceous mud-draped rippled sandstone, overlain by planar thin-bedded mudstones and sandstones (Figure 10) (thin section Stop 4). The upper part of the sandstone interval (section 30) consists of massive to planar laminated medium-grained arkosic sandstone with *Thallasinoides* burrows and coalified wood debris (up to 20-cm long) (lithofacies f) (Figure 8) (thin section GC914A).

The overlying NGC interval 29 to meter 378 consist of an underlying lower shoreface to middle shoreface parasequence overlain by a shelf to lower shoreface parasequence, suggesting a retrogradational parasequence set. Above this retrogradational parasequence set, 272 meters of lower Cowlitz Formation in the North Germany Creek section (section intervals 27 – 14) are lithologically correlative to the South Germany Creek section (intervals 11 – 1; Plate II and Figure 10). At least seven, and not more than eleven coarsening- and thickening-upward fossiliferous lower shoreface to middle and upper shoreface parasequences occur in this interval.

Section intervals 27 to 21 in the North Germany Creek (NGC) section and the correlative South Germany Creek (SGC) section contain at least three and as many as five lower shoreface successions. Each lower shoreface succession of the NGC section is

overlain by moderately well-sorted, medium-grained micaceous arkosic sandstones of the middle and upper shoreface (lithofacies c through f). The entire interval is about 80 meters thick. In the SGC section just below section interval 10, a 19-meter thick planar to hummocky bedded medium-grained micaceous arkosic sandstone interval (lithofacies e; thin sections LS, GW8C) overlies lower shoreface heterolithic siltstone and carbonaceous mudstone (lithofacies d) (Figure 9, Plate II). Concentrations of mica and carbonaceous plant debris define the thin, low angle planar-to swaley-laminations. *Thallasinoides* burrows are prevalent and concentrations of disarticulated bivalve casts such as *Venericardia clarki* and *Spisula* species (surf clams, macrofaunal sample LS; Nesbitt, 2000; Appendix B) are common in the upper part of the landslide exposed section (Plate II). A correlative hummocky to swaley medium-grained micaceous arkosic sandstone with *Venericardia clarki* and *Spisula* species surf clams (NGC interval 26) is overlain by a 90-cm basaltic lithic sandstone containing a 20-cm thick oyster hash lag.

At the top of this 80-meter thick sand-rich interval, (NGC section interval 21), a wavy-laminated silty fine-grained arkosic sandstone coarsens upward to planar-laminated medium-grained arkosic sandstone with 30 cm long *Ophiomorpha* burrows (lithofacies f), and is overlain by a contorted tangential cross-bedded coarse- to medium-grained arkosic sandstone (lithofacies h; Figure 10B). Interval NGC 21 best correlates to SGC interval 7 based on matching lithofacies and magnetic stratigraphy (Plate II).

Meter 530 to interval 18 of the North Germany Creek section is only 43% exposed, and contains a 5.1-meter thick coarsening-upward fossiliferous, medium- to coarse-grained basaltic sandstone bed (lithofacies g) at meter 485. Bivalves in this bed

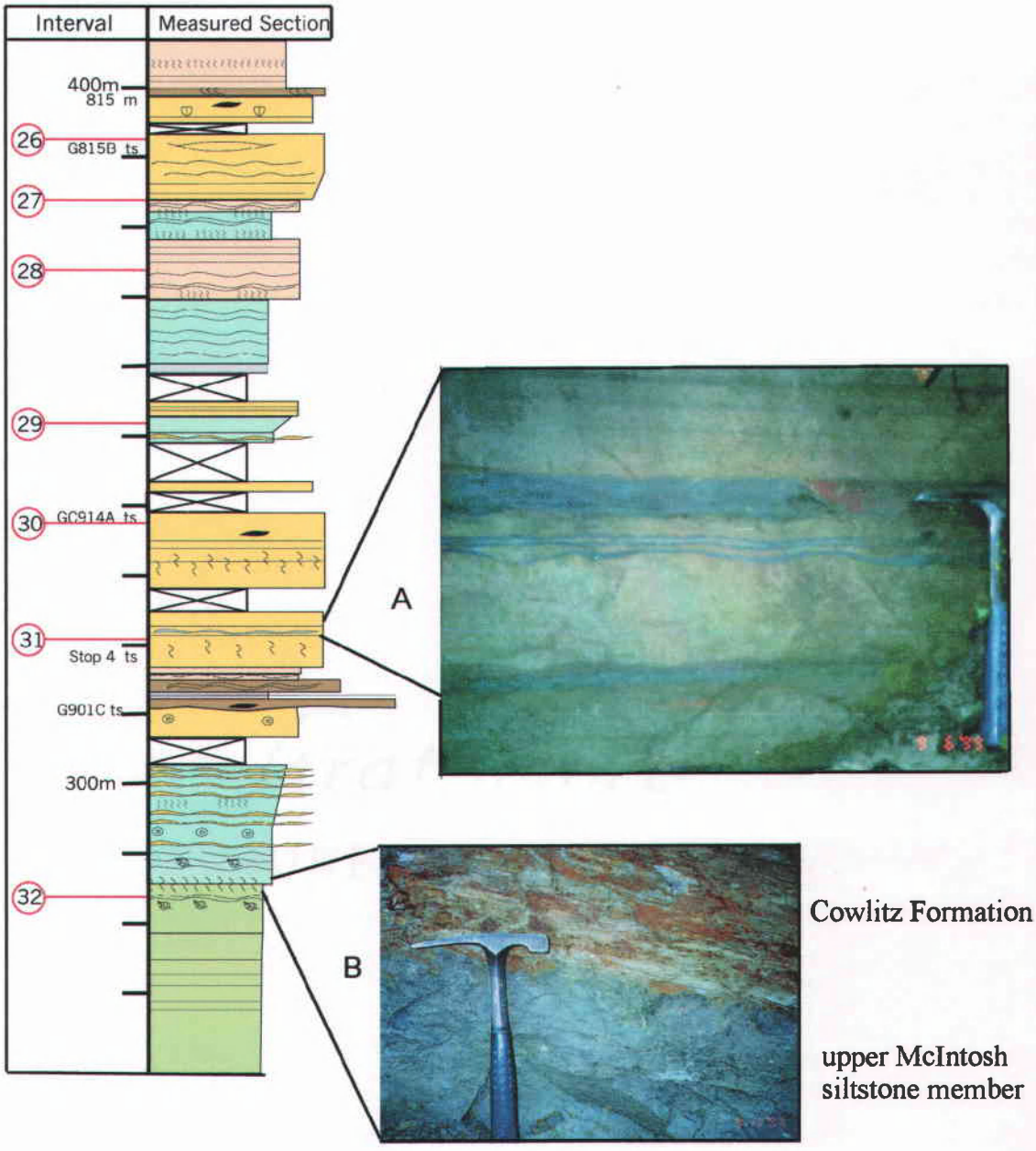

Figure 9. Sedimentary structures of the basal Cowlitz Formation, North Germany Creek.

A) Mud-draped, wave-rippled sandstone and interbedded tuffaceous, carbonaceous dark gray mudstone.

B) Scoured unconformable contact of buff, iron-stained, parallel-laminated, lower shoreface Cowlitz Formation silty sandstone abruptly overlying medium gray shelfal upper McIntosh Formation silty sandstone. Note 28 cm rock hammer for scale.

include robust *Venericardia clarki*, *Crassatellites dalli* clams and *Spisula* sp. surf clams (macrofaunal sample Str. BV; Nesbitt, 2000; Appendix B). Above the basaltic sandstone, two progradational sequences consists of middle shoreface hummocky-bedded sandstones and interbedded ripple- to planar-laminated silty sandstones of lithofacies e. The middle-shoreface beds are abruptly overlain by silty mudstones of the inner shelf (NGC meter 530), marking a marine flooding surface and the beginning of a prograding shelf to shoreface succession.

A dark, thinly laminated carbonaceous mudstone (lithofacies a) of the inner shelf at SGC meter 112 is the correlative flooding surface. Above the flooding surface, 50 to 78 meters of lower Cowlitz Formation, corresponding to NGC section meter 530 to interval 18, and SGC section intervals 6 to meter 191, consists of progradational sequences of inner shelf to shoreface facies. A 78-meter thick progradational sequence begins at the flooding surface at meter 113 (just below interval 6) in the SGC section with lithofacies a of the inner shelf. The bottom 27 meters of the lower progradational sequence consists of lithofacies a and b, of the shelf to lower shoreface transition. Above the lower 27 meters (SGC section 5 to the flooding surface at 190 meters) the sequence is dominated by middle shoreface storm-generated hummocky-bedded sandstones and fair-weather ripple-laminated carbonaceous silty sandstones of lithofacies e (Figure 9; Plate II). The lower 30 meters of the correlative NGC section (meter 530 to interval 18) consists of lithofacies a and b of the shelf to lower shoreface transition. A 21-meter thick upper shoreface, fossiliferous medium- to coarse-grained basaltic sandstone of lithofacies g overlies the lower shoreface facies. Four fossiliferous beds (~ 30 cm) in the basaltic

sandstone interval include specimens of *Turritella uvasana stewarti* (turret snail), *Acutostrea fettkei* (oyster), *Corbula dickersoni* (corbula clam), *Venericardia clarki*, and *Crassatellites dalli* (clams) (macrofaunal sample GF8E; Appendix B). Abruptly overlying the fossiliferous upper shoreface basaltic sandstone interval in the NGC is a massive dark gray mudstone of lithofacies a (inner shelf). This flooding surface is the datum used for correlating the lithofacies successions of the North Germany Creek section with the South Germany Creek section (Figure 9).

Inner shelf benthic foraminifers were recovered from the correlative silty mudstone at the base of a 70-meter thick progradational sequence in the SGC section (SGC section intervals 3 - 1; NGC section intervals 18 - 14) (microfaunal sample GCBM; Rau, 2000; Appendix A). Directly overlying the uppermost foreshore sandstone in the SGC section is a subaerial Grays River lava flow Ar^{40}/Ar^{39} dated at 40.09 ±0.34 Ma (Plate II, Figure 9).

In the correlative North Germany Creek section, interval 16 (Plate II) consists of a 16-meter thick medium-grained hummocky-bedded (lithofacies e) arkosic sandstone overlain by a planar laminated medium-grained fossiliferous sandstone (lithofacies f) (Figure 10). The overlying shoaling upward sequence consists of lower shoreface heterolithic ripple-laminated arkosic sandstone and carbonaceous, micaceous silty mudstone (section interval 15) capped by coarse-grained fossiliferous basaltic lithic sandstone containing *Lucinoma acutilineatus* (lucinid bivalve, previously not found in the Cowlitz Formation) and *Calyptraea diagoana* (slipper-shell gastropod) in growth position (macrofaunal sample GR8E; Appendix B).

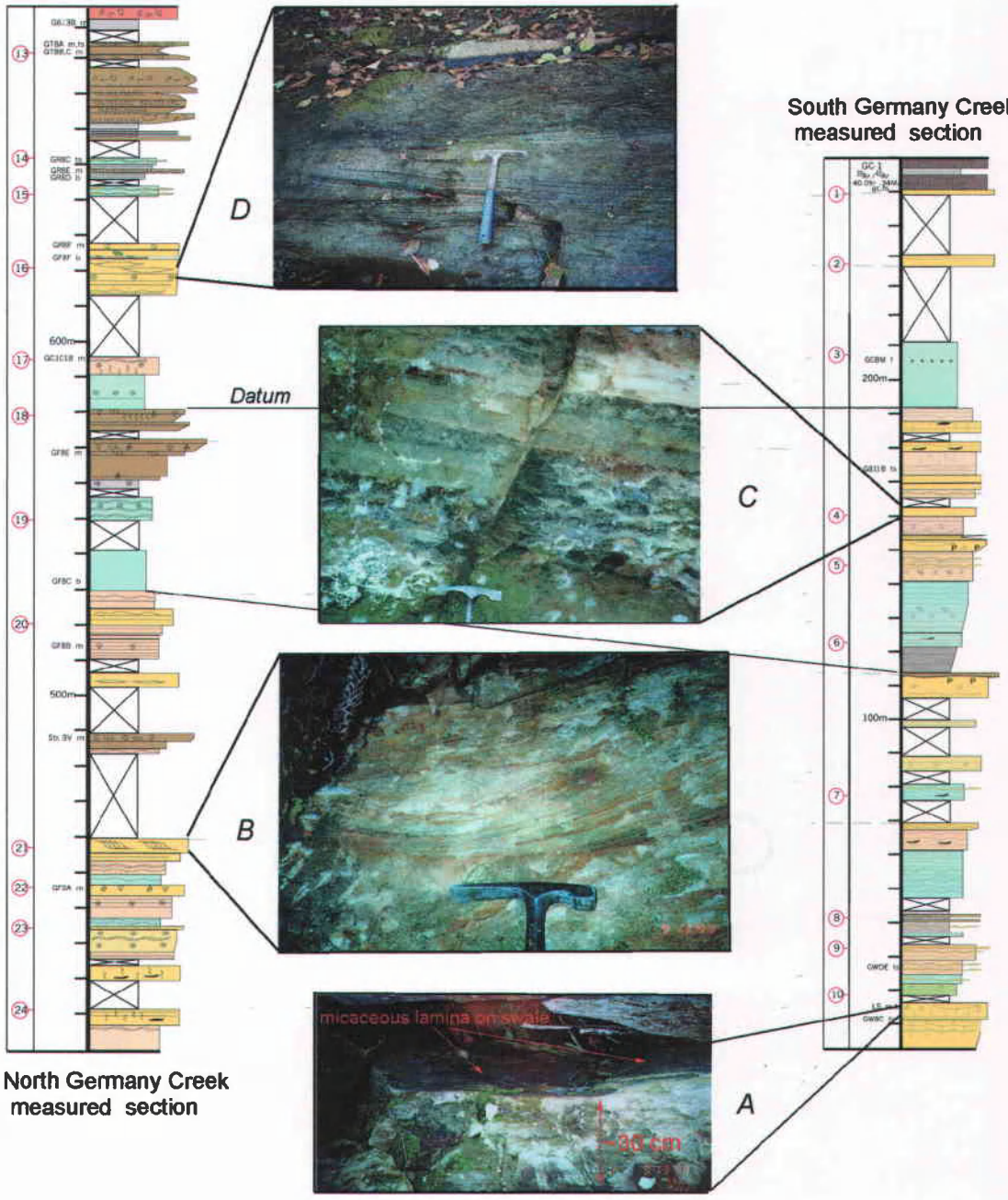

Figure 10. Lithofacies of the lower Cowlitz Formation of Germany Creek, Cowlitz Co., Washington.

A) Hummocky cross-stratified, micaceous, arkosic sandstone of the middle shoreface (lithofacies e).

B) Tangentially cross-bedded arkosic sandstone of a distributary bar or channel, possibly a flood-deposition event (lithofacies h).

C) Heterolithic fine-grained arkosic sandstone and carbonaceous, micaceous silty mudstone of the lower to middle shoreface (lithofacies d). Note 7 cm long rock hammer head for scale.

D) Low-angle, truncated hummocky cross-stratified arkosic sandstone of the middle shoreface (lithofacies e). Note 28 cm hammer for scale.

Beginning at NGC section interval 14, basaltic sandstone dominates the section. In order to allow greater stratigraphic resolution, this unit has been broken out from the Cowlitz Formation and mapped as Grays River Volcanic sedimentary rocks, unit 1 (Plate I, Tgvs1). It is a shallow-marine fossiliferous basaltic sandstone, conformable with the underlying arkosic sandstone dominated Cowlitz Formation and conformably underlying Grays River Volcanics subaerial basaltic lava flows (Plate II).

A 32-meter thick fossiliferous hyaloclastic basaltic sandstone and overlying lagoonal (?) mudstone section (section intervals 14 – 13) directly underlies subaerial Grays River lava flows Ar^{40}/Ar^{39} dated at 39.35 ±0.36 Ma (Plate II). Densely-packed, growth position bay oyster banks containing *Acutostrea fettkei* (oysters) and *Septifier dichotomus* (mussels) are interbedded with poorly sorted coarse-grained conglomeritic basaltic sandstone containing scattered cobble- to boulder-sized (1.2 meter diameter) clasts of Grays River basalt. The overlying lagoonal tuffaceous mudstone bearing juvenile bivalves (macrofaunal sample G613B; Appendix B) underlies 5 meters of clayey weathered palagonitic flow breccia below the dated Grays River Volcanics basal lava flow (Plate II).

Monahan Creek

The Cowlitz Formation measured and described in Monahan Creek is shown graphically in Figure 11. Three coarsening- and thickening-upward sequences are evident. The lithofacies associations are dominated by inner shelf transitions to wave-influenced shoreface successions.

Lithofacies of the 110 meters of Cowlitz Formation exposed in the ¾ mile transect of Monahan Creek (NE ¼ of Sec. 12, T 9 N, R 3 W) include: (a) inner to outer shelf micaceous mudstone and siltstone, (b) interbedded carbonaceous mudstone and current- and wave-ripple laminated micaceous silty sandstone of the shelf to lower shoreface transition, (c) lower shoreface silty carbonaceous mudstone with *Cruziana* ichnofacies, (d) lower to middle shoreface heterolithic sandstone and carbonaceous, micaceous siltstone, (e) massive to hummocky-bedded arkosic sandstone of the middle shoreface and (f) planar-laminated medium-grained arkosic sandstone of the upper shoreface to foreshore (Figure 11). Additional tide-influenced lithofacies in a 10.4 meter thick interval of the lower part of the Monahan Creek section include mud-draped cross-bedded sandstone foresets, mud-draped rippled sandstone, and tidally-formed sigmoidally cross-bedded arkosic sandstones (Figure 11).

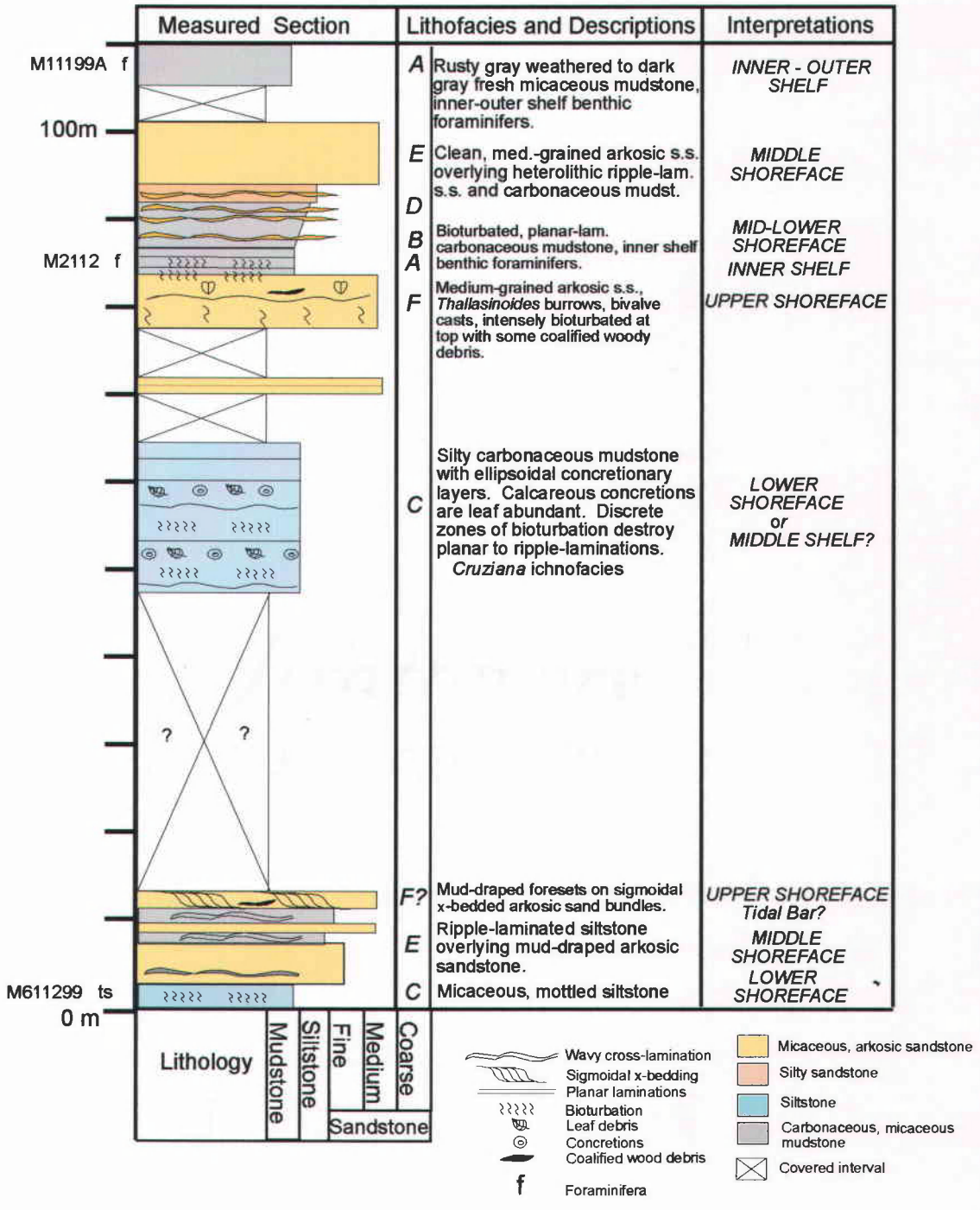

Figure 11. Monahan Creek measured section description and interpreted depositional environments of the Cowlitz Formation (see text for location; Plate I).

Arkansas Creek area

Discontinuous exposures of interbedded micaceous, carbonaceous mudstones and arkosic sandstones along landslide exposed cliffs and the creek bed of Arkansas Creek prevented accurate correlation between exposures. An estimated 70-meter thick section exposed in landslide head scarps along Arkansas Creek (SW ¼ of Sec. 24, T 10 N, R 3 W) provided a continuous but relatively thin section for description. Direct measurement of the exposure was unattainable due to the vertical face of the head scarp. Visual estimation of the lithology and thickness of the upper 30-35 meters was determined from the base.

The lowest exposure consists of 6 meters of micaceous siltstone with carbonized leaf debris along discontinous planar laminations and one 35-cm thick bed of clean fine-grained arkosic sandstone (lithofacies b). The siltstone grades evenly to heterolithic interbedded bioturbated rhythmically-bedded carbonaceous silty mudstone (4 – 6 cm thick) and buff swaley fine-grained arkosic sandstone interbeds (4 – 6 cm). The sandstone beds become thicker (30 – 40 cm) towards the top of the additional 10-meter thick interval (lithofacies c,d).

Overlying the lower shoreface heterolithic facies is a 5-meter thick planar to hummocky cross-bedded fine- to medium-grained arkosic sandstone bed overlain by a 40-cm thick ripple-laminated carbonaceous, micaceous mudstone (lithofacies e). Above this bed, another 5 to 6 meter thick amalgamated hummocky-bedded arkosic sandstone bed is overlain by a ripple-laminated muddy siltstone bed. An 8-meter thick bioturbated

micaceous siltstone (lithofacies c) overlies the middle-shoreface hummocky-bedded interval.

The overlying estimated 30 to 35 meters consists of generally coarser and thicker arkosic sandstones and interbedded heterolithic ripple-laminated siltstone and carbonaceous mudstone. A large, freshly cleaved boulder of fossiliferous medium-grained planar laminated arkosic sandstone could be clearly identified as belonging to a fresh face near the top of the ~70-meter cliff exposure. Shallow-marine or subtidal bivalves identified from the block include *Corbicula cowlitzensis*, *Tivelina valarensis* and *Spisulardia pakulii*, along with *Whitneyii sinuarta*, an ornate predatory gastropod (Nesbitt, personal communication, 2000).

Another landslide head scarp along a logging road above Arkansas Creek 2.3 km south of the cliff exposed section consists of flat-lying tidally-bedded arkosic sandstones and micaceous mudstones (N ½ of Sec.36, T 10 N, R 3 W; Plate I). Lithofacies recognized in the 21 meters of strata exposed include friable tangential cross-bedded arkosic sandstone and subtidal megaripple sigmoidally cross-bedded sandstone with mud-draped foresets and mud-couplets forming distinctive tidal bundles (subtidal bar or channel) (Figure 12). Other sedimentary structures include angular mud-rip clasts, clastic dikes and soft-sediment deformation of thin mudstone interbeds (Figure 12).

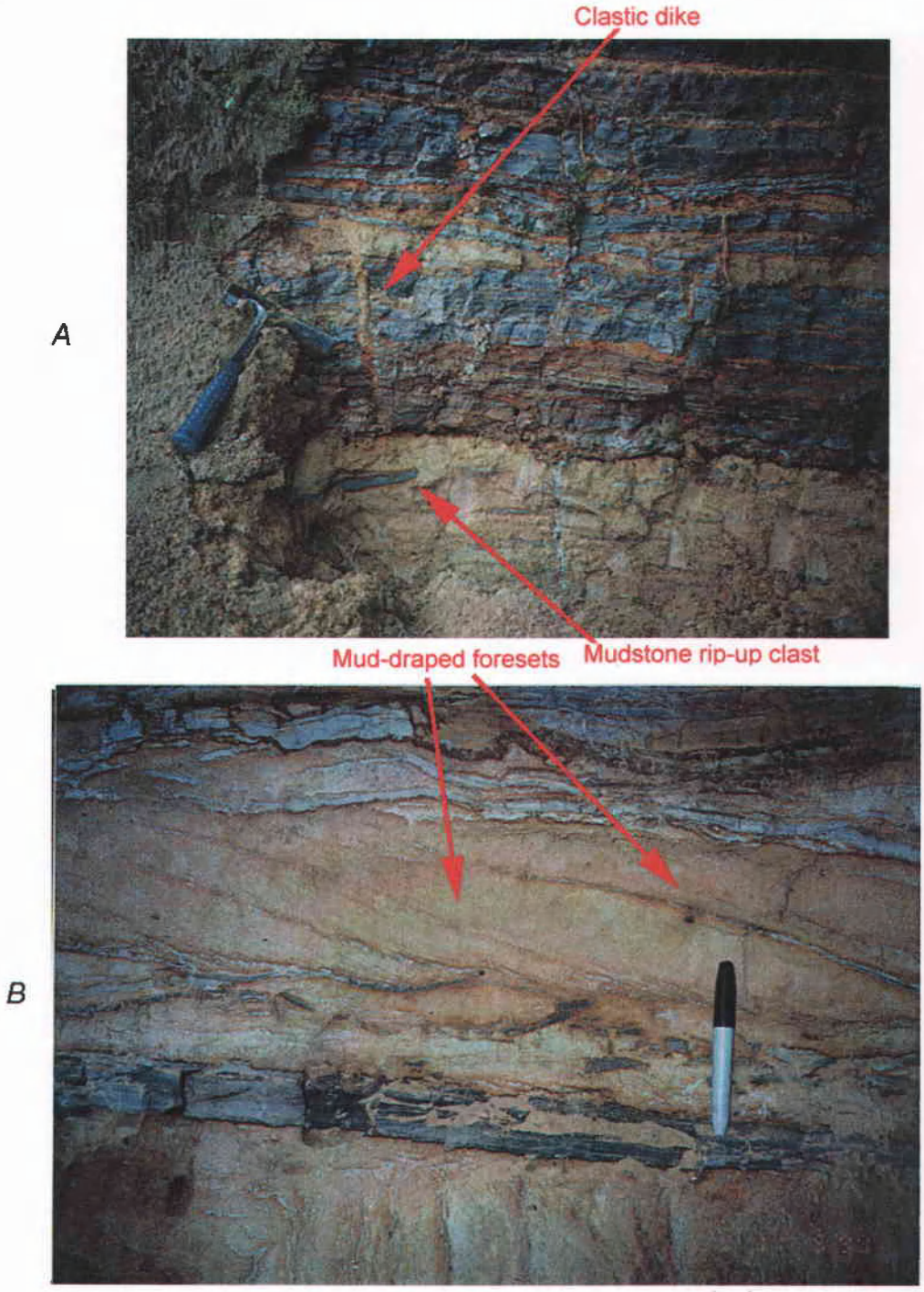

Figure 12. Lithofacies of the Cowlitz Formation exposed along a road cut near Arkansas Creek (N1/2 36-T10-R3; Plate I).

A) Heterolithic friable arkosic sandstone and carbonaceous mudstone, including clastic dikes and angular mud rip-up clasts, interpreted as a subtidal channel complex undergoing rapid deposition.

B) Sigmoidally cross-bedded mud-draped foreset arkosic sandstone interval, recording the deposition of a dominant tide called a tidal bundle. Note 28 cm hammer for scale.

Depositional Environment of the lower Cowlitz Formation

Germany Creek

Depositional environments of the basal 374 meters of Cowlitz Formation (North Germany Creek section and correlative South Germany Creek section) in the study area are inferred from well-exposed vertical lithofacies relationships, a variety of sedimentary structures, ichnofacies, as well as molluscan and benthic foraminiferal fossil assemblages (Figure 13). Depositional environments of the Germany Creek sections include: inner shelf (lithofacies a), shelf to shoreface (lithofacies b), lower shoreface to middle shoreface (lithofacies c,d,e), upper shoreface to foreshore (lithofacies f), reworked volcaniclastic debris flow deposits and channelized sandstones of the upper shoreface and foreshore (lithofacies g), and distributary channel or bar deposits of the upper shoreface and foreshore environments (lithofacies h).

Middle shelf silty mudstones and a few interbedded thin fine-grained sandstones of lithofacies a occur in three intervals of the Germany Creek sections (NGC int. 29, above 20; SGC int. 6, below 3, Plate II). This facies is marked by a predominance of mudstone and a lack of sedimentary structures. Microfauna sample GCBM from the SGC interval 3 contains the benthic foraminifers *Elphidium cf. E. minutum* and *Quinqueloculina imperalis*, indicating an inner to outer shelf depositional environment (Rau, written communication, 2000). The assemblage is typical of the inner shelf/prodelta facies of the Skookumchuck Formation interbedded with coal deposits of the Centralia, Washington area (Rau, written communication, 2000). Thin-bedded fine-

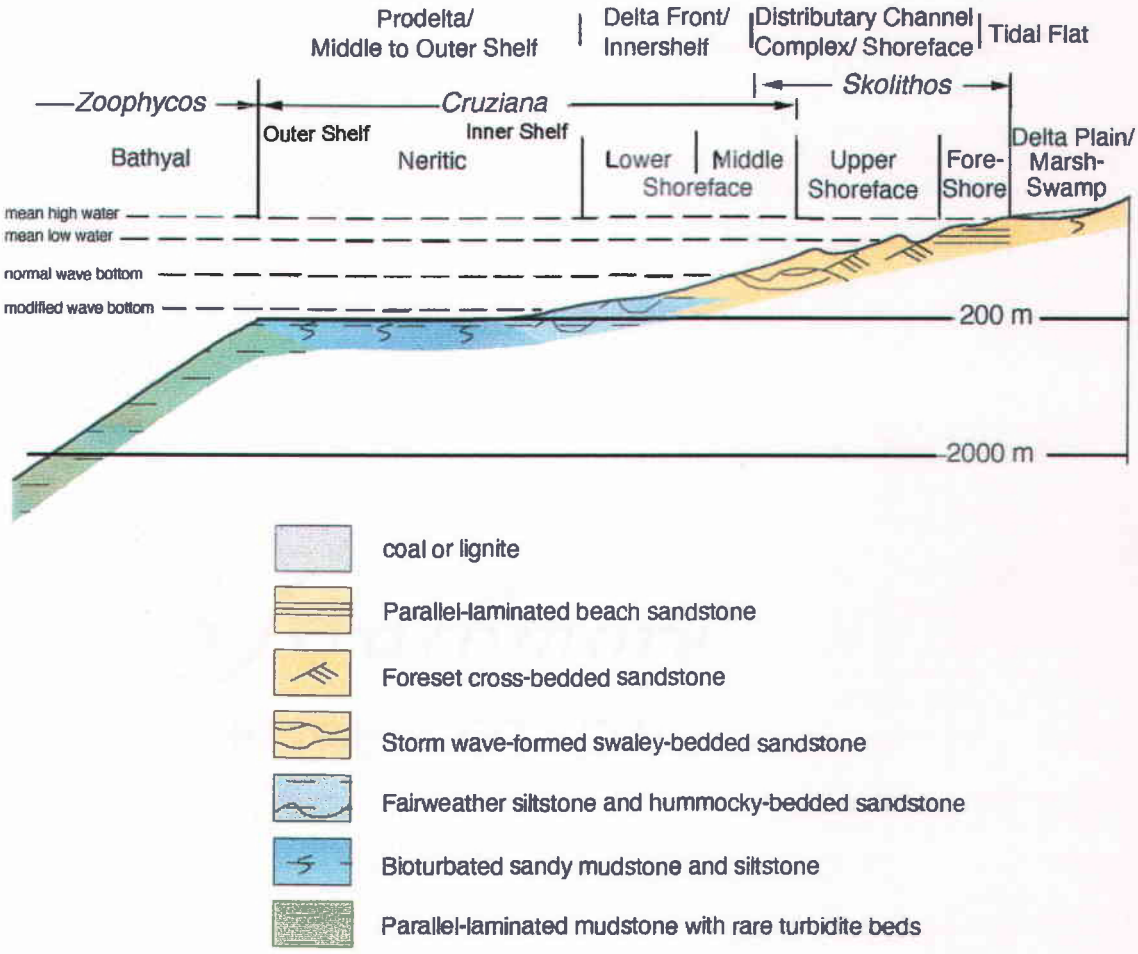

Figure 13. Profile of onshore-offshore depositional environments related to sedimentary structures and ichnofacies of the McIntosh Formation and normal marine units of the Cowlitz Formation (slightly modified from Payne, 1998; Berkman, 1990 and Robertson, 1997).

grained sandstones are interpreted to be turbidites or tempestites generated in shallow water by storm waves and flowing onto the shelf. These beds are interpreted to be deeper water equivalents to the storm-generated hummocky beds of the middle-shoreface/delta-front environment (Figure 13) (Chan and Dott, 1986).

The shelf to lower shoreface transitional interbedded carbonaceous mudstones and thin-bedded micaceous silty sandstone of lithofacies b occurs in five stratigraphic intervals of the Germany Creek sections (NGC int. 32, 27, 19, 18; SGC 10). This facies is a mixture of shelfal mudstone and an equal amount of thin-bedded bioturbated silty sandstone. An increasing frequency of interbedded sandstone indicates a higher energy depositional environment than lithofacies a. Lithofacies b is marked by an increase in bioturbation of the *Cruziana* ichnofacies (Figure 13) where thin sandstone beds (20-30 cm) show intense bioturbation at the tops overlain by ripply carbonaceous mudstone, suggesting relatively slow depositional rates without wave or current agitation (Chan and Dott, 1986). This depositional environment is common of the lower delta-front/prodelta transition, or deposition on the middle shelf (Chan and Dott, 1986).

A gradational change from interbedded carbonaceous mudstone and siltstones of lithofacies b to bioturbated siltstone with few if any carbonaceous mudstone interbeds marks the transition to the lower shoreface lithofacies c. Lithofacies c is characterized by intensely bioturbated to mottled micaceous siltstone (*Cruziana* ichnofacies).

Sets of asymmetrical current ripples and wave-formed oscillatory ripples with carbonaceous, micaceous silt- draped crests are common sedimentary structures where current and wave agitation is great enough to prevent deposition of clay-sized particles.

Lithofacies d and e are gradational with lithofacies c, showing increased storm-wave dominated deposition of sandstone on the lower to middle shoreface. Lithofacies d and e dominate the Germany Creek section, occuring in every progradational succession (Plate II, lithofacies d shown in orange, lithofacies e with hummocky-bedded symbol). The lower to middle heterolithic shoreface facies of lithofacies d contains abundant carbonaceous leaf debris, mica, and parallel to wavy-laminations, suggesting deposition in a slighty lower energy environment than the storm-wave hummocky-bedded, medium-grained arkosic sandstone dominated lithofacies e. Hummocky-bedded sandstones are common in delta-front and delta-margin environments and believed to form through the complex oscillatory motion of storm-waves as they impinge on the bottom at depths below fair-weather wave base (Chan and Dott, 1986) (Figure 13). *Thallasinoides* burrows of the *Skolithos* ichnofacies, as well as concretionary intervals and coalified woody debris are common in lithofacies e (Figure 13). Macofaunal sample GC1018 (Plate II, NGC int.17) was identified as containing *Pteria clarki*, a wing oyster that lives attached to seaweed in shallow marine depths, and *Laevidentalium* sp. (tusk shell dentalium), previously known only from the Tukwila Formation (Nesbitt, written communication, 1999; Appendix B).

Upper shoreface planar-laminated to massive medium-grained arkosic sandstone of lithofacies f commonly caps coarsening- and thickening-upward shoaling successions

in the Germany Creek sections (NGC int. 31,30,26,24,23,22; Plate II). These sandstone beds are 3 – 5 meters thick, commonly contain large (40-50 cm long) *Thallasinoides* and *Ophiomorpha* burrows of the *Skolithos* ichnofacies and articulated marine clams such as Venericardia (macrofaunal samples LS, Str.BV, GF8A, GR8F). The in-place marine fauna and vertical burrow traces suggest shallow-water deposition and high energy shoal-water conditions. The well-sorted sandstone suggests extensive wave-reworking and the planar laminations may be swash-formed beach deposits. These medium-grained sandstones may be reworked delta distributary mouth bars, deposited seaward of active distributary channels or upper shoreface environments that were peripheral to the delta system (delta-margin) (Chan and Dott, 1986).

One coarsening- and thickening-upward interval (NGC int. 21) is capped by a 4.1-meter thick pebbly, medium-grained, high-angle cross-bedded sandstone (lithofacies h) (Figure 10B). A 30-cm interval of the cross-bedded sandstone is contorted, suggesting rapid deposition and subsequent liquefaction due to sudden loading or seismic shock. The vertical stratigraphic relationship of the cross-bedded sandstone overlying marine facies suggests that these sandstones could be delta-distributary channel deposits, similar to the Eocene Coaledo Formation of southwestern Oregon (Chan and Dott, 1986). Strong wave action in a coastal setting generally reworks distributary channel deposits except during rapid deposition of sediment due to episodic flood events (Chan and Dott, 1986). However, lack of laterally continuous exposure prevents definitive identification of this individual bed.

Fossiliferous pebbly basaltic sandstone and minor basaltic pebble conglomerate associated with upper shoreface arkosic sandstones from lithofacies g of the upper shoreface to foreshore depositional environment. These basaltic sandstone intervals occur in five horizons of the NGC section (int. 31,25, Str. BV, 18, and 14; Plate II) and one interval of the SGC (int. 6; Plate II) correlative to the cross-bedded arkosic sand (distributary channel) of the NGC int. 21. The beds range in thickness from 1 to 8 meters. Commonly they display scoured, poorly sorted bases that coarsen upward. Macrofaunal assemblages gathered from these intervals are rich in bay oyster bank deposits containing *Acutostrea fettkei* oysters and *Septifier dichotomus*, *Mytilus* sp. mussels (macrofaunal samples GT8A,B,C; GF8E, 815). Two intervals contain *Calyptraea diagoana*, a slipper-shell gastropod that lives stuck to a hard substrate in the rocky intertidal zone (Nesbitt, written communication 2000; macrofaunal samples 815, GR8E). Sample 815, a wave-reworked lag deposit, contains an additional *Trochid* sp. snail believed to have grazed algae on a hard, rocky substrate in a shallow estuarine to marine bay environment (Nesbitt, written communication, 2000). Commonly interbedded above the oyster bank and hash deposits is the shallow-marine Turritella-Tivelina assemblage of Nesbitt (1995) locally consisting of *Turritella uvasana stewarti* (turret snail), *Crassatellites dalli*, *Venericardia clarki*, *Callista andersoni* (marine clams), and *Corbula dickersoni* (corbula clam) (Nesbitt, 2000; samples Str. BV, GF8E, int. 18; Appendix B). The pebbly basaltic sandstones are interpreted as debris flow deposits or channel sandstones periodically eroding from a nearby growing Grays River volcanic high to the southwest into the forearc basin. Bay oyster communities exploited the coarse

hard-substrate provided by periodic deposition of Grays River volcanic debris and with subsequent subsidence were reworked as hash-lag deposits and colonized by the shallow marine Turritella-Tivelina (Nesbitt, 1995) assemblage.

Monahan Creek

The 110 meters of Cowlitz Formation exposed in Monahan Creek contain the same vertical lithofacies associations, ichnofacies and benthic foraminifers of the Germany Creek section. Therefore, these strata are interpreted as also deposited in storm-wave shoreface/delta front depositional environments. Bioturbated carbonaceous micaceous silty mudstone of the inner to outer shelf occurs in two intervals (Figure 11; foraminiferal samples M2112, M11199A; Appendix A). Sample M11199A may reflect a slightly deeper environment of the outer shelf to uppermost upper bathyal water depth of deposition based on the presence of *Pullenia salisburyi* with *Quinqueloculina* sp (Rau, written communication, 2000). Microfaunal sample M2112, with the presence of abundant *Elphidium* sp. suggests an inner shelf depostional environment (Rau, written communication, 2000).

The lower to middle shoreface depositional environment of lithofacies b and c occurs in three intervals (meter 1, 50 and 87; Figure 11). Abundant carbonized leaf debris and calcareous concretion horizons characterize these deposits in the Monahan Creek section. Complex hook-shaped and vertical burrows of the lower to middle shoreface *Cruziana* ichnofacies are common.

Middle shoreface massive arkosic sandstone of lithofacies e caps one shoaling succession beginning at meter 94, Figure 11. Upper shoreface medium-grained micaceous arkosic sandstone with *Thallasinoides* burrows, broken bivalve casts and coalified woody debris occurs at meter 78, Figure 11. The upper contact of the upper shoreface sandstone is intensively bioturbated, indicating colonization of the subsiding sandy upper shoreface by the lower shoreface *Cruziana* ichnofacies. Mud-draped foresets and sigmoidal cross-beds occur at meter 13 of Figure 11, and are interpreted as representing a tidal bar deposit of the upper shoreface.

Arkansas Creek

The approximately 70-meter thick cliff-exposed section of Cowlitz Formation in Arkansas Creek (SW ¼ of Sec. 24, T 10 N, R 3 W; Plate I) contains at least two coarsening- and thickening-upward lower shoreface to foreshore (lithofacies b – f) successions similar in thickness and character to the Germany Creek and Monahan Creek section. Molluscan fauna recovered from a planar laminated sandstone bed include shallow marine or subtidal *Corbicula cowlitzensis*, *Tivelina valarensis* and *Spisulardia pakulii* (clams), and the ornate predatory gastropod *Whitneyii simuarta* (sample Ark 6; Nesbitt, personal communication, 2000; Appendix B).

The tide-dominated, landslide-exposed section above Arkansas Creek (N ½ of Sec. 36, T 10 N, R 3 W; Plate I) displays a different depositional environment than the shoreface successions of the other Cowlitz Formation stratigraphic sections (Figure 12). Subtidal channel fill facies are well-exposed in the approximately 15-meter thick interval.

Sedimentary structures present in the exposure (Figure 12) that are diagnostic of a subtidal channel environment include: multiple megaripple cosets consisting of sigmoidal cross-bedded sandstone, slack-water mud-draped bottomset couplets, contorted bedding and clastic dikes, mud rip-up clasts, and mud-draped reactivation surfaces (Nio and Yang, 1991) (Figure 12). The sigmoidal cross-bedded mud-draped arkosic sandstone intervals record the deposit of a single, dominant ebb or flood tide called a tidal bundle (Walker, 1992). Soft-sediment deformation (clastic dike, contorted bedding) and mud rip-up clasts suggest rapid deposition, possibly from flood events. Stratigraphically overlying the 5-meter thick mud-draped tidal bundle sequence is an approximately 10-meter thick extremely friable, micaceous arkosic sandstone containing sigmoidal cross-bedding and lacking mudstone drapes. Foreset and bottomset laminae are defined by concentrations of carbonaceous plant debris and mica. The cross-bed sets are about 1 meter thick and bounded by wavy reactivation surfaces. These cross-bed sets were probably deposited near the main axis of the channel where strong ebb and flood currents prevented the deposition of slack-water mud-drapes.

Summary

In summary, the basal 374-meters of middle Eocene Cowlitz Formation in Germany Creek consists of multiple wave-dominated coarsening- and thickening-upward progradational shelf to shoreface successions (Plate II). The 110-meter thick Monahan Creek section, although relatively poorly exposed, shows similar progradational shelf to shoreface lithofacies associations (Figure 11). The progradational sequences in the basal

Cowlitz Formation described in the study area are also described by Payne (1998) in the basal type-section Cowlitz Formation, and also from funnel-shaped curves on spontaneous potential and resistivity logs in the nearby Shell-Zion #1 well (Figure 1 for location). The 374-meter thick lower Cowlitz Formation of the study area correlates with the 275-meter thick informal basal Cowlitz Formation unit 1A and the lowest 100 meters of Payne's informal unit 1 B. This correlation is based on similar thickening- and coarsening-upward arkosic and basaltic sandstone lithofacies, molluscan and foraminiferal biostratigraphy, and lithostratigraphic position directly above the bathyal upper McIntosh siltstone member. Payne's (1998) informal unit 1A of the Cowlitz Formation consists of progradational shoreface successions. The overlying 283 meter thick unit 1 B consists of delta plain, tidal channel and tidal flat facies assocations. A 70-meter thick cliff outcrop along Arkansas Creek also exposes coarsening- and thickening-upward shoreface successions consistent with the basal part of the Cowlitz Formation. Higher in the section, a well-exposed outcrop above Arkansas Creek displays tide-dominated lithofacies of a channel fill (Figure 12) consistent with Payne's (1998) overlying unit 1 B.

MAGNETIC STRATIGRAPHY OF THE LOWER COWLITZ AND UPPER MCINTOSH FORMATIONS

The South and North Germany Creek measured sections were sampled by the author for paleomagnetic analysis. Samples were taken as oriented blocks of rock (3 samples per site) using simple hand tools. The North Germany Creek section was sampled at 28 sites and the South Germany Creek section was sampled at 11 sites (Plate II for locations). The samples were analyzed for magnetic inclination and declination at the California Institute of Technology under the supervision of Dr. Donald Prothero of Occidental College, Los Angeles, California. The results of the analysis were used in conjunction with paleomagnetic results from nearby measured sections including the type-Cowlitz Formation of southwest Washington, Clark and Wilson sandstone member of the Cowlitz Formation and Sunset Highway and Sweet Home Creek members of the Hamlet Formation of northwest Oregon, to provide regional magnetic stratigraphic correlations (Prothero et al., in press) (see Regional Stratigraphic Correlation section). For a complete discussion of the methods and detailed discussion of the results of the paleomagnetic analysis, see Prothero et al. *(in press)*. The results of this analysis of the Germany Creek sections are tabulated in Appendix F. Locations of sample sites are shown on the Plate II index map.

The magnetic stratigraphy of the two Germany Creek sections is shown in Figure 14 and Plate II. The Cowlitz Formation in the lower half of the 310-m thick South Germany Creek section is reversely polarized; the upper half is normally polarized. The South Germany Creek section is overlain by a normally polarized Grays River basaltic

lava flow dated at 40.09 ±0.34 Ma. The lower 270-m of the North Germany Creek section (upper McIntosh Formation) has reversed polarity. A normal polarity interval straddles the unconformable contact between the upper McIntosh and the basal Cowlitz Formation (Payne's unit 1A, 1998). The overlying 330-m of Cowlitz Formation unit 1 are mostly reversed in polarity, except for one short normal magnetozone (NGC intervals 19 – 18). A normal polarity interval begins directly below a conformably overlying basaltic lava flow dated at 39.35 ±0.36 Ma, capping the North Germany Creek section.

Based on the correlation to the worldwide paleomagnetic time scale of Berggren et al. (1995) and the radiometric date overlying the North Germany Creek section (Figure 14), the lower 270-m reversed polarity interval of upper McIntosh formation is correlative to Chron 19r (41.5 – 42.5 Ma). The normal magnetozone between the upper McIntosh and Cowlitz formations that straddles a period of nondeposition likely correlates to Chron 19n (41.2 – 41.5 Ma). The overlying dominantly reversed polarity magnetozone of Cowlitz Formation informal unit 1 correlates with Chron 18r (40.1 – 41.2 Ma), with the uppermost normally polarized Cowlitz Formation and Grays River Volcanics interval correlative to Chron 18n (38.4 – 40.1 Ma). Correlations for the South Germany Creek section indicate that the lower reverse polarity magnetozone is correlative to Chron 18r, and the upper normal polarity magnetozone to Chron 18n (Figure 14).

The amount of tectonic rotation of the Germany Creek sections was calculated from declination data (Appendix F) by Prothero et al. *(in press)* against the Eocene cratonic pole of Diehl et al. (1983). Error estimates were corrected using the method of

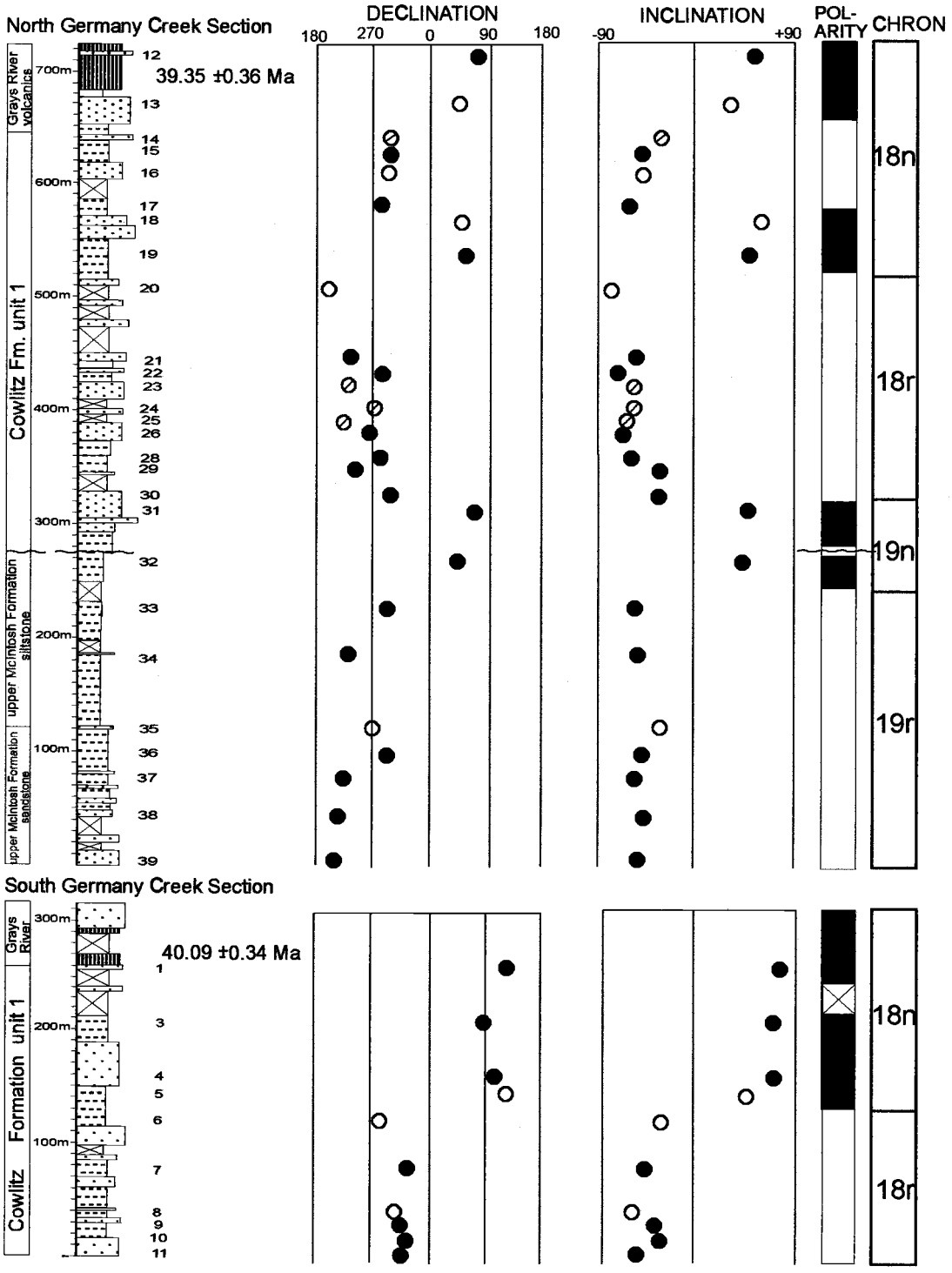

Figure 14. Magnetic stratigraphy of the Germany Creek sections. Solid circles are statistically distinct from a random distribution at the 95% confidence level; dashed circles indicate one sample was missing or rejected; open circles indicate sites where one sample was divergent, but the other two gave a clear indication of polarity (Prothero et al., *in press*). Sample sites indicated by numbers adjacent to strat. column.

Demarest (1993). The Germany Creek sections show clockwise rotation of 103 ±7 degrees and a negligible northward translation of 5 ±7 degrees relative to the Eocene cratonic pole (Prothero et al., in press) (Appendix F). Samples from other sections used in the study by Prothero et al., in press) show significant clockwise rotation, but show a wide range of rotational values in close proximity. Drilled oriented cores of basalt from the underlying Crescent Formation were analyzed byWells and Coe (1985). They reported a clockwise rotation of the Crescent Formation nearest the Germany Creek sections of 52 ±10 degrees (Domain 6 of Wells and Coe, 1985, eastern Willapa Hills). For nearby Grays River Volcanics (Goble Volcanics of Wells and Coe, 1985) overlying the Germany Creek sections, Wells and Coe (1985) report clockwise rotations of only 23 ±15 degrees. The wide scatter of data for rock units in proximity suggests problems in the standardization of the methods or techniques used to acquire the paleomagnetic data. Rotational disparity is greatest between sedimentary paleomagnetic samples and volcanic sample results. However, all results show significant clockwise rotation in discrete structural domains of northwest Oregon and southwest Washington (Wells and Coe, 1985; Prothero et al., 2001).

SEQUENCE STRATIGRAPHY OF THE UPPER MCINTOSH AND COWLITZ FORMATIONS

Sequence stratigraphy is the study of genetically related facies within a framework of chronostratigraphically significant surfaces (Van Wagoner et al., 1992). A depositional sequence is defined as a relatively conformable, genetically related succession of strata bounded by basinwide unconfomities or their correlative confomities known as sequence boundaries (Mitchum, 1977, in Van Wagoner et al., 1992). Sequence boundaries form in response to relative falls in sea level (Van Wagoner et al., 1992). Deposited during one relative sea level cycle (regression – transgression), a depositional sequence can be subdivided into system tracts using the following time-stratigraphic surfaces: (1) sequence boundaries, (2) a transgressive surface representing the first major marine flooding surface, and (3) a maximum flooding surface representing maximum relative sea level of the depositional cycle (Armentrout, 1996).

Depositional sequences can be further subdivided into lowstand (LST), transgressive (TST), highstand (HST) and shelf-margin (SMST) system tracts, defined by their relative positions within the sequence and their parasequence stacking patterns (Van Wagoner et al., 1992). A parasequence set (on the order of 10 to 200 meters thick) is defined as a succession of genetically related parasequences forming one of three characteristic stacking patterns: progradational, aggradational, and retrogradational parasequence sets (Van Wagoner et al., 1992). For example, an aggradational parasequence set is composed of vertically stacked individual coarsening- and thickening-upward parasequences of relatively equal thickness. The criteria that identify

the unconformable part of sequence boundaries in a single well-log, core or outcrop include a basinward shift in facies and a vertical change in parasequence stacking patterns (Van Wagoner, 1996). A parasequence (roughly tens of meters thick) is defined as a relatively conformable succession of genetically related beds or bedsets bounded by marine-flooding surfaces or their correlative surfaces (Van Wagoner et al., 1992). Parasequences have been identified in coastal-plain, deltaic, beach, tidal, estuarine, and shelf environments (Van Wagoner, 1985). The vertical facies associations of parasequences (coarsening-upward or fining-upward) are interpreted as progradational bedsets deposited in shoaling upwards depositional environments, which are abruptly overlain by deeper water deposits (marine flooding surface) of the next parasequence (Van Wagoner et al., 1992).

Applying these concepts to the Tertiary forearc basin of SW Washington, Armentrout (1987) delineated 4 major depositional sequences (6 to 21 m.y. in duration) related to regional tectonic events. According to the cycle time spans determined by Van Wagoner et al. (1996), these four depositional sequences are 2nd order megacycles (5 to 50 m.y. in duration). The McIntosh and Cowlitz formations and the lower Grays River Volcanics were deposited within Armentrout's (1987) sequence II (~6 m.y. in duration). Payne (1998) further subdivided the 1,000-m thick McIntosh Formation and the 1,240-thick Cowlitz Formation into five 3rd order cycles of 5 to 1 m.y. in duration (Van Wagoner et al., 1992). Payne (1998) determined the duration of the cycles was based on calculating an average sedimentation rate of a 1400-m section, from the base of the upper McIntosh Formation to the middle of the Cowitz Formation (Payne's unit 3). The upper-

lower McIntosh Formation contact and sequence boundary was correlated to the 42.5 Ma eustatic sequence boundary of Haq et al. (1987) providing an absolute date for the base of the section. A tuff in Cowlitz Formation unit 3 was Ar^{40}/Ar^{39} dated by Irving et al. (1996) at 38.9 Ma, providing an upper date that Payne (1998) used to calculate a sedimentation rate of 39 cm/1000 years for the 1400-m thick section. In this study a sedimentation rate of 22 cm/1000 years was calculated for the 690-m thick upper McIntosh and lower Cowlitz formations using the 42.5 Ma lower age of Chron 19r, coincident with the 42.5 Ma eustatic sequence boundary as correlative to the basal upper McIntosh Formation, and a Grays River lava flow Ar^{40}/Ar^{39} dated at 39.36 Ma conformably overlying the lower Cowlitz Formation (sample GR-2; Plate I, II).

Payne (1998) defined a lower sequence boundary separating the lower and upper members of the McIntosh Formation in Stillwater Creek due to an abrupt shoaling event and the absence of the lower to upper shoreface sandstone facies between the two members. Above the sequence boundary, upper McIntosh Formation parasequences of coal-bearing intertidal shoreface sandstone define a lowstand wedge of the lowstand system tract, resting on tuffaceous upper bathyal siltstones of the lower McIntosh Formation member. In the North Germany Creek section the lowest exposure (~9-m) consists of thin ripple-laminated heterolithic siltstone interbedded with thin micaceous mudstone of either the lower shoreface or tide-dominated prodelta depositional environments (see Depositional Environments) overlain by 50 m of subtidal sandstone bar facies. Due to the vertical juxtaposition of subtidal facies overlying lower shoreface facies, a sequence boundary is inferred between the two exposures, marking the

beginning of a depositional sequence. On the basis of stratigraphic position, relative thickness and facies associations, the subtidal lowest 50-m interval (SGC int. 39; Plate II) of Germany Creek is interpreted as correlative to the intertidal part of the upper McIntosh Formation sandstone member of Stillwater Creek (Payne, 1998), resting above the 42.5 Ma sequence boundary (Haq et al., 1987).

Beginning at meter 10 in the North Germany Creek section, two thickening and coarsening-upward parasequences of subtidal bar facies (up to 40-m thick) form a parasequence set interpreted to be a tide-dominated lowstand wedge prograding in an estuarine environment of a lowstand system tract (LST) of the upper McIntosh sandstone. Deposition of the lowstand wedge occurs after maximum sea level fall has caused exposure of the shelf and relative sea level slowly begins to rise. Deposition is restricted seaward of the previous shelf break (change from shelf to slope), and the lowstand-shoreline sequences are deposited on the previous shelf or upper slope (Van Wagoner et al., 1992).

At the NGC interval 38 – 35 (Plate II), a vertical succession of wave-dominated, progressively thinner and more distal coarsening- and thickening-upward parasequences form a characteristic retrogradational parasequence set of a transgressive system tract (TST). Although the transgressive surface separating the lower tide-dominated interval from the upper wave-dominated interval is not exposed in the Germany Creek section, the backstepping pattern of successively younger wave-dominated parasequences indicates flooding of the lowstand shelf and deposition of broad shoreface successions as the transgression continued. At meter 122 in the NGC section (thin section GC916C;

Plate II) an abundantly glauconitic silty micaceous mudstone is interpreted as the early part of a condensed section. Associated with intensive bioturbation and glauconite deposition, condensed sections usually represent a great deal of time due to continuous deposition of thin hemipelagic sediments as the shoreface parasequences step landward and the shelf is starved of terrigenous sediment (Van Wagoner et al., 1992). However, terrigenous sediment was deposited in this interval as an influx of fine-grained basaltic sandstone that may represent the either distal part of a grain flow introduced into the basin or lower shoreface reworked debris flow deposits. The condensed section may continue to section interval 35, where abundant bathyal benthic foraminifers are preserved (microfaunal sample 916D; Appendix A). A maximum flooding surface (MFS on Plate II) at this interval (NGC int. 35) representing the maximum relative sea level rise and subsequently the deepest paleo-bathymetry, is interpreted from the abrupt contact of the basaltic sandstone with overlying dark, benthic foramanifer-bearing, homolithic mudstone of the upper McIntosh silty mudstone.

The maximum flooding surface (MFS) or downlap surface marks the progression from a transgressive system tract to a highstand system tract (NGC int. 35 – 32), where the rate of relative sea level rise is at a minimum and parasequences begin to build basinward, downlapping the condensed section. The bathyal HST upper McIntosh silty mudstone is truncated by prograding inner shelf to lower shoreface successions of the Cowlitz Formation, indicating an abrupt change in water depth. The basinward shift in facies and observed scoured contact (Figure 9) suggest a sequence boundary between the two formations. Based on interval thickness, correlation with surrounding units,

magnetostratigraphy and benthic foraminifer age constraints, this sequence boundary defines the end of a complete sea level regression-transgression cycle or depositional sequence of the 3rd order (1 to 5 million years; Vail et al., 1977).

A rapid decrease in water depth is evident from the lithofacies and sedimentary structures (Figure 10) of the overlying depositional sequence of the lowest Cowlitz Formation from Germany Creek. The lowest shoreface succession (NGC int. 32 – 30; Plate II) consists of a 35-m thick coarsening- and thickening-upward parasequence overlain by a 40-m thick aggradational upper shoreface sequence interpreted as a delta front lowstand wedge (LST). Alternatively, this interval could represent a shelf-margin system tract (type-2 depositional sequence of Van Wagoner, 1996) or ramp margin lowstand wedge, due to the minor erosional truncation, lack of incised valley and thin wedge deposition observed. However, lacking the resolution to determine the basin geometries that define these particular types of system tract models, the more common type-1 model is applied (see Van Wagoner, 1996).

The overlying 38-m thick NGC interval 30-27 (Plate II) consists of two coarsening- and thickening-upward, backstepping, middle to lower shoreface parasequence interpreted as a transgressive system tract. The transgressive surface separating the two systems tracts is covered if present. An aggradational parasequence stacking pattern common to the early highstand system tract (HST) is interpreted from the 6 relatively equally thick progradational shoreface parasequences of NGC interval 27 – 21 (SGC int. 11 – 8) (Plate II).

Several shelf to upper shoreface progradational parasequences of the lower Cowlitz Formation interpreted as the late highstand system tract overlie the early HST aggradational parasequence set at NGC int. 21 – 13 (SGC int. 7-1). The progradational interval is 225-m thick, containing an increasing percentage of basaltic sandstone upward until conformably overlain by Grays River Volcanic lava flows causing cessation of the arkosic depositional system in the area.

Although no recent deep boreholes (some shallow coreholes have been drilled, Pauli, 2000, written communication), and no deep electric well-logs exist from the study area, subsurface data from a driller's log of the 1925 Castle Rock Oil and Gas Company Quigley No.1 well (TD = 2893 feet) were obtained from Washington Department of Natural Resources (center Sec. 18, T9N, R2W; Plate I and III). A simple stratigraphic column was sketched using the thicknesses and lithologies reported from the driller's log and compared with the Germany Creek measured sections to determine if lithologic correlations were possible. The lithostratigraphy and thicknesses of sandstone and shale units show a close lithostratigraphic correlation to the North Germany Creek section (Figure 15) (Plate III).

In figure 15, a thin coal-bearing sandstone interval at the base of the Quigley No. 1 well likely correlates to the lowstand, tidally-bedded upper McIntosh sandstone. Payne (1998) reported a thin coal bed overlying tidally-bedded sandstones in the upper McIntosh sandstone of Stillwater Creek. Overlying the thin coal-bearing sandstone of the

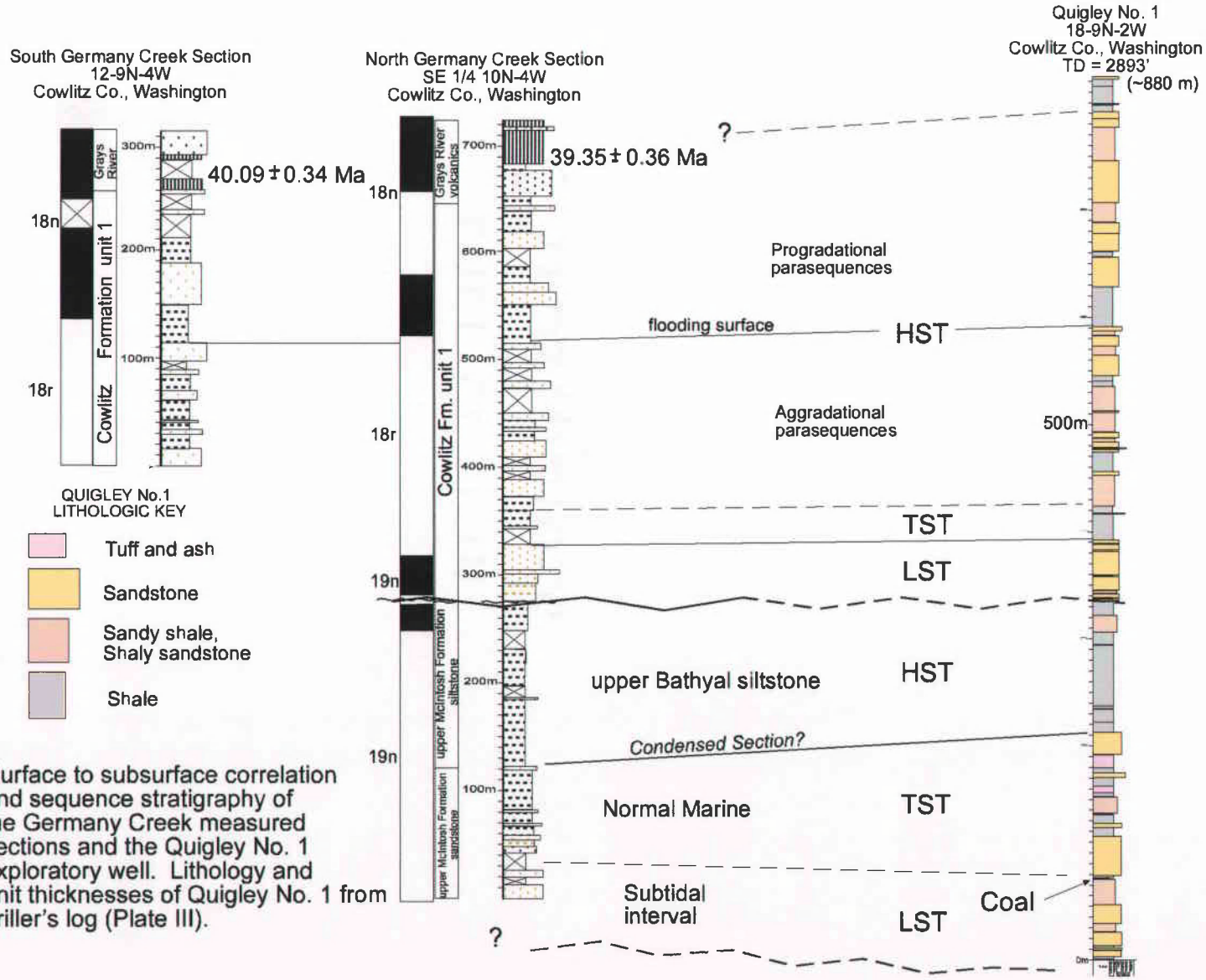

Figure 15. Surface to subsurface correlation and sequence stratigraphy of the Germany Creek measured sections and the Quigley No. 1 exploratory well. Lithology and unit thicknesses of Quigley No. 1 from driller's log (Plate III).

Quigley No.1 is a mixed normal marine sandstone and shale interval correlative to the backstepping transgressive system tract of the upper part of the lower McIntosh sandstone at Germany Creek. An overlying thick shale interval is correlative in thickness and lithology to the highstand system tract bathyal siltstone and minor thin-bedded turbidites of the North Germany Creek upper McIntosh siltstone unit. A ~50-m thick sandstone unit directly overlies the thick shale interval in the Quigley No.1 log, similar in thickness and lithology to the lowstand Cowlitz Formation unit 1 sandstone of Germany Creek. A 34-m thick shale interval overlies the ~50-m thick sandstone of the Quigley No.1 well is lithologically correlated to the transgressive sytem tract of the Germany Creek lower Cowlitz Formation. An aggradational sequence of thin sandstones and shaly sandstones of equal thickness is evident in the Quigley No. 1 log, correlative to the aggradational lower and middle shoreface sandstones of the lower Cowlitz Formation. A progradational shoreface sequence is interpreted overlying the aggradational interval from the Quigley No. 1 logs, similar in thickness and lithostratigraphy to the shelf to shoreface progradational interval from the upper part of the Germany Creek Cowlitz Formation (Figure 15).

The close correlation between surface exposed units of the Germany Creek measured sections (Cowlitz Formation informal unit 1A) to the west-northwest and the subsurface lithostratigraphy to the east-southeast suggests that the Cowlitz Formation forming the broad hills and valleys of the eastern part of the study area above the Quigley No. 1 well consist of Cowlitz Formation informal unit 1B or lower unit 2.

SEDIMENTARY PETROLOGY OF THE UPPER MCINTOSH AND LOWER COWLITZ FORMATIONS

Background

The 1979 discovery and development of a 60-70 BCF (Johnson et al., 1997) gas field near Mist, Oregon has shown the excellent reservoir production potential of the friable, arkosic sandstones of the Cowlitz Formation. Although some Cowlitz Formation sandstones contain high percentages of volcanic lithic grains, many have a micaceous feldspathic-quartzose mineralogy with porosities ranging from 14 to 41%, averaging 25%, and permeabilities ranging from 46 to 1,500 md, averaging 200 md (Armentrout and Suek, 1985). Reservoir sandstones of the Mist Gas Field are well-sorted and lack large amounts of volcanic rock fragments. These well-sorted feldspathic-quartzose sandstones are less susceptible to diagenetically formed pore-filling authigenic minerals than the lithic sandstones of other Cowlitz Formation horizons and depositional environments (Armentrout and Suek, 1985). Therefore, analagous potential reservoir rocks may exist locally in southwestern Washington in those areas of the middle to late Eocene coastal plain and shallow shelf where well-sorted feldspathic-quartzose arkoses accumulated with minimal intra-basinal volcanic rock fragment input.

Petrologic study of sixteen sandstone thin sections from the upper McIntosh and Cowlitz formations was conducted to determine the composition, provenance and diagenetic history (locations shown on Plate I and II; Appendix C). Four potential reservoir quality sandstones were stained with sodium cobaltinitrate to aid identification of potassium feldspar grains and point counted to determine the sandstone modal

composition of the framework grains. Results were then compared with the point counted reservoir sandstone (C&W sandstone) of the Mist Gas Field and the Skookumchuck Formation. Visual estimates of porosity and qualities of permeability were aided by commercial impregnation of blue dye into the pore spaces of the four lithic arkosic sandstones. X-ray diffraction (XRD) patterns and scanning electron microscopy analyses under the direction of Dr. Reed Glasmann of the Department of Geosciences, Oregon State University, were used to describe the clay mineralogy and morphology of the framework grains and intervening pore spaces to interpret the diagenetic history of one sandstone sample (G815B). This was performed by the author using a Phillips 3100 Automated X-Ray diffractometer (XRD) unit at the Department of Geosciences and a AMR 3100 scanning electron microscope under the direction of Al Soeldner in the Botany Department at Oregon State University.

LITHIC-ARKOSIC SANDSTONES

The four point-counted thin sections of the upper McIntosh and Cowlitz formations are identified as lithic arkoses according to the QFL sandstone classification of Folk (1974) (Figure 16). In this scheme, quartz grains (Q) include quartz and quartzite, feldspars (F) also include granitic and gneissic grains, and lithics (L) include all other rock fragments present. The samples were chosen from moderately well-sorted, friable, micaceous, fine- to medium-grained sandstones in the Germany Creek sections (Plate II). Sandstone sample 916E is from fine- to medium-grained, subtidal rhythmites of the upper McIntosh sandstone (NGC int. 39, Plate II). Sandstone sample 914A is a

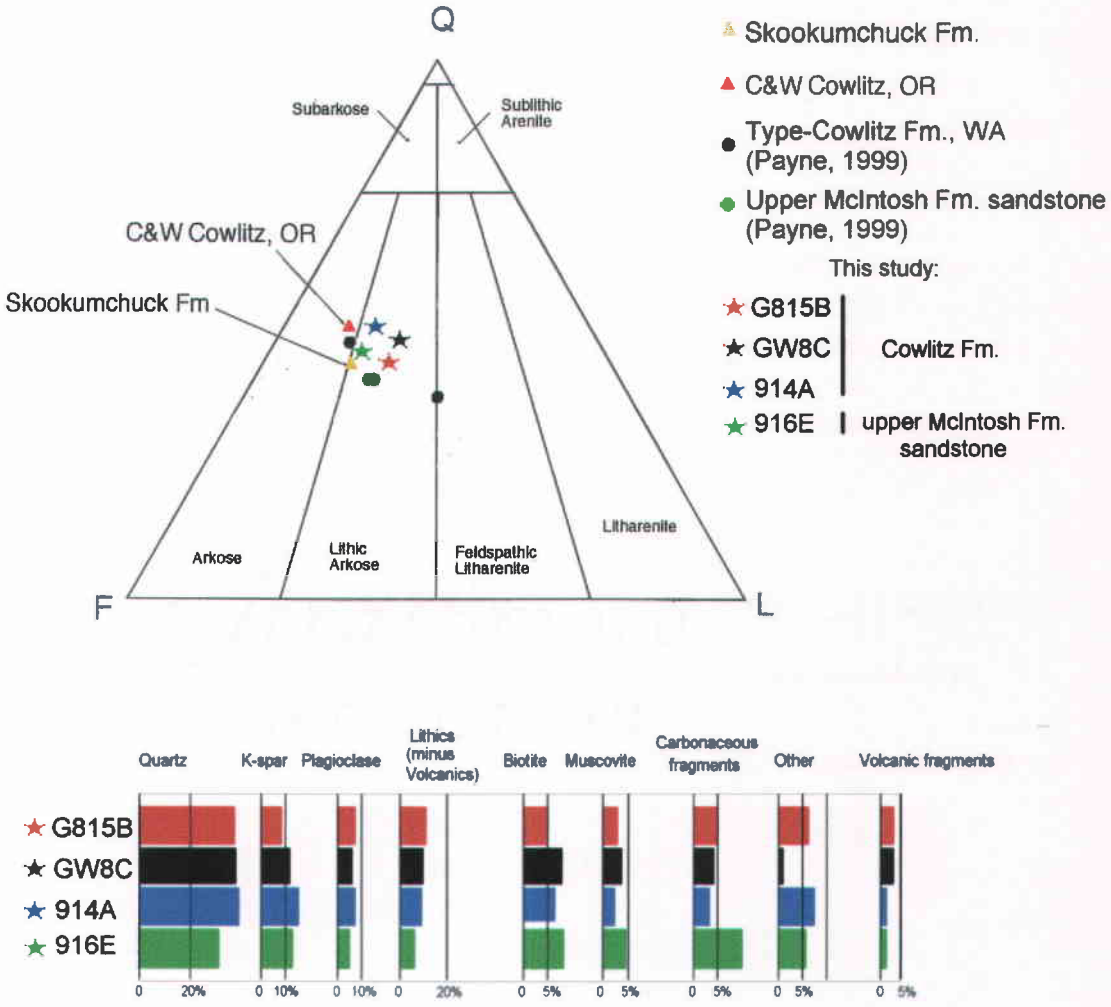

Figure 16. QFL ternary sandstone classification diagram (Folk, 1974) comparing mineralogic characteristics of reservoir and potential reservoir sandstones of the region.
The bottom bar diagram provides a more detailed framework grain composition summary of the upper McIntosh and Cowlitz formation potential reservoir sandstones of the study area.
Skookumchuck Formation and C&W member of the Cowlitz Formation data from Payne (1998).

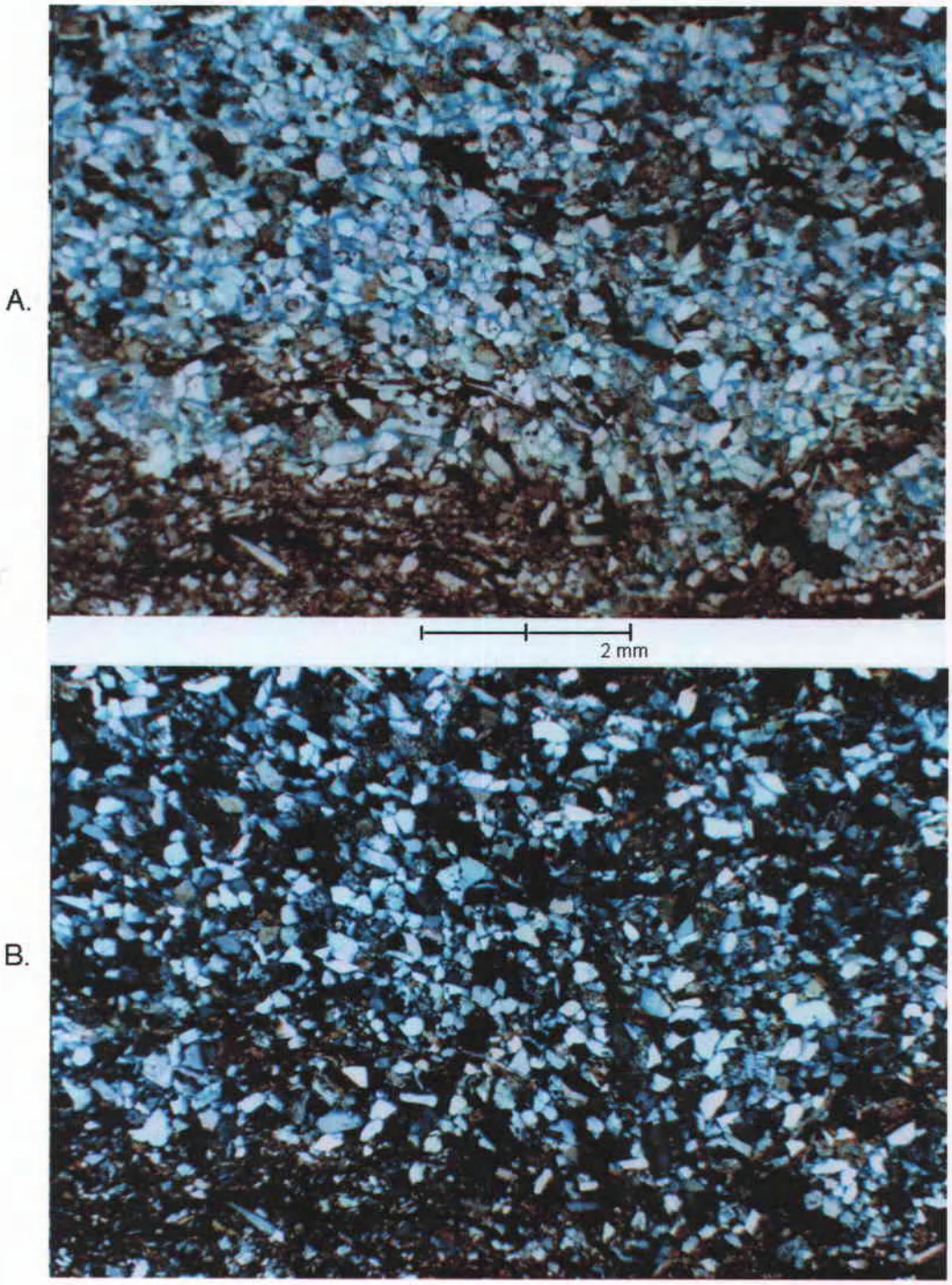

Figure 17. Photomicrograph of laminated, micaceous, carbonaceous lithic arkose from the upper McIntosh Formation sandstone (sample 916E, Plate I and II. Note dominant subangular monocrystalline quartz and feldspar grains, lateral interconnectivity of blue-dyed pore spaces vertically impeded by concentrations of carb. debris along laminae.
(A. Plane-polarized light, B. Crossed nicols)

medium-grained, upper shoreface sandstone from the first coarsening- and thickening-upward succession of the Cowlitz Formation (NGC int. 30; Plate II). Samples GW8C and G815B are from medium-grained, hummocky-bedded, middle shoreface sandstones of the Cowlitz Formation (SGC interval 10 and NGC interval 26, Plate II). Framework mineral grains identified during point counting include monocrystalline and polycrystalline quartz, plagioclase, potassium feldspar (K-spar), biotite, muscovite and minor hornblende and epidote (Appendix C). Rock fragments recognized include metamorphic clasts of schist and quartzite, myrmekitic microgranitic plutonic clasts, carbonaceous plant debris, and basaltic clasts with pilotaxitic, amygdaloidal and randomly oriented textures (Appendix C).

Framework grains of the micaceous, lithic arkosic sandstones mainly consist of subangular quartz and feldspars (Figures 16, 17 and 18). The sandstones lack a detrital clay fraction, classifying them as arenites. The quartz is dominantly monocrystalline, and is about twice as abundant as the feldspars (Figure 16; Appendix C). The ratio of potassium feldspar to albite-twinned plagioclase feldspar is roughly 2:1. Untwinned orthoclase feldspar is more abundant than gridiron twinned microcline. Lithic fragments are dominantly metamorphic, plutonic, and basaltic and comprise about 20% of the framework grains in these samples. Carbonized plant debris is common in the samples, with the greatestt concentration (10%) in the subtidal McIntosh sandstone (sample 916E). Additionally, the sandstones are highly micaceous, containing more biotite than muscovite, averaging 8 to 12% mica. Biotites are commonly brown and partially altered to greenish chlorite. Muscovite is not commonly deformed in the interstices between

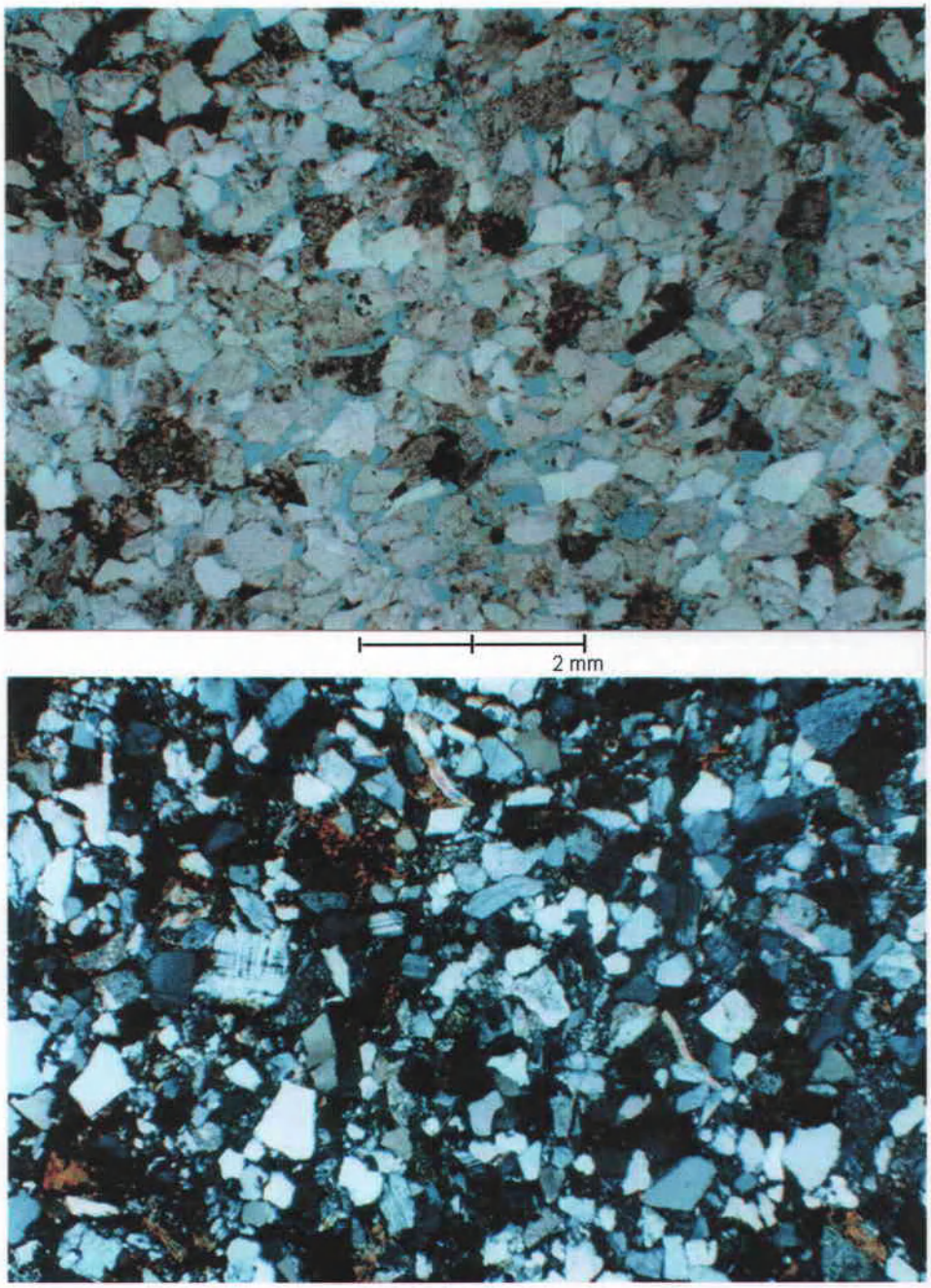

Figure 18. Photomicrograph of porous (blue-dye) micaceous, lithic arkosic sandstone of the Cowlitz Formation (sample G815B, Plates I and II). Note gridiron-twinned microcline and uncompressed muscovite flakes (B) between subangular monocrystalline quartz and feldspar grains. (A. Plane-polarized light, B. Crossed nicols. Photos from slightly different positions.)

A.

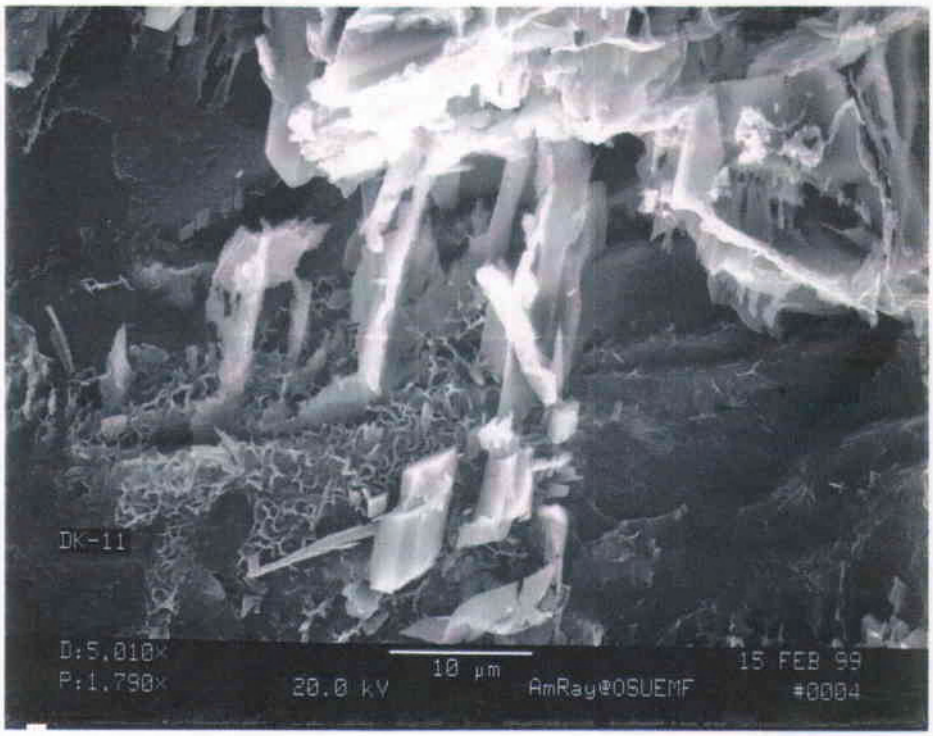

B.

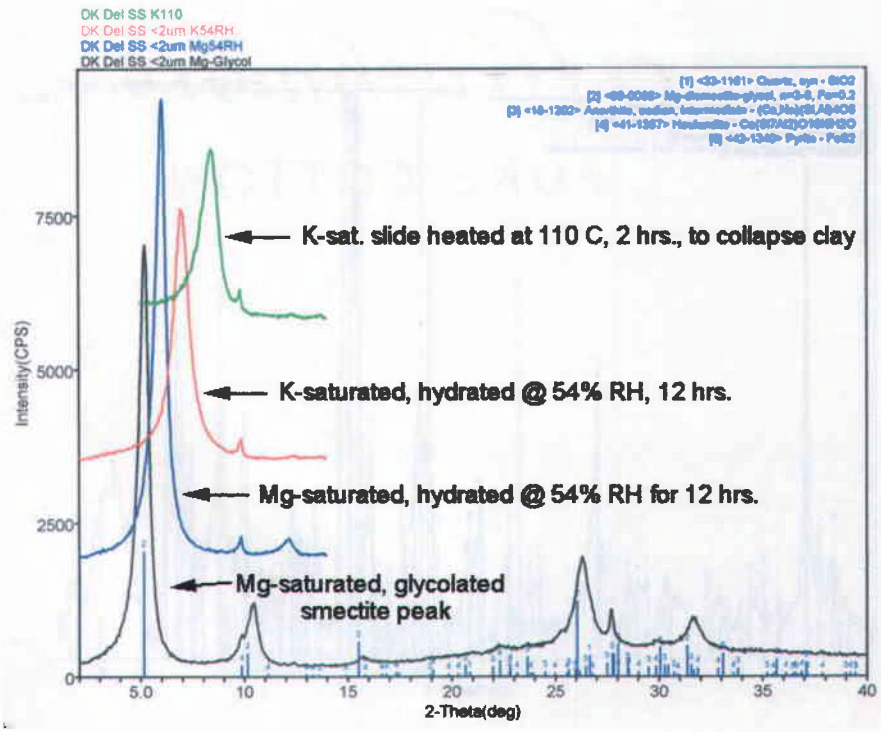

Figure 19. A) SEM image of a partially dissolved K-spar grain rimmed by leaf-like later-stage smectite overgrowths in Cowlitz Formation sandstone sample G815B.
B) XRD patterns from the clay-sized <2 micron fraction of sample G815B, showing a sharp-peaked, organized Mg-smectite.

more resistant framework grains, but some ductile schist, volcanic grains and carbonaceous plant debris have been deformed.

Basaltic fragments in the four lithic arkosic arenites are rare, but display a groundmass of plagioclase-phyric mixtures of pilotaxitic, amygdaloidal and randomly oriented textures. The pilotaxitic basalt grains have aligned plagioclase microlites similar to the Grays River Volcanics lava flows. Most basalt clasts have been partially altered to greenish celadonite, although some show a residual scoriaceous texture indicating little transport from the source to the site of deposition.

Grain contacts are commonly tangential indicating that the sandstone has not undergone intense burial compaction. Visual estimates of porosity by point counting of grains vs. pore spaces in the four impregnated samples (916E, 914A, GW8C, G815B) range from 16% to 19%. Porosity is mainly primary intergranular with minor secondary porosity formed by partial dissolution of plagioclase feldspar grains (Figure 19A) and volcanic rock fragments. The primary porosity is open and shows good interconnectivity, suggesting good permeability. However, vertical permeability in carbonaceous laminated sandstones (916E) is restricted. Pore throats are open between intergranular pores, with minor grain-rimming smectite clay the major authigenic cementing material present (Figure 19A). However, minor potassium feldspar overgrowths were observed on some grains. The source of the thin early diagenetic smectite may be from partial dissolution of *in situ* glassy basaltic fragments or altered volcanic ash fragments remobilized by pore water solution.

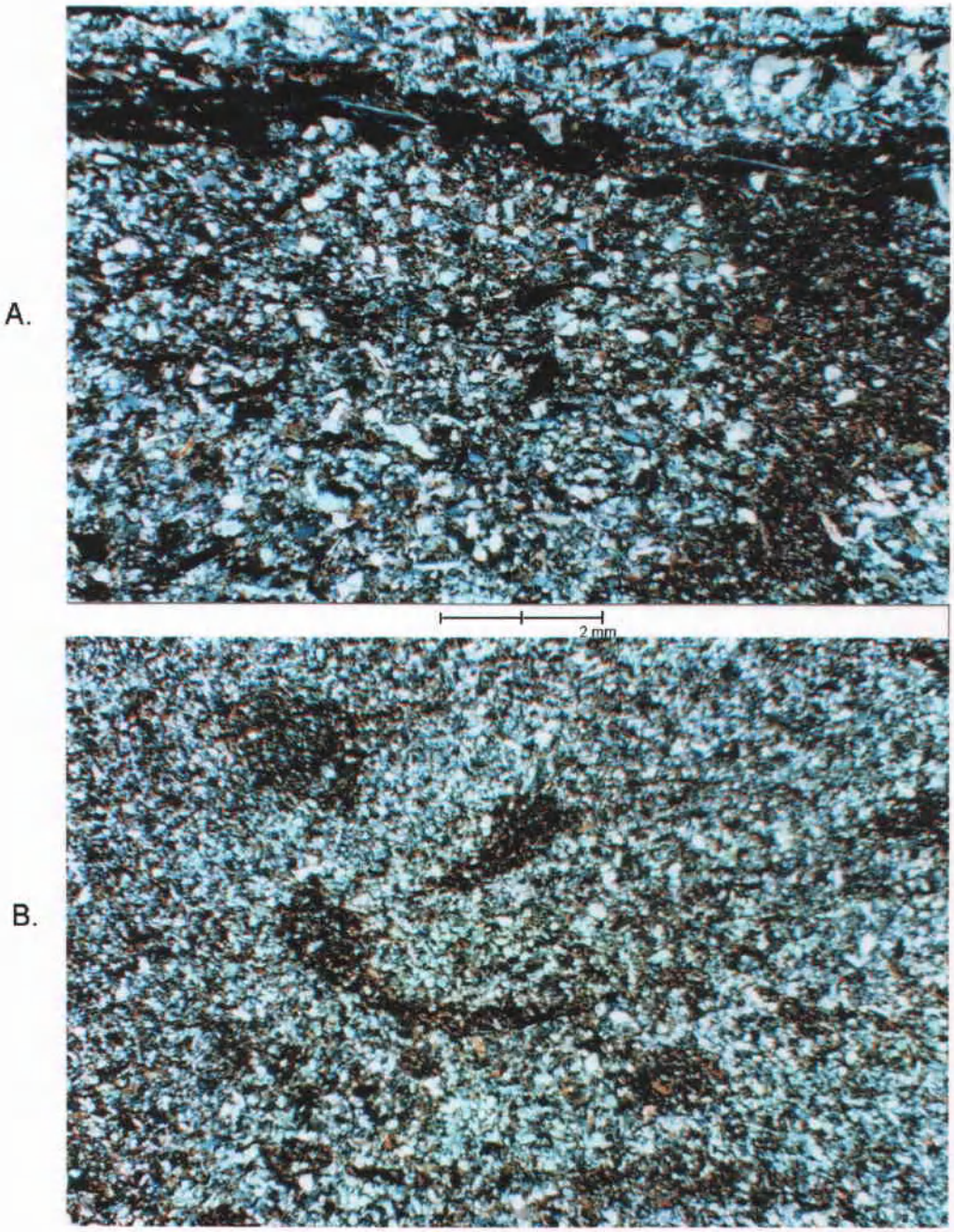

Figure 20. Photomicrographs of Cowlitz and McIntosh Formation siltstones.
A) Sample 811B (Cowlitz Fm.) ripple- to parallel-laminated lower shoreface siltstone. Note aligned black carbonaceous debris in lamina and abundance of fine mica (Plane-polarized light).
B) Sample 914H (upper McIntosh siltstone), bathyal turubidite siltstone. Note dark hook-shaped Phycosiphon burrows filled with organic debris and clay (Plane-polarized light).

Bulk powder clay mineral XRD analysis of sandstone sample G815B shows a pattern consisting of anorthite and albite, along with quartz, pyrite, smectite, and heulandite (a zeolite). The <2 micron fraction XRD pattern (Figure 19B) shows a sharp, narrow smectite peak that has been modeled using Newmod2 clay mineralogy software as a high N 12, Fe=1.7 mineral. Heulandite is also present in the <2 micron fraction, with minor secondary anorthite. SEM analysis of sample G815B shows smectite growing on a partially dissolved potassium feldspar grain Figure 19B). This relationship illustrates the diagenetic history of the sandstone, indicating that dissolution of potassium feldspars resulted in secondary porosity followed by formation of some later-stage smectite clay-rimming overgrowths. Some late stage zeolite (heulandite) grew on top of above the grain-rimming smectite clay (SEM and thin section analysis). Heulandite is a close mineralogic relative to clinoptilolite, which forms under shallow burial conditions.

SILTSTONES AND LITHIC SANDSTONES

Petrographic analysis of arkosic siltstone thin sections from the Germany Creek measured sections was conducted to compare lithologic and textural differences between Cowlitz Formation lower shoreface siltstones and a McIntosh Formation bathyal turbidite siltstone. Cowlitz Formation samples G811B and GR8C (above SGC int. 4; Plate II) were taken from a ripple- to planar-laminated carbonaceous siltstone of the lower shoreface facies (Figure 20A). The framework subangular, fine-grained sand- to silt-sized grains are dominated by monocrystalline quartz and feldspars (40%). There is an abundance of fine-grained biotite and muscovite, estimated at 25-30 % along with

abundant carbonaceous plant material (20-25%) in current-formed laminae (Figure 20A). Clay matrix is estimated at 10%, with little or no pore space.

Siltstone sample 914H was examined from the bathyal turbidite lithofacies of the upper McIntosh siltstone (NGC int. 34). It is characterized by 1-3 mm long hook-shaped *Phycosiphon* burrows (Figure 20B). Unlike the lower shoreface siltstones, very little carbonaceous plant debris was observed in thin section. Fine-grained to silt-sized, subangular quartz and feldspar grains form an estimated 50% of the rock volume, along with extremely fine-grained biotite (25%) and minor muscovite (5%). Clay-sized matrix is estimated at 5-10%, concentrated along *Phycosiphon* burrow traces (Figure 20B). Otherwise, clay-matrix is relatively minor from the unit as compared with the lower shoreface siltstones. Although there is likely more intergranular porosity in the bathyal siltstone relative to the shoreface siltstone due to an overall lack of carbonaceous material and clay-sized matrix, an estimated percentage of porosity was not determined due to the extremely small size of grains and microscopic pore spaces.

A poorly sorted, highly glauconitic, bioturbated lithic sandy siltstone from the upper McIntosh sandstone-siltstone contact was petrographically analyzed to further examine the mineralogy and texture of the unit (GC916C; below NGC int. 35; Plate II). Sample GC916C consists of an estimated 30-35% round green glauconite grains, minor fine- to medium-grained subangular quartz and feldspar (10%) and sub-rounded, coarse-grained plagioclase-phyric, pilotaxitic basaltic clasts (5-10%) within a carbonaceous muddy matrix (>50%). Some green grains may have relict cleavage suggesting clay alteration of feldspar. Minor fragments of collophane, possibly representing fossilized

A.

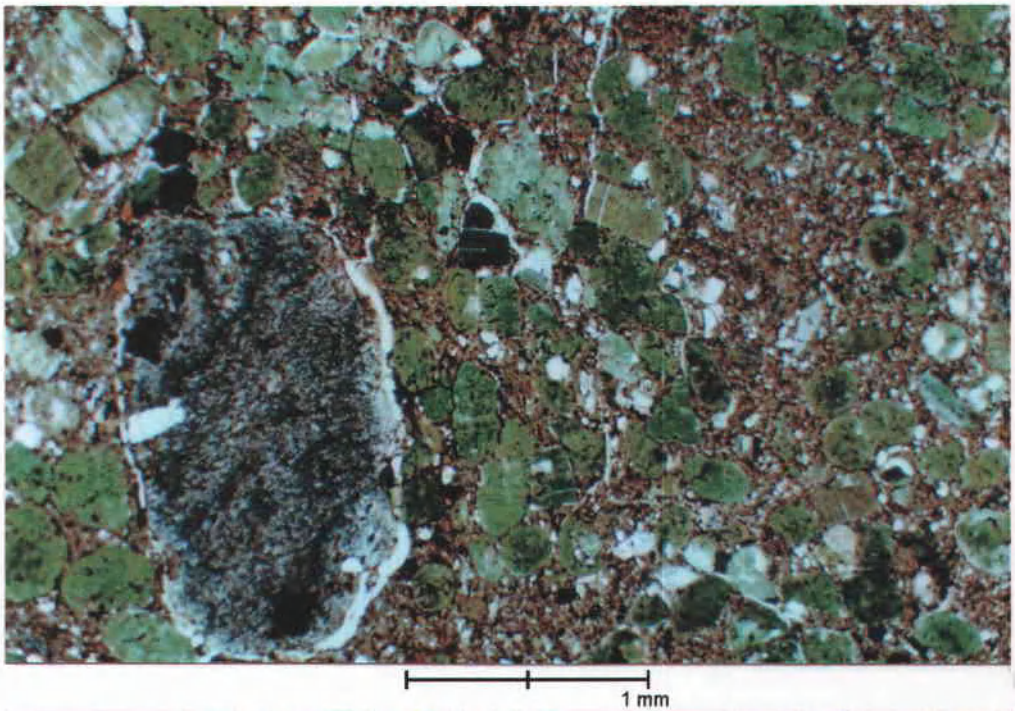

B.

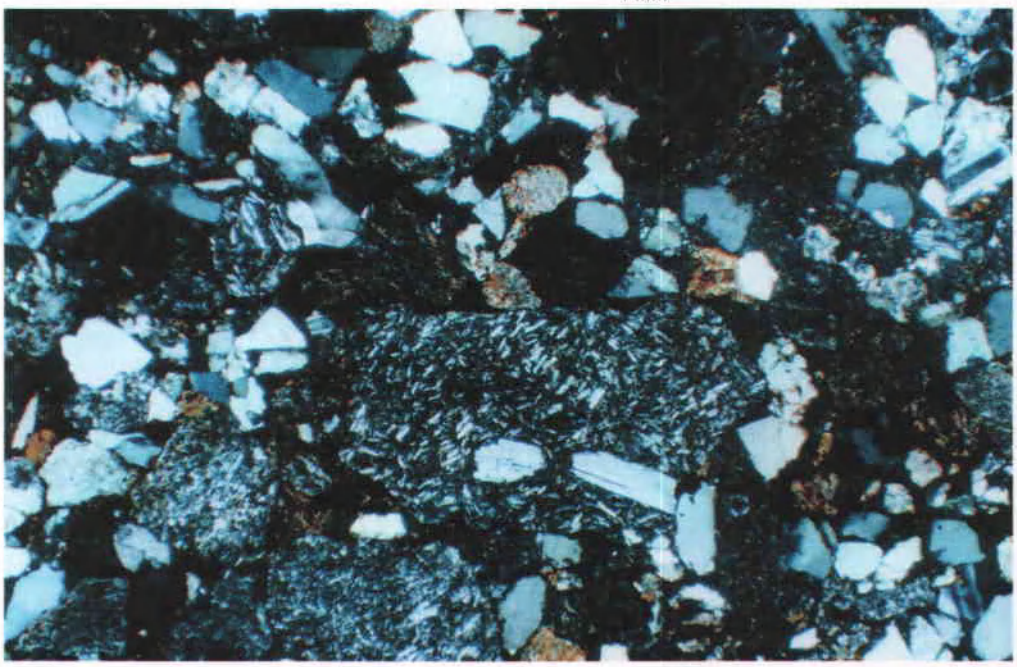

Figure 21. Lithic sandstones of the Cowlitz and upper McIntosh formations.
A) Sample GC916C, glauconitic, lithic sandstone from the base of a possible condensed section. Note rounded green glauconite grains and larger subrounded coarse sand-sized plagioclase-phyric basalt grain (upper McIntosh Fm., plane-polarized light).
B) Poorly sorted, basaltic sandstone of the Cowlitz Formation, sample G901C. Note mixture of textures of coarse basalt grains and fine- to medium-sand sized monocrystalline quartz and plagioclase (Crossed nicols).

fish scales were noted. Glauconite is believed to form under slightly reducing conditions authigenically on the seafloor by alteration of substrate materials such as fecal pellets in the earliest stages of deposition within the top few centimeters of muddy sediment, or the top few meters of coarse sandy sediment. Glauconite-rich sandstones and siltstones containing collophane (fish scales) are common features associated with condensed section deposition during the earliest stages of the transgressive system tract at or near the maximum flooding surface (Van Wagoner, 1996).

Basaltic lithic sandstones from the Cowlitz Formation (G901C, M711299) were analyzed petrographically to examine the basaltic grains for provenance determination. They are calcite cemented and are dominated by coarse sand-sized basaltic clasts. A coarse-grained basaltic lithic sandstone from the first coarsening- and thickening-upward succession of the lower Cowlitz Formation (sample G901C, Figure 21B) represents the first basaltic sandstone interbed described in the Germany Creek Cowlitz measured section (below NGC int. 31; Plate II). The sample is poorly-sorted, containing an estimated 40-50% subangular very coarse to coarse sand-sized plagioclase-phyric basaltic grains. The basaltic grains have randomly oriented, amygdaloidal and pilotaxitic textures and include minor scoriaceous fragments. Subangular fine to medium sand-sized quartz and feldspar grains make-up approximately 40% of the volume of sample G901C, with minor biotite (<5%) and clayey, carbonaceous matrix (5-10%). The basaltic fragments may have been originally transported from volcanic highland areas by fluvial processes or flood discharges and were subsequently reworked by shoreface processes and mixed with quartz and feldspar. The pilotaxitic basalt clasts have aligned plagioclase microlites

in an opaque-rich groundmass that is similar to the Grays River Volcanic lava flows (see Grays River Volcanics Petrology section). Four albite twinned plagioclase phenocryst compositions from very coarse grains of porphyritic basalt in sample G901C (Figure 21B) range from 67An to 81An (Labradorite) as determined using the Michel-Levy technique, consistent with a Grays River tholeiitic source.

The basaltic clasts in the basaltic lithic sandstones are interpreted to have been derived from a nearby Grays River intrabasinal volcanic highland based on lithology, subangular scoriaceous fragments, and their proximity to active basaltic volcanism. The presence of scoriaceous basaltic clasts suggests proximity to a volcanic vent as these delicate clasts would not likely survive extended transport or reworking. The dominance of basaltic grains and relatively meager amount of quartzose-feldspathic sand suggest only slight wave reworking in the shoreface environment prior to deposition. Also, the chemical composition of the plagioclase phenocrysts from the basaltic clasts in sample G901C are typical of an oceanic basaltic source such as the Grays River Volcanics. The basaltic clasts were most likely derived from the encroaching Grays River Volcanic high that eventually buried the Cowlitz Formation progradational shoreface deltaic successions of the Germany Creek area (Plate I).

SUMMARY

In summary, a general sequence of diagenetic events can be interpreted for the four point-counted friable lithic arkosic sandstones of the McIntosh and Cowlitz formations based on petrographic, XRD, and SEM analysis. As burial depth increased,

minor compaction squeezed some schist and carbonaceous plant debris between more durable quartz and feldspar grains. Mechanical compaction of quartz and feldspar grains is not observed. Most framework grain contacts are tangential, indicating only minor compaction by shallow burial. Partial dissolution of potassium feldspar resulting in secondary porosity and subsequent redeposition of potassium feldspar overgrowths likely occurred at maximum burial depth. Scanning electron microscope analysis shows grain-rimming smectite clays on secondary pore space of a partially dissolved potassium feldspar grain (Figure 19A). Authigenic smectite clay rims many framework grains acting as a weak cement, but has not filled much of the primary intergranular pore space in these lithic arkosic sandstones. The late stage zeolite (heulandite) is formed under shallow burial conditions, perhaps no greater than 2000 m (Glasmann, written communication, 1999). Porosities of the analyzed shoreface lithic arkoses in the study area are estimated at 16-19%, consisting of mainly primary intergranular porosity and represent potential reservoir sandstones.

Petrographic studies of the Cowlitz and McIntosh Formation lithic arkosic sandstones and siltstones, and volcanic lithic sandstones indicate a mixed extrabasinal felsic plutonic-metamorphic provenance and an intrabasinal basaltic source (Appendix C). The micaceous arkosic constituent sands of the Cowlitz and McIntosh Formation were fluvially transported from a dissected arc, most likely the Idaho Batholith. The basaltic clasts share textural and compositional affinities to the intrabasinal Grays River and Tillamook Volcanics of southwest Washington and northwest Oregon.

STRATIGRAPHY, PETROLOGY AND GEOCHEMISTRY OF THE GRAYS RIVER VOLCANICS AND ASSOCIATED SEDIMENTARY UNITS

Volcanic rocks including the high-titanium tholeiitic Grays River Volcanics erupted in the middle Eocene to upper Eocene (43 to 37 Ma) and accumulated around centralized volcanic centers or multiple vents in the forearc basin of southwest Washington and northwest Oregon. Eruptions of the Grays River Volcanics and Tillamook Volcanics of northwest Oregon at several volcanic centers has been related to middle to late Eocene forearc extension along a broad zone of right-lateral shear resulting from changes in Farallon-North American plate motion and convergence from 43 to 37 Ma (Armentrout, 1987). Both the Grays River and Tillamook Volcanics are oceanic-island tholeiitic basalts, consisting mainly of subaerial flows, although the lower Tillamook Volcanics consists of pillow lavas, breccia and feeder dikes (Snavely, 1987). In the study area, these basalt lava flows and mafic tuffs were referred to as the Goble Volcanics (arc derived) by Livingston (1966), however they were renamed by Phillips (1987) as Grays River Volcanics (forearc derived). Major geochemical differences in mean FeO, TiO_2 and SiO_2 percentage between the Grays River Volcanics and Goble volcanics enabled differentiation between the volcanic units (Phillips, 1987). A thick, extensive pile of Grays River Volcanics is located in the western half of the study area, and another smaller pile (Bebe Mountain) is located in the north-central part of the study area (Plate I, Figures 2 and 22).

The 46 to 42.5 Ma Tillamook Volcanics of northwest Oregon and the 42 to 37 Ma Grays River Volcanics of southwest Washington are chemically and petrologically

equivalent (Rarey, 1986; Kenitz, 1997). These volcanics are high-titanium oxide (3-4 % TiO_2), high iron-oxide (FeO) basalts, chemically distinct from the underlying lower TiO_2 and FeO Siletz-Crescent oceanic basalt basement and distint from the younger calc-alkaline Eocene to Oligocene Goble Volcanics to the east (Rarey, 1986). Lavas in both the Tillamook and Grays River Volcanics are characterized by pilotaxitic flow texture of aligned plagioclase microlites and titanoaugite within a black, glassy groundmass in thin section. However, the lavas of the Grays River Volcanics are dominantly basaltic in composition, whereas the Tillamook Volcanics contain some overlying more differentiated feldspar-phyric andesite and dacitic flows (Rarey, 1986).

A gravity study by the U.S. Geological Survey (Finn et al., 1991) reveals a large Bouguer gravity anomaly (>50 milligals) centered immediately north of the of the Columbia River that may be associated with a main eruptive center of the Grays River Volcanics (Figure 32). The Champlin Puckett well 13-36-5 on the south bank of the Columbia River (Sec. 36, T8N, R5W; Figure 22) drilled on the south flank of the gravity high and encountered about 1700 meters of Grays River Volcanic lava flows averaging 10-20 meters thick (Kenitz, 1997). However, this gravity high has also been related to thickened oceanic crust and relict seamount topography of the basement Siletz-Crescent basalts (Wells and Coe 1985; Stanley et al., 1996). Stanley et al. (1996) defined the discrete, fault-bounded crustal blocks of the Siletz terrane by gravity anomalies above 10 milligals (Figure 32). Alternatively, the very large (>50 milligal) anomaly may result from a composite effect of basement seamount topography overlain by a Grays River volcanic eruptive center.

Correlations of sedimentary and volcanic units in northwest Oregon indicate that the Tillamook Volcanics are stratigraphically lower than the Grays River Volcanics (Kenitz, 1997), suggesting that they are two separate volcanic centers. Kenitz (1997) and Robertson (1997) in subsurface stratigraphic studies of northwest Oregon concluded that the Tillamook Volcanics underlies the Cowlitz and Hamlet (upper McIntosh equivalent) formations and the overlying Grays River Volcanics are interbedded with the Clark and Wilson reservoir sandstone of the Cowlitz Formation (northern Mist Gas Field) (Figure 3).

Payne (1998) suggested that two subunits or episodes of Grays River volcanism based on stratigraphic (conformable – unconformable) relationships with underlying sedimentary units and radiometric ages collected across the oucrop belt of Grays River Volcanics in may be present in southwest Washington. An older and thicker pile crops out in the central and western part of the Willapa Hills, conformably overlying the Cowlitz Formation of the study area. (southwest quarter, Plate I). Another younger and thinner Grays River volcanic pile was mapped by Payne (1998) around Bebe and Abernathy Mountains (Figure 2, Plate I) and shown by mapping and subsurface corehole data (Pauli, 2000, written communication) to be unconformably overlying the Cowlitz Formation. Based on the conformable contacts of the dated Grays River basalt flows in Germany Creek with the underlying Cowlitz Formation and the presence of an angular unconformity between the two units around the Abernathy and Bebe mountain area (Plate I), this study suggests an intra-formational unconformity between the two Grays River Volcanic subunits at around 38-39 Ma (Plate I, cross section C – C').

LOCAL AGE DETERMINATION

Although the Tillamook and Grays River Volcanics are geochemically indistinguishable, they are largely time-separated units and can be separated stratigraphically. North of the Mist, OR area (Figure 2), flows of Grays River Volcanics increase in thickness; to the south of the Mist, OR area Tillamook Volcanic thickness increases (Kenitz, 1997). Most age dates of the Tillamook Volcanics are between 45 and 42 Ma, whereas ages of Grays River rocks range from 42 to 37 Ma (Kenitz, 1997). K-Ar ages from pillow basalts of the lower Tillamook Volcanics range from 46 to 43 Ma (Magill et al., 1981) with the upper subaerial part ranging from 43 to 42 Ma ($^{40}Ar/^{39}Ar$ dates; McElwee, in Payne, 1998). Niem et al. (1992) reported a $^{40}Ar/^{39}Ar$ date of 42.4 ±0.5 Ma for a flow near the top of the subaerial Tillamook Volcanics.

The lower Grays River Volcanics are interbedded with lower Narizian bathyal foraminifer of the Skamokawa Creek siltstone west of the study area, suggesting they could be as old as 43 Ma in the western Willapa Hills (Walsh et al., 1987) (Figure 22). Thus the Grays River Volcanics are perhaps partially age-equivalent with the uppermost Tillamook Volcanics of NW Oregon. The Ordway Creek porphyritic quartz monzonite and granodiorite stock (Wells, 1986), zircon fission track dated at around 41 Ma (Walsh, 1987), intruded the Grays River Volcanics to the west of the study area and contains inclusions of Grays River Volcanics. Four Grays River basalt samples from the study area were submitted to Dr. Robert Duncan of the College of Ocenaic and Atmospheric Sciences, Oregon State University, Corvallis for $^{40}Ar/^{39}Ar$ dating using a laser-fusion mass spectrometer. Two Grays River subaerial lava flows overlying Cowlitz Formation

shallow marine units from Germany Creek were $^{40}Ar/^{39}Ar$ dated at 40.01 ±0.34 Ma (GC-1) and 39.35 ±0.36 Ma (GC-2) (Appendix E, Plate I, Figures 22 and 23). Additionally two dikes with Grays River geochemistry intruding the Germany Creek measured sections have been $^{40}Ar/^{39}Ar$ dated at 39.98 ±0.29 Ma (914L) and 39.56 ±0.41 Ma (G810D) (Appendix E, Plate I, Figure 23). Of the four dates, only GC-1 and GC-2 can are significantly different in age, with GC-1 slightly older than GC-2.

A younger subunit of Grays River volcanic rocks was found from Abernathy and Bebe mountains to the northeast of the study area (Payne, 1998). The $^{40}Ar/^{39}Ar$ dates reported by Payne (1998) from this Grays River Volcanic subunit, as determined by Dr. Robert Duncan, from southwest to northeast are: (1) 38.64 ±0.40 Ma from southern Abernathy Mountain (Plate I) in the lower part of the pile, (2) 37.44 ±0.45 Ma from northwestern Bebe Mountain, and (3) 36.85 ±0.46 Ma from the upper part of the volcanic pile in Olequa Creek (Payne, 1998). Payne (1998), using subsurface corehole data penetrating Bebe Mountain and field-mapped relationships, established that the younger pile of Grays River Volcanics (Tgv2, this study) and associated sedimentary sequence (Tgvs2, this study) unconformably overlie the Cowlitz Formation. A $^{40}Ar/^{39}Ar$ age of 38.9 ±0.1 Ma was obtained from oligoclase crystals in a tuff bed from informal unit 3 (Payne, 1998) of the middle Cowlitz Formation in Olequa Creek (Irving et al., 1996). These dates constrain the unconformity between the Bebe Mountain pile of Grays River Volcanics and the Cowlitz Formation at 38 to 39 Ma.

However, in the study area the Cowlitz Formation south of Abernathy Mountain in Germany Creek is conformably overlain by Grays River subaerial flows dated at

40.01 ±0.34 Ma (GC-1) and 39.35 ±0.36 Ma (GC-2) (Plate I). A flow from the southern end of Abernathy Mountain unconformably overlying the Cowlitz Formation is dated at 38.64 ±0.40 Ma (Payne, 1998). Because the outcrop pattern of the Abernathy Mountain section of Grays River Volcanics is contiguous with the older, main outcrop distribution of Grays River to the south and west, an intra-formational unconformity and overlapping of the two piles of Grays River Volcanics is inferred in the study area (Plate I). The radiometric dates constrain the unconformity separating the lower Grays River Volcanics (Tgv1) conformably overlying the Cowlitz Formation from the upper Grays River Volcanics (Tgv2) unconformably overlying the lower Grays River pile and Cowlitz Formation to around 39 Ma (Plate I). The unconformity is not well-defined within the Grays River volcanic stratigraphy due to poor exposure, but is inferred from flat-lying flow tops of the upper pile overlying south dipping flow tops, exposed unconformable contacts between the Cowlitz Fm. and overlying Grays River flows, radiometric dates and magnetic stratigraphy.

MAGNETIC STRATIGRAPHY

A portable fluxgate magnetometer was used in the lab to determine the magnetic polarity of nine oriented basaltic rock samples from the field area (Plate I). Four samples (GC-1, GC-2, 914L and G810D) were tested again using another fluxgate magnetometer with the assistance of Dr. Paul Hammond of Portland State University. The re-test was conducted due to conflicting results of fluxgate determined basalt paleomagnetic polarities with interbedded sedimentary units run by Dr. Don Prothero of Occidental

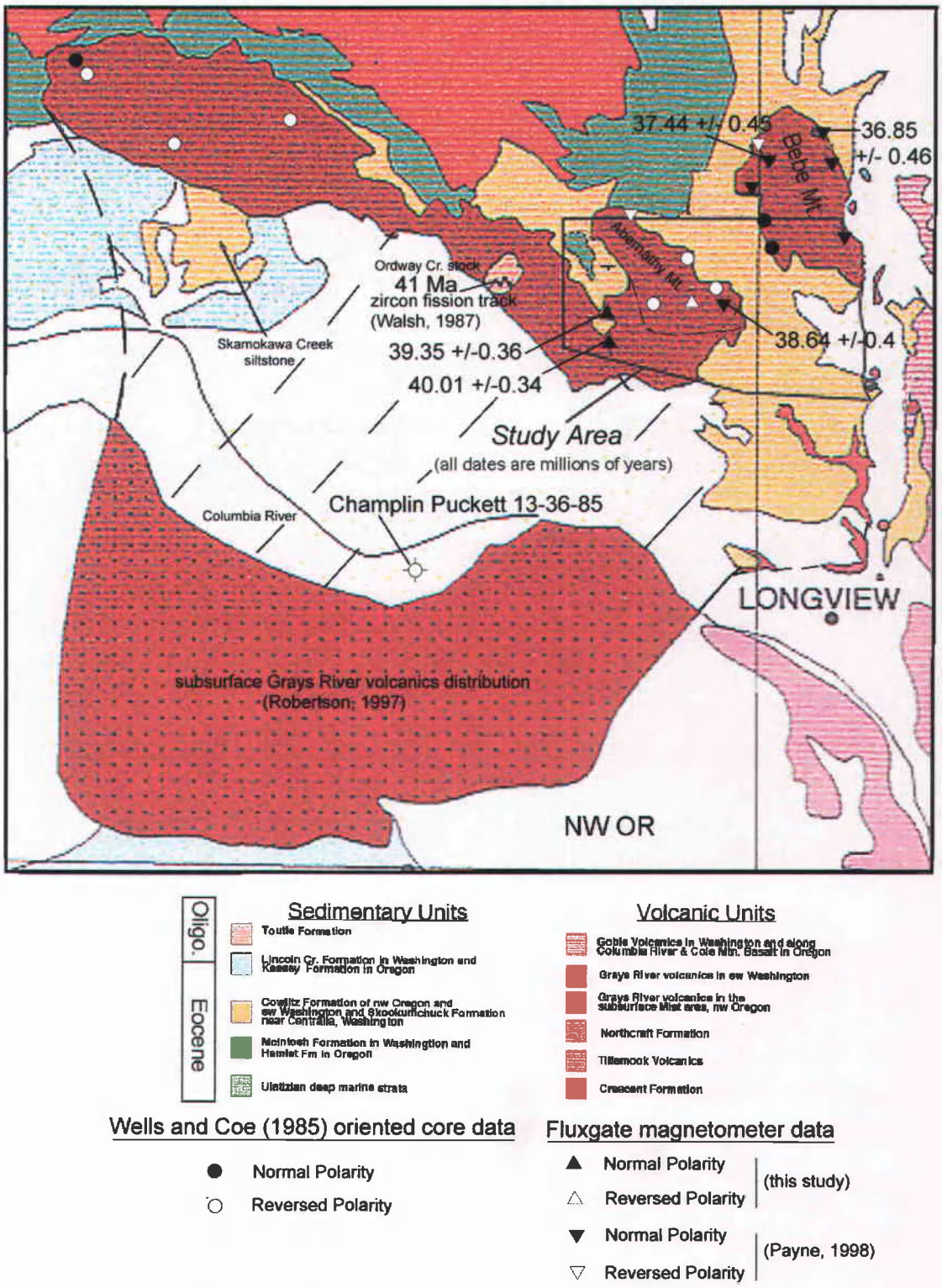

Figure 22. Grays River volcanics outcrop and subcrop map showing locations of radiometric age dates and magnetic polarity results.

College in Los Angeles using a 2G cryogenic magnetomer (for sedimentary section paleomagnetic results, see Regional Stratigraphy section). The signals of the basalt samples were weak and indeterminate for all but two of the nine samples of Grays River Volcanics. Fortunately, Wells and Coe (1985) sampled 5 sites of Grays River Volcanics in the study area using oriented drilled core samples which were analyzed at Stanford University with a cryogenic magnetometer (Figures 22 and 23). Also, Payne (1998) reported fluxgate-measured magnetic polarity for 3 sites from the Grays River Volcanics of the thesis area (Figure 22, 23).

The only direct results from this study regarding the polarity of Grays River Volcanics are from sample GC-1 (40.01 ±0.34 Ma; Plate I) normally polarized, and sample 626B NW ¼ of Sec. 11, T 9 N, R 3 W; Plate I), reversely polarized (Figure 22, 23). Oriented sample GC-2, dated at 39.35 ±0.36 Ma, was indeterminate. However, sample GC-2 conformably overlies normally polarized rocks (sedimentary section paleomagnetic site 13, NGC) and is conformably overlain by normally polarized site 12 (NGC), indirectly indicating that GC-2 is normally polarized (Plate II). The magnetic polarity of the dated Grays River dikes (914L and G810D) was indeterminate.

The oldest and lowest most flow of the Grays River Volcanics exposed in the study area (sample GC-1, 40.01 ±0.34 Ma) conformably overlies the Cowlitz Formation (SGC section, Plate II) and is normally polarized, placing it in Chron 18n (Figure 23). Also conformably overlying the Cowlitz Formation, slightly younger sample GC-2 (NGC, 39.35 ±0.36 Ma) is indirectly indicated to be normally polarized, placing it within Chron 18n (Figure 23). Based on age date correlation with the magnetic time scale of

Berggren and others (1995) (Figure 23), both dated Grays River dikes (914L and G810D) are correlated to Chron 18n. Reversely polarized sample 626B is from near the top of the Grays River volcanic pile (south central Abernathy Mt.) and is therefore correlated with the overlying Chron 17r (Figure 23).

The three magnetic sample sites collected by Wells and Coe (1985) are from the top of the Grays River Volcanics, southeast Abernathy Mt., and are reversely polarized (Figure 22). These reversely polarized rocks are correlated to Chron 17r, between 38.1 and 38.5 Ma (Figure 23). A normally polarized, 38.64 ±0.40 Ma (Payne, 1998) Grays River basalt flow from the same area of Abernathy Mt. unconformably overlying the Cowlitz Formation (Figures 22 and 23) may correlate to the uppermost part of Chron 18n.

The Bebe Mountain outcrop of the Grays River Volcanics has an age range of 37.44 ±0.45 to 36.85 ±0.46 Ma and best fits into magnetochronologic interval 17n (Figure 23) (Payne, 1998). Only one sample from the lower part of Bebe Mountain is reversed. This sample lies stratigraphically below the normally polarized 37.44 ±0.45 Ma dated Grays River flow, and likely correlates to one of the minor reversals within the base of Chron 17n.

In summary, the main pile of the Grays River Volcanics of the eastern Willapa Hills (Tgvs1; >41 Ma to 39.35 ±0.36 Ma) lies in Chrons 18r and 18n (Figure 23). Radiometric dates from the main pile of Grays River Volcanics in the south and west become younger to the north and east toward the youngest outcrops of Grays River Volcanics at Abernathy and Bebe mountains (Tgvs2, Plate I) (Figure 22, 23). A normal

polarity Grays River flow (Tgvs1) from Germany Creek (GC-2) dated at 39.35 ±0.36 Ma conformably overlies the Cowlitz Formation, whereas a normal polarity flow from south Abernathy Mountain (Tgvs2) dated at 38.64 ±0.40 Ma unconformably overlies the Cowlitz Formation (Payne, 1998). Thus, the local unconformity in the Germany Creek-Abernathy mountain area is between 39.35 ±0.36 and 38.64 ±0.40 Ma, equivalent to the uppermost part of Chron 18n and all of Chron 17r (Figure 23). The reversed polarity Grays River flows (Tgv2) of Wells and Coe (1985) are correlative with Chron 17r from 38.1 to 38.5 Ma, and unconformably overlap the normal polarity lower part of the main pile of Grays River Volcanics south of Abernathy Mountain. Farther to the northeast at Bebe Mountain, a younger pile (37.44 ±0.45 to 36.85 ±0.46 Ma) of dominantly normal polarity Grays River Volcanics, equivalent to Chron 17n, unconformably overlies the Cowlitz Formation, (Payne 1998).

GRAYS RIVER VOLCANIC STRATIGRAPHY

The volcanic rocks of Grays River (upper and lower) consist of augite-plagioclase phyric basalt flows interbedded with lesser mafic tuff, basaltic conglomerate, fluvial-lacustrine and marine lithic sandstone, and minor coaly intervals. The sequence was erupted in a southwest-deepening marginal-marine/deltaic environment (Phillips et al., 1989). On the east, Grays River subaerial lava flows are interbedded with shallow marine/deltaic arkosic sandstone and coal of the Cowlitz Formation (Figure 22) (Phillips et al., 1989). To the west the unit lies between deep-marine facies of the McIntosh Formation and the siltstone of Skamokawa Creek (Figure 22) (Phillips et al., 1989).

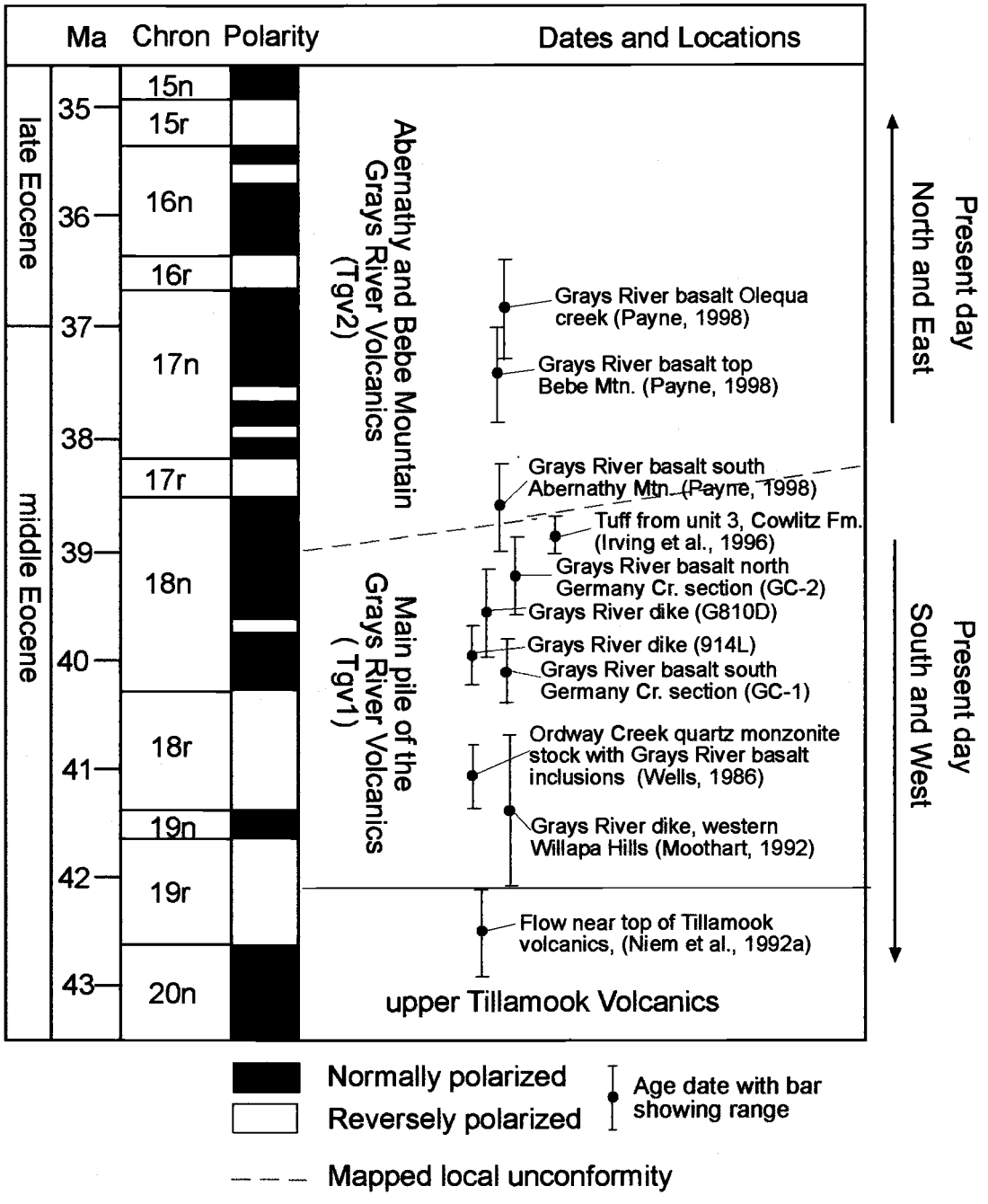

Figure 23. Magnetic polarity chart and radiometric age-dates of the Grays River Volcanics of the eastern Willapa Hills. Note decreasing age relationship of the Grays River Volcanics to the present-day north and east. Also note the two subunits of Grays River Volcanics are almost age continuous suggesting continued basaltic volcanism prior to, during and after the erosional unconformity formed between them. Locations and sources of age data are provided in the text.

The Grays River Volcanics in the study area consist of two mapped subunits (Tgv1 and Tgv2) separated by an intraformational unconformity, distinguished based on position of the unconformity above or below, age dates, magnetic stratigraphy, and structural attitudes. The lower subunit, Tgv1, has a maximum thickness of about 1250 m based on projection of structural dip and length of exposure along south Germany Creek (Plate I). The greatestt reported thickness of the Grays River Volcanics is from the Champlin Puckett 13-36-85 well (location shown on Figure 22) which penetrated 1700+ m of basaltic lava flow, tuff and volcaniclastic rock prior to ceasing drilling (Kenitz, 1997). The upper unit, Tgv2, is not well-defined in the thesis area, but is estimated to have a maximum thickness no greater than 300 m (Abernathy Mountain, Plate I, cross-section B – B'), averaging around 150 m. Both subunits have individual subaerial lava flows ranging in thickness from 3 to 25 meters.

Lower Grays River Volcanics

Unit Tgvs1 is defined as conformable between the overlying Grays River flows and underlying shallow marine, shoreface Cowlitz Formation sandstones, and consisting of a series of vertically stacked coarsening- and thickening-upward fossiliferous, pebbly basaltic sandstone and basaltic pebble to cobble conglomerate beds. Although difficult to define outside the Germany Creek measured section due to lack of continuous stratigraphic exposure, the conformable lower Grays River volcanic strata (Tgvs1) are also exposed at the NE ¼ of Sec. 15, T9N, R3W (Plate I). At this location, two 3 to 5 meter thick, thinly-bedded, coarsening-upward granular basaltic sandstone intervals are

overlain by fine-grained tuffaceous lithic sandstone beds (2 to 3 meters thick) containing unidentified bivalve casts and minor mica. This 20-m thick unit is identified as the lower Grays River volcanic strata based on similar structural attitude with the underlying Cowlitz Formation and apparently conformable overlying Grays River basalt flows (Plate I).

In Germany Creek, the 42 meters of the lower Grays River Volcanics strata include a bed containing a boulder-sized (100 cm x 90 cm), angular clast of Grays River Volcanics (Plate II, NGC meter 663). Bay oyster bank accumulations are common in this interval, owing to the abundance of hard substrate (see Cowlitz Formation Depositional Environment). This unit is interpreted as reworked debris flow deposits and channel deposits of Grays River Volcanic in the foreshore of a volcanic island. The uppermost part of this interval consists of a thin mudstone containing articulated juvenile bivalves, interpreted as a backshore lagoonal deposit. This lagoonal mud is overlain by 4 meters of clayey basal flow rubble and hyaloclastic deposits of a Grays River subaerial lava flow that entered the marginal-marine environment.

This augite-phyric, vesiculated-top, subaerial lava flow (sample GC-2, 39.35 ±0.36 Ma) is about 15 meters thick where exposed on the mainline road next to Germany Creek (SW ¼, Sec. 6, T9N, R3W). This flow is columnar-jointed and is vesiculated and slightly brecciated in the upper part. A 3.3-m thick interval of wavy-bedded carbonaceous mudstone and alternating tuffaceous, basaltic sandstone overlies the rubbly flow top. Overlying the interbedded sedimentary rocks is another subaerial lava flow, about 10 m thick. This flow is plagioclase- and augite-phyric, with a highly vesiculated,

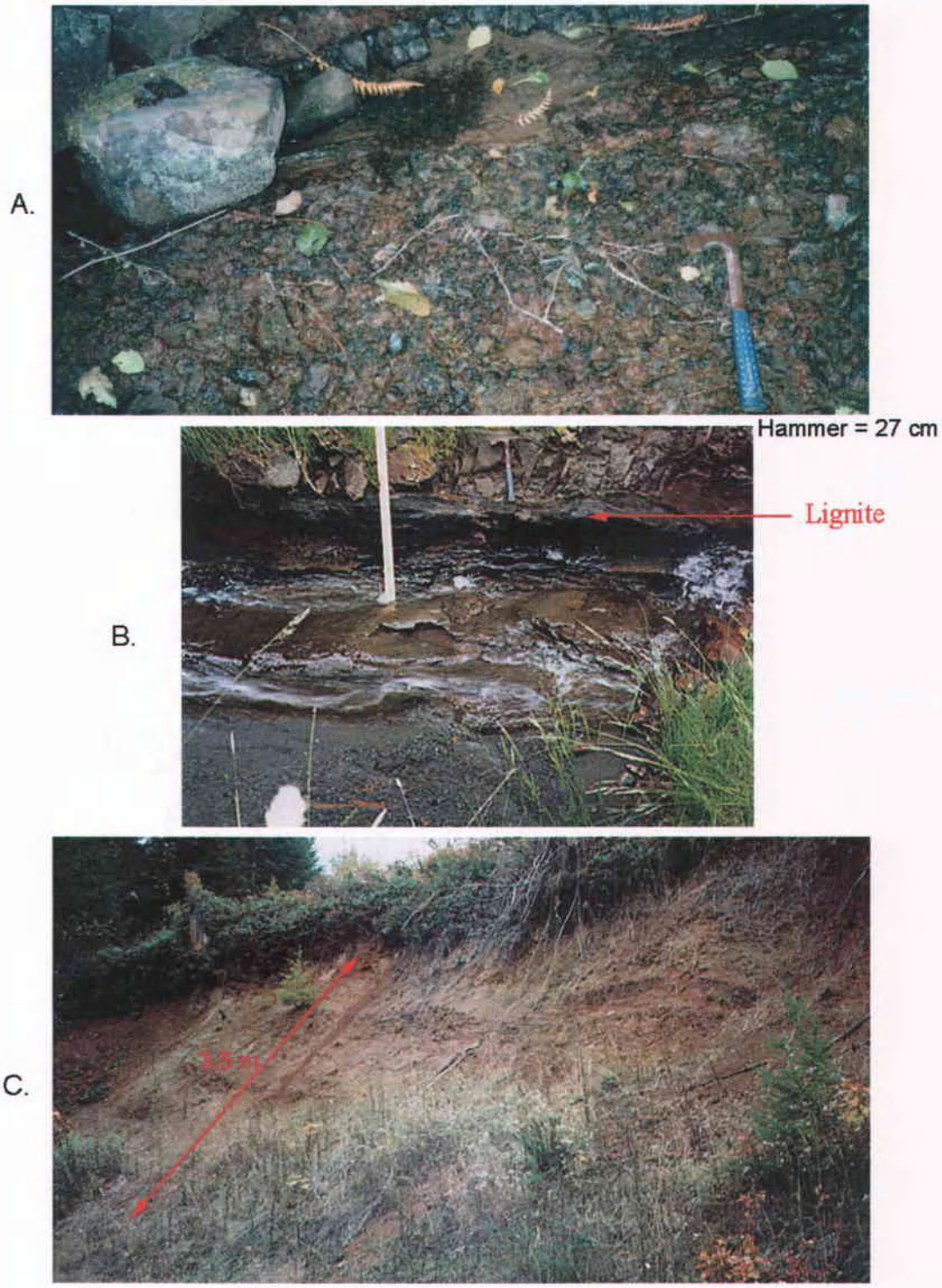

Figure 24. Outcrop pictures of Grays River sedimentary units.
A) 1.-m thick basaltic conglomerate interbed below subaerial lava flow (Germany Creek, SE 1/4, Sec. 14, T9N, R4W; Plate I).
B) Black lignite bed (30-cm thick) in tuffaceous sandstone (Tgvst, Plate I, Sec. 12, T9N, R4W).
C) Carbonaceous leaf-bearing tuff and siltstone in road exposure, Tgvs2 (NW 1/4, Sec. 1, T9N, R3W, Plate I).

scoriaceous base and top. The exposures of these two lava flows in Germany Creek are intruded by a 1.3-m thick basaltic dike. Overlying the second flow is a 1.5-m thick, sub-rounded, basaltic pebble (2 cm to 2 mm) conglomerate. The conglomerate is overlain by 1-m thick matrix-supported carbonaceous wood- and leaf-bearing basaltic conglomerate or mudflow deposit (NGC int 12). This is the last exposure north of the Germany Creek Fault (Plate I, see Structural Geology section).

The lowest exposed flow of the Grays River Volcanics (Tgv1) in the study area occurs in the South Germany Creek section, interval 1 (Plate II), where a subaerial lava flow sample (GC-1, dated at 40.01 ±0.34 Ma) conformably overlies a foreshore arkosic sandstone of the Cowlitz Formation. The baked bottom contact is abrupt with little or no scoriaceous flow breccia or hyaloclastic deposits. This grayish black augite-olivine-phyric to aphanitic flow (petrographic sample GC-1; Plate I and II) is about 3-m thick with a vesiculated top, overlain by a 65-cm thick lithic arkosic sandstone, in turn overlain by a 4-m thick, blocky to pseudo-colonnade, augite-olivine-phyric lava flow. Some larger vesicles are filled with zeolites and calcite.

Stratigraphically overlying these lowest flows in a tributary on the west side of Germany Creek is a 25 meter thick landslide-exposed coal-bearing, volcaniclastic tuffaceous sandstone interval (Tgvst, Plate I; SGC section, meter 292-315; Plate II). The basal part of the section consists of scoriaceous, vesicular basalt overlain by a 2-m thick, rusty-red to dark gray, tuffaceous, silty mudstone with leaf impressions. An overlying 70-cm thick, medium-grained basaltic sandstone fines upward and is capped by a 26 cm silty coal bed. Abruptly overlying the coal bed is a light gray claystone, grading upward

to a buff tuffaceous siltstone, 1.4-m thick. Above this interval, a 1-m thick, spheroidally weathered, massive, dark brown coarse-grained basaltic sandstone is overlain by a 5.6-m thick interbedded scoriaceous volcaniclastic sandstone with graded beds and tuffaceous mudstone intervals. A 1.6-m thick, overlying thin-bedded, scoriaceous volcaniclastic sandstone is capped by a 33 cm thick coal bed with anamolous interbedded sandy laminae (Figure 24B). The second coal is overlain by a fine- to medium-grained 1-m thick pebbly basaltic sandstone, deeply weathered to clay. The pebbly basaltic sandstone fines upward to basaltic lithic sandstone (1.4-m thick), overlain by a 15 cm thick lignitic coal bed. The coaly, tuffaceous sandstone interval (Tgvst, Plate I) is interpreted as a fluvial-lacustrine/swamp deposit between Grays River lava flows, possibly due to cyclic paleostream blockage by lava flows and subsequent coal marsh development.

Stratigraphically overlying the Tgvst interval are multiple (>34), stacked southwesterly-dipping Grays River volcanic lava flows averaging 10 m thick (ranging from 3 to 25 m thick) and minor interbedded, framwork supported, sub-rounded basaltic conglomerates (Figure 24A) and associated basaltic sandstones (averaging 3-6 m thick). Along with numerous covered intervals in south Germany Creek, and based on projection of flow-top dips to the south along the length of exposure to the southern border of the study area (Plate I), this interval is estimated at about 1250 m thick. A weathered, vesicular, augite-phyric basaltic flow (GC-4) from the uppermost part of this interval near the southern boundary of the thesis area was sampled for magnetic polarity (indeterminate) and geochemical analysis (see Petrology and Geochemistry of the Grays River Volcanics).

From interval 14 to 13 of the North Germany Creek measured section, shallow-marine basaltic sandstone dominates the section and is conformably overlain by clayey flow rubble and a dated subaerial lava flow (GC-2, 39.35 ±0.36 Ma). This 42-m thick interval was broken out of the Cowlitz formation, which it conformably overlies, and mapped as Tgvs1 to allow greater stratigraphic resolution in the study area.

The following discussion is from field mapping, sampling and observations of logging road and quarry outcrops of the generally southerly-dipping lower Grays River Volcanics (Tgv1) from the southwest quarter of the study area (Plate I). The rocks at sample site 51700 (NE ¼ of Sec.7, T9N, R3W; geochem.) consist of grayish-black, aphyric microcrystalline, slightly vesiculated basalt with minor (0.3 to 1 mm) augite phenocrysts (<5% of total) which weathers to rusty-brown. The exposed flow is approximately 4 meters thick with a blocky, pseudo-colonnade jointing. Other quarry exposures in the area (e.g. NW ¼ of Sec. 8, T9N, R3W; NW ¼ of Sec. 18, T9N, R3W, see outcrop map; Plate I) generally consist of 3 to 10 meter thick, columnar-jointed aphyric to augite- and plagioclase-phyric basalt flows with 1 to 2 meter thick vesiculated flow tops and clayey, rubbly, brecciated flow bottoms. A recent quarry excavation at the NW1/4 of Sec.17, T9N, R3W exhibits a 3-m thick vesiculated flow top overlain by a subangular fine-pebble basaltic conglomerate (1.5-m thick), grading upward into tuffaceous siltstone.

Upper Grays River Volcanics

A younger incised valley-fill sequence, the upper Grays River volcanic strata – unit 2 (Tgvs2) is inferred to partially overlie the lower Grays River Volcanics (Tgv1) south of Abernathy Mountain, around the Miocene Grande Ronde basalt capped mountain in the study area (SW quarter, Plate I). This interpretation is based on: (1) the mapped unconformity between the underlying Cowlitz Formation with the overlying Abernathy Mountain section of Grays River Volcanics (see NW quarter of Plate I), (2) radiometric age dates and magnetochronologic stratigraphy from various stratigraphic levels within the Grays River Volcanics (see Magnetic Stratigraphy section), (3) flat-lying upper flows overlying south (14 degrees) and north (17 to 31 degrees) dipping lower flows, and (4) the field-mapped, subsurface penetrated Grays River incised valley-fill strata present beneath Bebe Mt (Payne, 1998). The lack of laterally and vertically continuous exposures of Grays River Volcanics in the study area makes defining the position of the intra-formational unconformity and identifying the discontinuous upper Grays River unconformity-valley-fill unit (Tgvs2) difficult. The only diagnostic feature of unit Tgvs2 in the study area is its stratigraphic position above the unconformity. Both Grays River sedimentary units (Tgvs1 and Tgvs2) contain shallow marine interbeds, tuffaceous lithic sandstone, carbonaceous mudstone and basaltic pebble conglomerate.

Payne (1998) described the Grays River unconformity valley-fill strata underlying upper Grays River Volcanics flows of Bebe Mountain. The upper Grays River sedimentary unit is mainly evident in the subsurface under the western part of Bebe Mountain and the southern part of Abernathy Mountain, ranging in thicknes from 0 to

over 200 meters (Pauli, written communication, 1996 in Payne, 1998; cross section C-C, Plate I). The unit also crops out in places along the southwest margin of Bebe Mountain and the southern and western (this study) part of Abernathy Mountain (Tgvs2, Plate I) (Payne, 1998). The upper Grays River strata may have been deposited within down-dropped blocks of lower Grays River Volcanics and/or Cowlitz Formation after, or contemporaneously with an episode of uplift and erosion (see Regional Correlation and Structural Geology sections).

According to Payne (1998), the lower part of the upper Grays River volcanic-arkosic sandstone unit consists of reworked Cowlitz Formation lithic arkosic sandstone and siltstone, making identification and mapping of the part of the unit where it overlies Cowlitz Formation very difficult. The upper part of the sedimentary unit, consists of basaltic sandstone, tuffaceous siltstone and basaltic breccia; the unit directly underlies the Grays River Volcanics and has similar dip. Shallow-marine Tellina cowlitzensis clams were identified from a siltstone underlying the Grays River Volcanics at Abernathy Mountain (SW ¼ of Sec. 21, T10N, R3W; Plate I) (Payne, 1998). At the southern end of Abernathy Mountain, (NW ¼ of Sec. 1, T9N, R3W; Plate I) a thin-bedded, 5-m thick, leaf-bearing, basaltic tuff is exposed (Figure 24C). On the western flank of Abernathy Mountain (SE ¼ of Sec.24, T10N, R4W; Plate I) another outcrop of the upper Grays River sedimentary unit is exposed. At this locality, a 5-m thick, buff to white tuffaceous siltstone with leaf imprints and randomly oriented silicified stem debris unconformably overlies the Cowlitz Formation and is overlain by upper Grays River lava flows.

Conformably overlying the upper Grays River sedimentary unit (Tgvs2, Plate I), are subaerial, dominantly aphyric to microphyric columnar-jointed upper Grays River lava flows (Tgv2). To the north of the leaf- and woody-debris bearing tuffaceous siltstone of the upper Grays River sedimentary unit (Tgvs2, Plate I) of western Abernathy Mountain, a quarry exposes a 14-m thick, aphyric radially jointed upper Grays River lava flow (Figure 25A), interpreted to be a filled lava tube. Although no pillow-basalt structures were observed from the outcrop, it is possible the radial-jointing pattern could be the result of a subaqueous lava tube fill. To the south, but roughly stratigraphically equivalent to the radial-jointed upper Grays River basalt is a 15-m thick blocky to columnar-jointed subaerial lava flow with a 3 to 4 meter thick scoriaceous, vesiculated flow top (Figure 25B). The flow is sparsely vesicular and microphyric, with dispersed, small (1-2 mm) augite phenocrysts (5%) in a grayish black groundmass. Geochemistry sample 6170B (Quarry at the NW ¼ of Sec. 32, T10N, R3W, Plate I) was collected from an aphyric, extremely vesiculated, flat-lying upper Grays River lava flow. The basalt was analyzed geochemically to determine if it was a Miocene Grande Ronde flow or Eocene Grays River flow due to its stratigraphic position and textural similarities to the nearby exposures of Grande Ronde (Sentinel Bluffs unit) basalt. Geochemistry sample 626B (reversely polarized, upper Grays River Volcanics flow) was taken from a quarry exposure (NW ¼ of Sec. 11, T9N, R3W, Plate I) of three flows dipping to the northwest. The entire exposure is about 12-m thick, with each flow about 4 m thick. The columnar-jointed, aphyric flows have 1-m thick brecciated flow bottoms and vesiculated flow tops. An upper Grays River, aphyric, columnar-jointed basaltic lava flow with subordinate

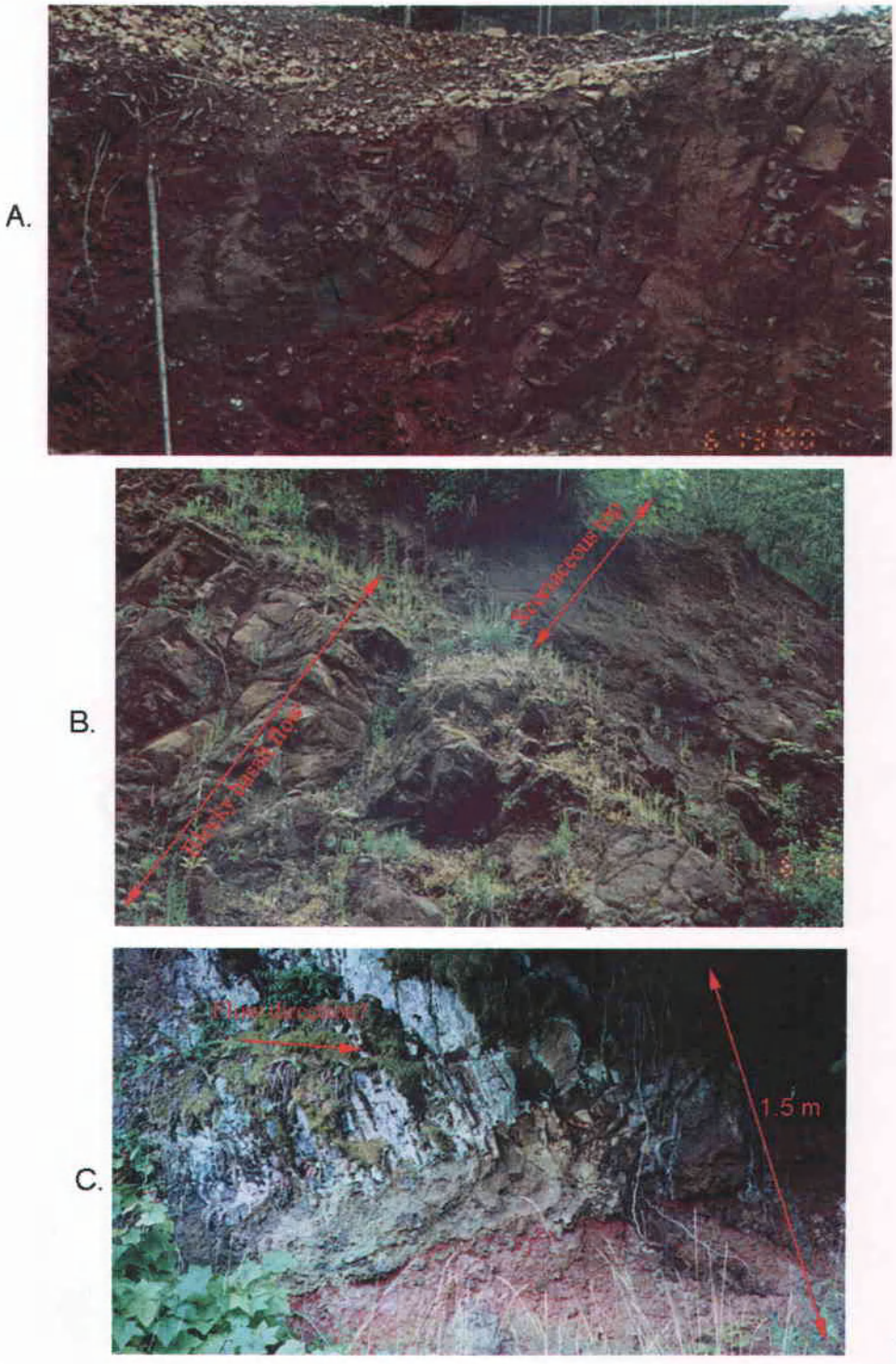

Figure 25. Outcrop photographs of upper Grays River basalt flows.
A) Quarry with radial-jointed aphyric basalt, ~14-m thick (NE 1/4, Sec. 24, T10N, R4W).
B) Road exposure of blocky, 15-m thick subaerial lava flow with less resistant scoriaceous top (NW 1/4, Sec. 32, T10N, R4W).
C) Reddish scoriaceous flow-base breccia and overlying bent relict-flow colonnade (SE 1/4 of Sec. 3, T9N, R3W).

interbedded tuffaceous strata is exposed in another quarry (SW ¼ of Sec. 32, T10N, R3W; Plate I) (geochemistry sample 51703). A very well-exposed flow base, most likely from an upper Grays River subaerial lava flow, but near the middle of the entire Grays River volcanic sequence is shown in Figure 25C (S ½ of Sec. 3, T9N, R3W). Reddish scoriaceous flowbase breccia abruptly underlies the augite-microphyric basaltic colonnade. The bottoms of the colonnade are locally bent in relict flow direction to the northwest (Figure 25C).

DIKES OF THE GRAYS RIVER VOLCANICS

Numerous thin dikes of Grays River basalt intruding the upper McIntosh and Cowlitz formations, and Grays River Volcanics are exposed along the Germany Creek measured sections (Plate I). Fifty-one, 1 to 12-meter thick dikes were mapped (averaging 2-3 meters thick), with at least an equal number of thinner dikes left unmapped (Plate I). The southwest-northeast trending dikes generally are sub-parallel to the strike of the intruded unit and perpendicular to the angle of dip. Subordinate conjugate northwest-southeast trending dikes are present. Dikes are also associated with some fault zones in Germany Creek (see Structural Geology section). The dikes cannot be traced laterally from the bed of Germany Creek, but appear to be tens to hundreds of meters in length.

The dikes range from plagioclase- and augite-phyric basalt with microcrystalline groundmass, to zoned dikes with aphyric margins and plagioclase-glomerophyric interiors with microcrystalline groundmass. Two peperite dikes were noted, one intruding Grays River Volcanics and consisting of brick red vesiculated clasts and

angular Grays River pebble-sized clasts. The other intrudes the upper McIntosh siltstone unit and consists of angular, glassy basalt and baked siltstone. At 12 m thick, the thickest dike described from the study area (sample 914L) displays a 3-4 meter chilled aphyric margin which encloses a distinctive radial, acicular to disc-shaped plagioclase glomeroporphyritic (20%) basalt with a microcrystalline groundmass (W ½ of Sec. 25, T10N, R4W). The subhedral, radial, plagioclase glomerocrysts are about 1 to 1.5 cm in diameter (Figure 26A). Other plagioclase glomeroporphyritic dikes with microcrystalline groundmass are present along Germany Creek (see Grays River Petrology section). Some spherical to ovoid amydaloidal basaltic dikes indicate shallow emplacement and declining pressure. The 1 to 5 mm amygdules are commonly filled with zeolites and calcite.

Two Grays River dikes were $^{40}Ar/^{39}Ar$ age dated: sample 914L, 39.98 ±0.29 Ma; and sample G810D, 39.56 ±0.41 Ma. Dike sample 914L intrudes the North Germany Creek section upper McIntosh siltsone near interval 34, just south and east of Abernathy Mountain and trends northwest-southeast. Dike sample G810D intrudes the South Germany Creek section lower Cowlitz Formation near interval 4 (Plate II), trending southwest-northeast. These relationships are discussed further in the Structural Geology section.

A.

B.

Figure 26. A) Radial glomeroporphyritic plagioclase phenocrysts of the 3 to 4 m thick interior of a 12-m thick Grays River dike, sample 914L. Note 27-cm rock hammer for scale (location in text).
B) Typical jointed Grays River aphyric dike intruding tan fine-grained Cowlitz Formation sandstone along the South Germany Creek section, near interval 3 (Plate II).

PETROLOGY AND GEOCHEMISTRY

For this study, fourteen thin sections of the Grays River Volcanics were commercially cut and mounted through financial assistance of the Washington Department of Natural Resources. Thin section samples were collected along the Germany Creek measured sections to determine the mineralogic and textural variation of the flows and dikes. Of these, four samples are from interbedded Grays River sedimentary units, two from the Grays River terrestrial sedimentary unit (samples 628GB and 628C; unit Tgvst) and two from the lower Grays River marine sedimentary unit (samples GT8A and GR8A; unit Tgvsl) (Plate I and II). The remaining ten thin sections consist of six glomeroporphyritic to microphyric Grays River basalt dikes (samples 914L, GC-4, G810D, GT8L, 617A and G815C) and four porphyritic Grays River basalt lava flows (samples GC-1, GC-2, GC-3 and GC-5) (Plates I, II).

Data from twelve samples analyzed for major oxide and trace element geochemistry characterize the geochemical composition of the Grays River basalt flows and dikes of the thesis area. Five Grays River basaltic dike samples in Germany Creek were collected for geochemical analysis: 914L, GC-4, G810D, GT8L, and M511299 (see Appendix D; Plate I and II, Figure 28). Seven Grays River basalt flows were analyzed: GC-1, GC-2, GC-3, 51700, 51703, 6170B and 626B (see Appendix, Plate I and II, Figure 28). Geochemical analyses of the twelve samples were provided by the Washington Department of Natural Resources, under the supervision of Tim Walsh and Karl Wegmann. The samples were submitted for x-ray fluorescence analysis (XRD) to the Washington State University GeoAnalytical Labratory. XRD analyses consist of 10

major and minor element oxides and a suite of 17 alkaline earth and transition trace elements (Appendix D). Six samples were also run using ICP-MS analysis at Washington State University GeoAnalytical Laboratory to determine 27 trace element amounts (4 of these are Grays River lava flows: 51700, 51703, 6170B and 626B; Appendix D).

Grays River Sedimentary Units

Thin section GR8A (Figure 27) is from the lowest part of the Grays River Volcanics sequence, mapped in the study area as nearshore, lower Grays River Volcanics sediments (Tgvs1) confomable with the Cowlitz Formation and overlying subaerial lower Grays River lava flows (Tgv1) (NGC int. 13; Plate II). The sample, illustrated in Figure 27A, is from the base of a 1.5-m thick bay oyster bank deposit. The coarse-grained, basaltic, silty sandstone consists of pilotaxitic, intersertal and altered glassy basaltic clasts (85% visual estimation). Some basaltic fragments groundmass have been altered to clay and are squeezed between more brittle framework grains as a pseudo-matrix during compaction. Minor plagioclase, monocrystalline quartz and clinopyroxene (augite) grains are also present. The sparry calcite cement of the sandstone was most likely derived from insitu dissolution of aragonitic mollusc shells. These basaltic clasts may have originally been transported from volcanic highland areas by fluvial processes, flood events, or debris flows, but were subsequently reworked by wave processes and mixed with minor quartz and feldspar in a shallow-marine or distributary mouth bar environment (Figure 27).

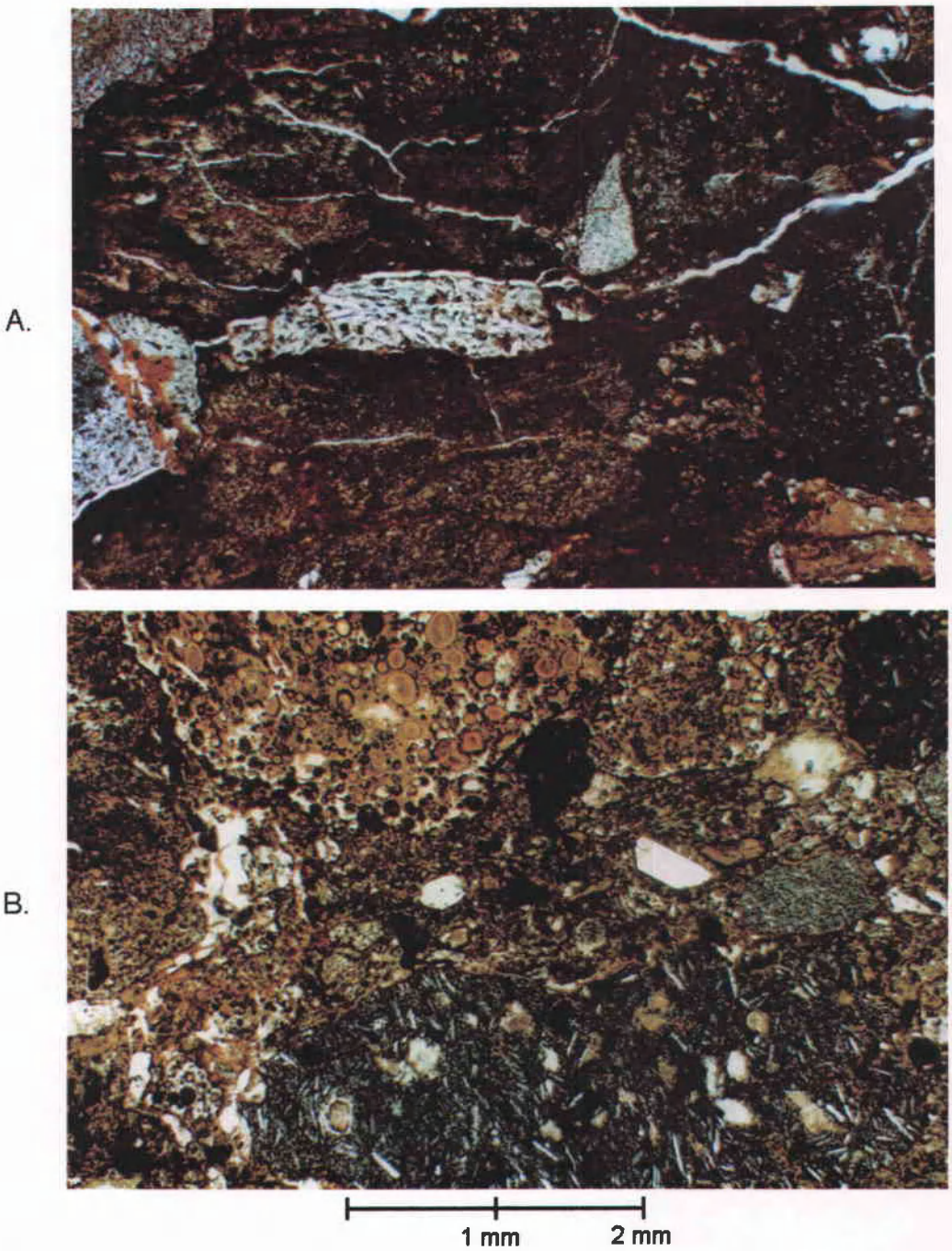

Figure 27. A) Lowermost Grays River volcanic strata-unit 1 (sample GR8A). Coarse-grained, shallow-marine basaltic sandstone. Note plagioclase-phyric basalt clasts with pilotaxitic texture and volcanic clasts altered to celadonite pseudo-matrix (Crossed-nicols).
B) Lower Grays River volcanic terrestrial unit (sample 628GB). Coarse-grained, scoriaceous basaltic sandstone, vesicles filled with green celadonite and nontronite. Note amygdular basalt and porphyritic basalt (Plane-polarized light).

The Grays River volcanic terrestrial strata consists of thin bedded, fluvial basaltic lithic sandstone and siltstone. These basaltic, tuffaceous, coaly interbedded sedimentary units are mapped in the area as Tgvst (Plate I). Volcanic clast textures and compositions in this coarse-grained basaltic sandstone include pilotaxitic, amygdaloidal and porphyritic basalt (75%), and altered irregularly-shaped scoriaceous clasts (10%). The vesicles are filled with fibrous zeolites and chlorophaeite, a yellowish brown concentrically-ringed mineraloid. Monocrystalline quartz and albite twinned plagioclase grains are present (5%). Albite twinned (labradorite) plagioclase phenocrysts from several of the coarse-grained porphyritic basalt clasts ranges from 64 An to 88 An, (n = 5, averaging 79 An) using the Michel-Levy technique. Fine-grained scoria altered to zeolite, Fe-rich nontronite or celadonite clay forms the matrix and cement between framework grains (10%) (Figure 27).

Lower Grays River Lava Flows

Above and interbedded with the lower Grays River volcanic sedimentar units are subaerial lower Grays River lava flows that were sampled for geochemical analysis and petrologic examination along Germany Creek and the southwestern part of the study area (GC-1, GC-2, GC-3; Plate I) (Figure 28). Two basal lava flows were also dated at 40.01 ±0.34 Ma (GC-1) and 39.35 ±0.36 Ma (GC-2) (Plate I). Thin section and geochemisty sample GC-3 comes from the upper part of the lower Grays River Volcanics subaerial flows (Tgvsl) (SE ¼ of Sec. 14, T 9 N, R 4 W) (Figure 28).

Based on the IUGS (International Union of Geological Sciences) classification of volcanic rocks that plots normalized weight percent of total alkalies ($K_2O + Na_2O$) versus silica (Le Bas et al., 1986) (Figure 28), the basal lower Grays River GC-1, GC-2 and sample 51700 subaerial flows classify as subalkaline basalts. Sample GC-3 from the upper part of the lower Grays River Volcanics pile classifies as a subalkaline basaltic andesite (Figure 28). Using Miyashiro's (1974) iron enrichment diagram, all three lower Grays River volcanic samples plot as tholeiitic in composition (Figure 28B).

The basal lava flow overlying the South Germany Creek Cowlitz Formation section (dated at 40.09 ±0.34 Ma) is an augite- and olivine-phyric tholeiitic basalt (sample GC-1) (Plate I and II; Figure 29A). The flow is characterized by large (4 – 14 mm) subhedral augite phenocrysts (15 %) with subordinant medium-grained (1-5 mm) subhedral olivine phenocrysts (5%). One large, embayed titanoaugite phenocryst has partially grown around a smaller subhedral, rounded olivine (Figure 29A). The large fractured titanoaugite phenocrysts commonly display resorbed edges and pits. Minor angular, broken, subhedral albite-twinned plagioclase phenocrysts are also present (1-3%). The groundmass has pilotaxitic texture with abundant opaque ilmenite, microlites of plagioclase, clinopyroxene and dark brown clay-altered devitrified glass (Figure 29A).

The basal lava flow overlying the North Germany Creek section (dated at 39.35 ± 0.36 Ma) is a tholeiitic basalt with phenocrysts of olivine, augite, and calcic plagioclase (Plate I and II). The flow displays a hypidiomorphic texture, containing euhedral olivine phenocrysts (1-5 mm) comprising about 10% of the rock. The olivines range in composition from Fo73 to Fo88 using 2V analysis of phenocrysts (Figure 29B). This

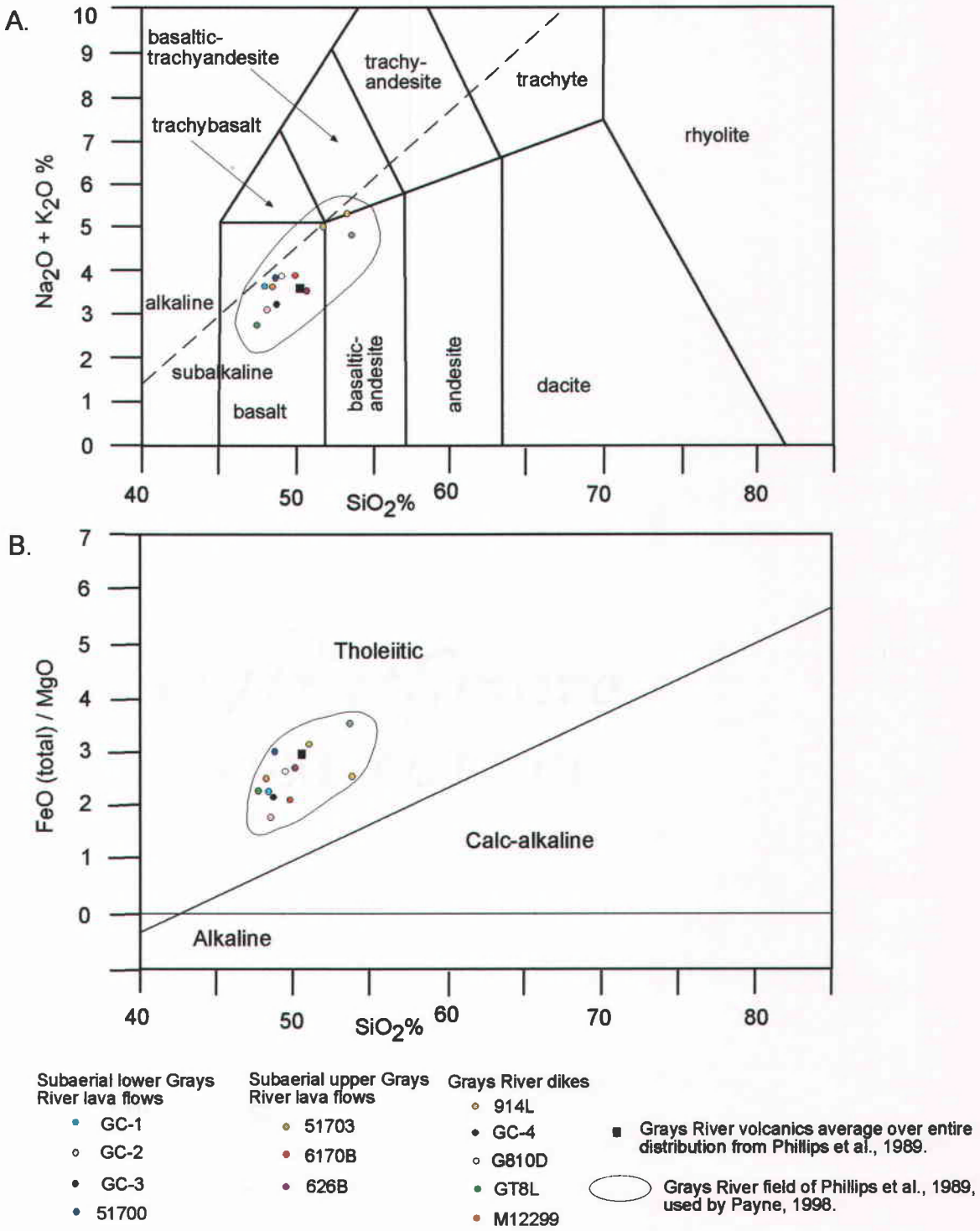

Figure 28. A) Basalts of the Grays River Volcanics from the thesis area plotted on a total alkali vs.SiO_2 (TAS) diagram using normalized weight percentage, based IUGS classification scheme of Le Bas et al., 1986. Note dotted line separating alkaline vs. subalkaline volcanic rocks from Irvine and Barager's (1971) classification.
B) Iron enrichment diagram of Miyashiro (1974). Most samples plot as subalkaline tholeiitic basalt; three samples plot as subalkaline basaltic andesites. (modified from Payne, 1998)

high magnesian olivine (forsterite) is characteristic of tholeiitic basalts (Philpotts, 1990). Olivine phenocrysts are generally resorbed and partially to completely altertered to iddingsite. Subhedral 1 – 9 mm titanoaugite phenocrysts comprise about 10% of the rock, and show a thin outer zoning and minor resorption (Figure 29B). Plagioclase phenocrysts (1-8 mm) form about 5-10 % of the rock, show albite- twinning, and are infrequently grouped in glomerocrysts. The plagioclase is commonly sericitized along cleavage planes. Alteration products also include yellowish green chlorophaeite and reddish brown iddingsite derived from alteration of olivine. The groundmass is a pilotaxitic texture of flow-aligned plagioclase microlites, clinopyroxene and opaques (Figure 29B).

The subaerial lava flow from the top of the lower Grays River volcanic pile (GC-3) is vesiculated, plagioclase-phyric tholeiitic basaltic-andesite which contains medium (1-5 mm) subhedral, lath-shaped plagioclase phenocrysts (5-10%) and minor small, altered anhedral clinopyroxene phenocrysts (1-5%). Vesicles are commonly filled with fibrous zeolite and calcite. The groundmass consists of plagioclase microlites in pilotaxitic flow texture, opaques, and microcrystalline clinopyroxene altered to clay. The rims of vesicles have been weathered to dark-brown, clay-altered devitrified glass.

Upper Grays River Lava Flows

Payne (1998) studied 21 basalts from Bebe and southeastern Abernathy Mountains of the upper Grays River lava flows. He also incorporated data for 21 major oxide and minor element geochemistry samples reported by previous workers from

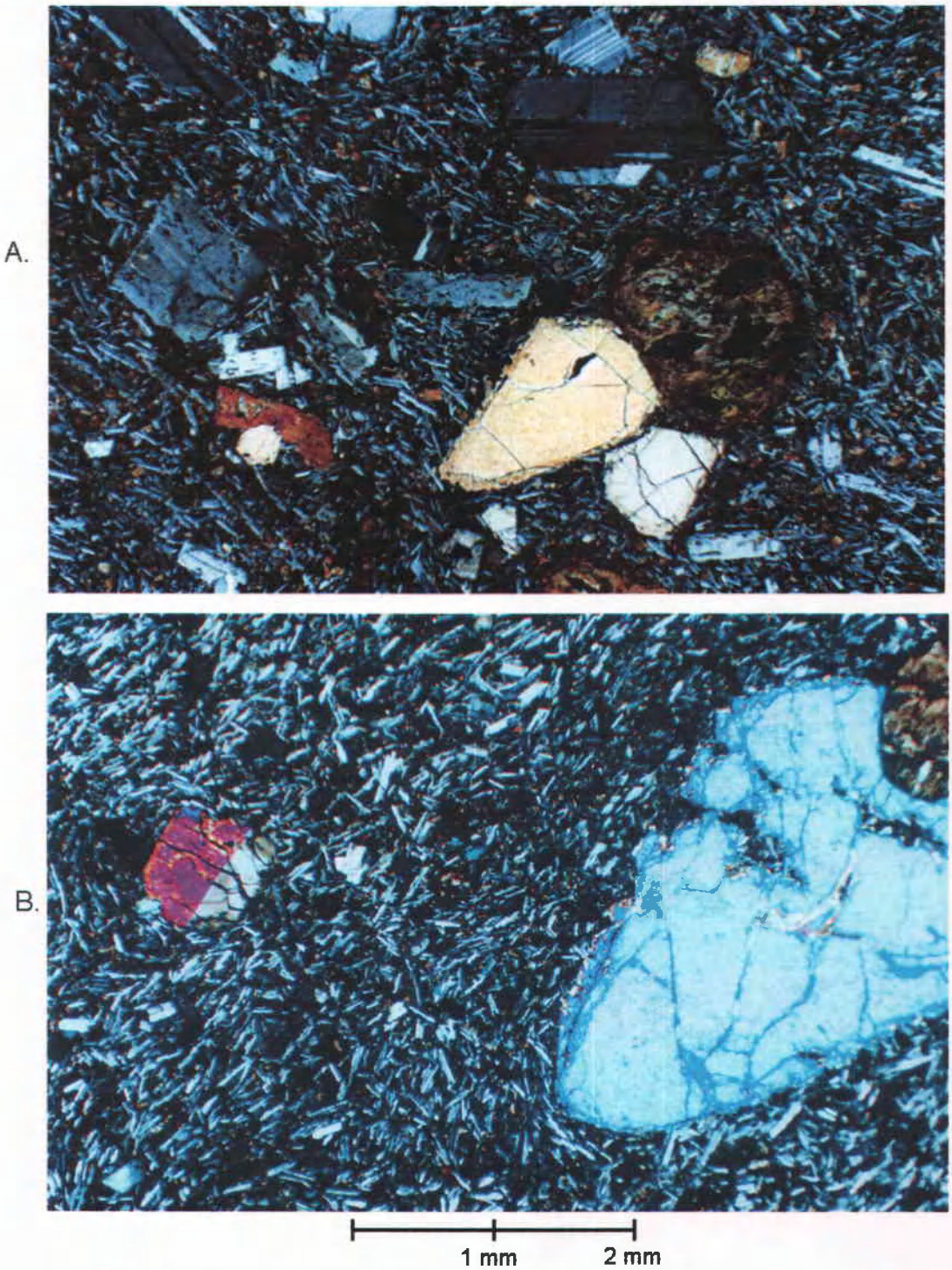

Figure 29. Photomicrographs of lower Grays River lava flows.
A) Augite- and olivine-plagioclase-phyric tholeiitic basalt (sample GC-1). Note iddingsite-altered olivine phenocrysts and flow aligned plagioclase microlites (Crossed-nicols).
B) Porphyritic tholeiitic basalt (sample GC-2). Note round altered olivine and large embayed titanoaugite phenocrysts (Crossed-nicols).

lower, middle and upper Bebe Mountain. All 21 samples from Bebe Mountain are from the upper Grays River Volcanics, and all classify geochemically as subalkaline tholeiitic basalts (Figure 28) (Payne, 1998). In this study, 4 basalts from the upper Grays River Volcanics also classify as subalkaline tholeiitic basalts, very close in proportion to the average field for Grays River Volcanics of Phillips et al., 1987 (Figure 28).

Payne (1998) noted three basaltic textures among the upper Grays River subaerial flows in the Bebe – southeastern Abernathy Mountain area: (1) a lower olivine-bearing (picritic) basalt (dated at 38.6 Ma from southeastern Abernathy Mountain, Plate I), (2) a middle intersertal to plagioclase glomerophyric unit (upper middle Bebe Mountain dated at 37.4 Ma), and (3) an upper aphyric pilotaxitic intra-canyon flow unit (Olequa Creek, dated at 36.8 Ma). The lowest flows on Bebe and Abernathy mountains (CP-94-76, CP-95-196; dated at 38.6 Ma) are characterized by medium-grained olivine phenocrysts in an intersertal finely crystalline groundmass of plagioclase, clinopyroxene and opaques (Payne, 1998). These flows bear a textural and mineralogic similarity to the lower Grays River subalkaline tholeiitic basalt sample GC-2 (dated at 39.4 Ma with overlapping age range, this study; Figure 23). The textures and mineralogic affinities of flows above and below the unconformity indicate that there was no change in the magma source for the lower and upper Grays River Volcanics. Subaerial flows (dated at 37.4 Ma; Payne, 1998) from the middle part of Bebe Mountain are characterized by distinctive plagioclase glomerocrysts, as well as olivine and plagioclase phenocrysts. Intra-canyon flows comprising the youngest part of the Grays River Volcanics at Bebe Mountain (dated at

36.8 Ma; Figure 23) are dominantly aphyric and all display a pilotaxitic flow texture (Payne, 1998).

Grays River Dikes

Six glomeroporphyritic to microphyric Grays River basalt dikes were analyzed petrographically (samples 914L, GC-4, G810D, GT8L, 617A and G815C; Plates I and II). Five Grays River basaltic dike samples were collected for geochemical analysis: 914L, GC-4, G810D, GT8L, and M511299 (Figure 28). Sample M511299 is from Monahan Creek, the rest of the samples are from the Germany Creek measured sections (Plates I and II).

The thickest dike in the study area is 12-m thick, SW ¼ of Sec. 25, T 10 N, R 4 W. It has a chilled microphyric margin (sample 914L; Plate I) and a glomerporphyritic central zone shown in Figure 26A. The chilled margin plots as a subalkaline tholeiitic basaltic andesite (Figure 28), with higher silica and alkali than any other sample from the study area. This sample contains sparse phenocrysts of pitted and resorbed euhedral augite with alteration on the cleavage planes (<5%). The groundmass is dominated by intergranular plagioclase microlites (60%) with altered clinopyroxene, opaques and intersertal glass (Figure 30). Sample 914L was $^{39}Ar/^{40}Ar$ dated at 39.98 ±0.29 Ma.

Two other Grays River dikes in Germany Creek (samples 815C, NE ¼ of Sec. 1, T 9 N, R 4W and G810D NE ¼ of Sec. 12, T 9 N, R 4 W) display large plagioclase glomerocrysts (5-15 mm) in a black vitric groundmass containing plagioclase microlites and clay-altered glass with minor clinopyroxene and some iddingsite altered small olivine

crystals (Figure 30). Sample 815C is less altered and contains larger plagioclase glomerocrysts, up to 20 mm in length. The plagioclase is albite-twinned and typically sericitized along cleavages (Figure 30A). This glomeroporphyritic texture is common to the Grays River dikes of the study area. Sample G810D is a subalkaline tholeiitic basalt (Figure 28), and has a $^{40}Ar/^{39}Ar$ age date of 39.56 ±0.41 Ma.

Evenly spaced, sperical vesicles are aligned along the margins of a 3-m thick dike that intrudes the lower Grays River lava flows in Germany Creek (sample GT8L; SW ¼ of Sec. 6, T 9 N, R 3 W). This aphyric dike with an intersertal texture of black glass and plagioclase microlites is a subalkaline tholeiitic basalt (Figure 28). The round vesicles are filled with zeolites and calcite with a dark clay-altered glassy rim. Sample GC-4 is from a thin dike intruding the lower Grays River volcanic sediments (SW ¼ of Sec. 6, T 9 N, R 3 W), and it also plots as a subalkaline tholeiitic basalt (Figure 28). In thin section it is porphyritic with medium-grained albite-twinned plagioclase (5-10%) and minor resorbed clinopyroxene (<5%). The groundmass consists of intersertal glass and plagioclase microlites with microcrystalline olivines, opaques and clinopyroxene.

There is evidence of mixing of two basaltic, plagioclase microlite-bearing magmatic fluids in Grays River dike sample 617A, occuring as clots of basalts of differing textures and colors. A darker, titanoagite and plagioclase vitrophyric portion of the thin section is mixed with a less glassy, intergranular to intersertal plagioclase-phyric clots. The euhedral titanoaugite phenocrysts are very large, with one up to 17 mm (10 % of black vitric zone) (Figure 30).

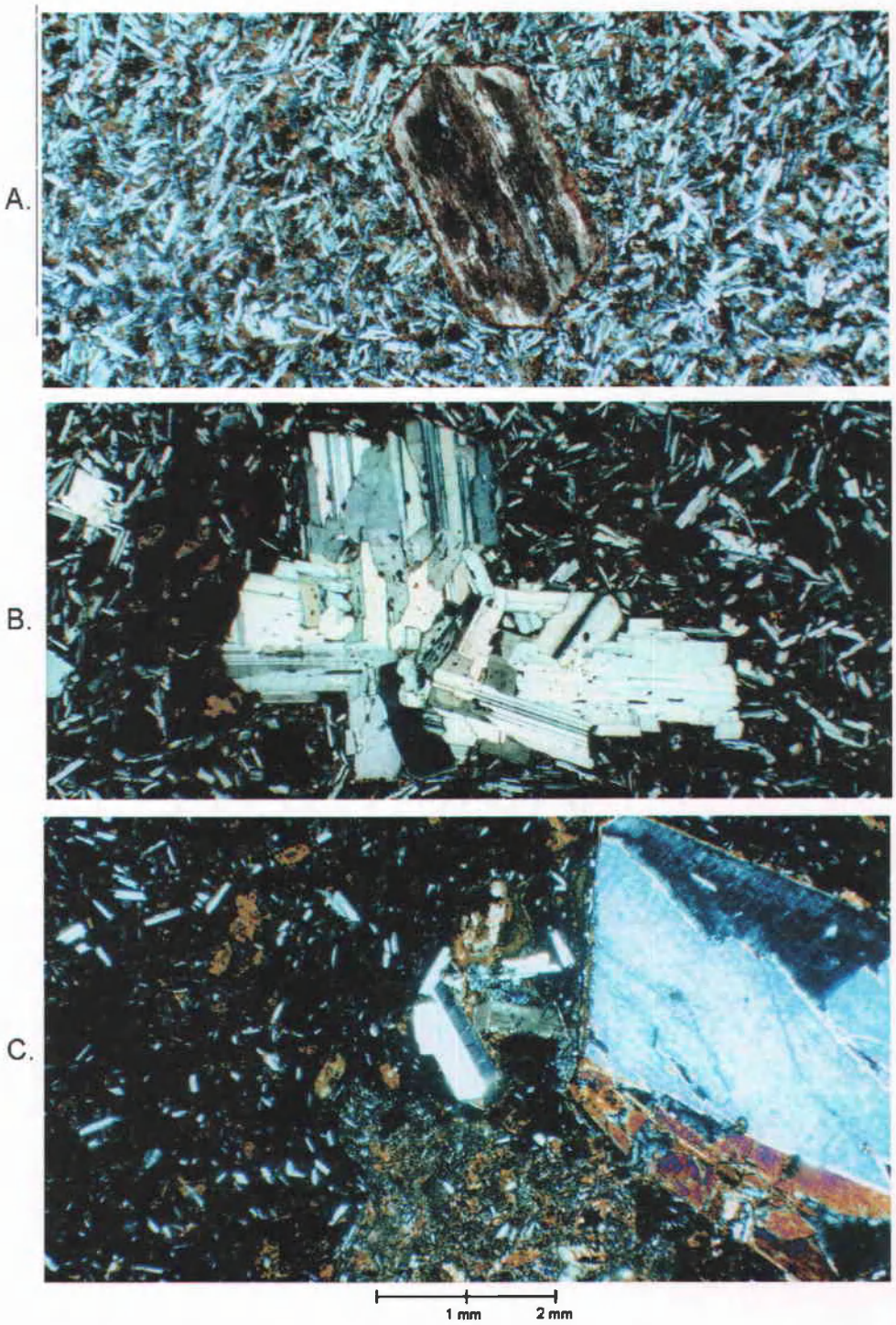

Figure 30. Photomicrographs of Grays River dikes.

A) Sample 914L, chilled margin of intergranular plagioclase microlites, opaque ilmenite and sparse clay-altered augite phenocrysts (Plane-polarized light).

B) Typical plagioclase glomeroporphyritic texture of Grays River dikes in the study area (815C; Crossed-nicols).

C) Sample 617A showing mixture of two glassy, plagioclase microlite magmas and large titanoaugite phenocryst (Crossed-nicols).

CONCLUSIONS AND INTERPRETATIONS

A diagrammatic summary of the radiometric dates, lithostratigraphy, magnetostratigraphy and geochemical sample positions of the Grays River volcanic lava flows and dikes of the study area is shown in Figure 31. The Grays River Volcanics of the study area are separated by an intraformational unconformity that defines informal lower (Tgv1) and upper (Tgv2) units. The lower Grays River Volcanics conformably overlie the middle Eocene Cowlitz Formation in the Germany Creek area, and are at least 1250 m thick in the southern part of the thesis area based on dip projection and exposure of numerous 2 – 5 meter thick flows along lower Germany Creek (Plate I). Two basal subaerial Grays River volcanic augite-, olivine- and plagioclase-pyric subalkaline tholeiitic lava flows (GC-1 and GC-2) have been $^{40}Ar/^{39}Ar$ dated at 40.01 ±0.34 Ma and 39.35 ±0.36 Ma, conformably overlying shoreface successions of the Cowlitz Formation (Plate I and II) (Figure 31). Interbedded sedimentary subunits within the lower Grays River include a discontinuous 42-m thick, fossiliferous basaltic sandstone unit Tgvs1 and ta 25-m thick, thin lignite-bearing, fluvial-lacustrine Tgvst interval. The lower Grays River Volcanics unit in the study area (~40 – 39 Ma) is correlated to Chron 18n based on radiometric age dates, interbedded normal polarity sedimentary units and a normal polarity oriented sample (GC-1) (Figure 31). Geochemical analysis of major- and minor-element oxides from 4 lower Grays River lava flows suggests the possibility of differentiation of the magma from the lowest flow subalkaline olivine tholeiitic basalt (samples GC-1, GC-2, 51700) to the uppermost flow subalkaline plagioclase-phyric basaltic andesite in Germany Creek (sample GC-3) (Figure 31). Basaltic andesite and

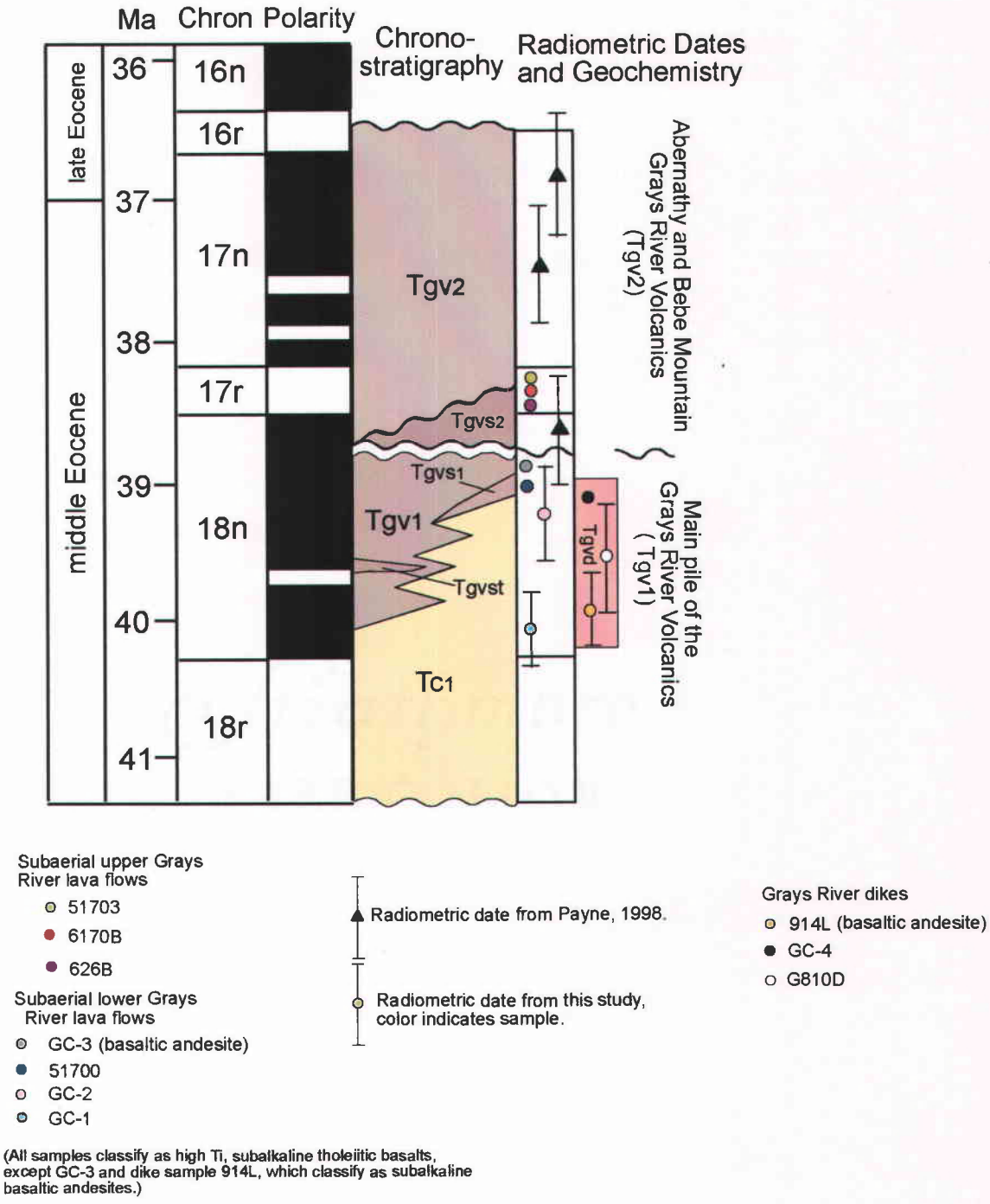

Figure 31. Diagram illustrating the chonostratigraphic, magnetostratigraphic and geochemical relationships of the Grays River volcanics of the study area. See text for locations of samples and sources of radiometric age data.

dacite has also been reported in the upper Tillamook volcanics of northwestern Oregon (Mumford, 1988; Safley, 1989).

The upper Grays River Volcanics unit of the study area (38.6 – 36.8 Ma) is exposed at Bebe and Abernathy mountains, where it is estimated to have a maximum thickness of 300 m, averaging about 150 m (Plate I). Flows are generally 2 – 3 meters thick. Underlying the subaerial lava flows is an unconformity valley-fill unit, Tgvs2 (0 – 200-m thick, Pauli, 1998; in Payne, 1998), consisting of reworked Cowlitz Formation arkosic sandstone and grading upward to shallow-marine basaltic sandstone, tuffaceous lithic siltstones and lapilli tuff-beds. This unconformable unit is poorly exposed in the thesis area, but likely was deposited in structural lows from erosion of exposed highlands consisting of lower Grays River Volcanics and Cowlitz Formation. Renewed or continuing Grays River volcanism produced the upper Grays River subalkaline olivine tholeiitic basalt flows that overlie the Grays River unconformity valley-fill sequence. The 21 upper Grays River basalt samples described by Payne (1998) and the 3 upper Grays River basalt samples from this study all classify as subalkaline tholeiitic basalts.

The integration of stratigraphic and geochemical analyses of the Grays River Volcanics to determine relative stratigraphic patterns produced few results. Both lower and upper Grays River Volcanics are dominated by high titanium-oxide, tholeiitic basalts. All Grays River basalts from the study area contain a high concentration of incompatible trace elements relative to MORB. It is noteable that of the 4 geochemically analyzed samples of lower Grays River Volcanics in the thesis area, sample GC-3 is the only basaltic andesite and is the stratigraphically highest sample taken. All 3 geochemical

samples of the upper Grays River Volcanics from the study area classify as subalkaline tholeiitic basalts. Additional sampling and geochemical analyses are needed to confirm or deny the possible differentiation of the lower Grays River Volcanics.

Lower Grays River Volcanics tholeiitic basalt subaerial lava flows and porphyritic dikes display large plagioclase glomerocrysts and evidence of olivine and augite phenocryst resorption. Rounded grain corners of euhedral olivine and subhedral titanoaugite phenocrysts are common in the lowest basalt flows of the study area (GC-1, GC-2). Plagioclase glomerocrysts are common in the interior of Grays River dikes. Chilled microphyric margins and multiple injections of basaltic magma are also observed from thin sections of Grays River dikes. These textural features associated with primitive subalkaline tholeiitic basalts are interpretated to indicate decompression melting of the mantle. Grays River dike geochemisry matches lower and upper Grays River flows, however no substantial amount of plagioclase glomerocrysts were observed in the Grays River flows. This textural difference between the majority of the Grays River dikes and the age-equivalent lower Grays River flows suggests the feeder dikes were not sampled, or the glomerocrysts in the dikes were reduced by further decompression melting during eruption. The high concentration of incompatible trace elements (Ti, K, Rb, Sr, Zr and Ba) in the Grays River Volcanics relative to MORB suggests a deeper mantle source that is not depleted compared to the shallower mantle sources under mid-ocean ridges (Philpotts, 1990).

Tholeiitic basalts containing a high concentration of trace elements relative to MORB are associated with episodic eruptions of flood basalts of intra-plate volcanic

provinces (Philpotts, 1990). A possible candidate for the primary magma of intra-plate flood basalt provinces is picritic, high magnesian-olivine basalt compatible with mantle olivine compositions (Philpotts, 1990). The basal flows of the lower and upper Grays River Volcanics of the study area are olivine-bearing tholeiites consistent with a picritic-derived primary magma. Resorption of the early-forming olivine crystals of intra-plate flood basalts during the rise and rapid decompression of the magma would occur, decreasing the effective bulk viscosity of the magma and allowing it to rise more rapidly causing greater rates of intrusion or extrusion (Philpotts, 1990). Resorption of olivine is observed in thin sections of the Grays River Volcanics.

Numerous sub-parallel, northwest- and dominant northeast-trending sub-vertical GraysRiver dikes attest to the dilation of the study area during emplacement of the Grays River Volcanics. Two dikes with different orientations, samples 914L and G810D, have overlapping $^{40}Ar/^{39}Ar$ age dates of 39.98 ±0.29 Ma and 39.56 ±0.41 Ma, indicating concurrent activity with the lower Grays River Volcanics. The plagioclase glomeroporphyritic texture common in the dikes of the area may have resulted from partial decompression melting of plagioclase (labradorite) crystals during intrusion and subsequent fusion due to crystal overgrowth during cooling (Philpotts, 1990). Although no dikes were observed as direct feeders to Grays River lava flows in the study area, the large number and vertical nature of the dikes are consistent with similar associations found in continental flood basalt provinces where numerous dikes are emplaced perpendicular to zones of crustal extension.

An alternative origin hypothesis is that the Grays River Volcanics represent shield volcanoes with centralized eruptive centers. The shield volcanoes could be associated with either spreading ridges or rising "hot spot" mantle plumes. The overlapping outcrop and subcrop distribution pattern of the Tillamook and Grays River Volcanics, both thickening toward the relative center location of the respective units suggests a central source and shield volcano structure. The orientations of Grays River dikes of the study area may belong to one region of radial dikes radiating from an eruptive center indicated by the thickest accumulation of lower Grays River Volcanics (1700+ m) penetrated by the Champlin Puckett 13-36-85 well on the flank of a large Bouguer gravity high (Figure 32). Very large boulder sized-clasts of Grays River Volcanics and very coarse conglomeratic volcaniclastic deposits are complexly interbedded with arkosic sandstones of the Cowlitz Formation at Mt. Solo, two miles west of Longview, Washington (McCutcheon, personal communication, 1999). Together these observations suggest that the Grays River Volcanics may have accumulated a moderate relief associated with a main eruptive center of a shield volcano. However, speculation about the gravity high being related to a thick Grays River volcanic center is weakened by the presence of thick, underlying seamount paleo-topographic highs of Crescent Formation oceanic basalt.

For future study, determination of subsidence or uplift of the basin prior to volcanism is important to indicate if the Grays River basalt volcanism was more closely related to an active rising deep mantle plume (hot spot), or a result of thinning of the lithosphere due to lithospheric extension and subsequent passive rising and decompression of the mantle (MORB-like). If the Grays River volcanism was a result of

a rising mantle plume, then thermal inflation and uplift of the lithosphere resulting in erosion of sediments would precede rifting and extrusion. However, if the volcanism was due to a passive rise of the mantle into zones of lithospheric extension, basin subsidence and sedimentation would precede thermal uplift and extrusion (Philpotts, 1990). The lower Grays River Volcanics appear to have been deposited in a rapidly subsiding basin, whereas the upper Grays River Volcanics were deposited after a period of uplift and erosion. Factors responsible for basin uplift or subsidence are complicated in the marginal marine middle Eocene forearc basin of the study area. Relative changes in sea-level recorded in the sedimentary record of the basin could be result of many factors including intra-basinal thermal dynamics (subsidence due to thinning, or uplift due to thermal inflation of the lithosphere), eustatic sea level fluctuations, and tectonic forearc basin deformation. A regional understanding of the structural and thermal evolution of the middle Eocene forearc basin is required to comprehensively interpret the driving factors of the mixed siliciclastic and volcanic stratigraphic record.

LINCOLN CREEK FORMATION

The Lincoln Creek Formation tuffaceous siltstone (Tlc on Plate I) is poorly exposed in a limited part of the thesis area where it is preserved beneath an isolated outcrop of Grande Ronde Basalt (vicinity of Sec. 9, T 9 N, R 4 W; Plate I). The approximately 70-meter thick Lincoln Creek Formation consists of light-gray to buff, bioturbated, tuffaceous siltstone and silty, very fine-grained sandstone containing fossiliferous shell-lag casts and molds of articulated bivalves and gastropods. Dr. Elizabeth Nesbitt (personal communication, 2000) identified Nuculana washingtonensis, found in both the Lincoln Creek and Cowlitz formations, from molluscan macrofaunal sample 725A (SE ¼ of Sec. 5, T 9 N, R 4 W; Plate I). All other molluscan fossils submitted from the formation were unidentifiable. Livingston (1966), in reconnaissance mapping reported a Refugian age benthic foraminifer locality (identified by Rau) at the SE ¼ of Sec. 5, T 9 N, R 4 W. Although no foramifers were found from the Lincoln Creek Formation in this study, the previously collected Refugian (latest Eocene – Oligocene) benthic foraminiferal assemblage indicates the tuffaceous siltstone is younger than the Late Narizian (middle Eocene) Cowlitz Formation and consistent in age with the (mainly Oligocene) Lincoln Creek Formation. Trace fossils identified from ditch exposures include hook-shaped *Phycosiphon* burrows, suggesting an outer shelf to bathyal depositional environment below wave-base, consistent with the fine-grained lithology, and massive bedding of the unit.

The relatively flat-lying Lincoln Creek Formation is inferred to nonconformably overlie the upper Grays River Volcanics in the study area based on magnetostratigraphy and radiometric dates of the late Narizian Grays River Volcanics and the Refugian age of the Lincoln Creek Formation. The Lincoln Creek Formation is unconformably overlain by the competent middle Miocene Sentinental Bluffs unit of the Grande Ronde Basalt (Columbia River Basalt Group). The Lincoln Creek Formation typically forms vegetated slopes and is prone to landslide failure.

GRANDE RONDE BASALT

The middle Miocene Grande Ronde Basalt member of the Columbia River Basalt Group in the study area is restricted to a continuous isolated cap-rock exposure located in Secs. 5 and 9, T 9 N, R 3 W, Plate I (Tgvsb on Plate I). The blocky, dark gray, aphyric, dikytaxitic basalt is well-exposed in a quarry at the SE ¼, Sec. 4, T 9 N, R 3 W; Plate I. Dikytaxitic texture refers to small, ubiquitous vesicles filling interstices between phaneritic crystals. No colonnade or columnar jointing is observed from exposures in the study area, however small scale blocky jointing resembling entablature texture is prevalent. The lower contact with the underlying Lincoln Creek Formation is not exposed, but is presumed to be an unconformity due to the juxtapostion of Oligocene strata (Lincoln Creek Formation) overlain by middle Miocene Columbia River basalts. Large angular blocks (1 to 5 meters in diameter) of Grande Ronde basalt are found in landslide debris where the incompetent underlying Lincoln Creek Formation has failed along the flanks of the in-place Grande Ronde basalt cap-rock (Plate I). The maximum thickness of the Grande Ronde basalt in the study area is estimated to be 50 to 60 m (Plate I) with the number of individual flows undetermined, but likely no more than 2 (see comments at end of section).

Geochemical analysis of the major- and minor-element oxides (sample 51705; see Appendix D) showed that the basalt in the quarry exposure is equivalent to either the high MgO Sentinel Bluffs or China Creek flow units of the Grande Ronde Basalt (Figure 32). A fluxgate magnetometer (lab analysis) indicated an oriented sample from the Grande

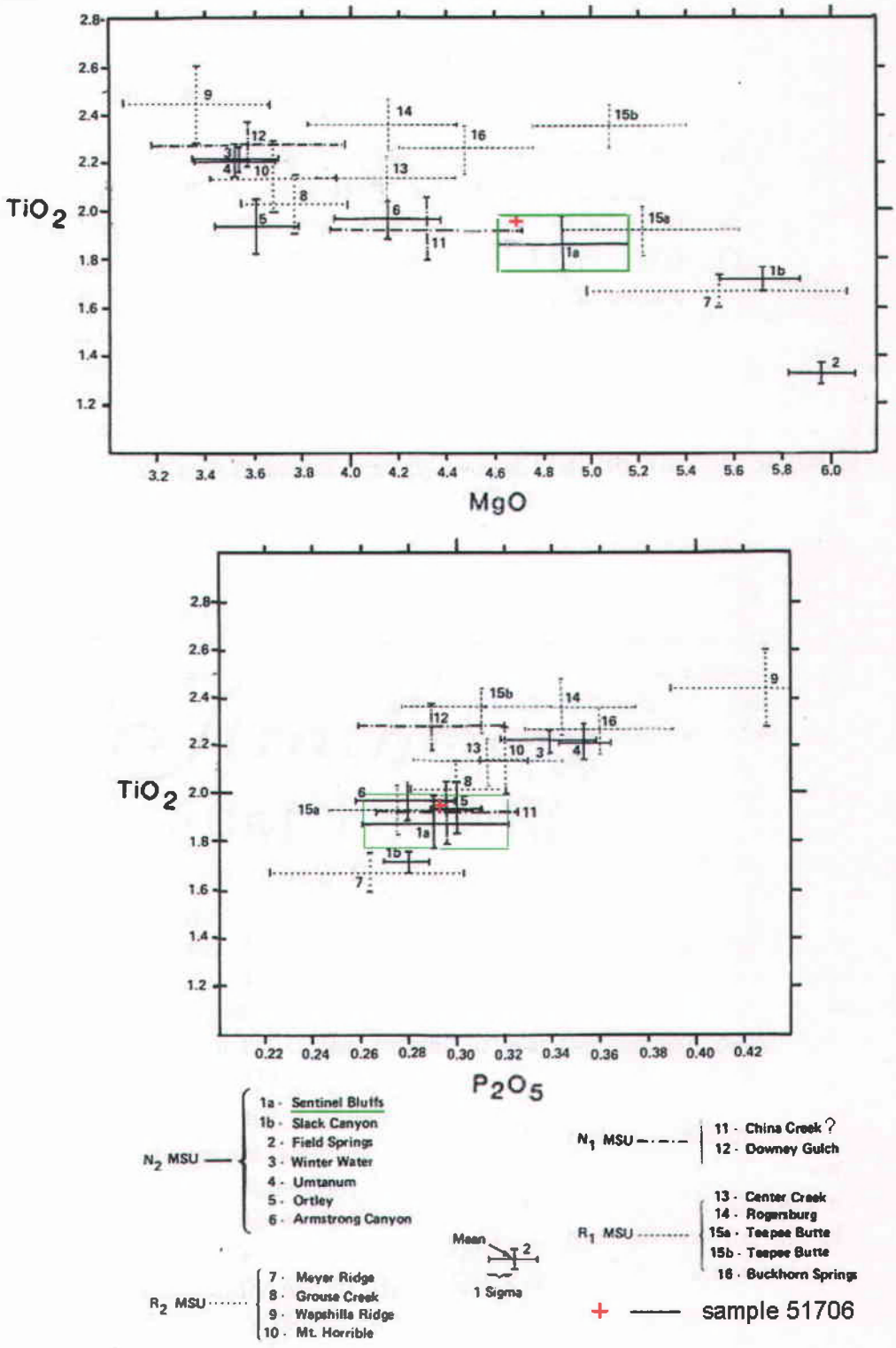

Figure 32. MgO vs. TiO2 and TiO2 vs. P2O5 variation diagrams for informal Grande Ronde flow units from Reidel et al. (1989). Normal polarity quarry sample 51706 is plotted as a red cross, most closely affiliated with 1a, Sentinel Bluffs unit (see Appendix D for complete chemical composition data).

Ronde quarry has normal polarity. Although both the China Creek and Sentinel Bluffs flow units have normal polarity, the China Creek flow unit occurs much lower stratigraphically than the Sentinel Bluffs flow unit and terminate about 100 km to the southeast of the study area (Reidel et al., 1989). Whereas, the Sentinel Bluffs flows are the highest stratigraphic units in the Grande Ronde basalt and are documented near the mouth and margins of the Columbia River in western Oregon and Washington. Also, dikytaxitic groundmass texture is characteristic of the Sentinel Bluffs flow unit. The Sentinel Bluffs unit of the Grande Ronde contains a total of 8 individual flows, dated at 15.6 Ma (Reidel et al., 1989). However, only two Sentinel Bluffs flows made it to western Oregon and Washington in the middle Miocene (Beeson and others, 1989).

QUATERNARY UNITS

The Quaternary age terrace units of the study area are primarily the result of sudden deposition of glacial flood and episodic lahar deposits along the major drainages of the eastern margin of the area. Probable Missoula flood slackwater silt deposits (unit Qtr) and at least two Holocene lahar deposits from Mt. Saint Helens (pre-1980 unit Qshu1 and 1980 unit Qshu3) are present along the lower Arkansas Creek and western bank of the Cowlitz River drainages (Plate I). Modern stream alluvium and landslide deposits are common throughout the study area (units Qal and Qls). This study relies heavily on the peri-glacial Pleistocene terrace unit (Qtr) mapping of Roberts (1958), Livingston (1966) and Waitt (1985) in Phillips et al. (1987). The description of the Quaternary Mt. St. Helens laharic units of the study area by Scott (1986), along lower Delameter and Arkansas creeks augmented the geologic map of this study.

MODERN LANDSLIDE DEPOSITS

The landslide deposits of the study area occur in various incompetent, oversteepened rock units of the study area, but are frequently associated with the friable arkosic sandstones and siltstones of the Cowlitz Formation and siltstones of the upper McIntosh formation where overlain by Grays River Volcanics. The deposits usually consist of chaotic, heterogeneous mixtures of basalt blocks and weakly consolidated sand, silt and clay derived from weathered sedimentary units. The deposits display hummocky and slump topography (Plate I). Many small slides occur along numerous

stream drainages throughout the study area where incompetent sedimentary units are undercut by seasonal flooding, frequently eroding the toes of previous slides and re-activating landslide movement.

LAHAR DEPOSITS OF A.D. 1980

Lahar deposits from the May 18th, 1980 eruption of Mt. St. Helens were carried into the Cowlitz River drainage in the study area from the confluence of the South Fork Toutle River to the north. The deposits consist of 2 to 9 m of clast-supported sandy gravel sharply overlain by 2 m to less than 20 cm of matrix-supported, unstratified mixtures of pumice, volcanic gravel and sand, where in place along the west bank of the Cowlitz River, north and south of Castle Rock, Washington (Gilkey, 1983; in Phillips et al., 1987). The lahar inundated the town of Castle Rock and clogged the Cowlitz River drainage. Today 10 to 12 meter high rectangular piles of lahar debris removed from Castle Rock line the western edge of Interstate-5 north and south of town.

LAHAR DEPOSITS (QSHU1)

Based on the eruptive nomenclature and event chronology for Mt. St. Helens used by Phillips et al. (1987), the thin, unconsolidated lahar deposits which form a broad terrace northwest of Castle Rock in the Arkansas Valley have been correlated to lahars of probable Kalama through Pine Creek age, >100 – 2500 yr B.P (Scott, 1986). The lahar deposits in the study area are poorly exposed under a well-developed soil. The deposits

consist of unconsolidated coarse andesitic sands and subangular pebble and cobbles within a clayey, ashey matrix. The pre-1980 lahar deposit is about 10 meters thick.

TERRACE DEPOSITS

Terrace deposits consisting of light-colored silts and minor framework supported polymict pebbles primarily consisting of porphyritic volcanic clastsa with minor quartzite and jaspers, forms a dissected terrace about 10-15 meters thick in Arkansas Valley (Sec. 31, 32, T 10 N, R 2 W). This unit is also present on the west bank of the Cowlitz River (Sec. 22, 29, T 9 N, R 2 W; Plate I) (Phillips, et al., 1987). While working in the Castle Rock – Toledo area, Roberts (1958) acquired from a local resident a mammoth facial bone that came from a terrace deposit. The facial bone was identified as *Mammathus primigenius* (Blumenback), and assigned to the Pleistocene (Livingston, 1966). Other fossil mammoth material was recovered from a probable contemporary terrace deposit during construction of U.S. Highway 99 near Kelso, Washington. Roberts (1958) reported the presence of granodiorite erratics in the terraces, interpreted to be ice-rafted debris from outburst floods of Glacial Lake Missoula. Phillips et al. (1987) also interpreted the terrace deposits to be late Pleistocene slackwater silt deposits from Glacial Lake Missoula outburst floods.

MIDDLE EOCENE TO LATE EOCENE REGIONAL CORRELATION AND STRATIGRAPHIC RELATIONSHIPS IN SOUTHWEST WASHINGTON AND NORTHWEST OREGON

The primary goal of this study is to determine the regional stratigraphic position of the middle to late Eocene units of the study area with the nearby type Cowlitz Formation of southwest Washington and the Cowlitz Formation in Mist Gas Field of northwest Oregon. Radiometric dating of conformably overlying Grays River basalt flows allowed comprehensive magnetostratigraphic sampling of the Germany Creek sections to be directly tied to the middle to late Eocene magnetic polarity chart of Berggren et al. (1995). Magnetostratigraphic sampling was also conducted on the Hamlet Formation and Clark and Wilson sandstone member of the Cowlitz Formation in northwest Oregon, as well as sections of the type Cowlitz Formation in southwest Washington (Prothero et al., 2001). Aided by magnetostratigraphy, molluscan and foraminifer ages, lithostratigraphy and and sequence stratigraphy, regional correlations of the middle to late-Eocene units of southwest Washington and northwest Oregon can be described with a higher resolution than previously available.

REGIONAL MAGNETIC CORRELATIONS

Previous authors have based correlation of the upper McIntosh Formation (southwest Washington) to the Hamlet Formation (northwest Oregon) (Payne, 1998; Niem, personal communication, 1999) on lithostratigraphy and biostratigraphy. These correlations were made from the type Cowlitz Formation (near the Zion well, Plate III) to the subsurface of the Mist Gas Field in northwest Oregon (Plate III, Figure 2, 3). The Germany Creek sections and the Quigley No. 1 well in the study area provide surface and subsurface stratigraphy between the type section and the Mist Gas Field. Paleomagnetic data from the Germany Creek sections (upper McIntosh-Cowlitz Formations) were incorporated into a regional paleomagnetic study involving six other measured sections including the Hamlet-Cowlitz Formation of northwest Oregon and the type Cowlitz Formation in southwest Washington (Prothero et al., 2001; Figure 33). The paleomagnetic data provide another stratigraphic tool to refine the middle to late Eocene stratigraphy of the region.

The results of the regional magnetic polarity correlation of the McIntosh-Hamlet and Cowlitz formations are shown in Figure 33 (modified from Prothero et al., in press). The Olequa Creek section (T11N, R2W, Lewis Co., Washington) follows the maps and sections of Weaver (1937) and partial section of Payne (1998). The Coal Creek section (T9N, R3W, Cowlitz Co., Washington) follows Weaver (1937). The Germany Creek sections were described and sampled by the author (Plate I, II, III). The Fall Creek section (T4N, R7W, Columbia Co., Oregon) of the Clark and Wilson (C&W) sandstone member of the Cowlitz Formation was described by Niem et al., (1994), as well as the

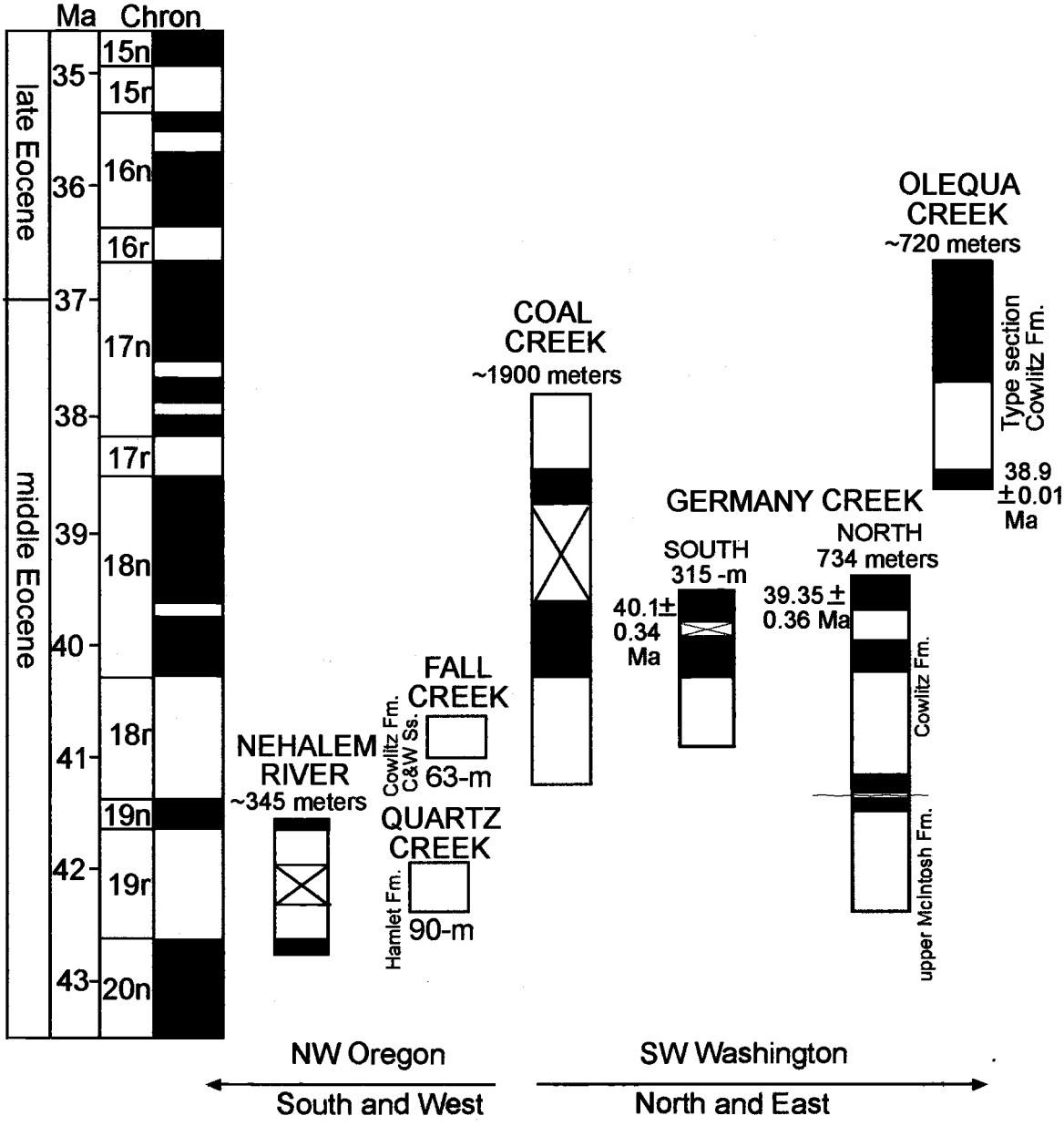

Figure 33. Regional magnetic polarity correlations of the middle to late Eocene McIntosh-Hamlet and Cowlitz formations of northwest Oregon and southwest Washington. See text for measured section locations (modified from Prothero et al., *in press*). Time scale after Berggren et al., 1995.

Quartz Creek section (T4N, R7W, Columbia Co., Oregon) of the Sunset Highway and the Sweet Home Creek members of the Hamlet Formation. The Nehalem River section (T3N, R7W, Columbia Co., Oregon) of the Hamlet Formation follows Nelson (1984).

The magnetic polarity correlations of the sections suggest that the Hamlet-McIntosh and Cowlitz formations of northwestern Oregon and southwestern Washington span most of the middle Eocene (Prothero et al., 2001). The upper McIntosh and Hamlet formations of the area correlate to Chron C19r (41.5 – 42.5 Ma) and the lower part of Chron C19n (41.5 – 41.2 Ma). In southwest Washington, the Cowlitz Formation spans from Chron C19n in Germany Creek and Coal Creek, to as young as Chron C17n (36.5 – 38.2 Ma) in Olequa Creek (Figure 33).

The magnetic polarity sections of Figure 33 are not drawn to scale with regard to total thickness. The sections containing radiometric dates provide starting points from which to correlate lithology and stratigraphic relationships with the magnetozone results from the individual section site units. The magnetozone (normal or reverse) thicknesses of the sections are drawn to scale to maintain the ratio of measured section thickness between the magnetozones, but the overall thickness of the entire sections are defined by correlation to the magnetic polarity chart of Berggren et al. (1995). The variable time-thicknesses of the individual sections likely reflect lack of precision in measurement or non-uniform sedimentation rates for different parts of the depositional system. The thickest sections spanning a relatively short amount of time (e.g. Coal Creek, Olequa Creek) are nearest the Chehalis basin centers and are interpreted as representing a higher

sedimentation rate associated with greater basin subsidence and accomodation space. The thinner sections spanning a relatively large amount of time (e.g. Germany Creek) were deposited along the southwest edge of the Chehalis basin on a structural high associated with the Willapa Hills uplift. Geologic mapping of the Willapa Hills uplift and seismic reflection data tied to well-log data from the Chehalis Basin show the McIntosh and Cowlitz formations thinning and onlapping a Crescent Formation basin high southwest of the Chehalis Basin (see Structural Geology section, Figure 34).

SURFACE TO SUBSURFACE REGIONAL STRATIGRAPHIC CORRELATIONS

Plate III illustrates the regional paleo-, magneto- and lithostratigraphic surface to subsurface stratigraphic correlations of the middle to late Eocene rock units of the Germany Creek sections. The study area lies between the Mist Gas Field in Columbia Co., northwest Oregon and the type-section Cowlitz Formation near the Zion well in Lewis Co., southwest Washington (index map, Plate III). Spontaneous potential and resistivity electric well-logs were used to interpret the lithostratigraphy of the subsurface Hamlet Formation, Grays River Volcanics and Cowlitz Formation in the Mist Gas Field as well as the upper McIntosh and Cowlitz formation from the Zion well. Robertson (1997) made subsurface stratigraphic correlations and lithologic interpretations of the Longview Fibre (LF) 25-33-65 (Mist Gas Field) and Clatskanie #1 well-logs used in this study. Interpretations from Payne (1998) and Pauli (2000, written communication) of the sequence stratigraphy of the Zion well were modified by the author with the additional data of the Germany Creek sections and Quigley No. 1 well-log thicknesses and cuttings

descriptions. Shallow corehole sp and resistivity well-log data from WK 157 (index map, Plate III) were correlated to the Zion well based on stratigraphic information and lithologic interpretations from Pauli (written communication, 2000).

The lowest unit described in this regional sequence stratigraphic correlation is a marine mudstone of the middle Eocene (lower Narizian)Yamhill Formation, underlying the Tillamook Volcanics in northwest Oregon (Clatskanie #1). The Yahmill Formation is correlative to the lower McIntosh Formation penetrated by the Zion well in southwest Washington. This lithostratigraphic relationship is corroborated with biostratigraphic correlation of bathyal to outer shelf benthic foraminifer assemblages from the lower McIntosh Formation of the Bulimina cf. B. jacksonensis zone, approximately 43 Ma (Rau, 1958), to coccolith assemblages collected from the Yamhill Formation of the Discoaster bifax subzone CP14a, which ranges from 44 to 40.3 ma (McDougall, 1997; in Payne, 1998). The lower McIntosh Formation was not penetrated or described in outcrop from the study area, and may thin or onlap the Crescent Formation basement high underlying the study area (see Figure 35).

The Tillamook Volcanics are interbedded with the Yamhill Formation in the Clatskanie #1 well (Plate III). A flow from outcrop exposure in the uppermost Tillamook Volcanics in northwest Oregon has been $^{40}Ar/^{39}Ar$ age dated at 42.5 Ma (Niem et al., 1992), with the lower part of the Tillamook Volcanics dated at 45-47 Ma (Kenitz, 1997). The geochemically and petrologically equivalent Tillamook Volcanics and Grays River Volcanics are stratigraphically separate eruptive centers (Kenitz, 1997). The high-TiO_2 tholeiitic Tillamook (42-45 Ma), lower Grays River (41-39 Ma) and upper Grays River

Volcanics (38.6-37 Ma) define an age progressive forearc basin basalt volcanic trend younger in age to the present-day north and east (Figure 22; Plate III).

The lithic arkosic sandstones of the Sunset Highway member of the middle Eocene Hamlet Formation unncomformably overlie the Tillamook Volcanics as interpreted from the Longview Fibre 25-33-65 and Clatskanie #1 well-logs, and as seen in outcrops in northwest Oregon (Robertson, 1997). The upper McIntosh sandstone member of southwest Washington is a lithologic and age correlative of the arkosic shelfal sandstone of the Sunset Highway member of the Hamlet Formation (Payne, 1998). Magnetic polarity results from the ~90-m thick Quartz Creek section of the Sunset Highway sandstone and lower contact of the Sweet Home Creek siltstonetone show the section to be entirely reversed (Chron 19r, 41.5 – 42.5 Ma; Prothero et al., in press; Figure 33). The lithostratigraphically correlative upper McIntosh sandstone and most of the upper McIntosh siltstone in the North Germany Creek section also have reversed polarity (Figure 33). The Nehalem River section of the Hamlet Formation also displays a largely reversed section that correlates to the upper McIntosh member of Germany Creek, but also contains a lower normal magnetozone not observed in Germany Creek. This lower normal magnetozone likely correlates with the uppermost part of Chron 20n (~42.6 Ma; Figure 33).

The Clark and Wilson sandstone member of the Cowlitz Formation overlies the Sweet Home Creek member of the Hamlet Formation, as interpreted by Robertson (1997) from the Longview Fibre 25-33-65 well-log of northwest Oregon (Plate III). Northeast (12.8 km) of the Longview Fibre 25-33-65 well, cuttings descriptions from the Clatskanie

#1 well show that the Grays River Volcanics overlie the Sweet Home Creek member of the Hamlet Formation (Plate III). An arkosic sandstone interval correlative to the C&W sandstone overlies the Grays River basalt in the Clatskanie #1 well. The interbedded Grays River basalt represents the onset of Grays River volcanism in the region, interpreted as near the base of the volcanic pile. To the north (29 km) in southwest Washington, the basal Grays River Volcanic flows conformably overlie ~370 m of arkosic shoreface successions of the lower Cowlitz Formation (informal unit 1A) of Germany Creek, dated at approximately 40.1 to 39.4 Ma (Plate III). This northwest Oregon to southwest Washington stratigraphic relationship illustrates the progressively younger ages and subsequently higher stratigraphic position of the Grays River Volcanics to the north (Plate III). The line of the section for Plate III is interpreted to cross the southeast flank of a thick accumulation of Grays River Volcanics, penetrated by the Champlin Puckett well (Figure 22 for location). The Grays River Volcanics thin in the subsurface to the southeast and southwest (Robertson, 1997; Kenitz, 1998). It is likely that the C&W sandstone of northwest Oregon and correlative arkosic sandstone of the lower to upper shoreface progradation successions of lower Cowlitz Formation in the study area are depositional equivalents (Chron 19n, 41.2 – 40.2 Ma) that skirted the southeast flank of a growing intra-basinal volcanic pile. Robertson (1997) interprets the geometry of lithofacies isopach maps of the C&W sandstone member in the Mist Gas Field as representing a wave-dominated delta front with minor distributary mouth bar deposits sheltered by the growing Grays River volcanic high. Robertson (1997) also noted that the isopach map of the parallel-bedded facies indicates that the main

distributary channel of the delta is oriented northeast-southwest suggesting that arkosic sandstone was transported from southwest Washington.

The C&W sandstone member of the Cowlitz Formation in northwest Oregon does not appear to correlate with the lowstand wedge and transgressive systems tract of the lowermost Cowlitz Formation in southwest Washington (Plate III). This interpretation is based on sequence stratigraphic correlation of the Germany Creek and Quigley No.1 sections to the 1 Zion well, and the observed thinning to the south and interpreted pinch-out of the lowstand and transgressive units. Based on this interpretation, it is likely that the C&W sandstone member correlates with the more proximal progradational to aggradational shoreface successions of the southwest Washington and overlying highstand systems tract succesions observed in outcrop and in well-logs (Plate III).

As shown in the 1 Zion well-log and in the type-section in Olequa Creek, overlying the progradational shoreface successions of the lower Cowlitz Formation is a coal-bearing, coastal or delta-plain facies, described by Payne (1998) as informal member subunit 1B. Numerous shallow coreholes were drilled on both flanks of the Arkansas Anticline in the north central part of the study area (Plate I) including corehole WK157 (Plate III; Pauli, written communication, 2000). Corehole WK157, from the southwest flank of the Arkansas Anticline, penetrated the upper Grays River Volcanics and underlying unconformity valley-fill sedimentary unit, Tgvs2, as well as two coal-bearing intervals (Plate III). The coal-bearing intervals are lithostratigraphically correlative to the thick coal seams of informal unit 1B of the lower Cowlitz Formation observed in the 1 Zion well and Olequa Creek (Pauli, written communication, 2000) (Plate III).

STRUCTURAL GEOLOGY

REGIONAL TECTONICS AND STRUCTURE

The study area lies within the Coast Range province of southwest Washington, a structural mountain range resulting from transtensional and transpressional strains caused by past and ongoing oblique subduction of Pacific basin plates (Kula, Farallon and Juan de Fuca) beneath the North American continental plate. A key feature of the geology of the Coast Range province is an early Eocene terrane of oceanic basalts called "Siletzia" forming the basement in western Oregon and Washington. This oceanic basalt is referred to as the Crescent Formation in southwest Washington, where it is exposed in the core of the Willapa Hills uplift (Figure 2). Elsewhere in the Coast Range, it forms the basement for Tertiary forearc basins, including the Chehalis Basin (Figure 34).

Bouguer gravity and aeromagnetic gradients (Finn, 1991) indicate that the dense, highly magnetic mafic volcanic rocks of Siletzia consist of many discrete blocks in southwest Washington (Stanely et al., 1996) (Figure 32). Stanley et al. (1996) inferred from gravity and magnetic data considerable variation in the thickness of the Siletzia terrane from Oregon (<30 km) to Washington (>6 km). Tertiary sedimentary basins likely formed where north-south contraction downwarped thinner zones of the mafic complex or where faulting produced tectonic subsidence (Stanley et al., 1996). Wells and Coe (1985) interpreted that the Siletzia (Crescent Formation) basement blocks (up to 30 km across) in southwest Washington are bounded by northwest- and west-striking dextral shear zones. Paleomagnetic studies of Crescent Formation in southwest Washington

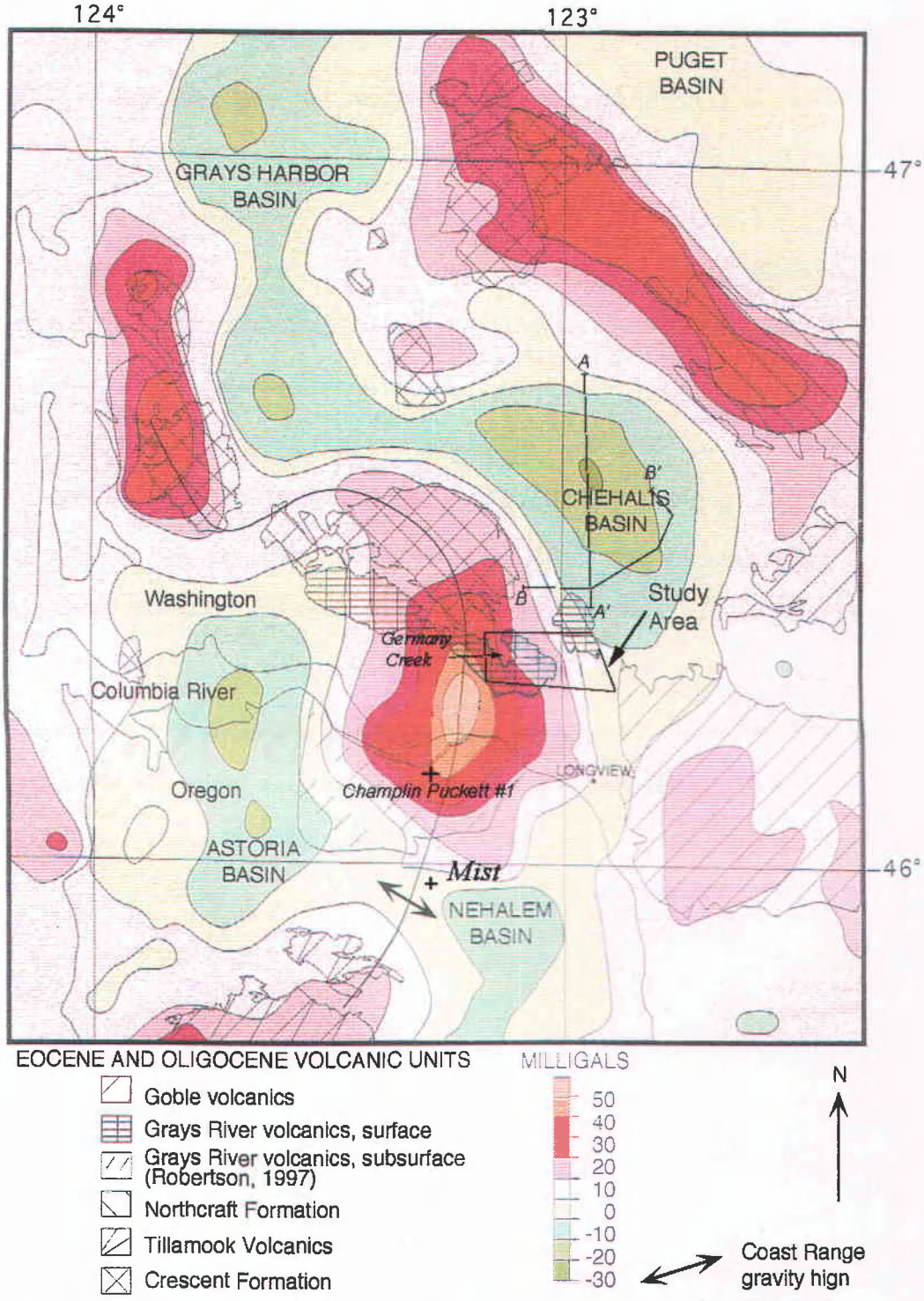

Figure 34. Residual wavelength-filtered gravity anomaly map and volcanic geology map superimposed to show relationship of dense subsurface crustal blocks of the Siletzia terrane to the mapped surface volcanic units. The anomalous high south of the Grays River outcrops has been related to the eruptive center of the Grays River volcanics. See text for discussion (modified from Finn et al., 1991; Walsh et al. 1987; Robertson, 1997; and Payne, 1998). Cross-section lines A-A' and B-B' refer to Figure 35.

indicated that most Siletzia tectonic blocks have been individually and/or collectively rotated clockwise by a combination of late Eocene dextral shear and late-middle Miocene to recent basin and range spreading (Wells and Coe, 1985; Stanely et al., 1996).

The relationship between geologic structures and tectonic rotation measured in the Crescent Formation of the Coast Range province is demonstrated by the (1) occurrence of zones of intense deformation bounding the rotated blocks, and (2) fold axis orientations (present-day north-northwest) within discrete blocks that are correlated with the amount of block rotation (Wells and Coe, 1985). The correlation between folding and rotation suggests that folding in the Crescent basement began prior to differential rotation as a result of accretion to the North American continental plate (Wells and Coe, 1985). Northeastward-oblique subduction of the Kula and Farallon oceanic plates moved the Siletzia seamount chain toward the subduction zone with the North American continent, resulting in northeast-southwest compression and formation of a northwest-southeast fault and fold trend, with consequent uplift and erosion (Armentrout, 1987). The onset of the Willapa Hills uplift was a result of the transpressional strain associated with the accretion of the Siletzia terrane along the continental margin around 46-48 Ma (Armentrout, 1987). Being too buoyant to subduct, the thick Siletzia terrane forced a jump in the line of the subduction zone to the west in the early middle Eocene forming the Cascadia subduction zone.

This early folding and accretion ocurred prior to formation of the forearc basin during the early middle Eocene, as judged from the onlap of the progradational late middle and upper Eocene McIntosh and Cowlitz formations against the folded Crescent

Formation basement high forming the eastern Willapa Hills (Wells, 1981) (Figure 35). Continued northeastward oblique subduction of the Farallon plate beneath North America and consequent dextral shear resulted in northeast-southwest tensional fault systems along which the Grays River Volcanics were erupted and extension of the McIntosh and Cowlitz Formations of the study area occurred (Armentrout, 1987).

A third major period of deformation of the Coast Range province of southwest Washington began in the late-early Miocene producing west-northwest open folds of the basinal sedimentary units, accentuated near margins of block uplifts (Wells and Coe, 1985). Subsequent regional tectonic events impacting the study area included backarc extension related to the opening of the Great Basin and renewed oblique dextral movement along northwest-southeast fault systems, deforming basalts of the middle Miocene Columbia River Basalt Group (17 – 12 Ma) (Armentrout, 1987). Another rotational phase of the Coast Range province during this time and continuing today is related to the extension of the Basin and Range province (Armentrout, 1987) and northerly translation of the Washington and Oregon Coast Range province due to transpressional forces from continued northeastward-directed subduction.

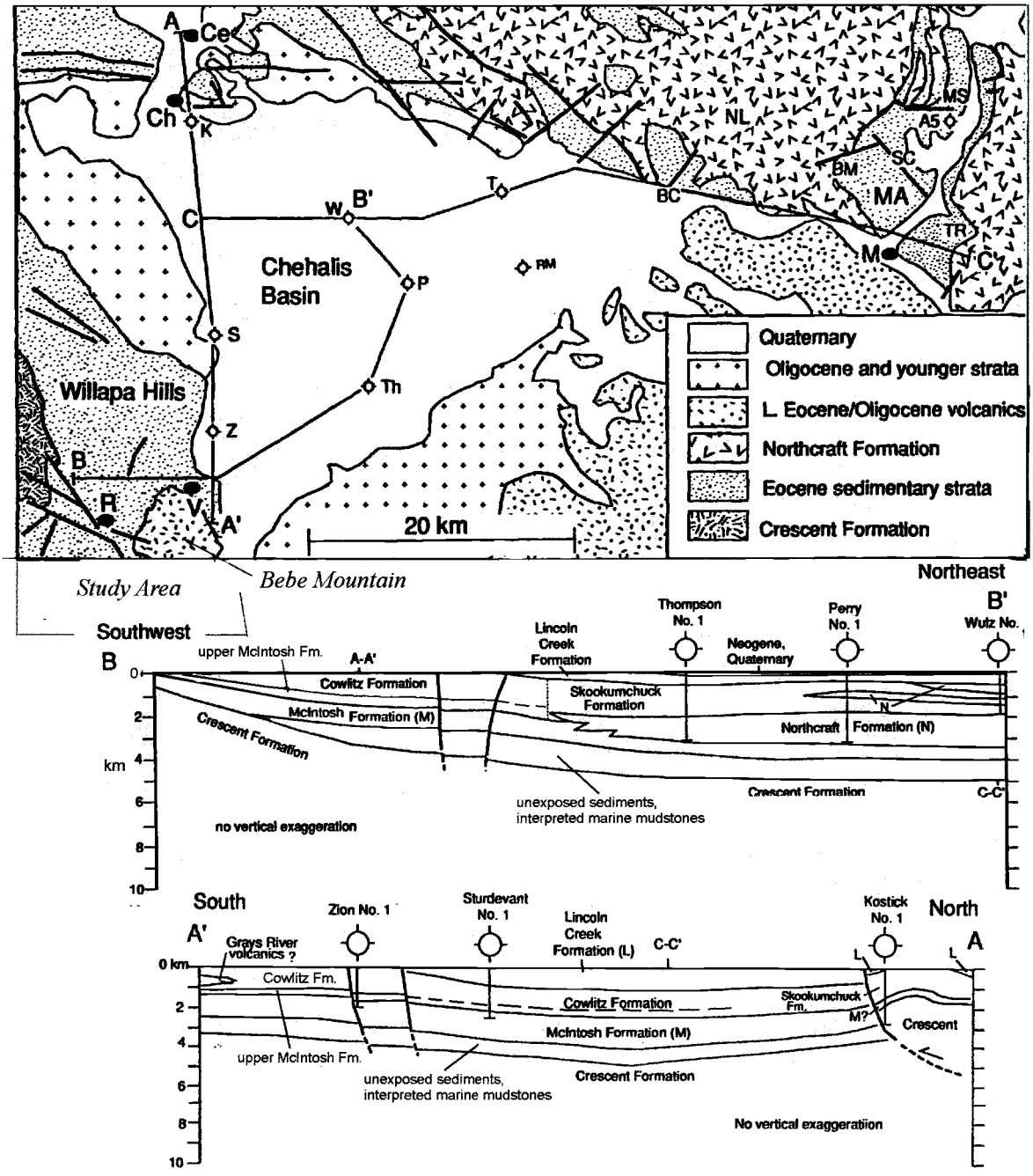

Figure 35. Geologic map of Chehalis basin and bounding uplifts. Abbreviations: Ce=Centralia, Ch=Chehalis; M=Morton, R=Ryderwood, S=Shell Sturdevant No.1 borehole; Th=Shell Thompson No.1 borehole; V=Vader Z=Shell Zion No.1 borehole. Schematic north-south cross section A-A' and southwest-northeast cross section B-B' are based on data from outcrop and borehole studies, seismic reflection profiles and magnetotelluric surveys (from Stanley et al., 1994). Note Eocene sedimentary units thin against the Willapa Hills basement high on the southwest margin of the basin, near the study area centered ~10 km south of Vader (slightly modifed from Stanley et al., 1994).

LOCAL STRUCTURE

The western study area is located on the southeast margin of the Willapa Hills uplift and the eastern study area on the southwest corner of the Chehalis basin (Figures 2, and 34). The oldest units (e.g. upper McIntosh Formation) are exposed in the mountainous northwest corner of the area, with the youngest units (e.g. Quaternary units, upper Cowlitz Formation informal unit 1) present in the river valleys of the southeast corner. Strata in the western study area generally dip 10° to 20° to the south-southeast, while strata in the relatively poorly exposed eastern study area generally dip to the northeast and southwest on either side of the northwest-trending Arkansas Anticline (Plate I, cross-section C – C'). Steeply dipping beds (>25°) usually result from proximity to faulting or slumping. Mapping of faults in the poorly exposed, densely forested study area was based on (1) exposure of fault planes in stream beds and roadcuts, (2) repetition of strata along stratigraphic sections, (3) field reconnaissance of lineations noted on aerial photos and (4) grouping of consistent attitudes of strata between lineations. Motion on the faults was determined by measuremening sub-horizontal slickensides on fault planes and vertical repetition of strata.

The mapped fault pattern in the study area generally matches the northwest- and northeast-trending fault systems mapped by other workers in the eastern Willapa Hills area, including Wells (1981), Wells and Coe (1985) and Payne (1998) (Figure 34; Plate I). There are three recognizable fault-sets and associated fault-related folds in the study area:

(1) North 30°- 50°W faults: occur as vertical to steep east-dipping faults with significant vertical offset and dextral slip components indicated by stratigraphic separation and slickensided fault surfaces. Payne (1998) defined two such faults that project into the study area near the western margin of Bebe Mountain, the west Pumphrey Mountain fault and the Bebe Mountain fault (Plate I). The Bebe Mountain fault has an estimated 800 m of dextral displacement and 60 m of normal vertical separation (west-side down), laterally juxtaposing the upper Grays River basalts against the Cowlitz Formation (Plate I) (Payne, 1998). The west Pumphrey Mountain fault offsets the axis of the Arkansas Anticline (Plate I). Wells (1981) mapped similar north-northwest-trending faults to the west and south. These faults displaced middle Miocene Columbia River basalts, suggesting they were active in the post-middle Miocene. Regional fault relationships suggest that some north-northwest-trending faults were active in the late Eocene and were reactivated in the post-middle Miocene (Payne, 1998; Niem, personal communication, 2000). A major north-northwest-trending regional fault mapped by Wells (1981) displaces the lower Grays River Volcanics in the southwest corner of the map area (Plate I; Figure 36). No estimate of the amount of lateral or vertical offset can be determined from exposures in the study area, although Wells (1981) showed this fault as an oblique-slip dextral fault with normal separation. In the northwest corner of the map area (Plate I; Figure 34) a steeply dipping (71° N), north-northwest-trending fault with approximately 50-60 m of normal vertical separation offsets the upper McIntosh sandstone. This fault appears to be a splay or is truncated by the west-northwest-trending

dextral oblique-slip Loper Creek Fault (Plate I). There are no fault-related folds associated with these faults in the study area.

(2) North 70°-80°W dextral oblique-slip faults: form the longest fault traces in the study area, including the Germany Creek fault and the Loper Creek fault (Plate I; Figure 36). The faults are generally steeply dipping to vertical, with vertical and dextral-slip separation. The Germany Creek fault is the most prominent structure in the study area, and is well exposed where it crosses Germany Creek (Plate I; Figure 36). The fault has north-side down, normal vertical displacement of 315 m based on repetition of stratigraphic section (South Germany Creek section). Grays River basalt on the upthrown south-side of the Germany Creek fault is dated at 40.01 ±0.34 Ma (GC-1), while the downthrown north-side of the fault contains a Grays River flow dated at 39.35 ±0.36 Ma (GC-2), confirming the sense of vertical motion and relative amount of vertical separation (Plate I). Subhorizontal slickensides, 15° from horizontal, on the Germany Creek fault plane indicate that the latest motion of the fault was right-lateral. The amount of lateral displacement seems to be subordinate to the vertical displacement based on the regional outcrop continuity of the Grays River Volcanics. The Germany Creek fault produced a drag-fold anticline, trending 30° to the fault along the upthrown south side of the fault. This drag-fold anticline recognized from the strikes and dips of strata along the South Germany Creek section, (Plate I, cross-sections) deforms the Cowlitz and presumably the underlying McIntosh formations, as well as several Grays River dikes. To the east and west of Germany Creek, the fault trace forms a well-developed lineation

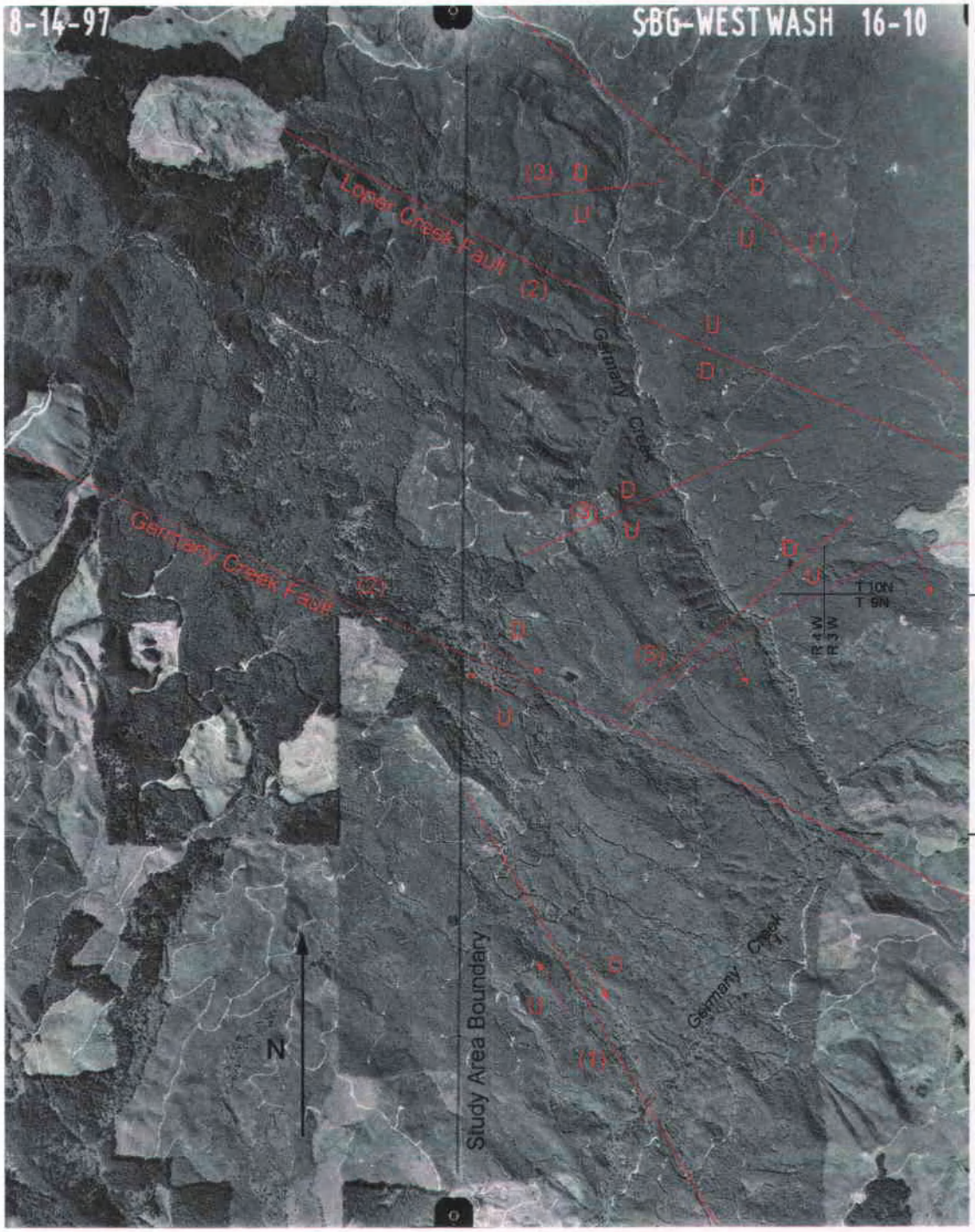

Figure 36. Aerial photo showing lineations of the Germany Creek drainage basin, western study area, northwest Cowlitz Co., Washington.
(1) North-northwest-trending dextral oblique-slip faults.
(2) Northwest-trending dextral oblique-slip faults, including the Germany Creek fault with a vertical displacement of 315 m.
(3) Northeast-trending normal faults, with possibly some sinistral displacement.
See Plate I and text for a complete discussion.

(Figure 36), but lack of exposure prevented accurate measure of the vertical and horizontal separation elsewhere in the study area.

Also associated with the deformation along the Germany Creek fault are smaller, sub-parallel normal faults (north-side down), that may or may not have dextral displacement (Plate I; Figure 34). It is undetermined whether these minor faults formed in response to the right-lateral shearing that produced the sub-horizontal slickensides on the Germany Creek fault, or were developed during the previous extensional period.

The Loper Creek fault, sub-parallel to and less exposed than the Germany Creek fault, shows less vertical separation (~50 m based on stratigraphic repetition, North Germany Creek Cowlitz and upper McIntosh section) with the south-side down. No slickensides or indications of lateral displacement were found associated with the Loper Creek fault, although it is probable that there is some amount of dextral displacement along the fault. The mapped Loper Creek fault position was determined from exposure in Germany Creek and correlation to a corresponding lineation on aerial photos (Figure 36). Together the Germany Creek and Loper Creek faults are the boundary faults of an intervening graben (Plate I, cross-section B – B'). The Loper Creek fault is associated with a Grays River volcanic dike swarm that trends sub-parallel to the fault trace. Dike sample 914L, dated at 39.98 ±0.29 Ma trends sub-perpendicular (~60°) a few feet north of the Loper Creek fault (Plate I).

The Germany Creek and Loper Creek faults were active in the late Eocene as evidenced by the deformation of Grays River dikes and associated dike swarms of the Loper Creek fault. Lack of exposure due to landslides and cover limits the interpretation

of how recently these faults were active, neither of them appear to offset the Lincoln Creek Formation or Grande Ronde Basalt Sentinel Bluffs unit (Plate I). However, because exposures of both the Lincoln Creek and Grande Ronde basalt are restricted to the intervening down-dropped graben between the Germany Creek and Loper Creek faults it is likely that these faults were active in the post-middle Miocene dextral-shearing event. Other northwest-trending faults in the region offset the Columbia River Basalts (Wells, 1981).

(3) North 40°-60°E faults: are shorter, north-side down normal faults, generally restricted to blocks between larger, bounding northwest-trending conjugate faults. Some northeast-trending faults mapped with sinistral displacement (Payne, 1998) are projected into the map area from the north (Plate I). The northeast-trending faults appear to be closely associated with numerous sub-parallel Grays River dikes. Although not associated with a fault, a northeast-trending Grays River dike (sample G810D) intruding the Cowlitz Formation in the South Germany Creek section was dated at 39.56 ±0.41 Ma (Plate I). The normal displacement on the faults crossing Germany Creek is estimated through repetition of Cowlitz strata to be approximately 30-50 meters. The late middle Eocene period of extension represented by the northeast-trending dikes likely produced the earlier-formed northeast-trending normal faults in the graben between the northwest-trending Germany Creek and Loper Creek faults (Plate I), and could represent early dextral transtension forming conjugate strike-slip fault pairs. Some small fault-related folds are associated with these faults. A small drag-fold anticline deforming the upper McIntosh sandstone, parallels a northeast-trending fault intruded by a dike in the

northwest corner of the map (Sec. 25, T 10 N, R 4 W; Plate I). A monocline trends parallel to three northeast-trending normal faults in the Germany Creek graben (Plate I, cross-section A – A').

In the subsurface at the Mist Gas Field in northwest Oregon, similar middle to late Eocene horst and graben style northwest- and northeast-trending normal faults offset the Cowlitz Formation and underlying Tillamook Volcanics (Niem, et al., 1992; Payne, 1998). Many of these faults do not displace the overlying upper Eocene to Oligocene Keasey Formation (partial Lincoln Creek equivalent) (Robertson, 1997). Likewise, a northwest- and northeast-trending conjugate normal fault system offsetting the Cowlitz Formation, but terminating at the unconformity between the overlying Grays River sedimentary sequence (Tgvs2) was recognized by Pauli (1995, in Payne, 1998) through subsurface correlation of exploration coreholes beneath and surrounding Bebe Mt (Plate I). Some of these faults were subsequently reactivated, offsetting the unconformable Grays River sedimentary sequence and overlying upper Grays River Volcanics (Payne, 1998).

Left-lateral displacement of some northeast-trending faults north of the study area offset the axis of the post-middle Miocene Arkansas Anticline up to 2 km, suggesting reactivation of the older structures (Plate I, cross-section C-C'). These reactivated northeast-trending faults could represent *en echelon* faults or Riedel shears formed in response to continued northwest-trending strike-slip to oblique-slip faults in a wrench tectonic setting (Payne, 1998).

The offset axis of the broad, northwest-trending Arkansas Anticline lies between Bebe and Abernathy mountains, generally paralleling the Arkansas valley in the eastern study area (Plate I). The anticline has been interpreted as the eastward extension of the Willapa Hills uplift (Wells, 1981; Payne, 1998). The post-middle Miocene regional compressional event deformed both the middle Eocene Cowlitz Formation and the overlying upper Grays River Volcanics of the study area, as well as younger Oligocene to middle Miocene units outside the study area (Wells, 1981). Russ Evarts of the U.S. Geological Survey identified an anticlinal fold along trend in the Miocene volcanics of the Washington Cascades to the southeast that may be an extension of the Arkansas Anticline (personal communication, 1999). Due to poor exposures, landslides, and the numerous faults, mapping of the axis of the Arkansas Anticline at 1:24,000 scale is difficult. However, in general, strata southwest of the Arkansas Valley strata to the southwest, whereas strata to the northeast of the valley generally dip to the northeast (Plate I, cross-section C-C').

Paleomagnetic declinations of Germany Creek samples indicate clockwise tectonic rotation, corroborating the interpretation that the study area underwent right-lateral shear. A clockwise (dextral) rotation of 103 ±7° was calculated for the Germany Creek sections by Prothero et al. (2001). Results from surrounding sections (see Regional Stratigraphy section) showed comparable rotations, but none as high as the Germany Creek section, indicating that the study area has undergone considerable dextral-shearing. However inclination data show that the Germany Creek section has had no significant northward translation (Prothero et al., 2001; Appendix F).

SUMMARY

Three fault sets and fault-related folds in the study area, as well as the Arkansas Anticline and its subsequent offset can be related to two main periods of deformation recognized in the Oregon and Washington Coast Ranges post Siletzia accretion in the early middle Eocene. The (1) north-northwest- and (2) northwest-trending dextral oblique-slip faults and (3) subordinate northeast-trending conjugate normal faults are related to dextral transtension of the Coast Range resulting in horst and graben style faulting. This style of faulting also occurs in the subsurface at the Mist Gas Field in northwest Oregon and Bebe Mountain in the study area. This period of transtensional deformation likely coincides with emplacement of the middle Eocene Grays River dikes of the study area, beginning at between 39.98 ±0.29 to 39.56 ±0.41 Ma, and terminating prior to the unconformably overlying upper Grays River Volcanics dated at 38.64 ±0.4 Ma (southeast Abernathy Mt., Plate I).

The second period of deformation is related to transpressional deformation of the Coast Range that produced dextral faults, fault re-activation and broad regional folding of the middle Miocene Columbia River Basalts throughout southwest Washington. This post-middle Miocene transpressional event resulted in continued uplift of the Willapa Hills and formation of the Arkansas Anticline in the northern part of the study area. Niem et al. (1992) contend that many northwest- and northeast-trending Eocene normal faults were reactivated with dextral motion during this post-middle Miocene deformation. As this deformation proceeded, the Arkansas Anticline was offset by new or reactivated northeast-trending left-lateral strike-slip faults. These left-lateral faults are believed to

have formed in a wrench tectonic setting as conjugate fault pairs or Riedel shears to the dominant right-lateral faults of the dextral transpressional deformation due to continued oblique subduction at the Cascadia subduction zone (Wells and Coe, 1985).

HYDROCARBON POTENTIAL

Since 1979, approximately 70 BCF (Johnson et al., 1997) has been produced from the Cowlitz Formation at the Mist Gas Field of nearby northwestern Oregon. Despite that success there has been limited exploration in the related Eocene units of southwest Washington. About 20 wells with depths greater than 3,000 ft (914 m) have been drilled in or around the Chehalis basin (Figure 2; Figure 34, 35), many in the 1950's and early 1960's (Johnson et al., 1997). At present, there is no oil or gas production in southwest Washington. However, the improving stratigraphic and structural resolution between producing units in northwest Oregon and southwest Washington has provided an exploration strategy for the study area and surrounding region, defined as the Cowlitz-Spencer gas play (407) by Johnson et al. (1997).

Using the Mist Gas Field as an analog, the exploration premise for this play is that methane gas generated from Eocene marine mudstone or non-marine carbonaceous mudstone and coal has migrated into reservoirs in overlying or interbedded Eocene deltaic, shallow-marine or submarine fan arkosic sandstone (Johnson et al., 1997). Traps are provided by horst and graben-style small block faults or small anticlines, and possibly some stratigraphic pinch-outs. Interbedded siltstones or overlying marine mudstones form the seals.

POTENTIAL RESERVOIRS

In the study area, four reservoir-quality micaceous arkosic sandstones in the upper McIntosh Formation sandstone unit and lower Cowlitz Formation have been studied. Potential micaceous lithic arkosic reservoir sandstones occur in the upper McIntosh sandstone and in the lowstand and early highstand system tracts of the lower Cowlitz Formation, deposited prior to encroachment of the Grays River Volcanics from the south into the study area. The sandstones (samples 916E, 914A, GW8C, G815B) which plot as lithic arkoses on the QFL diagram of Folk (1974), are nearly identical in mineralogy and texture to the producing reservoir sandstones of the Mist Gas Field and the Skookumchuck Formation storage sandstones of the Chehalis Basin (Jackson Prairie gas storage wells) (Johnson, et al. 1997). Visual estimates of porosity through point counting grains vs. pore spaces in four impregnated samples (916E, 914A, GW8C, G815B; Appendix C) range from 16% to 19%. Porosity is mainly primary intergranular with minor secondary porosity formed by partial dissolution of plagioclase feldspar grains (Figure 19A) and volcanic rock fragments. The primary porosity is open and shows good interconnectivity, suggesting homogeneous permeability particularly in the shoreface sandstones of the Cowlitz Formation. However, vertical permeability in the upper McIntosh carbonaceous laminated subtidal bar sandstones (916E) is somewhat restricted due to aligned carbonaceous material and mica flakes along laminae. In all the sandstones pore throats are open between intergranular pores. Minor grain-rimming smectite clay acting as a weak cement in these moderately friable sandstones (Figure

19A). Grain contacts are commonly tangential in the clean arkoses indicating that the sandstones have not undergone intense burial compaction.

POTENTIAL SEALS

The lowstand and transgressive upper McIntosh subtidal to shoreface sandstones are overlain by at least 130 m of highstand bathyal mudstones and siltstones of the upper McIntosh Formation siltstone, providing an effective seal (Plate II). The lower part of the upper McIntosh siltstone may also contain a 5-t o 10-m thick organic-rich condensed section (see Upper McIntosh Formation; Sequence Stratigraphy sections) providing a potential source rock. However, further organic geochemical analysis would be necessary to evaluate the source rock potential of these dark gray bathyal siltstones. Interbedded outer shelf mudstones and distal shoreface siltstones may provide seals for potential reservoir sandstones in the lower Cowlitz Formation of the study area (Plate II). These interbedded units may also serve to compartmentalize potential Cowlitz sandstone reservoir targets, or provide stratigraphic traps.

STRUCTURAL TRAPS

The Mist Gas Field structural style of numerous small late Eocene-formed horst and graben fault block traps is analogous to the study area (Johnson et al., 1997). The fault pattern of the entire study area is likely consistent with the western half of the map (Plate I) where northwest- and northeast-trending conjugate pairs of normal faults have offset the Cowlitz and underlying formations (Plate I). Due to poorer exposures, the

mapped fault pattern of the eastern part of the study area is much less comprehensive than the better-exposed western map area (Plate I). However, there does not appear to be a southwest Washington analog to the northwest Oregon Nehalem arch, the regional structure considered responsible for hydrocarbon migration out of the deep, mature zones of the Nehalem and/or Astoria basins into the reservoirs of the Mist Gas Field (Johnson et al., 1997) (Figure 34).

HYDROCARBON GENERATION AND MIGRATION

At the Mist Field, hydrocarbon generation was most likely initiated as early as 33 Ma at depths of 3,000 m (10,000 ft) or more in the Nehalem or Astoria basins based on a calculated Lopatin time-temperature index (TTI) model (Armentrout and Suek, 1985). Generation probably began in gas-prone, kerogen-bearing marginal marine-deltaic rocks (coals) and/or deeper bathyal mudstones downdip from the reservoir rocks after the reservoir rocks had been sealed and undergone initial faulting (Armentrout and Suek, 1985). The gas is largely methane with a carbon and oxygen isotope composition that suggests both insitu biogenic and migratory thermogenic sources (Armentrout and Suek, 1986).

In southwest Washington, the limiting factor in development of large gas accumulations has been the relatively low maturity of source rocks (Johnson et al., 1997). The calculated thermal gradient and therefore the maturation depth of 3,000 m (10,000 ft.) determined for northwest Oregon is a reasonable estimate for the thermal gradient and depth of maturation in southwest Washington, unless an area of higher heat flow was

encountered. The burial history of southwest Washington differs from northwest Oregon in that maximum burial and inferred generation and migration of hydrocarbons occurred in the early to middle Miocene, following marine deposition of the Oligocene Lincoln Creek Formation (Johnson et al., 1997). Today, bathyal marine mudstone of the lower McIntosh Formation are at sub-3,000 m depths in the central Chehalis basin (Figure 35). During the early to middle Miocene maximum burial it is likely that the lower Cowlitz Formation in the Chehalis basin of southwest Washington was also within the hydrocarbon window. Tertiary intrusions, Grays River dikes and interbedded Northcraft and overlying Grays River Volcanics along the margins of the basin may have provided a significantly higher heat flow allowing earlier (post late Eocene) generation of hydrocarbons in organic-rich carbonaceous mudstones and lignites of the upper McIntosh and Cowlitz marginal marine rocks.

Subsequently, migration of hydrocarbons out of the Chehalis basin depocenter could have been initiated updip toward potential traps in the study area from the early Oligocene to the middle Miocene. Today the potential upper McIntosh sandstone and lower Cowlitz reservoirs of the eastern part of the study area are updip from potential source rocks in the south-central Chehalis basin (Figures 2 and 34). If hydrocarbons were generated and migrated from the early Oligocene to middle Miocene, the migration pre-dates the post-middle Miocene transpressional deformation that formed the Arkansas Anticline. Small conjugate fault blocks formed during the late Eocene transtensional deformation could have provided structural traps similar to the Mist Field. Subtidal bar sandstones of the upper McIntosh Formation encased in carbonaceous siltstones may

provide local stratigraphic traps. In the western study area, continued uplift and erosion has breached and exposed potential reservoir sands of the upper McIntosh and lower Cowlitz formations. The breached Arkansas Anticline in the eastern study area exposes informal unit 1 of the lower Cowlitz Formation, but the underlying potential target upper McIntosh subtidal sandstone is preserved (Plate I).

PREVIOUS EXPLORATION

The 1925 Castle Rock Oil and Gas Co. Quigley No. 1 is the only deep exploratory well (TD = 2893', 900 m) drilled within the study area (center 18-T9-R2; Plate I, Plate III). Based on lithostratigraphic correlations (Plate III), the penetrated interval of Quigley No. 1 corresponds to the potential reservoir upper McIntosh sandstone up to informal unit 1B shoreface successions of the Cowlitz Formation. A "good show oil" was reported on the driller's log from the upper McIntosh sandstone interval in the Quigley No. 1 well cuttings descriptions. A 1.22 m "coaly" interval was also noted overlying the oil show sandstone (Plate III). No pressure data are available. A "brackish water" contact may be present 10.6 m above the coaly interval. Another "show oil" interval from the well log corresponds to the interpreted reservoir-quality aggradational shoreface successions of the early highstand systems tract of the Cowlitz Formation (Plate III). The data suggest that some hydrocarbons may be present within potential reservoirs of the study area.

FUTURE EXPLORATION

Based on the factors outlined for hydrocarbon exploration strategy in the vicinity of the study area and the gathered data, the most likely deep play involves the upper McIntosh Formation sandstone. Several reservoir quality, arkosic shoreface sandstones within the upper McIntosh Formation could be as thick as 5-10 meters (Plate II, Plate III). Small fault block traps (~1 square mile, 2.4 square km) could provide structural traps throughout the Chehalis basin and in unexplored areas of the Arkansas Creek Anticline. An effective seal, the overlying upper McIntosh bathyal siltstone, is present in all locations.

Important small-scale facies changes documented in this study can further refine exploration strategies for the upper McIntosh Formation sandstone member. The interpreted subtidal bar facies of the distal lowstand upper McIntosh sandstone of the western study area (Germany Creek sections) correlates to proximal intertidal channel sandstones of the Zion No. 1 well to the northeast (Plate III). The overlying transgressive lower shoreface silty sandstones in the upper McIntosh of Germany Creek correlate with medium-grained, hummocky cross-stratified middle shoreface sandstones in the Zion No. 1 well (Plate III). The 1.22 m "coaly" interval overlying the tide-dominated, lowstand upper McIntosh sandstone in the Quigley No.1 well lithostratigraphically correlates to a ~5-m thick coaly interval interpreted from the Zion No.1 well-log (Plate III). This coaly interval overlying the tide-dominated upper McIntosh sandstone was also reported by Payne (1998) exposed in Stillwater Creek to the north of the study area (Figure 1). However, this coal is not present in the Germany Creek section, where facies

relationships suggest time-equivalent, deeper water, distal depositional environments. Therefore in the study area, exploration targets within the upper McIntosh sandstone would probably have greater success if they were restricted to fault-bounded blocks on a north-south line east of Quigley No.1 (Plate I). No coals were found in the overlying lower Cowlitz Formation of Germany Creek, which show slightly deeper water facies equivalents to eastern measured sections and well-logs of the Cowlitz Formation (Plate III). However a Hampton Tree Farms employee, Longview, Washington recalled (1999) a coal seam burn from 1996 near the SW ¼ of Sec. 24, T 10 N, R 3 W, on the northeast flank of the Arkansas Creek Anticline, stratigraphically above the Arkansas Creek Cowlitz Formation section described in the study area (Plate I for location). Despite repeated attempts, this coal seam exposure could not be located.

Shallow wells (e.g. <300 m) penetrating Cowlitz Formation unit 1B and 3 coal seams in the Arkansas Creek valley area are now being tested by dewatering for potential commercial accumulations of coal bed methane. If these prove to be commercially viable, then similar potential coal bed methane plays may exist east of Quigley No. 1 in the more proximal coastal/delta plain facies of the Cowlitz Formation.

GEOLOGIC HISTORY

During the early-middle Eocene, northeastward-oblique subduction of the Kula and Farallon oceanic plates moved the Siletzia basaltic seamount chain toward the subduction zone of the North American continent, resulting in northeast-southwest compression and formation of a northwest-southeast fault and fold trend, with consequent uplift and erosion (Wells and Coe, 1985; Armentrout, 1987). The onset of the Willapa Hills uplift was a result of the transpressional strain associated with the accretion of Siletzia terrane along the continental margin around 46-48 Ma (Armentrout, 1987). The study area continued to be directly affected by the plate-boundary reorganization induced by the accretion of the thick, bouyant Siletzia terrane throughout the Eocene.

Rapid subsidence of the Siletzia terrane basement (Crescent Formation) in the middle Eocene due to crustal extension formed a large forearc basin with sub-basins extending from present-day southern Oregon to Vancouver Island, Canada (Niem et al., 1992). At the southern edge of the Chehalis basin, bathyal mudstone and minor arkosic sandstone of the lower McIntosh Formation onlap the Crescent Formation in the Willapa Hills, suggesting the area formed an Eocene basement high attributed to seamount topography at the top of the Crescent Formation (Stanley et al., 1994) (Figure 35). Alternatively, Wells and Coe (1985) attributed the onlapping of the middle and upper Eocene sedimentary units as a result of the uplifted Crescent Formation basement, i.e. Willapa Hills uplift, forming a structural paleo-topographic high within the subsiding forearc basin.

A relative fall in sea level of approximately 20-80 m based on juxtaposition of lithofacies is recorded in the sequence boundary that separates the upper shoreface, subtidal sandstones of the upper McIntosh Formation from the outer shelfal siltstone deposits of the lower McIntosh Formation (Plate III) (Payne, 1998). In the study area, this sequence boundary may be exposed near the base of the North Germany Creek section (Plate II). The sequence boundary has been correlated by Payne (1998) to the 42.5 Ma eustatic sequence boundary of Haq et al.(1987).

Subtidal bar facies of the upper McIntosh sandstone unit (up to 40-m thick) form a parasequence set interpreted to be a tide-dominated lowstand wedge prograding in an estuarine environment of a lowstand system tract (LST) (Figure 37). Deposition of the lowstand wedge occurs after maximum sea level fall has caused exposure of the shelf and relative sea level slowly begins to rise. Deposition is restricted seaward of the previous shelf break (change from shelf to slope), and the lowstand-shoreline sequences are deposited on the previous shelf or upper slope (Van Wagoner et al., 1992).

Overlying the subtidal facies, a vertical succession of wave-dominated, progressively thinner and more distal coarsening- and thickening-upward parasequences form a characteristic retrogradational parasequence set of a transgressive system tract (TST) in the upper McIntosh sandstone unit. Although the transgressive surface separating the lower tide-dominated interval from the upper wave-dominated interval is not exposed in Germany Creek, the backstepping pattern of successively younger wave-dominated parasequences indicates flooding of the lowstand shelf and deposition of broad shoreface successions as the transgression continued. Overlying this interval, a

glauconite-rich silty micaceous mudstone of the upper McIntosh Formation is interpreted as the early part of a condensed section. A maximum flooding surface representing the maximum relative sea level rise and subsequently the deepest paleo-bathymetry, is interpreted from the overlying dark, benthic foraminifer-bearing, homolithic mudstone of the upper McIntosh silty mudstone. The maximum flooding surface (MFS on Plate II) or downlap surface marks the progression from a transgressive system tract to a highstand system tract where the rate of relative sea level rise is at a minimum and parasequences began to build basinward, downlapping the condensed section. The bathyal HST upper McIntosh siltstone member is truncated by prograding inner shelf to lower shoreface successions of the Cowlitz Formation, indicating an abrupt change in water depth of at least 20-80 m based on inferred water depths from sedimentary structures and ichnofacies. The upper McIntosh Formation sandstone and siltstone members (270 m) are reversely polarized and correlate to Chron 19r (41.5 – 42.5 Ma).

The abrupt basinward shift in facies and observed scoured contact (Figure 9B) indicate a sequence boundary between the upper McIntosh siltstoneone member and the lower Cowlitz Formation. Based on interval thickness, correlation with surrounding units and benthic foraminifer age constraints, this sequence boundary defines the end of a complete sea level regression-transgression cycle or depositional sequence of the 3rd order (1 to 5 million years; Vail et al., 1977). A normal magnetozone between the upper McIntosh and Cowlitz formations straddles this sequence boundary and correlates to Chron 19n (41.2 – 41.5 Ma).

A rapid decrease in water depth of approximately 20 – 80 m is evident from the lithofacies and sedimentary structures (Figure 10) of the overlying depositional sequence of the lowest Cowlitz Formation in Germany Creek. The lowest shoreface succession consists of a 35-m thick coarsening- and thickening-upward parasequence overlain by a 40-m thick aggradational upper shoreface sequence interpreted as a wave-dominated delta front lowstand wedge (LST). The overlying 38-m thick interval consists of two coarsening- and thickening-upward, backstepping, middle to lower shoreface parasequences interpreted as a transgressive system tract. An aggradational parasequence stacking pattern of the early highstand system tract is represented by the overlying relatively equal thickness progradational shoreface parasequences of the lower Cowlitz Formation. Several shelf to upper shoreface progradational parasequences of the lower Cowlitz Formation interpreted as the late highstand system tract overlie the early highstand aggradational parasequences. The basal reversely polarized lowstand, transgressive and aggradational sequences of the Cowlitz Formation correlate to Chron 18r (40.1 – 41.2 Ma), with the uppermost normal polarity progradational sequences correlative to Chron 18n (38.4 – 40.1 Ma; Figure 33). The progradational interval is 225 m thick, containing an increasing percentage of basaltic sandstone upward until conformably overlain by subaerial Grays River Volcanic lava flows causing cessation of the arkosic deltaic/coastal plain depositional system.

Beginning at 40.09 ±0.34 Ma (sample GC-1,), subaerial augite-, olivine- and plagioclase-phyric subalkaline tholeiitic lava flows of the lower Grays River Volcanics progressed north into the study area, conformably overlying shoreface sandstone

successions of the Cowlitz Formation (Figure 37, Plate II). A second slightly younger lower Grays River Volcanics subaerial flow (GC-2) located to the north of GC-1, was $^{40}Ar/^{39}Ar$ dated at 39.35 ±0.36 Ma, demonstrating a regional trend of younger Grays River volcanism to the north, beginning with the Tillamook Volcanics in the subsurface of the Mist Gas Field. As the lower Grays River flows continued to encroach northward along the shoreface successions of the Cowlitz deltaic/coastal plain, the tidal channel complexes of Cowlitz Formation informal unit 1B (Arkansas Creek lithofacies, Figure 12) likely developed in response to tidal currents focused by the emergent Grays River volcanic high within the basin. Interbedded sedimentary subunits within the lower Grays River include the discontinuous 42-m thick, fossiliferous basaltic sandstone unit Tgvs1 and the 25-m thick, thin lignite-bearing, fluvial-lacustrine Tgvst interval. The estimated 1250 m lower Grays River Volcanics in the study area (~40 – 39 Ma) are correlated to Chron 18n based on radiometric age dates, interbedded normal polarity sedimentary units and a normal polarity basalt flow sample (GC-1) (Figure 31).

The lower Grays River Volcanics are associated with a period of dilation and emplacement of northeast- and minor northwest-trending Grays River dikes (> 100 dikes noted) beginning at between 39.98 ±0.29 to 39.56 ±0.41 Ma ($^{40}Ar/^{39}Ar$ dated dikes, 914L and G810D). Although no dikes were found age-equivalent to the unconformably overlying upper Grays River Volcanics dated at 38.64 ±0.4 Ma (Payne, 1998; southeast Abernathy Mt., Plate I), it is likely that dike activity continued throught the eruption of the lower and upper Grays River Volcanics. This period of dextral transtension induced clockwise tectonic rotation of the Coast Range and produced horst and graben style,

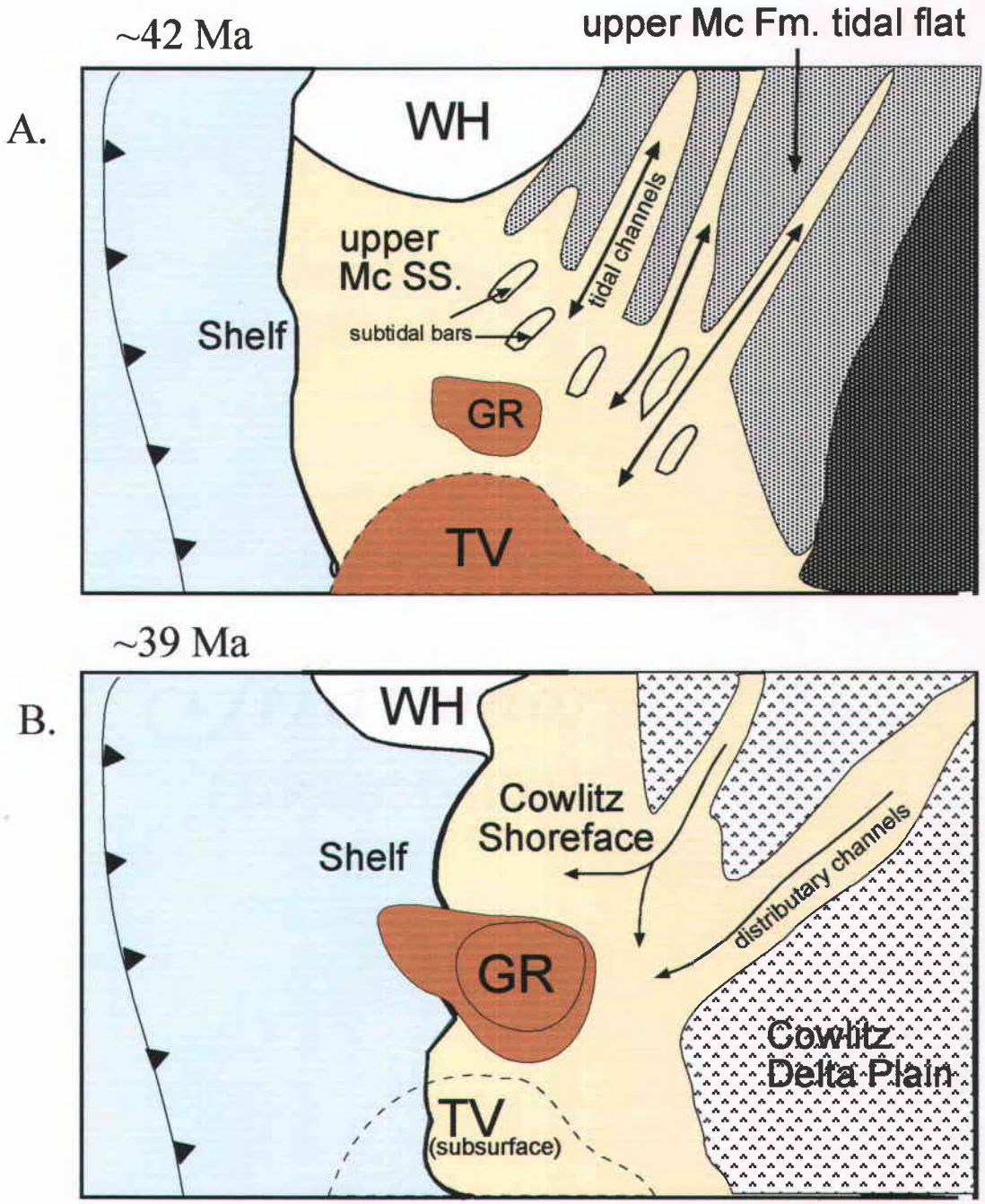

Figure 37. Schematic paleogeographic reconstructions of the (A) lowstand tide-dominated upper McIntosh sandstone member, ~42 Ma; and the (B) highstand prograding shoreface deposits of the lower Cowlitz Formation, ~40 Ma. WH = Willapa Hills structural high; GR = Grays River Volcanics; TV = Tillamook Volcanics.

north-northwest and northwest-trending dextral oblique-slip faults and subordinate northeast-trending conjugate normal faults which offset middle Eocene units and the lower Grays River Volcanics.

This late Eocene extensional period culminated in formation of a tectonically controlled erosional unconformity associated with a period of northeast-directed oblique subduction of the Farallon plate beneath North America (~38 Ma major Sequence Boundary II of Armentrout, 1987). In the study area, ongoing or reactivated Grays River olivine tholeiitic basaltic volcanism of the upper Grays River Volcanics of Abernathy and Bebe mountains, likely led to inflation of the crust, leading to uplift and erosion of the Cowlitz and lower Grays River strata about 38 Ma (Payne, 1998). The thick (<200 m), basal valley-fill sequence of the upper Grays River Volcanics sedimentary unit (Tgvs2), underlying the flows of the upper Grays River basalts (36.8 – 38.6 Ma, <300 m), was probably deposited in down-dropped blocks of normal-faulted and eroded Cowlitz and possibly upper McIntosh formations (Plate I; Payne, 1998). These normal faults offset the Cowlitz Formation and lower Grays River Volcanics but terminate at the overlying upper Grays River sedimentary sequence and upper Grays River flows (Pauli, 1997, in Payne, 1998).

Continuing plate-boundary readjustment associated with formation of the Cascadia subduction zone resulted in subsidence exceeding sediment supply in the shelf-margin basin of the study area beginning around 36-35 Ma (Armentrout, 1987). Arc magmatism of the newly developing Western Cascade Mountains produced tuffaceous

deep-marine deposits of the Lincoln Creek Formation that transgressed the subsiding upper Grays River Volcanics in the study area.

Late early Miocene (~18 Ma) readjustment of plate configuration continued dextral rotation of the Coast Range and uplifted the Lincoln Creek and underlying formations forming a regional unconformity (Regional Unconformity II of Armentrout, 1987). Backarc extension of the Great Basin accompanied extrusion of the Columbia River Basalt Group. A high MgO middle Miocene Grande Ronde Basalt flow interpreted to be Sentinel Bluffs basalt (15.6 Ma, Reidel et al., 1989) based on normal polarity and geochemical affinity (Figure 32), was deposited unnconformably overlying the late Eocene to early Oligocene Lincoln Creek Formation in the study area.

Post-middle Miocene transpression resulted in continued uplift and clockwise rotation of the Willapa Hills and formation of the northwest-trending Arkansas Anticline. The anticline has been interpreted as the eastward extension of the Willapa Hills uplift (Wells, 1981; Payne, 1998). This post-middle Miocene regional compressional event deformed both the middle Eocene Cowlitz Formation and the overlying late Eocene upper Grays River Volcanics of the study area, as well as younger Oligocene to middle Miocene units outside the study area (Wells, 1981). As this deformation proceeded, the Arkansas Anticline was offset by new or reactivated northeast-trending left-lateral strike-slip faults.

A late Pliocene to early Pleistocene regional unconformity (Regional Unconformity I of Armentrout, 1987) formed by erosion of areas uplifted by the ongoing northeast-directed compression forced by the subduction of the Juan de Fuca plate

beneath North America. Quaternary terrace units of the study area are primarily the result of sudden deposition of glacial flood and episodic lahar deposits along the major drainages of the eastern margin of the area. Probable Missoula flood slackwater silt deposits (unit Qtr) and at least two lahar deposits from Mt. Saint Helens (pre-1980 unit Qshu1 and 1980 unit Qshu3) are present along lower Arkansas Creek and the western and eastern banks of the Cowlitz River drainages (Plate I).

CONCLUSIONS

Based on detailed lithofacies descriptions of 3 measured sections (1160 m total), sampling of macro- and microfossils, magnetic stratigraphy and $^{40}Ar/^{39}Ar$ dates, the local stratigraphy was correlated to related regional units and used to interpret the middle to late Eocene unconformity-bound sequences and depositional systems. Geologic mapping of the 62 square mile study area at 1:24,000 coupled with petrographic analysis of potential reservoir sandstones of the upper McIntosh and Cowlitz formations allowed interpretations of the structural geology of the area, interaction of forearc basaltic volcanism with deltaic sedimentation, and preliminary hydrocarbon prospect targets. In summary, the results and interpretations of the study are:

1. The middle Eocene upper McIntosh sandstone member is at least 132 m thick and is composed of two systems tracts. The basal 52-m thick tide-dominated lithofacies arkosic sandstone and carbonaceous mudstone parasequences are interpeted as prograding lowstand wedge subtidal bars. The overlying 80-m thick wave-dominated lithofacies arkosic sandstone and siltstone parasequences are interpreted as transgressive lower to middle shoreface deposits. The two subunits define a lowstand to transgressive systems tract progression. A lowstand tide-dominated delta is interpreted to have deposited prograding subtidal bars along a partially flooded embayment of the shelf during the early stages of sea level rise. Continued sea level rise and subsequent transgression deposited broad retrogradational wave-dominated shoreface parasequences across the shelf.

2. The middle Eocene 163-m thick bathyal upper McIntosh Formation siltstone member is interpreted as a distal highstand systems tract. Glauconite-rich silty mudstones at the base of the upper McIntosh siltstone member represent a condensed section deposited on a starved shelf. Planktonic and bathyal foraminifers recovered from mudstones between thin-bedded turbidites facies indicate deep-marine, open ocean deposition. The uppermost McIntosh siltstone member is truncated by an unconformity at the base of the Cowlitz Formation.

3. The 374-m thick shoreface successions of the middle Eocene Cowlitz Formation in Germany Creek is composed of three systems tracts. A rapid decrease in water depth is evident from the change in lithofacies and truncation of the upper McIntosh siltstone by the basal 75-m thick lower shoreface to delta-front Cowlitz Formation lowstand wedge. Two overlying backstepping lower to middle shoreface parasequences are interpreted as a 38 m thick transgressive system tract interval. The uppermost 273-m thick Cowlitz Formation interval of shallow marine mollusk- and inner shelf benthic foraminifer-bearing aggradational and progradational lower to upper shoreface parasequences is interpreted as a highstand delta. Basaltic sandstone beds increase in thickness and frequency toward the upper contact of the shallow marine Cowlitz Formation with conformably overlying Grays River subaerial basalt flows (dated at 39.35 ±0.36 Ma and 40.09 ±0.34).

4. Lithofacies of the Cowlitz Formation in Monahan Creek and Arkansas Creek contain coarsening- and thickening-upward arkosic lower to upper shoreface parasequences similar to the highstand Cowlitz Formation in Germany Creek. Well-

exposed tide-dominated lithofacies in a roadcut above Arkansas Creek area are interpreted as subtidal channel fills, consistent with Payne's (1998) Cowlitz Formation informal unit 1B, which overlies the informal basal unit 1A.

5. Based on 39 magnetic sample sites and a 39.35 ±0.36 Ma age of a basalt flow conformably overlying the North Germany Creek section, the lower 270-m upper McIntosh Formation reversed polarity interval is correlative to Chron 19r (41.5 – 42.5 Ma). The normal magnetozone between the upper McIntosh and Cowlitz formations straddles a period of nondeposition, and likely correlates to Chron 19n (41.2 – 41.5 Ma). The overlying dominantly reversed polarity magnetozone of Cowlitz Formation informal unit 1 correlates with Chron 18r (40.1 – 41.2 Ma), with the uppermost normally polarized interval correlative to Chron 18n (38.4 – 40.1 Ma). Based on the 40.09 ±0.34 Ma conformably overlying basalt flow, the lower reverse polarity magnetozone of the South Germany Creek section is correlative to Chron 18r, and the upper normal polarity magnetozone to Chron 18n. The Germany Creek sections show an anomalously large clockwise rotation of 103 ±7 degrees and a negligible northward translation of 5 ±7 degrees relative to the Eocene cratonic pole (Prothero et al., 2001) (Appendix F).

6. There is a strong lithologic correlation between units of the Germany Creek measured sections (Cowlitz Formation informal unit 1A) and strata penetrated by the 1925 Castle Rock Oil and Gas Company Quigley No.1 well (Plate III). This correlation suggests that the Cowlitz Formation forming the broad hills and valleys in the eastern part of the study area near the Quigley No. 1 well consists of Cowlitz Formation informal unit 1B or lower unit 2. Thickening of the Cowlitz Formation to the southeast is

consistent with regional well and seismic observations that the Cowlitz and McIntosh Formations thin and onlap the Crescent Formation basement uplift of the Willapa Hills to the northwest of the study area.

7. Diagenetic events from McIntosh and Cowlitz lithic arkoses suggest shallow burial with partial dissolution of potassium feldspar resulting in minor secondary porosity and later redeposition of potassium feldspar overgrowths. Later stage authigenic smectite clay rims many framework grains, but has not filled much of the primary intergranular pore space. XRD determined heulandite is formed under shallow burial conditions, no greater than 2000 m. Primary intergranular porosities of the analyzed potential reservoir sandstones are estimated at 16-19%. Thin section analysis of the Cowlitz and McIntosh Formation lithic arkosic sandstones and volcanic sandstones indicate a mixed extrabasinal plutonic-metamorphic source (Idaho Batholith) and a local basaltic source. The basaltic clasts were derived from erosion of Grays River and/or Tillamook volcanics of southwest Washington and northwest Oregon.

8. Grays River Volcanics of the study area are subdivided locally by an intraformational unconformity that defines the lower (Tgv1, ~1250-m thick) and upper (Tgv2) units. Lower Grays River Volcanics conformably overlie the Cowlitz Formation in the Germany Creek area. Two basal Grays River basalt flows were $^{40}Ar/^{39}Ar$ dated at 40.01 ±0.34 Ma and 39.35 ±0.36 Ma. Interbedded volcaniclastic sedimentary subunits within the lower Grays River include the discontinuous 42-m thick, molluscan-bearing basaltic sandstone unit Tgvs1 and the 25-m thick, thin lignite-bearing, fluvial-lacustrine Tgvst unit. Lower Grays River Volcanics in the study area are correlated to Chron 18n

based on radiometric ages, interbedded normal polarity strata and normal polarity of flow sample GC-1 (Figure 31). Geochemistry of major- and minor-element oxides ofs lower Grays River lava flows suggests possible differentiation from lowest flow subalkaline olivine tholeiitic basalt to upper flow subalkaline plagioclase-phyric basaltic andesite (Figure 31).

Upper Grays River Volcanics (38.6 – 36.8 Ma, ~150-m thick) are exposed at Bebe and Abernathy mountains. Underlying the subaerial lavas is an unconformity valley-fill unit, Tgvs2, that unconformably overlies Cowlitz Formation arkosic sandstone and grades upward to shallow-marine basaltic sandstone, tuffaceous lithic siltstones and lapilli tuff-beds. These strata were probably deposited in structural lows highlands of lower Grays River Volcanics and Cowlitz Formation. Renewed or continuing Grays River volcanism produced the upper Grays River basalt flows that overlie the Grays River valley-fill sequence. Upper Grays River basalts all classify as subalkaline tholeiitic basalts.

9. Lower Grays River Volcanics lava flows and porphyritic dikes contain olivine and augite phenocrysts and plagioclase-glomerocrysts. Rounded, resorbed euhedral olivine and subhedral titanoaugite phenocrysts are common in the lowest basalt flows. Some Grays River dikes have plagioclase glomerocrysts in the interior. Chilled microphyric margins suggest multiple injections of basaltic magma. These textural features and chemical compositions in the primitive subalkaline tholeiitic basalts indicate decompression melting of the mantle. Higher concentration of incompatible trace elements (Ti, K, Rb, Sr, Zr and Ba) in the Grays River Volcanics relative to MORB

suggests a deeper mantle source that is not depleted compared to shallower mantle sources under mid-ocean ridges (Philpotts, 1990). Basal flows of the lower and upper Grays River Volcanics are olivine-bearing tholeiites consistent with a picritic-derived primary magma.

10. Numerous sub-parallel, northwest- and northeast-trending sub-vertical GraysRiver dikes attest to the crustal extension of the study area during emplacement of the Grays River Volcanics in the mid-Eocene. Two dikes have overlapping $^{40}Ar/^{39}Ar$ ages of 39.98 ±0.29 Ma and 39.56 ±0.41 Ma, indicating the intrusions were concurrent with the eruption of the lower Grays River Volcanics.

11. Lower Grays River Volcanics appear to have been erupted in a subsiding basin, whereas the upper Grays River Volcanics were formed after a brief period of uplift and erosion. Factors responsible for basin uplift or subsidence are complex in this marginal marine middle Eocene forearc basin of the study area. If the Grays River volcanism is a result of a remanent mantle plume, then thermal inflation and uplift of the lithosphere resulting in erosion of sediments would precede eruption. If the volcanism is due to a passive rise of the mantle into zones of lithospheric extension, basin subsidence and sedimentation would precede extrusion (Philpotts, 1990).

12. The early Oligocene Lincoln Creek Formation (~70-m thick) consists of bioturbated, tuffaceous siltstone and interbedded sandstone containing casts and molds of articulated bivalves and gastropods. Benthic foraminifers from the tuffaceous siltstone are assigned to the Refugian stage. Trace fossils include hook-shaped *Phycosiphon* burrows, suggesting an outer shelf to bathyal depositional environment.

The Lincoln Creek Formation is unconformably overlain by the middle Miocene Sentinel Bluffs unit of the Grande Ronde Basalt.

13. Grande Ronde Basalt in the study area is a blocky, dark gray, aphyric, dikytaxitic basalt. The maximum thickness of the Grande Ronde Basalt is estimated to be 50 to 60 m, consisting of 1 or two flows. Geochemistry of the major- and minor-element oxides, normal polarity of the basalt, and dikytaxitic texture indicate that it is most likely Sentinel Bluffs basalt (15.6 Ma).

14. The magnetic polarity correlations of regional middle Eocene measured sections suggest that the Hamlet-McIntosh and Cowlitz formations of northwestern Oregon and southwestern Washington span most of the middle Eocene. The upper McIntosh and Hamlet formations correlate to Chron C19r (41.5 – 42.5 Ma) and the lower part of Chron C19n (41.5 – 41.2 Ma). In southwest Washington, the Cowlitz Formation spans from Chron C19n in Germany Creek and Coal Creek, to as young as Chron C17n (36.5 – 38.2 Ma) in Olequa Creek (Figure 33). Variable time-thicknesses of the individual sections may reflect a non-uniform sedimentation rate for the different parts of the depositional system.

15. The line of the stratigraphic section from Plate III is interpreted as crossing the southeast flank of a thick accumulation of Grays River Volcanics, penetrated by the Champlin Puckett well (Figure 22 for location). This unit thins in the subsurface to the southeast (Robertson, 1997). It is likely that the C&W sandstone member of the Cowlitz Formation of northwest Oregon correlates with the lower Cowlitz Formation highstand systems tract shoreface successions (unit 1A and lower 1B) seen in outcrops and well-

logs in southwest Washington (Plate III). Cowlitz Formation coal-bearing intervals in northwest Oregon are lithostratigraphically correlative to the thick coal seams of informal unit 1B of the lower Cowlitz Formation (Plate III).

16. The three fault sets, fault-related folds and the Arkansas Anticline can be related to two extensive periods of deformation. The (1) north-northwest- and (2) northwest-trending dextral oblique-slip faults and (3) subordinate northeast-trending conjugate normal faults are related to dextral transtension of the Coast Range resulting in horsts and grabens as seen in the subsurface at Mist and Bebe Mountain. This period of transtensional deformation likely coincided with emplacement of the Grays River dikes in the study area, beginning at between 39.98 ±0.29 to 39.56 ±0.41 Ma, and terminating prior to the eruptions of the upper Grays River Volcanics (dated at 38.64 ±0.4 Ma). The second period of deformation produced dextral faults, fault re-activation and broad regional folding of the middle Miocene Columbia River Basalts throughout southwest Washington. This post-middle Miocene transpressional event resulted in continued clockwise rotation and uplift of the Willapa Hills and formation of the Arkansas Anticline. As this deformation proceeded, the Arkansas Anticline was offset by new or reactivated northeast-trending left-lateral strike-slip faults.

17. The most likely play in the study area involves the upper McIntosh Formation sandstone. The reservoir quality sands (17% porosity) in the upper McIntosh Formation could be as thick as 5 to10 meters (Plate II, Plate III). Small fault block traps similar to the Mist Gas Field (~1 square mile, 2.4 square km) provide potential structural traps throughout southwest Washington. The overlying upper McIntosh bathyal siltstone could

be an effective seal. In the central Chehalis basin the lower McIntosh Formation bathyal marine mudstone is at the sub-3,000 m calculated hydrocarbon generation window (Figure 33). During the early to middle Miocene maximum burial, it is likely that the lower Cowlitz Formation was also within the hydrocarbon window. Tertiary intrusions and interbedded volcanics along the margins of the basin may have provided higher heat flow allowing earlier (post late Eocene) generation of hydrocarbons in carbonaceous mudstones and lignites of the upper McIntosh and Cowlitz Formation. Migration of hydrocarbons out of the Chehalis basin depocenter could have been initiated from the early Oligocene to the middle Miocene. Upper McIntosh sandstone and lower Cowlitz reservoirs of the eastern study area are updip from potential source rocks in the south-central Chehalis basin. If hydrocarbons were generated and migrated from the early Oligocene to middle Miocene, the migration occurred after the late Eocene faulting event but pre-dated the post-middle Miocene transpressional deformation that formed the Arkansas Anticline. Therefore, hydrocarbons may have accumulated in fault traps as in the Mist Gas Field.

REFERENCES

Armentrout, J.M., 1977, Cenozoic stratigraphy of southwestern Washington, in Brown, E.H. and Ellis, R.C., eds., Geological Excursions in the Pacific Northwest: Geological Society of America 1977 Annual Meeting, p. 227-264.

Armentrout, J.M., and Suek, D.H., 1985, Hydrocarbon exploratoin in western Oregon and Washington: American Association of Petroleum Geologists Bulletin, v. 69, p. 627-643.

Armentrout, J.M., 1987, Cenozoic stratigraphy, unconformity-bounded sequences, and tectonic history of southwestern Washington, in Schuster, J. E., ed., Selected papers on the geology of Washington: Washington Department of Natural Resources, Division of Geology and Earth Resources Bulletin 77, p. 291-320.

Berggren, W.A., Kent, D.V., Swisher, C.C., and Aubry, M.P., 1995, A revised Cenozoic geochronology and chronostratigraphy: in Berggren, W.A., Kent, Aubry, M.P., and Hardenbol, J., eds., Geochronology, time scales and global stratigraphic correlation: SEPM Special Publication No. 54, p. 129-212.

Berkman, T.A., 1990, Surface-subsurface geology of the middle to upper Eocene sedimentary and volcanic units, western Columbia County, northwest Oregon: unpublished M.S. thesis, Oregon State University, Corvallis, 413 p.

Buckovic, W.A., 1979, The Eocene deltaic system of west-central Washington, in Armentrout, J.M., Cole, M.R., and TerBest, J., Jr. eds., Cenozoic paleogeography of the western United States: Pacific Coast Paleogeography Symposium 3, SEPM Pacific section, p. 147-163.

Bukry, D., 1975, Coccolith and silicoflagellate stratigraphy, northwestern Pacific Ocean, Deep Sea Drilling Project Leg 32: Washington D.C., Initial reports of the Deep Sea Drilling Project, v. 32, p. 677-701.

Chan, M.A., and Dott, R.H., Jr., 1986, Depositional facies and progradational sequences in Eocene wave-dominated deltaic complexes, southwestern Oregon: American Association of Petroleum Geologists Bulletin, v. 70, no. 4, p. 415-430.

Demarest, H.H., Jr., 1983, Error analysis for the determination of tectonic rotation from paleomagnetic data: Journal of Geophysical Research, v. 88, p. 4321-4328.

Diehl, J.F., Beck, M.E., Jr., Beske-Diehl, S., Jacobsen, D., and Hearn, B.C., Jr., 1983, Paleomagnetism of the Late Cretaceous-early Tertiary north-central Montana alkalic province: Journal of Geophysical Research, v. 88, p. 10593-10609.

Duncan, R.A, 1982, A captured island chain in the Coast Range of Oregon and Washington: Journal of Geophysical Research, v. 87, p. 10,827-10,837.

Evarts, R., U.S. Geological Survey, Western Regional Branch, Menlo Park California, written and personal communication, 1999-2000.

Finn, C., Phillips, W.M., and Williams, D.L., 1991, Gravity anomaly and terrain maps of Washington: U.S. Geological Survey Geophysical Investigations Map GP-988.

Flores, R.M. and Johnson, S.Y., 1995, Sedimentology and lithofacies of the Eocene Skookumchuck Formation in the Centralia coal mine, southwest Washington, in Fritsch, A.E., ed., Cenozoic paleogeography of the western United States-II: SEPM Pacific Section, book 75, p. 274-290.

Folk, R.L., 1974, Petrology of sedimentary rocks: Austin, Texas, Hemphill, 182 p.

Gilkey, K.E., 1983, Sedimentology of the North Fork and South Fork Toutle River mudflows generated during the 1980 eruption of Mt. St. Helens: University of California at Santa Barbara Master or Arts thesis, 254 p., 2 plates

Glasmann, J.R, Professor of Geology, Oregon State University, personal communications, 1999.

Grieff, J., Micropaleontologist, University of Washington Burke Museum, written communication, 2000.

Hammond, P.E., Prof. of Geology, Portland State University, personal comm., 2001.

Haq, B.U., Hardenbol, J., and Vail, P.R., 1987, Chronology of fluctuating sea levels since the Triassic: Science, v. 235, p. 1156-1167.

Henriksen, D.A., 1956, Eocene stratigraphy of the lower Cowlitz River area, eastern Willapa Hills area, southwestern Washington: Washington Division of Mines and Geology Bulletin 43, 122 p.

Irvine, T.N., and Barager, W.R.A., 1971, A guide to the chemical classification of the common volcanic rocks: Canadian Journal of Earth Sciences, v. 8, p. 523-548.

Irving, A.J., Nesbitt, E.A, and Renne, P.R., 1996, Age constraints on earliest Cascade arc volcanism and Eocene marine biozones from a feldspar-rich tuff in the Cowlitz Formation, southwest Washington: EOS Transactions of the American Geophysical Union, v. 77, no. 46, p. F-814.

Johnson, S.Y., Tennyson, M.E., Lingley W.S., Jr., and Law, B.E., 1997, Petroleum geology of the state of Washington: U.S.G.S. Professional Paper 1582, 40 p.

Kenitz, S., 1997, Correlation of Volcanic Rocks within Middle Late Eocene (Narizian Stage) Sedimentary Rocks in the Mist Gas Field Area, Columbia County, Oregon: unpublished M.S. thesis, Portland State University, 70 p.

Le Bas, M.J., Le Maitre, R.W., Streckeisen, A., and Zanettin, B., 1986, A chemical classification of volcanic rocks based on the total alkali-silica diagram: Journal of Petrology, v. 27, p. 745-750.

Livingston, V.E., Jr., 1966, Geology and mineral resources of the Kelso-Cathlamet area, Cowlitz and Wahkiakum counties, Washington: Washington Division of Mines and Geology Bulletin 54, 110 p.

Magill, J., Cox, A., and Duncan, R., 1981, Tillamook Volcanic Series: Further evidence for tectonic rotation of the Oregon Coast Range: Journal of Geophysical Research, v. 86, p. 2953-2970.

Mitchum, R.M., 1977, Seismic stratigraphy and global changes of sea level, Part 1, *in* C.E. Payton, ed., Seismic stratigraphy-applications to hydrocarbon exploration: AAPG Memoir 26, p. 53-62.

Miyashiro, A., 1974, Volcanic rock series in island arcs and active continental margins: American Journal of Science, v. 274, p. 321-355.

Moothart, S.R., 1992, Geology of the middle and upper Eocene McIntosh Formation and adjacent volcanic and sedimentary rock units, Pacific County, southwestern Washington: unpublished M.S. thesis, Oregon State University, Corvallis, 265 p.

Mumford, D.F., 1988, Geology of the Elsie-lower Nehalem River area, south-central Clatsop and northernmost Tillamook counties, northwestern Oregon: unpublished M.S. thesis, Oregon State University, Corvallis, 392 p.

Myers, D.A., 1970, Availability of groundwater in western Cowlitz County, Washington: Washington Department of Ecology Water-Supply Bulletin 35, 63 p., 2 pl., in Phillips, W.M., 1987, Geologic map of the Mount St. Helens quadrangle, Washington: Washington Division of Geology and Earth Resources Open File Report 87-4, 63 p., 1 plate, scale 1:100,000.

Nelson, D.E., 1984, Geology of the Fishhawk Falls-Jewell area, Clatsop County, Oregon: unpublished M.S. thesis, Oregon State University, 360 p.

Nesbitt, E.A., 1995, Paleoecological analysis of molluscan assemblages from the middle Eocene Cowlitz Formation, southwest Washington: Journal of Paleontology, v. 69, no. 6, 1060-1073.

Nesbitt, E.A., Research Associate, Thomas Burke Memorial Washington State Museum written and personal communication, 1999-2000.

Niem, A.R., Professor of Geology, Department of Geosciences, Oregon State University, Corvallis, written and personal communication 1998-2001.

Niem, W.A., MacLeod, N.S., Snavely, P.D., Jr., Huggins, D., Fortier, J.D., Meyer, H.J., Seeling, A., and Niem, W.A., 1992, Onshore-offshore geologic cross section, northern Oregon Coast Range to continental slope: Oregon Department of Geology and Mineral Industries Continental Margin Transect OGI-26, 10 p. 1 plate.

Niem A.R., and Niem, W.A., 1984, Cenozoic geology and geologic history of western Oregon, in Kulm, L.D. et al., eds., Western North America continental margin and adjacent ocean floor off Oregon and Washington: sheet 17.

Nio, S., and Yang, C., 1991, Diagnostic attributes of clastic tidal deposits: a review, in Smith, D.G., Reinson, G.E. Zaitlin, B.A, and Rahmani, R, A., eds., Clastic tidal sedimentology: Canadian Society of Petroleum Geologists, Memoir 16, p. 3-28.

Pauli, D., Exploration Geologist, Weyerhaeuser Minerals Division, Tacoma, Washington, written and personal communication, 1999-2001.

Payne, C.W., 1998, Lithofacies, Stratigraphy, and Geology of the middle Eocene type Cowlitz Formation and associated volcanic and sedimentary units, eastern Willapa Hills, southwest Washington: unpublished M.S. thesis, Oregon State University, Corvallis, 235 p.

Pease, M.H., and Hoover, L., 1957, Geology of the Doty-Minot Peak area, Washington: United States Geological Survey Oil and Gas Investigations Map OM-188, scale 1:62,500.

Pemberton, S.G., and MacEachern, J.A., 1992, Trace fossil facies models: Environmental and allostratigraphic significance; in Walker, R.G., and James, N.P., eds., Facies Models: Response to sea level change: Geological Association of Canada, p. 47-72.

Phillips, W.M., 1987, Geologic map of the Mount St. Helens quadrangle, Washington: Washington Division of Geology and Earth Resources Open File Report 87-4, 63 p., 1 plate, scale 1:100,000.

Phillips, W.M., Walsh, T.J., and Hagen, R.A., 1989, Eocene transition from oceanic to arc volcanism, southwest Washington: United States Geological Survey Open File Report, 89-178, p. 199-256.

Philpotts, A.R., 1990, Principles of igneous and metamorphic petrology: Englewood, New Jersey, Prentice Hall, p. 53, 286-290, 450-451.

Prothero, D.R., and Armentrout, J.M., 1985, Magnetostratigraphic correlation of the Lincoln Creek Formation, Washington: Implications for the age of the Eocene/ Oligocene boundary: Geology, v. 13, p. 208-211.

Prothero, D.R., Sanger, E., Nesbitt, E., Niem, A., and Kleibacker, D., in press, Magnetic stratigraphy and tectonic rotation of the middle Eocene Cowlitz and Hamlet Formations, western Oregon and Washington, in press, Cenozoic paleogeography of the western United States: Pacific Coast Paleogeography Symposium, SEPM Pacific section.

Rarey, P.J., 1985, Geology of the Hamlet-North Fork of the Nehalem River area, southern Clatsop and northernmost Tillamook counties, northwest Oregon: unpublished M.S. thesis, Oregon State University, Corvallis, 457 p.

Rau W.W., 1958, Stratigraphy and foraminiferal zonation in some Tertiary rocks of southwest Washington: U.S. Geological Survey, Oil and Gas Investigation, Chart O.C. 57, 2 sheets.

Rau, W.W., Micropaleontologist, written communication, 2000.

Reidel, S.P., Tolan, T.L., Hooper, P.R., Beeson, M.H., Fecht, K.R., Bentley, R.D., and Anderson, J.L., 1989, The Grande Ronde Basalt, Columbia River Basalt Group; Stratigraphic descriptions and correlations in Washington, Oregon and Idaho, in Reidel, S.P., and Hooper, P.R., eds., Volcanism and tectonism in the Columbia River flood-basalt province: Boulder, Colorado, Geological Society of America, Special Paper 239.

Roberts, A.E., 1958, Geology and coal resources of the Toledo-Castle Rock district, Cowlitz and Lewis Counties, Washington: U.S. Geological Survey Bulletin 1062 71 p.

Robertson, C.L., 1997, Subsurface-surface facies distribution of the Eocene Cowlitz and Hamlet Formations, northwest Oregon: unpublished M.S. thesis, Oregon State University, Corvallis, 143 p.

Safley, L.E., 1989, Geology of the Rock Creek-Green Mountain area, southeast Clatsop and northernmost Tillamook counties, northwestern Oregon: unpublished M.S. thesis, Oregon State University, Corvallis, 245 p.

Schasse, H.W., compiler, 1987, Geologic map of the Centralia quadrangle, Washington: Washington Division of Geology and Earth Resources Open-File Report 87-11, 27 p., 1 pl., scale 1:100,000.

Scott, K.M., 1986, Lahars and lahar-runout flows in the Toutle-Cowlitz River system, Mount St. Helens, Washington—Magnitude and frequency: U.S. Geological Survey Open-File Report 86-500, 95 p.

Snavely, P.D., Jr., Rau, W.W., Hoover, Linn, Jr., Roberts, A.E., 1951, McIntosh Formation, Centralia-Chehalis coal district, Washington: American Association of Petroleum Geologists Bulletin, v. 35, no. 5, p. 1052-1061.

Snavely, P.D., Jr., Brown, R.D., Jr., Roberts, A.E., Rau, W.W., 1958, Geology and coal resources of the Centralia-Chehalis district, Washington, with a section on microsopical character of Centralia-Chehalis coal, by J.M. Schopf: U.S. Geological Survey Bulletin 1053, 159 p. 13 pl.

Snavely, P.D., Jr., 1987, Tertiary geologic framework, neotectonics, and petroleum potential of the Oregon-Washington continental margin, in Scholl, D.W., Grantz, A., western North America and adjacent ocean basins- Beaufort Sea to Baja California: Circum-Pacific Council for Energy and Mineral Resources, Earth Sciences Series, v. 6., p. 305-335.

Stanley, W.D., Johnson, S.Y., and Nuccio, V.F., 1994, Analysis of deep seismic-reflection and other data from the southern Washington Cascades, U.S. Geological Survey Open File Report 94-159.

Stanley, W.D., Johnson, S.Y., Qamar, A.I., Weaver, C.S. and Williams, J.M., 1996, Tectonics and Seismicity of the Southern Washington Cascade Range, Bulletin of the Seismological Society of America, v. 86, no. 1A, p. 1-18.

Vail, P.R., Mitchum, R.M., and Thompson, S., III, 1977, Seismic stratigraphy and global changes of sea level, part 3: relative changes of sea level from coastal onlap, in C.W. Payton, ed., Seismic stratigraphy applications to hydrocarbon exploration: AAPG Memoir 26, p 63-97.

Van Wagoner, J.C., Mitchum, R.M., Campion, K.M., and Rahmanian, V.D., 1992, Siliciclastic sequence stratigraphy in well logs, cores, and outcrops: American Association of Petroleum Geologist Methods in Exploration Series 7, 55 p.

Waitt, R.B., Jr., 1985, Case for periodic, colossal jokulhlaups from Pleistocene glacial Lake Missoula: Geological Society of America Bulletin v.96, no.10, p.1271-1286.

Walker, R.G., 1992, Facies, Facies Models and Modern Stratigraphic Concepts, in Walker R.G., and James, N.P., eds., Facies models response to sea level change: Geological Association of Canada, p.1-25.

Walsh, T.J., Korsec, M.A., Phillips, W.M., Logan, R.L., and Schasse, H.W., 1987, Geologic map of Washington – southwest quadrant: Washington Division of Geology and Earth Resources Geologic Map GM-34, 2 pl. 28 p.

Walsh, T.J., 1987, Geologic map of Astoria and Ilwaco Quadrangles, Washington and Oregon: Washington Division of Geology and Earth Resources Open File Report 87-7, 32 p., 1 pl., scale 1:100,000.

Weaver, C.E., 1912, A preliminary report on the Tertiary paleontology of western Washington: Washington Geological Survey Bulletin 15, 80 p.

Weaver, C.E., 1937, Tertiary stratigraphy of western Washington and northwestern Oregon: University of Washington publications V.4, Seattle, 166 p., 15 pls.

Wells, R.E., 1981, Geologic map of the eastern Willapa Hills, Cowlitz, Lewis, Pacific, and Wahkiakum Counties, Washington: United States Geological Survey Open-File Report 81-674, scale 1:62,500.

Wells, R.E., and Coe, R.S., 1985, Paleomagnetism and geology of Eocene volcanic rocks of southwest Washington, implications for mechanisms of tectonic rotation: Journal of Geophysical Research, v. 90, no. B2, p. 1925-1947.

Yett, J.R., 1979, Eocene Foraminifer from the Olequa Creek Member of the Cowlitz Formation, southwestern Washington: M.S. thesis, University of Washington, Seattle, 145 p.

APPENDICES

(sample sites on Plates I and II,
page 219)

APPENDIX A Microfauna
Foraminifera Identification (Rau, 2000):

C = Common
F = Few
R = Rare
? = Questionably ident.

Species	Sample NO. 914F	914G5	916-D	M-11998	M8112	CRBM
Lenticulina cf. L. inornatiss (d'orbigny)	C	C	C			R
Eponides cf. E yeguaensis weinzierl and Applin	R					
Plectofrondicularia packardi Packardi Cushman and schenck	F					
Bulimina schenck. Beck	F	R	F		R	
Bolivina cf. B. jacksonensis Cushman and Applin	F	R				?
Bolivina cf. B. basiseensis Cushman and stone	R	C	F	R		
Gyroidina condoni (Cushman and schenck)	R	R				
?Guttulina sp.	R					
Dentalina spp.	R	F		R		
Globobulimina spp.	F					
Angulogerina hannai Beck	F					
Plectofrondicularia cf. P. jenkinsi	F					
Gyroidina soldanii octocamerata Cushman and Gd. Hanna		?				
Lenticulina welchi (Church)		F				
Globobulimina pacifica Cushman		R	?			
Globobulimina cf. B. papoides (d'orbigny)		C	F	C		
Globigerina bulloides d'Orbigny		R				
Globocasidulina globosa (Hantken)		R				
Lenticulina cf. L. texanus Cushman and Applin			R			
Uvigerina cf. U. churchi Cushman and Siegfus			R			
Nonionella sp.			R			
Nonion cf. N. inflatum Cushman and Ellisor			F		R	
Lenticulina spp.				F		
Quinqueloculina cf. Q minuta Beck				R		
Quinqueloculina imperalis Hanna and Hanna				F	R	
Pullenia salisburyi R.E. and K.C. Stewart				R		
Elphidium cf. E. minutum Cushman					F	R
Elphidium smithi Cushman and Dusenbury					?	

Foraminifera Identification (Rau, 2000):

914F

This assemblage is characteristic of my *Bulimina schencki-Plectofrondicularia cf. P. jenkinsi* zone of the upper part of the Narizian Stage of late or late-middle Eocene (Rau. 1981). It can be found in the deeper water facies of the Skookumchuck Formation (Snavely et al. 1958) (upper to middle bathyal depths). With respect to the Cowliz Fm., it depends on what is mapped as Cowlitz Fm. Although many of the species listed by Beck (1943), are not present. a few are. I suspect much of what has been called Cowliz Fm. is equivalent to the Skookumchuck Fm.

914165

This assemblage is similar to that if 914F as far as key elements are concerned, (*Bulimina schencki. Bolivina cf. B. basisensis. and Gyroidina condoni).* Additiona significant eliments, *Lenticulina welchi.* and abundant *Globobulimina* spp best suggest an upper bathyal environment of the above mentioned age for 914F.

916D

Again this assemblage may be referred to the above listed zone of southwestern Washington. Together with *Bulimina schencki. Bolivina cf. B. basisensis. Globobulimina sp.. Uvigerina churchi. and Nonion cf. N. inflata* suggest a correlation with the deep water facies (upper bathyal) of the Skookumchuck Fm.

M11199A

This assemblage. although poorly preserved suggests a similar age as the above other assemblages. The additional taxa of *Pullenia salisburyi.* and species of *Quinqueloculina* suggest a slightly shallower water depth of deposition, perhaps outer shelf to uppermost upper bathyal depths.

M2112

The presents of abundant *Elphidium* suggests shallow water conditions (inner shelf). This assemblage is typical of the shallow water facies of the Skookumchuck Fm. that is interbedded with coal deposits of the Centralia, Washington region. I would place it in the same zone as the others. uppermost Narizian Stage.

GCBM

This assemblage. although poorly preserved. suggests the same age as the others and with *Elphidium and Quinqueloculina* present it would suggest a shallow environment on the shelf either inner or outer shelf depths.

Fossils from George Creek, Cowlitz County, Washington

1	LS	*Venericardia clarki* (thick-shelled carditid clam), *?Spisula* species (surf clam), possibly *Aturia angustata* (nautilus),	Cowlitz Fm. - only poor-quality molds, but probably normal marine,
2	GT8 A	*Acutostrea fettkei* (oyster), very rare *Septifer dichotomus* (mussel),	Cowlitz Fm. - bay oysters bank plus this unique, but common, Cowlitz mussel[1]
3	GT8 B-C "South of the bridge"	*Acutostrea fettkei* (oyster), and the large flattened, horizontal burrow	Cowlitz Fm. - bay oyster bank, or simply transported shells from and oyster bank
4	GR8 E	*Lucinoma acutilineatus* (lucinid bivalve) and *Calyptraea diagoana* (slipper-shell - gastropod)	this bivalve is **not** found in Cowlitz Fm., but is found in Lincoln Creek Fm, the gastropod is found in both (does this make any sense stratigraphically?) - normal marine, intertidal to shallow subtidal.
5	GR8 F	nothing	
6	GC101 8	*Pteria clarki* (wing oyster), *Tellina* sp., *Laevidentalium* sp. (tusk shell)	*Pteria clarki* is only found in the Cowlitz Fm. They live, attached to seaweed in normal marine, shallow subtidal depths. The dentalium has only been found (so far) in the ?Tukwila Fm.[2], Cowlitz in age
7	GF8 E	molds of *Mytilus* (mussel) and *Acutostrea fettkei* (oyster)	Cowlitz Fm. - bay oyster bank
8	striped BV	*Venericardia clarki* (thick-shelled carditid clam), *Crassatellites dalli*, *Spisula* sp. (surf clam)	Cowlitz Fm. - normal marine hat lived at shallow subtidal depth - but may have been washed in, as these are both very thick, robust shells
9	GF8 A	*Turritella uvasana stewarti* (turret snail), *Acutostrea fettkei* (oyster), *Crassatellites dalli* (clam) *Venericardia clarki* (thick-shelled carditid clam), *Callista andersoni* (small venus clam), *Corbula dickersoni* (corbula clam)	Cowlitz Fm. -normal marine, shallow subtidal

Out of section

A	roadcrop	wood, gastropod impressions that may be *Liracassis* gastropd (from the helmit shell family)	If they are this genus, then it is probably lower Lincoln Creek or Toutle Fm.
B	M7 11299	nothing	
C	914 M	mold of shell probably *Tellina townsendensis* (tellin clam)	lower Lincoln Creek or Toutle Fm.

[1] See assemblage description in my J. Paleontology paper, 1995.
[2] In my short paper, Washington Geology, vol. 26 #1, 1998.

Macrofauna Identification:

ARK 6 - Corbicula, probably C. cowlitzensis. But definitely Cowlitz Fm.

61300C - only one mold is identifiable to the gastropod Scaphander - but this doesn't allow an age call

6143 - mostly just piles of sand wrapped up in tissue paper! The shells may be Crassatellites, but that is a possibility only. So not age call.

724A - Nuculana washingtonensis which is found in both Cowlitz and Lincoln Creek (and all equivalent formations of this age!)

616C - juvenile bivalve molds only. Perhaps Spisula, Callista or Pitar. No age call

6170A - mold of part of gastropod that may be Siphonalia sopehahensis. If that is so it is Cowlitz - but it's very little to go on.

G613B - mostly juvenile bivalves, as above they could be Spisula or Callista. But one good gastropod mold that looks like Bruclarkia sp., which would make it Lincoln Creek. If you have more of that I may be able to work with it. But as it stands, I can't make a reliable age call. Hope this isn't too disappointing.
and that is it - not other identifiable fossils present. H

Liz

Liz Nesbitt
Curator, Geology Division
Burke Museum of Natural History and Culture
Box 353010, University of Washington
Seattle, WA 98195-3010

APPENDIX C

Point Count Data:

	916E		GC914A		GW8C		G815B	
	# of points	%	# of points	%	# of points	%	# of points	%
monocrystalline quartz	119	29.75	141	35.25	133	33.25	147	36.75
polycrystalline quartz	17	4.25	21	5.25	27	6.75	14	3.5
biotite	33	8.25	25	6.25	29	7.25	22	5.5
muscovite	19	4.75	9	2.25	15	3.75	13	3.25
clinopyroxene	0	0	1	0.25	0	0	0	0
plagioclase	18	4.5	29	7.25	24	6	34	8.5
potassium feldspar	48	12	52	13	43	10.75	39	9.75
hornblende	6	1.5	7	1.75	4	1	2	0.5
epidote	0	0	0	0	3	0.75	1	0.25
carbonaceous material	41	10.25	14	3.5	16	4	21	5.25
meta-clasts (schist, gneiss)	29	7.25	33	8.25	39	9.75	40	10
quartzite	4	1	12	3	9	2.25	6	1.5
plutonic (myrmekitic texture)	38	9.5	23	5.75	43	10.75	27	6.75
pilotaxitic basalt	4	1	2	0.5	2	0.5	5	1.25
amygdaloidal basalt	0	0	0	0	3	0.75	2	0.5
randomly oriented basalt	2	0.5	3	0.75	7	1.75	4	1
glass	0	0	0	0	0	0	0	0
other	22	5.5	28	7	3	0.75	23	5.75
Total	400	100%	400	100%	400	100%	400	100%

APPENDIX D

Grays River basalt geochemistry:

Longitude 123°:	06.911	Germany Creek	08.078	07.820	Germany Creek	GC-1 copy	06.830	06.814	122° 59.669
Latitude 46°:	16.737	17.280	15.612	18.898	17.375		17.078	17.261	17.127

	WAL	WAL	WAL	WAL	WAL	WAL	WAL	WAL	WALM51
	GC1	GC2	GC3	914L	GC4	GC7	G810D	GT8L	12299
Date	20-Jan-00	20-Jan-00	20-Jan-00	20-Jan-00	20-Jan-00	20-Jan-00	20-Jan-00	20-Jan-00	20-Jan-00
	Unnormalized Results (Weight %):								
SiO2	47.05	47.85	51.13	52.17	47.42	46.98	47.52	45.59	46.71
Al2O3	14.59	16.60	17.00	14.57	13.96	13.81	15.33	14.49	14.28
TiO2	3.493	2.728	4.190	2.898	3.279	3.261	3.271	2.662	3.964
FeO	11.48	10.18	8.81	10.77	12.15	13.11	11.16	12.12	12.85
MnO	0.182	0.163	0.115	0.210	0.187	0.183	0.177	0.223	0.208
CaO	11.54	12.00	6.51	7.33	11.18	11.14	11.03	12.42	10.09
MgO	4.95	5.51	2.47	4.24	5.65	5.65	4.08	5.52	5.19
K2O	0.75	0.51	1.26	1.27	0.62	0.61	0.92	0.41	0.80
Na2O	2.76	2.51	3.83	3.36	2.55	2.55	2.88	2.20	2.66
P2O5	0.409	0.326	0.897	0.728	0.395	0.392	0.468	0.321	0.538
Total	97.20	98.38	96.21	97.55	97.39	97.68	96.84	95.95	97.39
	Normalized Results (Weight %):								
SiO2	48.40	48.64	53.14	53.48	48.69	48.09	49.07	47.51	47.96
Al2O3	15.01	16.87	17.67	14.94	14.33	14.14	15.83	15.10	14.66
TiO2	3.59	2.773	4.36	2.971	3.37	3.34	3.38	2.774	4.07
FeO*	11.81	10.35	9.15	11.04	12.47	13.42	11.52	12.63	13.20
MnO	0.187	0.166	0.120	0.215	0.192	0.187	0.183	0.232	0.214
CaO	11.87	12.20	6.77	7.51	11.48	11.40	11.39	12.94	10.36
MgO	5.09	5.60	2.57	4.35	5.80	5.78	4.21	5.75	5.33
K2O	0.77	0.52	1.31	1.30	0.64	0.62	0.95	0.43	0.92
Na2O	2.84	2.55	3.98	3.44	2.62	2.61	2.97	2.29	2.73
P2O5	0.421	0.331	0.93	0.75	0.406	0.401	0.483	0.335	0.552
	Trace Elements (ppm):								
Ni	102	69	18	10	95	99	29	116	71
Cr	195	144	20	16	155	144	47	292	86
Sc	26	36	27	22	25	28	29	34	24
V	399	328	297	206	373	371	325	311	359
Ba	174	142	343	300	163	169	227	138	214
Rb	11	5	18	26	5	6	20	3	18
Sr	450	425	651	410	428	430	480	412	504
Zr	233	171	337	381	210	213	252	162	259
Y	34	28	61	52	31	31	37	25	37
Nb	41.4	28.1	66.0	60.1	34.6	36.2	43.9	28.9	45.6
Ga	27	20	28	25	24	23	25	23	21
Cu	106	122	30	36	95	101	57	101	128
Zn	122	103	164	139	118	113	118	125	127
Pb	0	0	6	0	1	0	1	5	4
La	27	31	51	49	28	17	29	18	36
Ce	59	50	136	102	63	53	76	40	77
Th	2	4	6	5	4	1	2	2	1
	Major elements are normalized on a volatile-free basis, with total Fe expressed as FeO.								
	"*" denotes values >120% of our highest standard.								

WSU GeoAnalytical Laboratory

Grays River basalt minor element geochemistry:

Sample ID	La ppm	Ce ppm	Pr ppm	Nd ppm	Sm ppm	Eu ppm	Gd ppm	Tb ppm	Dy ppm
WAL GC-1	29.60	61.33	7.44	32.82	8.32	2.71	8.17	1.22	7.15
WAL GC-2	22.07	45.92	5.71	25.17	6.56	2.18	6.38	1.02	6.00
WAL GC-3	62.44	120.33	14.21	60.92	14.08	4.43	13.70	2.00	11.63
WAL 914L	50.76	103.01	12.42	52.60	12.83	3.85	12.32	1.91	11.08
WAL GC-4	27.72	57.25	6.96	30.86	7.81	2.54	7.62	1.16	6.69
WAL GC-7	27.42	56.31	6.86	30.12	7.77	2.50	7.40	1.15	6.66
WAL G810D	36.79	75.42	9.05	39.11	9.45	2.94	8.92	1.38	7.97
WAL GT8L	21.27	44.22	5.37	23.71	6.05	2.00	5.83	0.90	5.36
WAL M511229	37.46	76.35	9.43	41.18	9.91	3.19	9.45	1.42	8.04

Ho ppm	Er ppm	Tm ppm	Yb ppm	Lu ppm	Ba ppm	Th ppm	Nb ppm	Y ppm	Hf ppm	Ta ppm
1.36	3.28	0.44	2.49	0.37	191	3.03	38.60	33.29	5.73	2.51
1.14	2.90	0.39	2.25	0.34	153	2.26	28.09	28.75	4.40	1.89
2.23	5.45	0.72	3.92	0.59	361	5.74	66.99	61.65	8.60	4.66
2.14	5.53	0.77	4.39	0.67	309	5.52	61.14	54.82	9.52	4.03
1.29	3.12	0.41	2.31	0.35	182	2.82	36.12	31.82	5.37	2.37
1.26	3.08	0.41	2.29	0.35	178	2.71	35.31	31.13	5.21	2.32
1.52	3.79	0.52	2.98	0.44	260	4.03	44.78	37.75	6.53	2.97
1.01	2.49	0.34	1.90	0.30	147	2.16	28.58	24.74	4.06	1.89
1.48	3.61	0.48	2.71	0.40	239	3.50	47.32	37.96	6.54	3.09

U ppm	Pb ppm	Rb ppm	Cs ppm	Sr ppm	Sc ppm
0.83	1.63	11.1	0.14	466	35.0
0.62	1.34	5.3	0.15	443	33.1
1.33	2.04	17.6	0.13	652	27.3
1.55	3.19	26.5	0.22	427	23.3
0.77	1.58	6.8	0.15	445	33.3
0.79	1.62	6.8	0.15	436	32.4
1.06	2.64	21.1	0.22	489	31.9
0.58	1.14	3.9	0.06	414	38.7
0.97	1.91	19.1	0.14	511	31.0

WSU GeoAnalytical Laboratory

Basalt geochemistry:

Longitude 123°:	**05.992**	**05.087**	**03.133**	**05.517**	**01.770**	**122° 54.465**
Latitude 46°:	**16.854**	**18.183**	**17.208**	**18.842**	**17.049**	**20.008**

	WEG 51700	WEG 51703	WEG 51706	WEG 6170B	WEG 626B	WEG 6280
Date	24-Sep-00	24-Sep-00	24-Sep-00	24-Sep-00	24-Sep-00	24-Sep-00
Unnormalized Results (Weight %):						
SiO2	47.93	51.02	54.04	48.82	49.40	53.31
Al2O3	14.04	17.09	13.95	13.61	13.90	16.37
TiO2	3.666	2.887	1.964	3.248	3.975	2.074
FeO	13.78	9.82	11.15	12.33	12.84	8.52
MnO	0.216	0.205	0.209	0.162	0.176	0.176
CaO	9.59	8.68	8.63	9.88	9.33	9.37
MgO	4.58	3.19	4.64	5.90	4.56	4.15
K2O	0.80	1.13	1.25	0.84	0.63	0.50
Na2O	2.98	3.74	2.94	2.73	3.07	3.81
P2O5	0.592	0.581	0.301	0.536	0.501	0.296
Total	98.18	98.34	99.07	98.05	98.38	98.58
Normalized Results (Weight %):						
SiO2	48.82	51.88	54.55	49.79	50.21	54.08
Al2O3	14.30	17.38	14.08	13.88	14.13	16.61
TiO2	†3.73	2.936	1.982	†3.31	†4.04	2.104
FeO*	14.04	9.99	11.25	12.57	13.05	8.64
MnO	0.220	0.208	0.211	0.165	0.179	0.179
CaO	9.77	8.83	8.71	10.08	9.48	9.51
MgO	4.67	3.24	4.68	6.02	4.63	4.21
K2O	0.81	1.15	1.26	0.86	0.64	0.51
Na2O	3.04	3.80	2.97	2.78	3.12	3.87
P2O5	0.603	0.591	0.304	0.547	0.509	0.300
Trace Elements (ppm):						
Ni	38	12	13	107	38	14
Cr	43	16	36	247	28	30
Sc	25	22	37	26	34	33
V	341	227	351	307	320	367
Ba	239	287	470	197	193	191
Rb	7	22	29	11	7	10
Sr	435	496	309	375	462	401
Zr	279	286	152	239	248	145
Y	40	43	34	38	39	29
Nb	47.2	48.3	11.0	39.2	40.4	12.5
Ga	22	21	21	21	23	21
Cu	73	45	29	104	23	†185
Zn	134	122	114	128	131	106
Pb	4	5	10	1	0	0
La	31	42	20	35	38	12
Ce	93	89	43	86	98	34
Th	3	4	0	1	7	5

Major elements are normalized on a volatile-free basis, with total Fe expressed as FeO.
"R" denotes a duplicate bead made from the same rock powder.
"†" denotes values >120% of our highest standard.

Karl Wegmann - WA Dept. of Natural Resources 12/07/2000

Sample ID	Tm ppm	Yb ppm	Lu ppm	Ba ppm	Th ppm	Nb ppm	Y ppm	Hf ppm	Ta ppm	U ppm	Pb ppm	Rb ppm
WEG 51700	0.52	3.06	0.44	253	3.82	48.64	40.62	7.04	3.24	0.92	2.05	7.8
WEG 51703	0.63	3.72	0.57	290	4.30	50.37	44.72	7.39	3.30	1.14	2.26	22.6
WEG 51706	0.51	3.08	0.48	467	3.73	11.49	35.17	4.30	0.75	0.94	5.66	29.2
WEG 6170B	0.52	2.97	0.44	217	3.30	41.86	39.75	6.20	2.78	0.80	1.74	12.1
WEG 626B	0.52	2.98	0.45	213	3.16	42.27	40.72	6.55	2.82	0.85	1.76	6.9
WEG 6280	0.44	2.66	0.41	192	1.82	12.18	30.33	3.83	0.81	0.54	2.48	9.3

Karl Wegmann - WA Dept. of Natural Resources 12/07/2000

Sample ID	La ppm	Ce ppm	Pr ppm	Nd ppm	Sm ppm	Eu ppm	Gd ppm	Tb ppm	Dy ppm	Ho ppm	Er ppm
WEG 51700	38.27	78.36	9.67	42.17	10.21	3.28	9.81	1.52	8.72	1.60	3.98
WEG 51703	40.33	81.12	9.75	41.92	10.04	3.26	9.86	1.57	8.99	1.76	4.56
WEG 51706	19.50	39.34	4.90	22.14	5.87	1.93	6.18	1.07	6.71	1.36	3.64
WEG 6170B	33.57	69.61	8.63	38.19	9.47	3.04	9.04	1.43	8.14	1.53	3.87
WEG 626B	33.32	69.48	8.65	38.11	9.63	3.33	9.55	1.47	8.41	1.55	3.94
WEG 6280	16.74	35.68	4.55	20.61	5.61	1.93	5.75	0.96	5.94	1.17	3.17

Karl Wegmann - WA Dept. of Natural Resources 12/07/2000

Sample ID	Cs ppm	Sr ppm	Sc ppm	Zr ppm
WEG 51700	0.06	419	28.7	272
WEG 51703	0.16	488	22.7	286
WEG 51706	0.79	309	41.1	154
WEG 6170B	0.07	370	32.7	239
WEG 626B	0.09	458	32.3	253
WEG 6280	0.25	394	37.3	140

APPENDIX E

40Ar/39Ar Age Dates:

(run by Dr. Robert Duncan, OSU School of Oceanography, 2000)

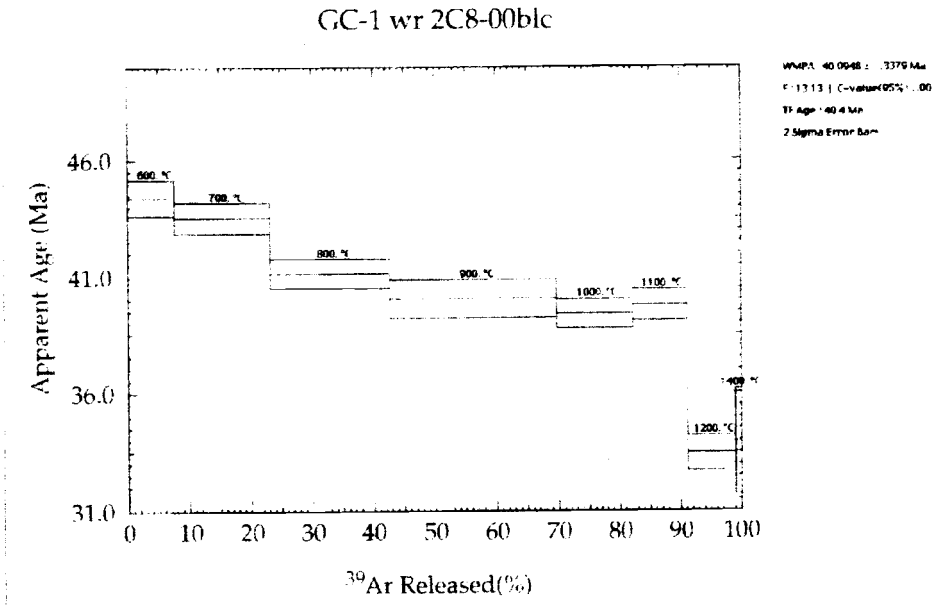

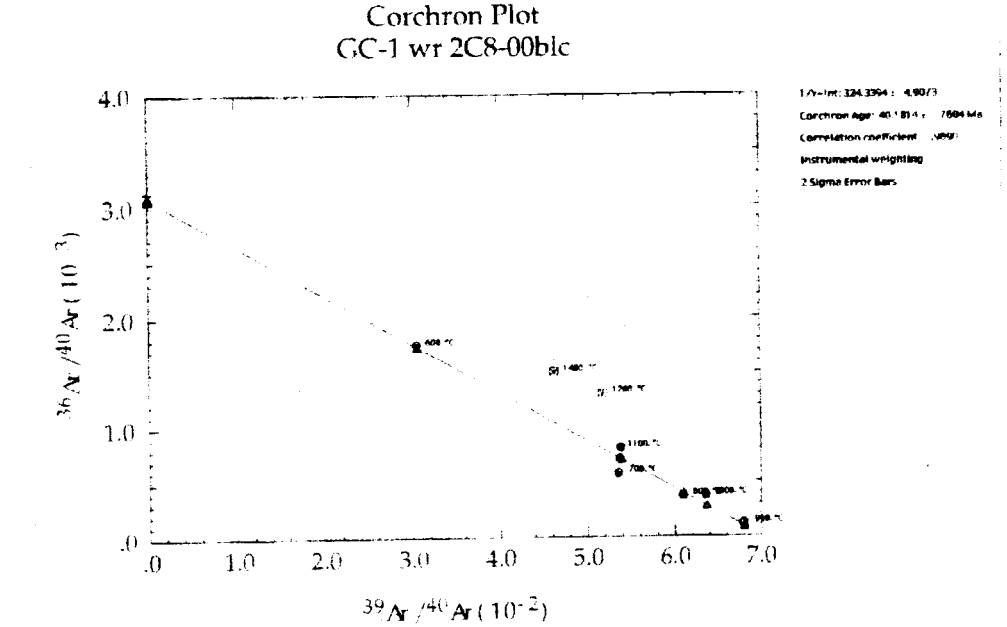

40Ar/39Ar Age Dates:

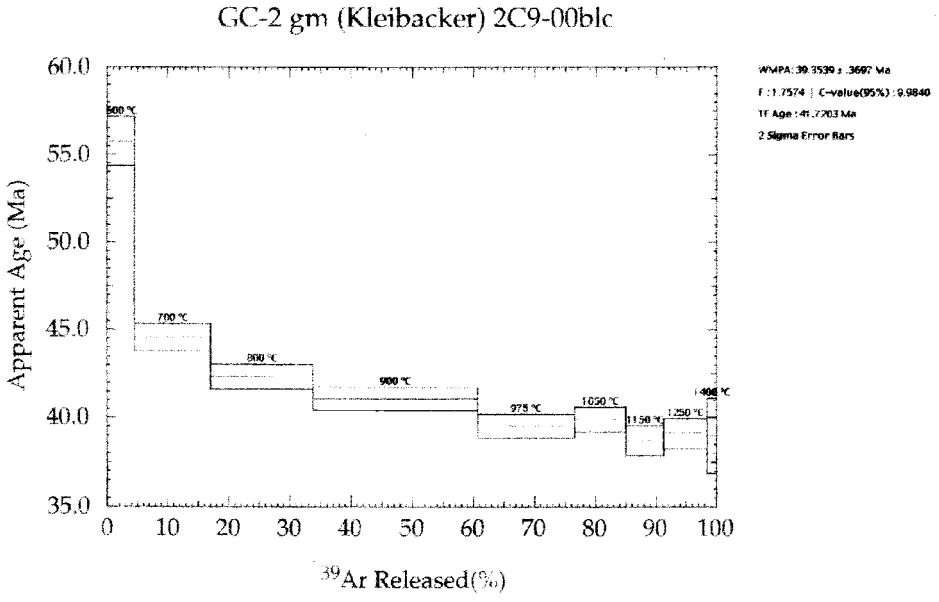

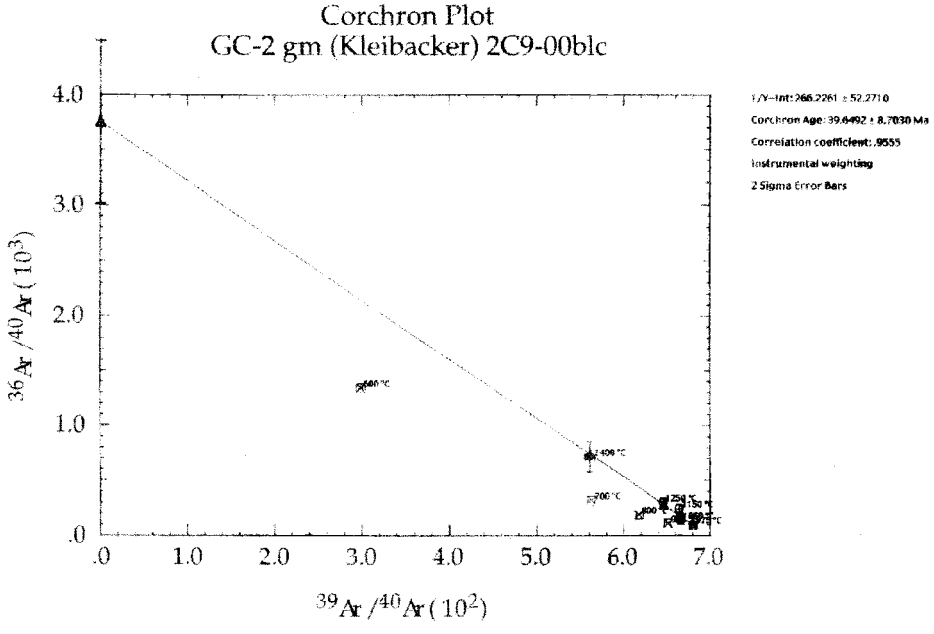

40Ar/39Ar Age Dates:

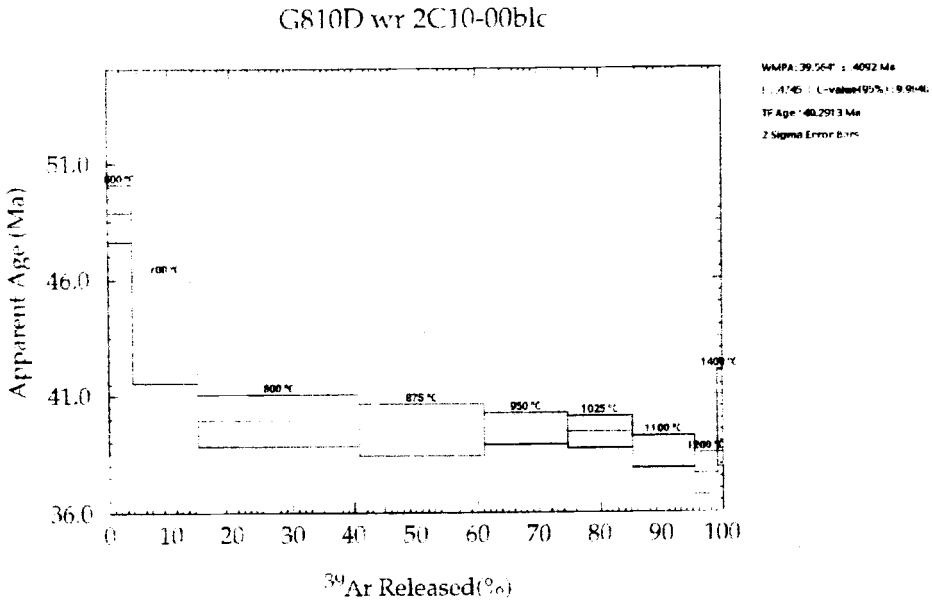

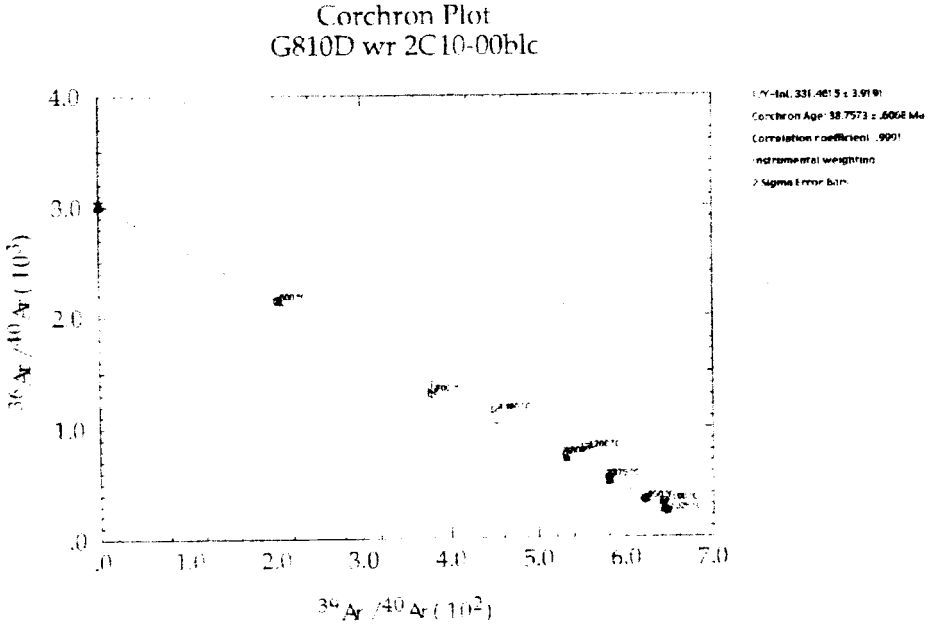

40Ar/39Ar Age Dates:

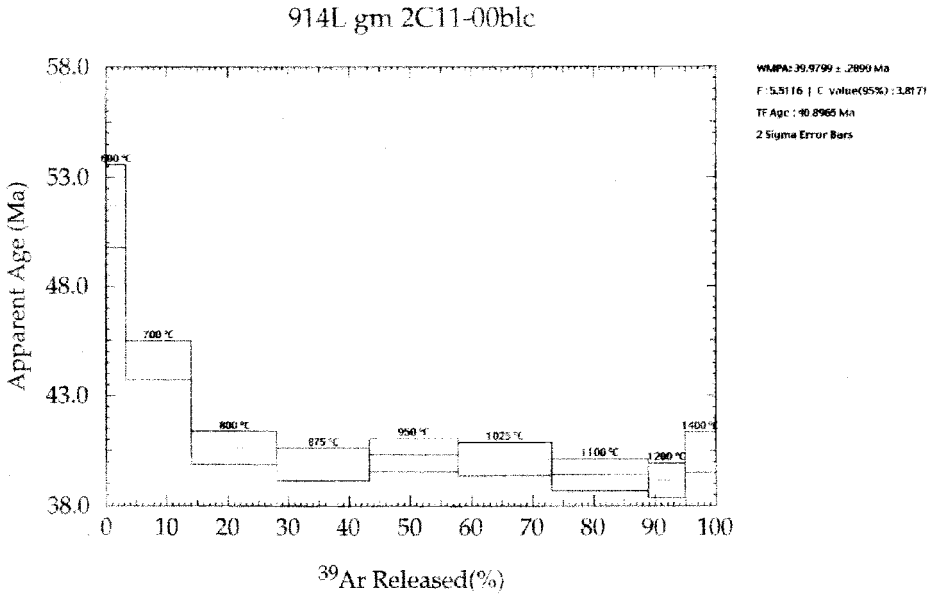

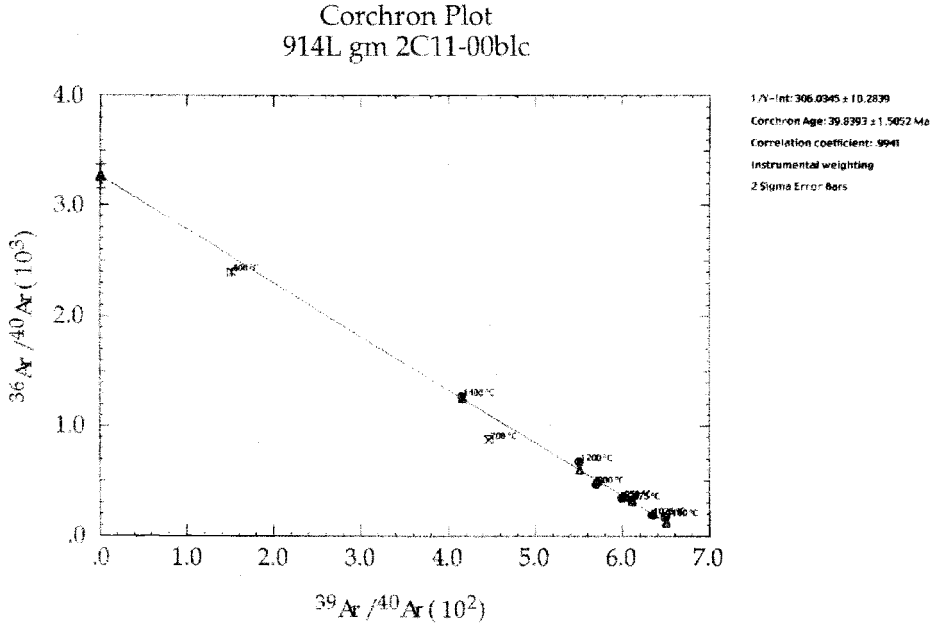

APPENDIX F

Paleomagnetic Results: Site numbers as in Plate II; N: number of samples per site; D, I: declination, inclination; k, alpha, precision parameters (data analysis from Dr. Donald Prothero, 2000). Locations given on pg. 218.

Site	N	D	I	k	α_{95}
Germany Creek					
1	3	118.9	82.8	133.2	10.7
3	3	85.7	74.8	83.8	13.6
4	3	96.6	71.6	265.0	7.6
5	3	138.4	48.3	4.1	70.5
6	3	284.1	-34.2	4.7	65.1
7	3	315.5	-51.6	53.6	17.0
8	3	296.6	-62.4	1.6	180.0
9	3	326.7	-34.5	27.0	24.2
10	3	7.5	-27.7	33.8	21.6
11	3	309.1	-49.1	88.7	13.2
12	3	75.7	59.3	69.7	14.9
13	3	28.8	34.5	1.9	151.1
14	2	325.0	-35.5	34.3	44.0
15	3	320.5	-45.1	44.3	18.7
16	3	303.5	-51.4	7.1	50.2
17	3	295.2	-66.5	21.0	27.6
18	3	53.0	74.6	2.4	109.3
19	3	56.6	50.5	7.1	50.4
20	3	197.8	-80.8	4.5	67.1
21	3	242.4	-54.5	10.2	40.8
22	3	288.4	-61.7	67.8	15.1
23	2	229.1	-46.2	6.3	130.3
24	2	277.2	-50.9	14.0	72.9
25	2	244.8	-72.1	3.3	180.0
26	3	272.4	-64.3	12.7	36.1
28	3	288.7	-62.4	6.5	52.9
29	3	251.1	-29.9	76.6	14.2
30	3	295.4	-26.1	16.9	31.0
31	3	65.7	50.7	7.0	50.8
32	3	53.5	55.1	11.7	37.7
33	3	289.8	-67.8	5.5	58.9
34	3	229.3	-61.2	18.6	29.4
35	3	276.1	-33.5	3.1	87.5
36	3	290.7	-55.2	13.2	35.4
37	3	235.3	-52.4	13.1	35.6
38	3	233.7	-40.1	5.7	57.3
39	3	215.0	-61.4	8.4	45.4
Germany Creek normal mean	8	74.2	67.2	11.6	17.0
Germany Creek reversed mean	27	273.5	-56.5	6.6	11.7
Germany Creek locality mean	35	93.9	60.6	8.9	8.6

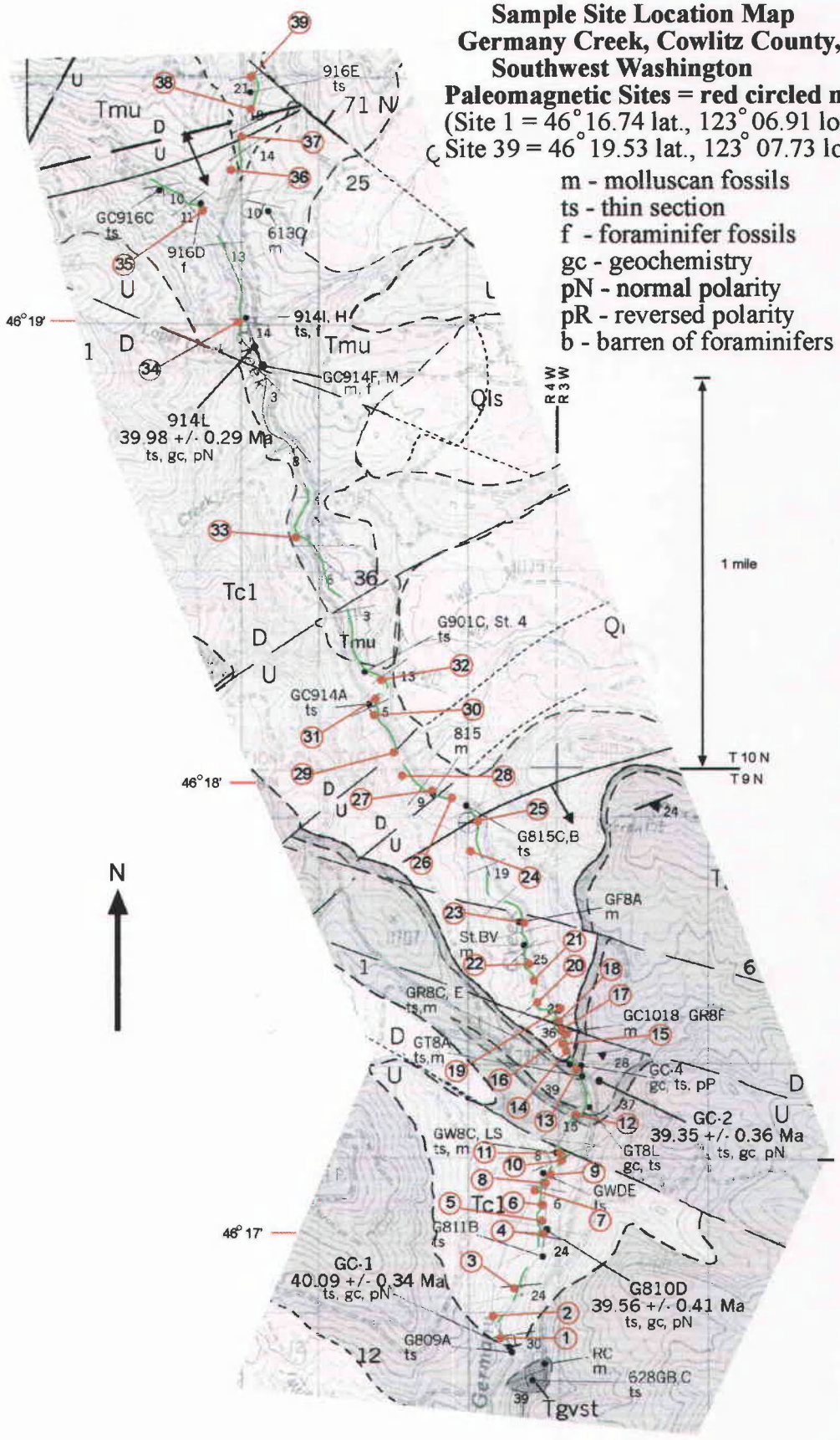
Sample Site Location Map
Germany Creek, Cowlitz County,
Southwest Washington
Paleomagnetic Sites = red circled numbers.
(Site 1 = 46°16.74 lat., 123°06.91 long.,
Site 39 = 46°19.53 lat., 123°07.73 long.)
m - molluscan fossils
ts - thin section
f - foraminifer fossils
gc - geochemistry
pN - normal polarity
pR - reversed polarity
b - barren of foraminifers
916E ts
GC916C ts
916D f
613C m
914I, H ts, f
914L 39.98 +/- 0.29 Ma ts, gc, pN
GC914F, M m, f
G901C, St. 4 ts
GC914A ts
815 m
G815C,B ts
GF8A m
St.BV m
GR8C, E ts,m
GT8A ts,m
GC1018 GR8F m
GC-4 gc, ts, pP
GC-2 39.35 +/- 0.36 Ma ts, gc, pN
GW8C, LS ts, m
GT8L gc, ts
GWDE ts
G811B ts
GC-1 40.09 +/- 0.34 Ma ts, gc, pN
G810D 39.56 +/- 0.41 Ma ts, gc, pN
G809A ts
RC m
628GB,C ts
Tmu
Tc1
Tc16
Tgvst
Qls
Qt
71 N
25
36
1
12
6
T
L
U
D
46°19'
46°18'
46°17'
R4W
R3W
T10N
T9N
1 mile
N